UNIVERSIDADE FEDERAL DE VIÇOSA

Bioaccessibility and metabolism of anthocyanins: effects of fermentation, encapsulation, and microbiota interactions

Larissa Lorrane Rodrigues Borges
Doctor Scientiae

VIÇOSA - MINAS GERAIS
2025

LARISSA LORRANE RODRIGUES BORGES

Bioaccessibility and metabolism of anthocyanins: effects of fermentation, encapsulation, and microbiota interactions

Thesis submitted to the Food Science and Technology Graduate Program of the Universidade Federal de Viçosa in partial fulfillment of the requirements for the degree of *Doctor Scientiae*.

Adviser: Paulo Cesar Stringheta

Co-advisers: Pedro H. Campelo Felix
Monique Renon Eller
Frederico A. R. de Barros

VIÇOSA - MINAS GERAIS
2025

Ficha catalográfica elaborada pela Biblioteca Central da Universidade Federal de Viçosa - Campus Viçosa

T
B732b
2025

Borges, Larissa Lorrane Rodrigues, 1996-
Bioaccessibility and metabolism of anthocyanins: effects of fermentation, encapsulation, and microbiota interactions / Larissa Lorrane Rodrigues Borges. – Viçosa, MG, 2025.
1 tese eletrônica (193 f.): il. (algumas color.).

Orientador: Paulo César Stringheta.
Tese (doutorado) - Universidade Federal de Viçosa, Departamento de Tecnologia de Alimentos, 2025.
Inclui bibliografia.
DOI: https://doi.org/10.47328/ufvbbt.2025.047
Modo de acesso: World Wide Web.

1. Fermentação. 2. Compostos bioativos. 3. Antocianinas - Metabolismo. 4. Microbioma gastrointestinal. I. Stringheta, Paulo César, 1952-. II. Universidade Federal de Viçosa. Departamento de Tecnologia de Alimentos. Programa de Pós-Graduação em Ciência e Tecnologia de Alimentos. III. Título.

CDD 22. ed. 664.024

Bibliotecário(a) responsável: Euzébio Luiz Pinto CRB-6/3317

LARISSA LORRANE RODRIGUES BORGES

Bioaccessibility and metabolism of anthocyanins: effects of fermentation, encapsulation, and microbiota interactions

Thesis submitted to the Food Science and Technology Graduate Program of the Universidade Federal de Viçosa in partial fulfillment of the requirements for the degree of *Doctor Scientiae*.

APPROVED: January 23, 2025.

Assent:

Larissa Lorrane Rodrigues Borges
Author

Paulo Cesar Stringheta
Adviser

ACKNOWLEDGMENTS

To God, for guiding me, blessing me, and granting me the strength, wisdom, and patience to face every challenge.

To my family, especially my parents, Gina Maria Rodrigues Borges and Geraldo Valdeir Alves Borges, for their constant love, support, and everything they have done for me.

To my advisor, professor Paulo César Stringheta, I express my deep gratitude for your guidance, patience, and dedication. Your valuable advice, continuous encouragement, and expertise were essential to the development of this study and to my academic growth.

To my co-advisors, Frederico Augusto Ribeiro de Barros, Monique Renon Eller, and Pedro Henrique Campelo Felix, and to Professor Evandro Martins, I sincerely thank you for all your support, teachings, and contributions to the development of this study.

To my co-advisor at Texas A&M University, Dr. Stephen Talcott, and to Dr. Susanne Talcott, for giving me the great opportunity to join their lab as a visiting scholar student. Thank you for your support, mentorship, teachings, patience, and kindness during my time abroad.

To everyone from LaCBio, especially my friends Valdeir, Hélia, Janaina, Amanda and Mariane, I am deeply grateful for all the support and moments shared throughout this journey. I would also like to thank Ana, Elizabeth, Sergio, Shannon, Tara, and Dr. Giulliana for their friendship and support in the lab at Texas A&M. The collaboration, talks, and companionship from each of you have made this path lighter and more inspiring.

To all my lifelong friends and those I've met along the way, I am eternally grateful for your support, care, and presence throughout my journey.

To the professors and staff of the Department of Food Technology at the Universidade Federal de Viçosa, thank you for all the teachings and support.

To CAPES for financing my scholarship and CAPES-PrInt for financing my training at Texas A&M University as a visiting scholar.

This study was financed in part by the Coordenação de Aperfeiçoamento de Pessoal de Nível Superior – Brasil (CAPES) – Finance Code 001.

ABSTRACT

BORGES, Larissa Lorrane Rodrigues, D.Sc., Universidade Federal de Viçosa, January, 2025. **Bioaccessibility and metabolism of anthocyanins: effects of fermentation, encapsulation, and microbiota interactions**. Adviser: Paulo Cesar Stringheta. Co-advisers: Pedro Henrique Campelo Felix, Monique Renon Eller and Frederico Augusto Ribeiro de Barros.

Anthocyanins have been widely studied for their health benefits; however, these compounds exhibit low bioaccessibility and bioavailability due to degradation and limited absorption in the gastrointestinal tract, which may restrict their effects. Therefore, innovative strategies to enhance the stability and maximize the benefits of anthocyanins are essential, especially for applications in food and supplements. In this context, this study investigated the bioaccessibility and metabolism of anthocyanins, focusing on digestion, interactions with gut microbiota, and the effects of fermentation and encapsulation on the stability and bioactivity of these compounds. The biotransformation of phenolic compounds was studied during the production of jabuticaba wine, and the results showed that anthocyanins underwent biotransformation. Significant increases were observed in total phenolic compounds (4.91 ± 0.07 times), total anthocyanins (5.62 ± 1.17 times), cyanidin-3-glucoside (C3G) (2.05 ± 0.74 times), gallic acid (GA) (57.02 ± 3.70 times), and protocatechuic acid (PA) (3.70 ± 0.51 times) compared to the non-fermented control. Additionally, an increase in the bioaccessibility of C3G, GA, and PA was observed. Jabuticaba wine also exhibited antiproliferative effects against cancer cells, antioxidant activities, and enzymatic inhibition properties. To improve anthocyanin stability during digestion, jabuticaba extract was encapsulated with whey protein (WP) or pea protein (PP) combined with gum arabic (GA). Encapsulation improved anthocyanin bioaccessibility, particularly in the PP:GA 1:2 (v/v) and WP:GA 1:2 (v/v) samples, with increases of 33% and 25%, respectively, compared to the unencapsulated extract. Encapsulation also delayed degradation, increased anthocyanin retention, and enhanced the production of metabolites and short-chain fatty acids (SCFAs) during the colonic phase. Cyanidin-3-glucoside exhibited superior antioxidant and anti-inflammatory effects compared to its main metabolites, significantly reducing reactive oxygen species and pro-inflammatory markers in colon cancer cells (HT29-MTX). The encapsulation of the extract using chitosan (CH) and GA as wall materials was also investigated, increasing bioaccessibility and targeted release of anthocyanins to the colon. The in vitro metabolism of anthocyanins and SCFA production were analyzed in individuals with different body mass

index (BMI) values. It was observed that the microbiota metabolized 37.45–54.01% of C3G in the lean group, 40.84–61.74% in the overweight group, and 36.06–69.16% in the obese group after 48 hours. These results showed variations in anthocyanin metabolism within each group, indicating that even among individuals with similar BMI, differences in gut microbiota composition may impact C3G metabolism. The anthocyanin extract also altered SCFA levels compared to control fermentations (without the extract). In summary, this thesis provided an overview of anthocyanin metabolism and bioaccessibility, demonstrating how fermentation and encapsulation influenced metabolism and increased the bioaccessibility of these compounds. Additionally, individual variability in gut microbiota composition was identified as an important factor in anthocyanin metabolism, highlighting the need to consider these variations when studying the health benefits of anthocyanins.

Keywords: cyanidin-3-glucoside; jabuticaba; short-chain fatty acids (scfas); microbiota; digestion

RESUMO

BORGES, Larissa Lorrane Rodrigues, D.Sc., Universidade Federal de Viçosa, janeiro de 2025. **Bioacessibilidade e metabolismo de antocianinas: efeitos da fermentação, encapsulamento e interações com a microbiota**. Orientador: Paulo Cesar Stringheta. Coorientadores: Pedro Henrique Campelo Felix, Monique Renon Eller e Frederico Augusto Ribeiro de Barros.

As antocianinas têm sido amplamente estudadas por seus benefícios à saúde; no entanto, esses compostos apresentam baixa bioacessibilidade e biodisponibilidade devido à degradação e limitada absorção no trato gastrointestinal, o que pode restringir seus efeitos. Assim, estratégias inovadoras para melhorar a estabilidade e potencializar os benefícios das antocianinas são essenciais, especialmente para aplicações em alimentos e suplementos. Neste contexto, este estudo investigou a bioacessibilidade e metabolismo das antocianinas, com foco na digestão, interações com a microbiota intestinal e efeitos da fermentação e encapsulamento na estabilidade e bioatividade desses compostos. A biotransformação de compostos fenólicos foi estudada durante a produção do vinho de jabuticaba, e os resultados mostraram que as antocianinas sofreram biotransformação. Aumentos significativos foram observados nos compostos fenólicos totais (4,91 ± 0,07 vezes), antocianinas totais (5,62 ± 1,17 vezes), cianidina-3-glicosídeo (C3G) (2,05 ± 0,74 vezes), ácido gálico (GA) (57,02 ± 3,70 vezes) e ácido protocatecuico (PA) (3,70 ± 0,51 vezes) em comparação ao controle não fermentado. Além disso, foi observado um aumento na bioacessibilidade de C3G, GA e PA. O vinho de jabuticaba também apresentou efeitos antiproliferativos contra células cancerígenas, atividades antioxidantes e propriedades inibitórias contra enzimas. Para melhorar a estabilidade das antocianinas durante a digestão, o extrato de jabuticaba foi encapsulado com proteína do soro de leite (WP) ou proteína de ervilha (PP) combinadas com goma arábica (GA). O encapsulamento melhorou a bioacessibilidade das antocianinas, especialmente nas amostras PP:GA 1:2 (v/v) e WP:GA 1:2 (v/v), com aumentos de 33% e 25%, respectivamente, comparado ao extrato não encapsulado. O encapsulamento também retardou a degradação, aumentou a retenção de antocianinas e potencializou a produção de metabólitos e ácidos graxos de cadeia curta (AGCC) durante a fase colônica. A cianidina-3-glicosídeo demonstrou efeitos antioxidantes e anti-inflamatórios superiores aos de seus principais metabólitos, reduzindo significativamente espécies reativas de oxigênio e marcadores pró-inflamatórios em células de câncer de cólon (HT29-MTX). O encapsulamento do extrato usando quitosana (CH) e GA como materiais de parede também foi investigado, aumentando

a bioacessibilidade e a liberação direcionada das antocianinas para o cólon. O metabolismo in vitro das antocianinas e a produção de AGCC foram analisados em indivíduos com diferentes índices de massa corporal (IMC). Observou-se que a microbiota metabolizou 37,45–54,01% de C3G no grupo magro, 40,84–61,74% no grupo com sobrepeso e 36,06–69,16% no grupo obeso após 48 horas. Esses resultados mostraram variações no metabolismo das antocianinas dentro de cada grupo, indicando que, mesmo entre indivíduos com IMC semelhante, diferenças na composição da microbiota intestinal podem impactar a metabolização da C3G. O extrato de antocianinas também alterou os níveis de AGCC em comparação às fermentações controle (sem extrato). Em resumo, esta tese forneceu uma visão geral do metabolismo e bioacessibilidade das antocianinas, mostrando como a fermentação e o encapsulamento influenciaram o metabolismo e aumentaram a bioacessibilidade desses compostos. Além disso, a variabilidade individual na composição da microbiota intestinal foi identificada como um fator importante no metabolismo das antocianinas, destacando a necessidade de considerar essas variações ao estudar os benefícios à saúde das antocianinas.

Palavras-chave: cianidina-3-glicosídeo; jabuticaba ; ácidos graxos de cadeia curta (agcc); microbiota; digestão

SUMMARY

1. GENERAL INTRODUCTION

Anthocyanins are a well-known group of phenolic compounds that have attracted scientific and industrial interest due to their color characteristics and diverse bioactive properties, including antioxidant, anti-inflammatory, and anti-diabetic effects, in addition to potential cardioprotective and neuroprotective properties (FALLAH et al., 2020; FALLAH; SARMAST; JAFARI, 2020; KALT et al., 2020; SHARMA; PANDITA; BHOSALE, 2023; XIN et al., 2024). Despite these benefits, anthocyanins are recognized for their low bioaccessibility and bioavailability in the human body, with only a minimal percentage (< 2.0%) of intact anthocyanins absorbed after consumption (DE FERRARS et al., 2014; MUELLER et al., 2017; STALMACH et al., 2012; ZHONG et al., 2017). This has raised questions about the actual role of anthocyanins in their original form versus the metabolites produced during digestion (BRAGA et al., 2018a; MUELLER et al., 2018). Addressing these questions is essential to maximize their beneficial health effects, but also to develop strategies that improve their stability and enable the application of these compounds in foods and supplements.

Jabuticaba is a fruit native from Brazil, that represent a unique and promising source of anthocyanins and other phenolic compounds. The jabuticaba fruit, especially its pigmented peel, contains a high concentration of cyanidin-3-glucoside, tannins, and several phenolic acids (INADA et al., 2020; NEVES et al., 2018, 2021). However, despite its potential health benefits, jabuticaba is primarily consumed fresh and its peel is often discarded, leading to a loss of valuable bioactive compounds. Fermentation of jabuticaba to produce jabuticaba wine is an alternative to explore the nutritional and functional benefits of this fruit, minimizing post-harvest losses. During fermentation, phenolic compounds are extracted from the peel, and can undergo biotransformation into other bioactive metabolites, potentially enhancing their antioxidant and health-promoting properties (BRAGA et al., 2018b; CHEN et al., 2023; DONG et al., 2023). Additionally, jabuticaba peel is a potential source of anthocyanin extraction for several applications.

Given the rising incidence of chronic diseases and the growing interest in functional foods, there is increasing market demand for anthocyanins, which are used as natural colorants and functional components in foods, beverages and dietary supplements (RESEARCH AND MARKETS, 2024). Therefore, innovative and effective approaches are needed to enhance anthocyanin stability. Various encapsulation techniques, including spray drying, complex coacervation, ionic gelation, liposomes, and molecular inclusion, have been investigated for

this purpose. These techniques aim to improve anthocyanin stability under different pH and temperature conditions, protect them from degradation during digestion, and provide controlled release and targeted delivery to specific regions of the gastrointestinal tract, such as the colon (NASCIMENTO et al., 2023; SHEN et al., 2022).

The gut microbiota is recognized as critical in affecting the bioavailability, bioactivity, and health effects of anthocyanins (CARDONA et al., 2013; EKER et al., 2020). Once in the colon, anthocyanins are metabolized by the gut microbiota into lower molecular weight metabolites, which may have greater bioavailability and distinct biological activities compared to their parent compounds (OZDAL et al., 2016; WANG; QI; ZHENG, 2022). Results from previous studies also suggested that anthocyanins positively impact the gut microbiota composition, promoting the growth of beneficial bacteria such as *Bifidobacterium* and *Lactobacillus*, and/or reducing potentially harmful species (BOTO-ORDÓÑEZ et al., 2014; GUERGOLETTO et al., 2016; MOLAN; LIU; PLIMMER, 2014; PENG et al., 2021). This interaction between anthocyanins and the gut microbiota might be essential in understanding the health effects of anthocyanins and metabolites. However, the complexities of anthocyanin metabolism along with interindividual variability in microbiota composition, highlight the importance for targeted research into how these compounds are metabolized across different population groups.

In this context, this thesis aimed to provide a comprehensive investigation of the bioaccessibility and metabolism of anthocyanins, focusing on their digestion, interactions with the gut microbiota, and the impact of fermentation and encapsulation techniques on their stability and bioactive potential.

REFERENCES

BOTO-ORDÓÑEZ, M. et al. High levels of Bifidobacteria are associated with increased levels of anthocyanin microbial metabolites: A randomized clinical trial. **Food and Function**, v. 5, n. 8, p. 1932–1938, 2014.

BRAGA, A. R. C. et al. Bioavailability of anthocyanins: Gaps in knowledge, challenges and future research. **Journal of Food Composition and Analysis**, v. 68, p. 31–40, 2018a.

BRAGA, A. R. C. et al. Lactobacillus fermentation of jussara pulp leads to the enzymatic conversion of anthocyanins increasing antioxidant activity. **Journal of Food Composition and Analysis**, v. 69, p. 162–170, 2018b.

CARDONA, F. et al. Benefits of polyphenols on gut microbiota and implications in human health. **Journal of Nutritional Biochemistry**, v. 24, n. 8, p. 1415–1422, 2013.

CHEN, W. et al. Improvement in color expression and antioxidant activity of strawberry juice fermented with lactic acid bacteria: A phenolic-based research. **Food Chemistry: X**, v. 17, p. 100535, 2023.

DE FERRARS, R. M. et al. The pharmacokinetics of anthocyanins and their metabolites in humans. **British Journal of Pharmacology**, v. 171, n. 13, p. 3268–3282, 2014.

DONG, X. et al. Effect of lactic acid fermentation and *in vitro* digestion on the bioactive compounds in Chinese wolfberry (*Lycium barbarum*) pulp. **Food Bioscience**, v. 53, p. 102558, 2023.

EKER, M. E. et al. A Review of Factors Affecting Anthocyanin Bioavailability: Possible Implications for the Inter-Individual Variability. **Foods**, v. 9, n. 2, p. 1–18, 2020.

FALLAH, A. A. et al. Impact of dietary anthocyanins on systemic and vascular inflammation: Systematic review and meta-analysis on randomised clinical trials. **Food and Chemical Toxicology**, v. 135, p. 110922, 2020.

FALLAH, A. A.; SARMAST, E.; JAFARI, T. Effect of dietary anthocyanins on biomarkers of oxidative stress and antioxidative capacity: A systematic review and meta-analysis of randomized controlled trials. **Journal of Functional Foods**, v. 68, p. 103912, 2020.

GUERGOLETTO, K. B. et al. *In vitro* fermentation of juçara pulp (*Euterpe edulis*) by human colonic microbiota. **Food Chemistry**, v. 196, p. 251–258, 2016.

INADA, K. O. P. et al. Bioaccessibility of phenolic compounds of jaboticaba (*Plinia jaboticaba*) peel and seed after simulated gastrointestinal digestion and gut microbiota fermentation. **Journal of Functional Foods**, v. 67, p. Article 103851, 2020.

KALT, W. et al. Recent Research on the Health Benefits of Blueberries and Their Anthocyanins. **Advances in Nutrition**, v. 11, n. 2, p. 224–236, 2020.

MOLAN, A. L.; LIU, Z.; PLIMMER, G. Evaluation of the effect of blackcurrant products on gut microbiota and on markers of risk for colon cancer in humans. **Phytotherapy Research**, v. 28, n. 3, p. 416–422, 2014.

MUELLER, D. et al. Human intervention study to investigate the intestinal accessibility and bioavailability of anthocyanins from bilberries. **Food Chemistry**, v. 231, p. 275–286, 2017.

MUELLER, D. et al. Encapsulation of anthocyanins from bilberries – Effects on bioavailability and intestinal accessibility in humans. **Food Chemistry**, v. 248, p. 217–224, 2018.

NASCIMENTO, A. L. A. A. et al. Exploring strategies to enhance anthocyanin bioavailability and bioaccessibility in food: A literature review. **Food Bioscience**, v. 56, p. 103388, 2023.

NEVES, N. DE A. et al. Flavonols and ellagic acid derivatives in peels of different species of jabuticaba (*Plinia* spp.) identified by HPLC-DAD-ESI/MSn. **Food Chemistry**, v. 252, p. 61–71, 2018.

NEVES, N. DE A. et al. Identification and quantification of phenolic composition from different species of Jabuticaba (*Plinia* spp.) by HPLC-DAD-ESI/MSn. **Food Chemistry**, v. 355, p. Article 129605, 2021.

OZDAL, T. et al. The reciprocal interactions between polyphenols and gut microbiota and effects on bioaccessibility. **Nutrients**, v. 8, n. 2, p. 1–36, 2016.

PENG, Y. et al. Prebiotic effects *in vitro* of anthocyanins from the fruits of *Lycium ruthenicum* Murray on gut microbiota compositions of feces from healthy human and patients with inflammatory bowel disease. **LWT**, v. 149, p. 111829, 2021.

RESEARCH AND MARKETS. Anthocyanin Market by Product Type, Source, End User - Global Forecast 2025-2030.

SHARMA, S.; PANDITA, G.; BHOSALE, Y. K. Anthocyanin: Potential tool for diabetes management and different delivery aspects. **Trends in Food Science and Technology**, v. 140, p. 104170, 2023.

SHEN, Y. et al. Advanced approaches for improving bioavailability and controlled release of anthocyanins. **Journal of Controlled Release**, v. 341, p. 285–299, 2022.

STALMACH, A. et al. Gastrointestinal stability and bioavailability of (poly) phenolic compounds following ingestion of Concord grape juice by humans. **Molecular Medicine Reports**, v. 56, p. 497–509, 2012.

WANG, X.; QI, Y.; ZHENG, H. Dietary Polyphenol, Gut Microbiota, and Health Benefits. **Antioxidants**, v. 11, n. 6, p. 1212, 2022.

XIN, M. et al. Anthocyanins as natural bioactives with anti-hypertensive and atherosclerotic potential: Health benefits and recent advances. **Phytomedicine**, v. 132, p. 155889, 2024.

ZHONG, S. et al. Characterization of Wild Blueberry Polyphenols Bioavailability and Kinetic Profile in Plasma over 24-h Period in Human Subjects. **Molecular Nutrition and Food Research**, v. 61, n. 12, 2017.

2. CHAPTER 1: Bioaccessibility and bioavailability of anthocyanins: A comprehensive review of current insights and challenges

Abstract

Anthocyanins are widely recognized for their bioactive properties and have been extensively studied for their health-promoting potential. However, despite the benefits associated with anthocyanin consumption, these compounds have low bioaccessibility and bioavailability due to degradation during digestion and limited absorption in the gastrointestinal tract. This review explores the factors influencing anthocyanin metabolism, including their degradation during the different phases of digestion (oral, gastric, small intestine and large intestine), and details how these factors contribute to their reduced bioaccessibility and bioavailability. Recent advances in encapsulation techniques to improve anthocyanin stability are also discussed. By consolidating insights from *in vitro* and *in vivo* studies, this review summarizes challenges and emerging solutions regarding anthocyanin bioaccessibility and bioavailability.

Keywords: Anthocyanin degradation, *In vitro* digestion; Gut microbiota; Functional foods; Anthocyanin absorption; Encapsulation.

1. Introduction

Anthocyanins are one of the major classes of phenolic compounds that possess numerous bioactive activities that can contribute positively to human health. Previous studies had indicated that anthocyanins possess antioxidant activities, anti-inflammatory activity, and anti-obesity activity (ESCALANTE-ABURTO et al., 2023; FALLAH et al., 2020; FALLAH; SARMAST; JAFARI, 2020). Anthocyanins can also provide cardioprotective, neuroprotective, and anticarcinogenic properties and have been associated with a reduction in the risks of hypertension and diabetes type II (DE ARRUDA NASCIMENTO et al., 2022; KALT et al., 2020; SHARMA; PANDITA; BHOSALE, 2023; XIN et al., 2024).

Despite the beneficial properties of anthocyanins, these compounds are known for their low bioaccessibility and bioavailability in the human body, which has raised questions about the actual role of parent anthocyanins in the human health (BRAGA et al., 2018; MUELLER et al., 2018). To more effectively correlate anthocyanin consumption with health benefits, it is very important to understand the digestion and metabolism of anthocyanins in the gastrointestinal tract, along with the absorption of both the parent anthocyanins and metabolites (HAN et al., 2019). During digestion, anthocyanins can undergo extensive degradation due to factors such as pH, enzymes and microbiota (AYVAZ et al., 2023). Then, the bioavailability of

parent anthocyanins is very low, with values below 2% (DE FERRARS et al., 2014; MUELLER et al., 2017; STALMACH et al., 2012; ZHONG et al., 2017). However, if the degradation products, phase I and phase II metabolites (formed through oxidation, reduction, hydrolysis, or conjugation reactions), and microbiota-derived metabolites are included, the total bioavailability may be higher (LILA et al., 2016).

The demand for anthocyanins in the global market is growing, especially for their utilization as natural colorants and in the development of functional foods, beverages, and dietary supplements. The market for anthocyanins increased from USD 392.12 million in 2023 to USD 415.46 million in 2024 and is expected to reach USD 591.75 million by 2030 (RESEARCH AND MARKETS, 2024). Therefore, enhancing the stability of anthocyanins is a challenge for the development of food products and nutraceuticals. The primary techniques explored for this purpose are encapsulation methods, with approximately 1200 research articles published between 2018 and 2023 (NASCIMENTO et al., 2023). These methods are used to enhance the stability of anthocyanins in conditions such as pH and temperature, and to control retention time and release rate for higher bioaccessibility and bioavailability of these compounds (SHEN et al., 2022).

In this context, in this review we discuss the bioaccessibility and bioavailability of anthocyanins, exploring the mechanisms of digestion and metabolism of anthocyanins in the gastrointestinal tract, the challenges associated with their low bioaccessibility and bioavailability, and encapsulation techniques designed to enhance their stability.

2. Anthocyanins structure

Anthocyanins are water-soluble natural pigments that gives red, blue or purple colors to fruits, flowers, grains and some vegetables (BURTON-FREEMAN; SANDHU; EDIRISINGHE, 2016). Chemically, anthocyanins are molecules that belong to the flavonoid group and are polyhydroxy or polymethoxy derivatives of the flavylium cation (GUO; XIA, 2018). They have a main structure of 15 carbons, arranged in two six-carbon benzene rings (A and B) and a three-carbon heterocyclic ring (C), which includes the oxygen atom and connects rings A and B (Figure 1) (GUO; XIA, 2018).

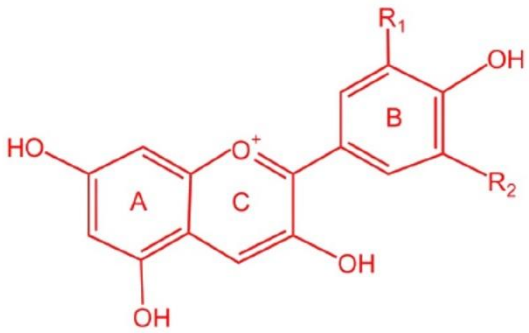

Anthocyanidin	R_1	R_2
Cyanidin	OH	H
Delphinidin	OH	OH
Malvidin	OCH_3	OCH_3
Pelargonidin	H	H
Peonidin	OCH_3	H
Petunidin	OH	OCH_3

Figure 1 - Basic structure of anthocyanidins and substituent groups of the six main types of molecules found in nature (KAMILOGLU et al., 2015). R_1 and R_2 represent the functional groups attached to the B-ring of the anthocyanidin structure.

Anthocyanins are the glycosylated forms of anthocyanidins (aglycones). Anthocyanidins are unstable and therefore rarely found in nature. Because of this instability, they are usually found in glycosylated forms (KENT; HÖLZEL; SWARTS, 2018). The hydroxyl groups on the aglycone may be substituted by sugar moieties at specific positions, primarily at the C3, C5, and C7 positions of the anthocyanidin structure (CELLI; TAN; SELIG, 2018; HE; MONICA GIUSTI, 2010). These sugars may also be linked to additional sugars through glycosidic bonds or acylated with aromatic or aliphatic organic acids (CELLI; TAN; SELIG, 2018; HE; MONICA GIUSTI, 2010). More than 600 anthocyanins are known and are mainly derived from six anthocyanidins: cyanidin, delphinidin, pelargonidin, peonidin, petunidin and malvidin (Figure 1) (MUKHERJEE, 2019; REYES et al., 2017).

The different types of anthocyanins are distinguished according to the different numbers and positions of hydroxyl and methoxyl groups in the B ring and by the type, number and position of the glycosidic moieties (GUO; XIA, 2018). Sugars like glucose, galactose, rhamnose, arabinose, xylose, and rutinose are commonly linked to anthocyanidins by replacing hydroxyl groups at positions 3 and 5 (CELLI; TAN; SELIG, 2018). Additional structures found are 3-diglycosides, 3-diglycosides-5-monoglycosides, and 7-glycosides (CELLI; TAN; SELIG, 2018).

Anthocyanins are highly susceptible to pH changes, and their structures undergo modifications according to pH values, resulting in different colors at different pH values due to the ionic properties of their molecular structure (XUE et al., 2024). In aqueous solution, the main equilibrium species of anthocyanins are the flavylium cation, the quinoid base, the

pseudobase carbinol, and the chalcone (Figure 2) (GIULIANI; CERRETANI; CICHELLI, 2016). Under acidic conditions (pH < 2.0), anthocyanins exist as red-colored flavylium cations, their most stable form. As the pH becomes slightly acidic to neutral (pH 3-6), they transition to a colorless carbinol pseudo-base or hemiketal form due to proton loss and molecular rearrangement (Figure 2). Within this range, the structure may also break and rearrange into a yellow chalcone form. At higher pH levels (around pH 7-10), anthocyanins shift to a purple or blue quinoidal base form (Figure 2). The relative amounts of the four forms of anthocyanins under equilibrium conditions vary according to pH values (WANG; LI; ZHOU, 2014; XUE et al., 2024).

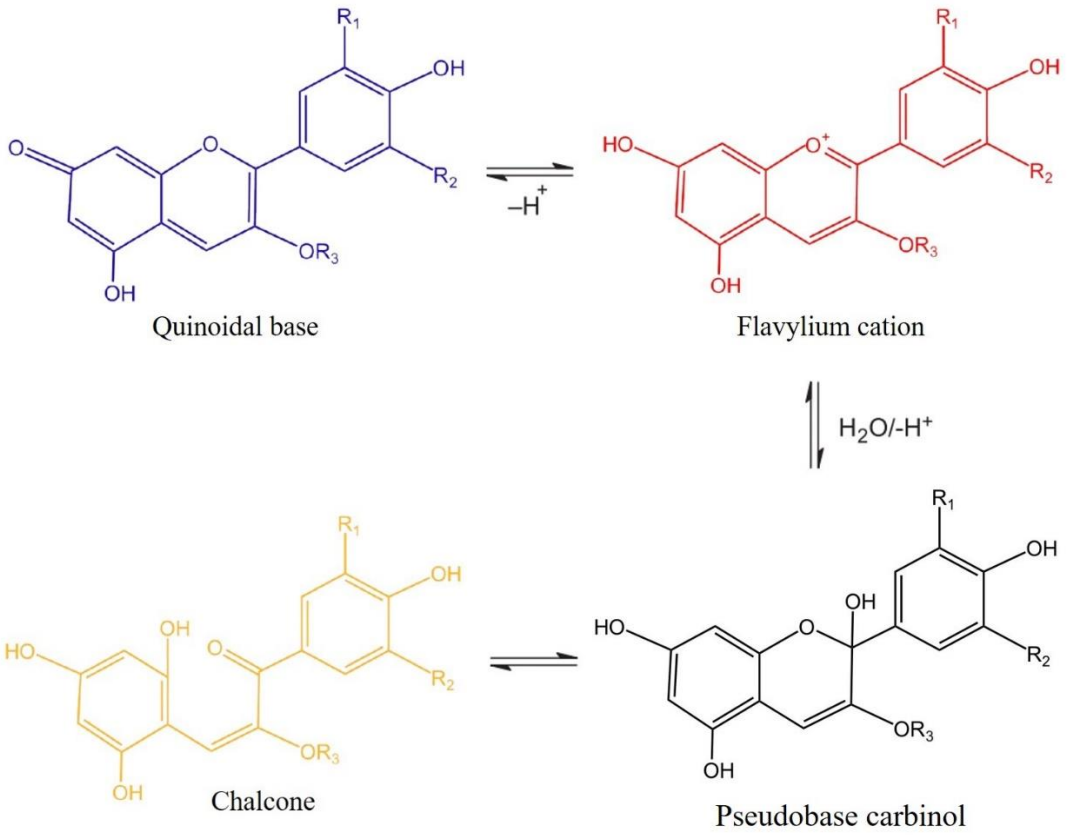

Figure 2 - Different structures of anthocyanins at different pH values (GIULIANI; CERRETANI; CICHELLI, 2016). *R1 and R2 represent the substituent groups on the anthocyanin molecule and R3 is a sugar moiety.

3. Anthocyanin metabolism

3.1. Oral digestion

During oral digestion (pH 6.6~7.1), anthocyanins begin to be metabolized, however, they remain relatively stable compared to later stages in the digestive tract, which may be associated with the short time that anthocyanins stay in the oral cavity (XUE et al., 2023). It has been suggested that anthocyanins metabolism begins in the oral cavity and is influenced by the pH condition and enzymes produced by the oral microbiota, which contains a wide variety of bacterial species (AYVAZ et al., 2023; HAN et al., 2019). A human study investigated the intraoral metabolism and retention of black raspberry anthocyanins (MALLERY et al., 2011). Key enzymes that metabolize anthocyanins were found in human oral tissues, saliva, and oral microbiota, including β-glucosidase, which converts anthocyanins into the aglycone form. Various black raspberry rinse formulations were evaluated, and several metabolites of black raspberry anthocyanins were detected, including their aglycone forms, glucuronidated conjugates, and low concentrations of protocatechuic acid (MALLERY et al., 2011). Initial levels of cyanidin-3-rutinoside, the primary anthocyanin, decreased from approximately 2287 µg/mL to 0.05 µg/mL over 240 minutes (MALLERY et al., 2011). Another study investigated the impact of anthocyanin (ACN) structure on their degradation, stability, and bioavailability within the oral cavity, using red grape and chokeberry juices as sources with distinct ACN profiles (KAMONPATANA et al., 2014). It was found that delphinidin-3-glucoside was more susceptible to salivary degradation than cyanidin, peonidin, and petunidin or malvidin glycosides. On average, total ACN degradation during the 5-minute mouth retention was 12.5 ± 1.6% for chokeberry juice and 15.3 ± 1.8% for red grape juice (KAMONPATANA et al., 2014).

3.2. Gastric digestion

Under gastric conditions, anthocyanins do not undergo significant changes due to the acidic pH (pH = 1.0-2.0). In an acidic environment, anthocyanins are in the flavyl cation form with red color and are stable (AYVAZ et al., 2023). Evidence of the fast appearance of anthocyanins in plasma after ingestion was an initial indication of the absorption of anthocyanins by the gastric wall (TALAVERA et al., 2003). Furthermore, some studies have already demonstrated the ability of anthocyanins to be transported/absorbed in a gastric cell barrier model with MKN-28 cells (differentiated cells from gastric adenocarcinoma) (HAN et al., 2020; PEIXOTO et al., 2016). The absorption efficiency of anthocyanins from jambo, jabuticaba and jamelão was 19.7, 9.7 and 14.1%, respectively (PEIXOTO et al., 2016). In another study, chinese red wine anthocyanins were transported through gastric MKN-28 cells

with transport efficiencies ranging from 4% to 9% (HAN et al., 2020). These studies indicated that the gastric mucosa may play an important role in the absorption of anthocyanins. However, the mechanism of anthocyanin absorption in the stomach remains not fully understood. It has been suggested that the bilitranslocase transporter, an anion carrier located in the gastric mucosa, may play a role in this process (PASSAMONTI et al., 2003). GLUT1 (glucose transporter 1) and GLUT3 glucose transporters have also been associated with the gastric absorption of anthocyanins (OLIVEIRA et al., 2019).

3.3. Small intestine digestion

The fraction of anthocyanins that is not absorbed in the stomach reaches the small intestine, with more neutral pH conditions. The intestine is the primary site for nutrient absorption and is divided into three distinct regions: the duodenum, jejunum, and ileum and the pH ranges from approximately 5.0–7.0 (HAN et al., 2019). Anthocyanins can be absorbed in their intact form or undergo hydrolysis, losing the glycosidic moiety and releasing their corresponding aglycone. These aglycones are then further degraded into phenolic acids and phloroglucinol aldehyde (PGA) (Figure 3) (KAWABATA; YOSHIOKA; TERAO, 2019; LIANG et al., 2024; MAKAREWICZ et al., 2021). Due to structural variations in the B-ring of the six main anthocyanins, each produces a distinct phenolic acid upon degradation. However, the A-ring is consistent across all six anthocyanins, making PGA a common metabolite. These metabolites may be derived from spontaneous degradation due to the pH in the intestine or by enzymatic activity. The enzymes identified as responsible for the hydrolysis of the glycosidic portion of anthocyanins are lactase phloridizin hydrolase and cytosolic β-glucosidase, found in the brush border of the small intestine and within epithelial cells (GONÇALVES; NUNES; ALVES, 2021). In a study investigating the bioavailability and intestinal accessibility of anthocyanins from bilberries in humans, including both healthy individuals and ileostomists, gallic acid (GA), protocatechuic acid (PCA), and phloroglucinol aldehyde (PGA) were identified as the predominant degradation products of anthocyanins in ileostomy fluid (MUELLER et al., 2017). The presence of these metabolites in the ileostomy effluent showed that conditions within the small intestine contribute to anthocyanin breakdown (MUELLER et al., 2017). Other studies support these findings by showing that absorbed metabolites concentrations are often higher than those of the parent anthocyanins, further suggesting that anthocyanins undergo degradation before absorption (DE FERRARS et al., 2014; ZHONG et al., 2017). Anthocyanins can be absorbed by the intestinal epithelial cells via passive transport

and active transport (HAN et al., 2019) and candidates for anthocyanin transporters are glucose transporters (SGLT1 and GLUT2) (EKER et al., 2020; KAMILOGLU et al., 2015). The absorption of cyanidin-3-O-glucoside was significantly reduced using the inhibitors of SGLT1 (phloridzin) and GLUT2 (phloretin) in human colon carcinoma cell (Caco-2) model (ZOU et al., 2014). These results indicated that both SGLT-1 and GLUT2 played an important role in regulating the absorption of cyanidin-3-O-glucoside (ZOU et al., 2014).

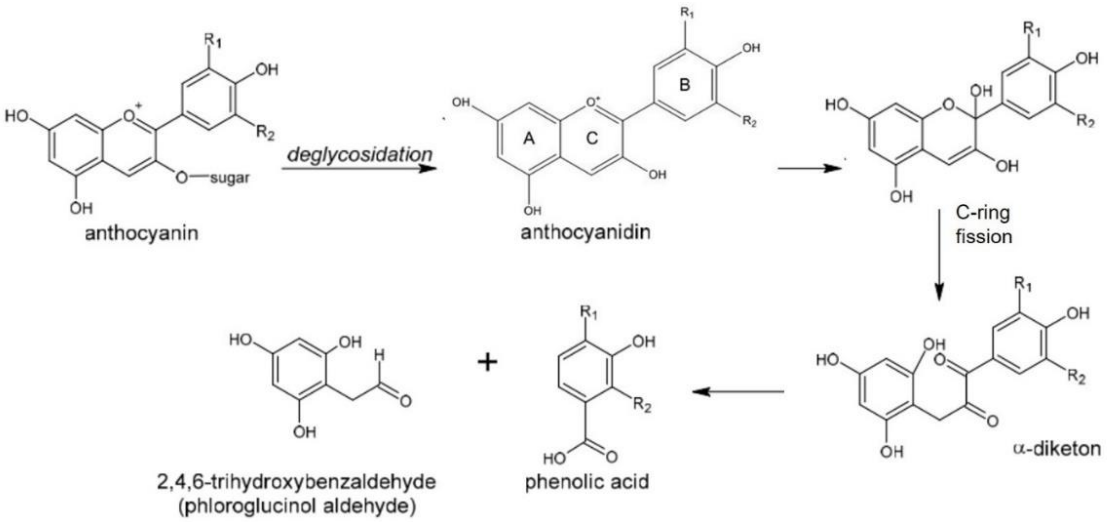

Figure 3 - Degradation pathway of anthocyanins (KAWABATA; YOSHIOKA; TERAO, 2019; MAKAREWICZ et al., 2021).

3.4. Colon digestion

Anthocyanins that are not absorbed or degraded in the stomach or small intestine reach the large intestine, where they undergo biotransformation by the gut microbiota into low-molecular-weight phenolic metabolites (WANG; QI; ZHENG, 2022). These metabolites may be derived from spontaneous degradation due to the pH in the large intestine (7.0–8.0) or microbial metabolism. The incubation of purified anthocyanin extracts from black rice and bilberry with fecal samples from humans showed that anthocyanin degradation occurs both spontaneously and through bacterial activity (SHEHATA et al., 2023). Cyanidin-3-glucoside degraded rapidly in the presence of live microbiota, with an initial degradation rate of 16.8 μM/h in the first two hours (SHEHATA et al., 2023). In contrast, the same compound in autoclaved microbiota showed a slower spontaneous degradation rate of 12.7 μM/h (SHEHATA et al., 2023). Also, incubating cyanidin-3-O-glucoside with the intestinal bacteria

resulted in a significant accumulation of protocatechuic acid, 2,4,6-trihydroxybenzaldehyde and other metabolites (DE FERRARS et al., 2014; HANSKE et al., 2013). The gut microbiota produces enzymes that can break down the glycosidic bonds in the structure of anthocyanins, leading to the release of their aglycone forms. Enzymes such as β-glucosidases are produced by specific bacterial species in the colon (EKER et al., 2020; LIANG et al., 2024). After the glycosidic bonds are broken, the aglycone forms of anthocyanins are further degraded into smaller phenolic compounds, including phenolic acids and PGA (Eker et al., 2020; Liang et al., 2024). The formed phenolic compounds can undergo further metabolism, resulting in smaller molecules like benzoic acids, phenylpropionic acids and phenylacetic acids (MAKAREWICZ et al., 2021). The detailed degradation and metabolism of anthocyanins in the presence of intestinal microbiota proposed by MAKAREWICZ et al., (2021) is presented in Figure 5. The resulting colonic metabolites of anthocyanins can be absorbed by epithelial cells and are transported to the liver to be further metabolized and distributed to the circulating system (KAN et al., 2022). Consequently, biotransformation of anthocyanins by the gut microbiota is considered a key step in the absorption and biological activity of anthocyanins. Comparing the absorption of anthocyanins in subjects with an intact healthy gut compared to ileostomies with an interrupted intestinal passage lacking a colon, the amounts of anthocyanins in the plasma and urine of healthy subjects were 79% and 44% higher, respectively, than in the plasma and urine of ileostomists (MUELLER et al., 2017).

Few studies have explored the exact function of gut bacteria in converting anthocyanins and their phenolic metabolites, and details about the particular species involved in this process and how the metabolism of anthocyanins varies among individuals remain lacking. There is also evidence that anthocyanin consumption has a prebiotic effect, because anthocyanins can promote the proliferation of beneficial bacterial species and inhibit the growth of pathogenic species (BOTO-ORDÓÑEZ et al., 2014; GUERGOLETTO et al., 2016; HIDALGO et al., 2012; MOLAN; LIU; PLIMMER, 2014; PENG et al., 2021; VENDRAME et al., 2011). Then, the relationship between anthocyanins and the human gut microbiota is considered a two-way interaction (KAN et al., 2022).

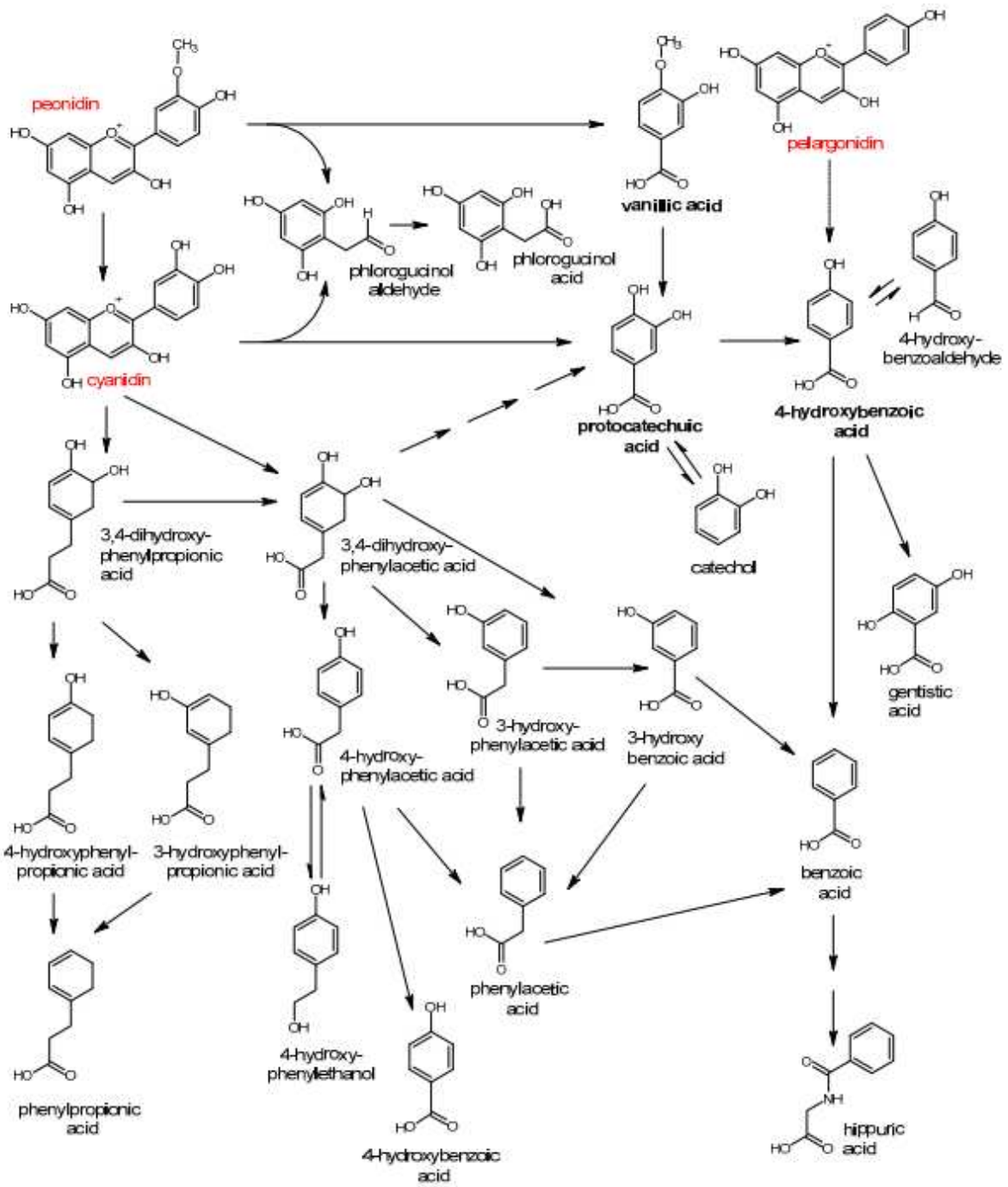

Figure 4 - Biodegradation of anthocyanins and their main metabolites (Reproduced from (MAKAREWICZ et al., 2021).

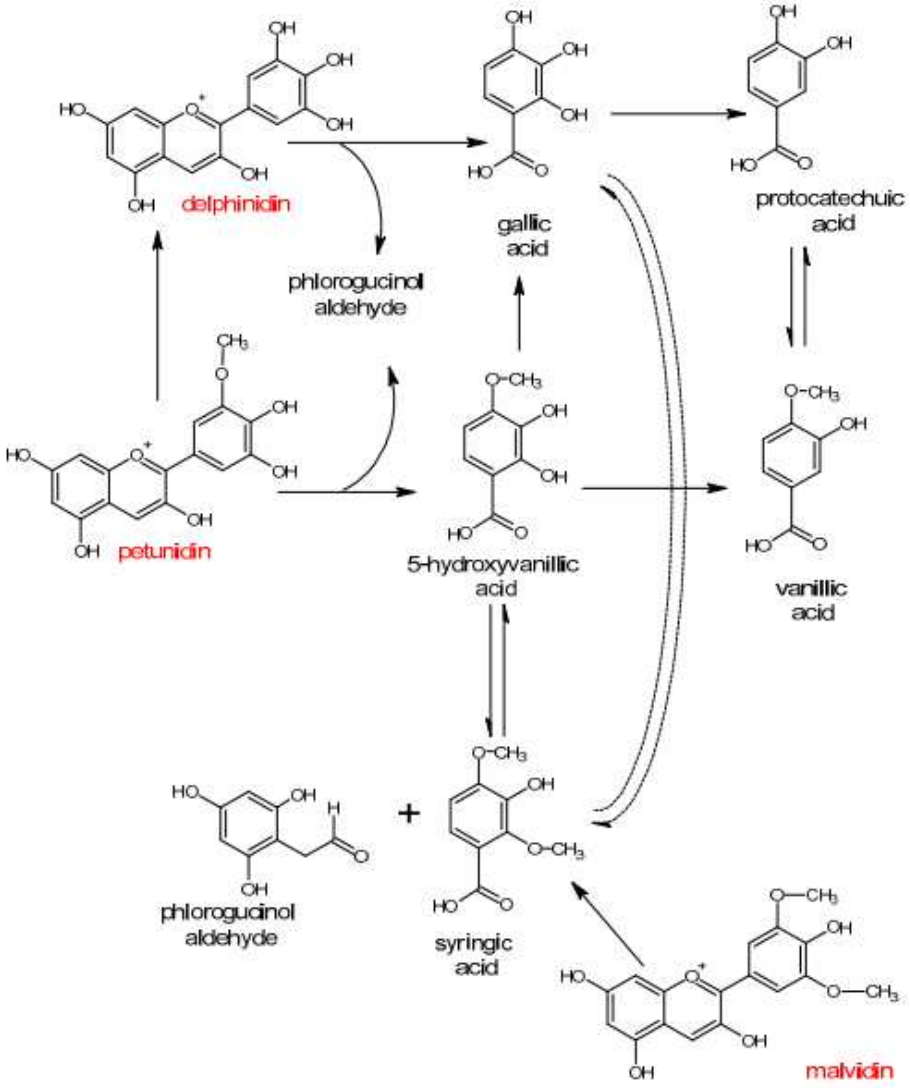

Figure 4 (continued)

3.5. Anthocyanins distribution and excretion

Anthocyanins and their metabolites can be metabolized in the intestine, liver, and kidneys through phase I (oxidation or O-demethylation) and phase II (glucuronidation, sulfation or methylation) metabolism by enzymes (CASSIDY; MINIHANE, 2017; EKER et al., 2020). This helps enhance the reactivity and solubility of these compounds, assisting their circulation and excretion (CASSIDY; MINIHANE, 2017; EKER et al., 2020). Afterward, anthocyanins and metabolites may enter the bloodstream and be absorbed by specific organs and tissues, excreted through the bile, undergo enterohepatic recirculation, and/or be eliminated through urine and feces (CASSIDY; MINIHANE, 2017; EKER et al., 2020).

4. Bioaccessibility and bioavailability of anthocyanins

Anthocyanins are recognized for their potential health benefits due to their diverse biological activities (BURTON-FREEMAN; SANDHU; EDIRISINGHE, 2016). However, the total amount of these molecules present in foods does not necessarily reflect the amount that will be absorbed and metabolized when consumed. To promote any biological action, anthocyanins must remain in a bioactive form until they reach their site of action. To validate the prominent health benefits reported in many *in vitro* models, it is necessary to consider the bioaccessibility and bioavailability of anthocyanins (HORNEDO-ORTEGA et al., 2021). Bioaccessibility refers to the portion of an ingested compound that becomes available for absorption following digestion, whereas bioavailability is defined as the fraction of the ingested compound that enters the circulation and reaches target organs and tissues to perform its biological function (LILA et al., 2016).

In vitro simulated digestion methods have been used to verify changes in the structure and bioactive properties of various compounds, such as anthocyanins. For this purpose, digestion models are used to simulate the physicochemical and physiological events that occur in the human gastrointestinal tract. These models are important for evaluating the stability and elucidating the effects on structural changes of bioactive compounds, prior to absorption (ALMINGER et al., 2014; GUTIÉRREZ-GRIJALVA et al., 2017; VICTORIA-CAMPOS et al., 2022). Simulated *in vitro* digestion aims to mimic the physiological conditions of the gastrointestinal tract, specifically, the chemical composition of digestive fluids, enzyme activities, pH, and residence time (HU et al., 2023). Although *in vitro* systems are limited in effectively reproducing the complexity of the gastrointestinal tract, these models have been increasingly used because they are faster and cheaper than *in vivo* analyses, and are being considered efficient in determining the stability of phytochemical compounds under gastrointestinal conditions (GUERRA et al., 2012; HERRERA-BALANDRANO et al., 2021).

After sample digestion, there are different methods to simulate the bioaccessibility of compounds. Dialysis and centrifugation are the two most common techniques that have been used to estimate the bioaccessible fraction of foods in *in vitro* assays (ETCHEVERRY; GRUSAK; FLEIGE, 2012; WOJTUNIK-KULESZA et al., 2020). In the solubility model, samples are centrifuged, generating a supernatant (soluble compounds that can potentially be absorbed) and a precipitate (non-absorbed compounds) (WOJTUNIK-KULESZA; ONISZCZUK; ONISZCZUK, 2020). In the dialysis model, a dialysis tube or bag containing a buffer is added to the samples after the *in vitro* gastric digestion phase, so that the pH gradually

increases as it happens in intestinal digestion (ETCHEVERRY; GRUSAK; FLEIGE, 2012). After this, bile salts and pancreatin are added to the samples and intestinal digestion is performed. At the end, the dialyzed fraction represents the sample capable of crossing the semipermeable membrane and that is possibly available for absorption (ETCHEVERRY; GRUSAK; FLEIGE, 2012). Meanwhile, the fraction outside the dialysis membrane represents the sample not available for absorption and that would reach the colon, where it would be metabolized by the intestinal microbiota (ETCHEVERRY; GRUSAK; FLEIGE, 2012; WOJTUNIK-KULESZA; ONISZCZUK; ONISZCZUK, 2020). Bioaccessibility is expressed as a percentage and is calculated as the ratio of the concentration of a compound in the soluble or dialyzed fraction to the concentration of the compound in the undigested sample (DE MORAIS et al., 2020).

A comparison between *in vivo* and *in vitro* digestion models revealed that after acute ingestion of Concord grape juice by ileostomy volunteers, the recovery of anthocyanins and other phenolic compounds in ileal fluid was consistent with findings from the *in vitro* digestion model (STALMACH et al., 2012). The authors suggested that the quantity of phenolic compounds detected in the ileal fluid of ileostomists could indicate the amount that would pass from the small to the large intestine in healthy individuals with a functioning colon (STALMACH et al., 2012). Similarly, in another study, the polyphenol composition in ileal fluid from an ileostomy subject after consuming lingonberries was compared with lingonberry extracts subjected to simulated *in vitro* digestion and fecal fermentation (BROWN et al., 2014). Similar patterns of lingonberry phenolic metabolism after the *in vivo* and *in vitro* digestion were also observed (BROWN et al., 2014). These studies emphasize the potential of *in vitro* digestion models as effective methods for understanding the bioaccessibility of polyphenols.

Studies on the bioaccessibility of anthocyanins from different sources revealed substantial variations, with some fruits presenting low bioaccessibility and others showing higher values. Low bioaccessibility values were reported in jabuticaba peel powder, ranging from 0.08% to 2.3% (QUATRIN et al., 2020). Similarly, mulberries had very low anthocyanin bioaccessibility after intestinal digestion, with recoveries of only 0.34% (for the inside sample) and 4.58% (for the outside sample) (LIANG et al., 2012). For blackberries, the main anthocyanin, cyanidin-3-O-glucoside, exhibited only 1.8% bioaccessibility (VAN DE VELDE; PIROVANI; DRAGO, 2018). Also, purified anthocyanins from multiple sources were stable during the gastric phase but the bioaccessibility dropped during the small intestinal phase to as low as 0.07–2.21% (VICTORIA-CAMPOS et al., 2022). On the other hand, higher bioaccessibility values were observed in other studies. For example, passion fruit peel showed

a bioaccessibility of 12.64±1.04% (CAO et al., 2021), while fresh blueberries had a value of 47.9±4.2% for anthocyanin bioaccessibility (MUÑOZ-FARIÑA et al., 2023). Further studies on blueberry anthocyanin extract showed that specific compounds like cyanidin-3-glucoside and petunidin-3-galactoside reached bioaccessibility rates of over 50%, while malvidin glycosides, comprising 55% of total anthocyanins, exhibited bioaccessibility between 27% and 35% (HERRERA-BALANDRANO et al., 2023). These variations indicate that bioaccessibility of anthocyanins is strongly influenced by the food matrix, digestive environment, and anthocyanin structure, with some anthocyanin structures and fruit extracts showing higher stability than others. Also, these results indicate that a considerable portion of anthocyanins degrade when exposed to the physiological conditions of the small intestine, emphasizing the challenges of maintaining anthocyanin integrity during digestion.

Anthocyanin bioavailability can be determined using *in vivo* systems, such as animal models or human clinical trials, or *in vitro* experiments, which are usually performed using cell culture systems. Using *in vivo* models, bioavailability can be determined by quantifying the concentration of anthocyanins and metabolites in the blood, urine and feces after ingestion of foods or beverages rich in anthocyanins (NASCIMENTO et al., 2023). *In vitro*, the bioavailability of compounds can be assessed by determining the absorption/transport of compounds by Caco-2 cells (ETCHEVERRY; GRUSAK; FLEIGE, 2012). Caco-2 cells belong to a line of human epithelial cells derived from a human colon adenocarcinoma, which behave much like intestinal cells in culture (ETCHEVERRY; GRUSAK; FLEIGE, 2012).

In *in vitro* studies using cellular models and anthocyanins from different food sources, the bioavailability of anthocyanins was very low. These studies showed that anthocyanins can be transported intact across Caco-2 cell monolayers, with anthocyanin transport/absorption efficiency of less than 5% (CARDONA; MERTENS-TALCOTT; TALCOTT, 2015; HAN et al., 2020; KUNTZ et al., 2015; PEIXOTO et al., 2016; ZOU et al., 2014). In Chinese red wine, the main anthocyanins, malvidin-3-glucoside and malvidin-3,5-diglucoside, showed transport rates between 3% and 5% in Caco-2 cells (HAN et al., 2020). For the Brazilian fruits jambo, jabuticaba e jamelão, the transport efficiencies of their anthocyanins ranged from 0.2% to 0.8% (PEIXOTO et al., 2016). Grape and blueberry extracts had lower absorption rates for compounds like malvidin and peonidin-3-glucosides, ranging from 0.001% to 0.06%, while diglucoside forms were undetected (KUNTZ et al., 2015). In açaí, the absorption rates for cyanidin-3-glucoside and cyanidin-3-rutinoside were 1.38% and 1.06%, respectively (CARDONA; MERTENS-TALCOTT; TALCOTT, 2015). Cyanidin-3-glucoside (10, 20, 40

μmol/L), used as a standard, showed transport efficiency between 0.8% and 2.4% (ZOU et al., 2014).

In *in vivo* studies, the bioavailability of anthocyanins was also estimated as very low, with recoveries of less than 2% of the ingested anthocyanin dose (STALMACH et al., 2012). In a study on the gastrointestinal stability and bioavailability of phenolic compounds from Concord grape juice, anthocyanins demonstrated low stability in the gastrointestinal tract, with significant degradation occurring before reaching the bloodstream (STALMACH et al., 2012). Peak plasma concentrations (Cmax) of anthocyanins ranged from 1.0 nmol/L to 2 nmol/L. Urinary excretion, as an indicator of bioavailability, were similarly low. The overall urinary excretion percentage of total anthocyanins was 0.26 ± 0.05% of intake, indicating that most of the ingested anthocyanins were either metabolized or not absorbed (STALMACH et al., 2012).

A low absorption of anthocyanins was also observed after the consumption of grape/blueberry juice (841mg ACN/liter) and smoothie (983 mg ACN/liter) (KUNTZ et al., 2015). The anthocyanins malvidin-3-glucoside and peonidin-3-glucoside were the most abundant in plasma, reaching peak concentrations (Cmax) of 1.5 nmol/L and 0.80 nmol/L, respectively, after grape/blueberry juice consumption, and 1.00 nmol/L and 0.46 nmol/L, respectively, after smoothie consumption (KUNTZ et al., 2015). The cumulative urinary excretion for malvidin-3-glucoside reached 2.46 nmol/L for juice and 2.64 nmol/L for smoothie, while peonidin-3-glucoside was 2.65 nmol/L for juice and 2.22 nmol/L for smoothie (KUNTZ et al., 2015). The metabolites of these anthocyanins, malvidin-3-glucuronide and peonidin-3-glucuronide, also showed high urinary levels, with Peo-3-glucuronide peaking at 3.61 nmol/L (juice) and 4.01 nmol/L (smoothie), and Mal-3-glucuronide at 1.2 nmol/L (juice) and 1.3 nmol/L (smoothie) (KUNTZ et al., 2015).

Analyzing the bioavailability and kinetic profile of wild blueberry polyphenols, it was found that the bioavailability of wild blueberry anthocyanins was 1.1% (ZHONG et al., 2017). Parent anthocyanins reached peak plasma concentrations around 2 h post-ingestion. Phase II metabolites, such as glucuronide conjugates of peonidin, delphinidin, cyanidin, and petunidin, reached their maximum levels at approximately 2.6, 6.3, 7, and 8.8 h, respectively (ZHONG et al., 2017). Phenolic acid metabolites showed peak concentrations between 0.5 and 24 h, and the concentrations detected were higher than those of the anthocyanins (ZHONG et al., 2017).

In another study, following the oral administration of cyanidin-3-glucoside (500 mg) in healthy participants, seventeen labeled compounds, including various phenolic acids, were identified in serum, urine, and feces (DE FERRARS et al., 2014). Cyanidin-3-glucoside reached a maximum concentration (Cmax) of 141 nM in the serum around 1.8 h post-consumption (DE

FERRARS et al., 2014). Most anthocyanin metabolites had a Cmax ranging from 10 to 2000 nM and showed varied elimination half-lives, indicating extended circulation for metabolites compared to the parent compound (DE FERRARS et al., 2014). The primary metabolites, including hippuric acid and vanillic acid, reached peak concentrations of around 1962 nM and 1845 nM, respectively, suggesting that these metabolites may play an important role in the health effects associated with anthocyanin consumption (DE FERRARS et al., 2014).

Higher amounts of metabolites than anthocyanins also reached the circulation after bilberry extract consumption (MUELLER et al., 2017). The bioavailability of anthocyanins in plasma (over 8 h after BE intake) was low, corresponding to only 0.02% of ingested anthocyanins. In urine samples, 0.03 ± 0.02% of ingested anthocyanins over the entire 24 h were found (MUELLER et al., 2017).

All studies showed that parent anthocyanins are poorly absorbed, while their metabolites are present in higher levels in the plasma and urine. This raised an important question: is it more important to prioritize increasing the bioavailability of intact anthocyanins or to focus on their degradation products, which showed higher absorption rates? (BRAGA et al., 2018; MUELLER et al., 2018). These compounds might have a greater impact on the physiological benefits associated with anthocyanins. However, the precise roles of parent anthocyanins compared to their metabolites in promoting human health are still under investigation, and determining the distinct effects of each is an important focus of study (JAKOBEK; BLESSO, 2023).

5. Application of encapsulation techniques to enhance the bioaccessibility and bioavailability of anthocyanins

Due to the low stability of anthocyanins in the gastrointestinal tract and their limited absorption in the human body, various strategies have been developed to enhance their bioaccessibility and bioavailability, primarily through different delivery systems using encapsulation techniques (NASCIMENTO et al., 2023; SHEN et al., 2022; XUE et al., 2024). These approaches have been discussed in details in previous reviews (NASCIMENTO et al., 2023; SHEN et al., 2022; XUE et al., 2024) and aim to protect anthocyanins from degradation, improve their intestinal absorption, and maximize their health-promoting effects.

Encapsulation methods such as spray drying, complex coacervation, ionic gelation, liposomes, and molecular inclusion, offer promising results by enhancing anthocyanin stability and providing a controlled release throughout digestion (NASCIMENTO et al., 2023; SHEN et

al., 2022; XUE et al., 2024). They include lipid-based, polysaccharide-based and protein-based anthocyanin complexes (NASCIMENTO et al., 2023; SHEN et al., 2022; XUE et al., 2024). In general, the studies demonstrated that encapsulation enhances the bioaccessibility of anthocyanins. β-Cyclodextrin encapsulation protected blackberry anthocyanins from degradation, resulting in about 7% higher bioaccessibility compared to non-encapsulated forms in simulated gastrointestinal conditions (FERNANDES et al., 2018). A ~8-10% improvement in bioaccessibility of maqui berry anthocyanins was observed through encapsulation, which helped protect these compounds from the degradative effects of intestinal pH (FREDES et al., 2018). Similarly, an increase of around 10% bioaccessibility for encapsulated anthocyanins using taro starch was reported (ROSALES-CHIMAL et al., 2023). Carbohydrate-based encapsulation also increased the bioaccessibility of encapsulated purple flesh potato anthocyanins in the intestine by 20% (VERGARA et al., 2020).

Few studies have considered the colonic phase during *in vitro* digestion when evaluating the release and digestion of anthocyanins. Since the colon is considered a primary site for the biotransformation and absorption of anthocyanin metabolites (LIANG et al., 2024; WANG et al., 2024), including this phase is critical for assessing the efficiency of encapsulation techniques. Evaluating the colonic phase can provide valuable insights into how encapsulated anthocyanins are metabolized by gut microbiota, potentially influencing their bioavailability and health benefits.

In a study using four different wall materials (gelatin, soy protein isolate, maltodextrin, and Arabic gum) to encapsulate blueberry anthocyanin extract, findings indicated that encapsulated anthocyanins displayed unique release patterns while undergoing fecal fermentation, which were impacted by the choice of wall material (WU et al., 2020). Anthocyanins encapsulated with soy protein isolate and gelatin were found to release anthocyanins at a slower rate compared to those encapsulated with arabic gum, maltodextrin, or unencapsulated samples, which extended the duration of exposure to gut microbiota (WU et al., 2020). The encapsulation also increased short-chain fatty acid production and changed the gut bacteria composition by increasing Bacteroidetes and reducing Firmicutes (WU et al., 2020).

A different study investigated the use of cyclodextrins (CDs) to encapsulate anthocyanins and analyzed their impact on gut microbiota, stability, and release in a simulated human colon model (FLORES et al., 2015). Results demonstrated that although there was a quick release in the first 30 minutes, encapsulation notably delayed the degradation of anthocyanins (FLORES et al., 2015). The prolonged release permitted a slow microbial

metabolism, leading to the generation of phenolic acids like gallic and syringic acids (FLORES et al., 2015). The anthocyanins and their breakdown products had a positive impact on the gut microbiota by promoting the growth of beneficial bacteria and inhibiting the growth of harmful bacteria, particularly *Clostridium histolyticum* (FLORES et al., 2015).

Some studies also showed higher intestinal transport efficiency of complexed or encapsulated anthocyanins compared to free anthocyanins. Lipid-based complexes with sweet potato anthocyanins (P-SPAs) showed improved stability and recovery under simulated gastrointestinal conditions, with higher intestinal transport efficiency than free anthocyanins (CHENG et al., 2018). Apparent permeability coefficient (Papp) values of P-SPAs absorption and excretion in Caco-2 cells were approximately 1.6 times and 1.3 times higher than those of free anthocyanins, respectively (CHENG et al., 2018). Phospholipids (PL) and terpenes (TP) also enhanced the transport of açaí anthocyanins across Caco-2 cells, suggesting that these compounds can enhance bioavailability by facilitating anthocyanin passage through intestinal barriers (CARDONA; MERTENS-TALCOTT; TALCOTT, 2015). Treatments containing PL resulted in transport enhancements of around 200% at the highest concentration assessed (5000 mg/L). When TP (50 mg/l) was added to PL at this concentration, an increase in transport higher than 300% was observed, compared to samples containing no aiding agents (CARDONA; MERTENS-TALCOTT; TALCOTT, 2015).

A protein-based anthocyanin complex with α-casein also showed increased absorption in animals (LANG et al., 2023). The excretion of anthocyanins was examined in rats treated with bilberry extract, both alone and in combination with α-casein (LANG et al., 2023). The results showed that, in the presence of α-casein, the anthocyanin content decreased in feces and urine while increasing in the blood. This indicates that α-casein can enhance the absorption of anthocyanins, leading to greater bioavailability (LANG et al., 2023).

In other study, analyzing the absorption and biodistribution of free versus nanoencapsulated radiolabeled anthocyanin (cyanidin-3-O-glucoside) in mice, the results indicated that nanoencapsulated anthocyanins are absorbed and distributed differently from their free form (ROSALES et al., 2024). After oral administration, nanoencapsulated anthocyanins were detected in various tissues, including the blood, spleen, bladder, pancreas, and bone, whereas unencapsulated anthocyanins were confined to the kidneys and bladder (ROSALES et al., 2024). Additionally, nanoencapsulated anthocyanins were absorbed more effectively than free anthocyanins, with significant differences observed at several time points (0.75, 1, 2, 3, and 24 h after ingestion) (ROSALES et al., 2024). Nanoencapsulated anthocyanins reached an absorption level of 5.65×10^{-6} % of the total injected mass over 24

h—nearly double the 2.96×10^{-6} % of free anthocyanins (ROSALES et al., 2024). This suggests that nanoencapsulation is effective in enhancing anthocyanin absorption and enables targeted delivery to specific tissues (ROSALES et al., 2024).

In humans, the encapsulation of bilberry extract (BE) with either whey protein (WP) or citrus pectin (CPC) was studied to evaluate their influence on the bioavailability and intestinal accessibility of anthocyanins in healthy subjects and ileostomists (MUELLER et al., 2018). WPC encapsulation modulated bioavailability by reducing anthocyanins in plasma by 28% but increased urinary excretion by 108%, suggesting enhanced elimination (MUELLER et al., 2018). The differences between the results from plasma and urine samples were associated with different sampling periods (MUELLER et al., 2018). CPC encapsulation, on the other hand, stabilized anthocyanins during intestinal passage, with 24% more anthocyanins recovered in ileal effluents (MUELLER et al., 2018). However, CPC did not enhance anthocyanin absorption, as plasma and urinary levels were lower than with pure BE, showing that CPC improves intestinal retention without increasing bioavailability (MUELLER et al., 2018).

The results from the studies showed that encapsulation could be a promising approach to increase the bioaccessibility and bioavailability of anthocyanins. The different techniques applied in the studies protected anthocyanins from degradation during gastric and small intestinal digestion to some extent and enhanced their absorption, increasing their bioavailability. However, most of the current data are based on *in vitro* or animal studies. Future studies could focus on improving the efficacy of these techniques and also on ensuring that encapsulation materials are compatible with food matrices without negatively impacting taste, texture or color. Furthermore, scaling up of these methods is also necessary to achieve successful commercialization.

6. Final considerations

This paper reviewed anthocyanins metabolism during the different phases of digestion and summarized the evidence of *in vivo* and *in vitro* studies regarding their bioaccessibility and bioavailability. Many studies have confirmed that anthocyanins have bioactive properties that can offer benefits to human health. However, their low bioaccessibility and bioavailability after consumption can limit their bioactivity. Factors, such as pH, fast degradation in the small intestine, and limited absorption, present major challenges. Therefore, the development of techniques to optimize the bioaccessibility and bioavailability of anthocyanins remains an

important focus of research. Different studies showed that encapsulation could improve the stability of anthocyanins to a certain extent, providing controlled release, and increased bioaccessibility and bioavailability by protecting them from degradation during gastric and small intestine digestion. Despite some progress in this area of research, these delivery systems still need to be optimized and validated through *in vivo* human trials. Additional studies on how the gut microbiota metabolizes encapsulated and non-encapsulated anthocyanins and how individual differences can influence this process are also important, as recent findings showed the role of microbiota in affecting the metabolism and health properties of anthocyanins and their metabolites. Expanding knowledge in this area could lead to more effective applications of anthocyanins in functional foods and nutraceuticals.

7. References

ALMINGER, M. et al. *In vitro* models for studying secondary plant metabolite digestion and bioaccessibility. **Comprehensive Reviews in Food Science and Food Safety**, v. 13, n. 4, p. 413–436, 2014.

AYVAZ, H. et al. Anthocyanins: Metabolic Digestion, Bioavailability, Therapeutic Effects, Current Pharmaceutical/Industrial Use, and Innovation Potential. **Antioxidants**, v. 12, n. 1, p. 1–39, 2023.

BOTO-ORDÓÑEZ, M. et al. High levels of Bifidobacteria are associated with increased levels of anthocyanin microbial metabolites: A randomized clinical trial. **Food and Function**, v. 5, n. 8, p. 1932–1938, 2014.

BRAGA, A. R. C. et al. Bioavailability of anthocyanins: Gaps in knowledge, challenges and future research. **Journal of Food Composition and Analysis**, v. 68, p. 31–40, 2018.

BROWN, E. M. et al. Comparison of *in vivo* and *in vitro* digestion on polyphenol composition in lingonberries: Potential impact on colonic health. **BioFactors**, v. 40, n. 6, p. 611–623, 2014.

BURTON-FREEMAN, B.; SANDHU, A.; EDIRISINGHE, I. Anthocyanins. Em: GUPTA, R. C. (Ed.). **Nutraceuticals**. 1. ed. London: Academic Press, 2016. p. 489–500.

CAO, Q. et al. Phenolic compounds, bioactivity, and bioaccessibility of ethanol extracts from passion fruit peel based on simulated gastrointestinal digestion. **Food Chemistry**, v. 356, p. 129682, 2021.

CARDONA, J. A.; MERTENS-TALCOTT, S. U.; TALCOTT, S. T. Phospholipids and terpenes modulate Caco-2 transport of açaí anthocyanins. **Food Chemistry**, v. 175, p. 267–272, 2015.

CASSIDY, A.; MINIHANE, A.-M. The role of metabolism (and the microbiome) in defining the clinical efficacy of dietary flavonoids. **The American Journal of Clinical Nutrition**, v. 105, p. 10–22, 2017.

CELLI, G. B.; TAN, C.; SELIG, M. J. Anthocyanidins and anthocyanins. Em: MELTON, L.; SHAHIDI, F.; VARELIS, P. (Eds.). **Encyclopedia of Food Chemistry**. 1. ed. [s.l.] Elsevier, 2018. p. 218–223.

CHENG, M. et al. Caco-2 cell transport of purple sweet potato anthocyanins- phospholipids complex. **Journal of Food Science**, v. 55, n. 1, p. 304–312, 2018.

DE ARRUDA NASCIMENTO, E. et al. *In vitro* anticancer properties of anthocyanins: A systematic review. **Biochimica et Biophysica Acta - Reviews on Cancer**, v. 1877, n. 4, p. 188748, 2022.

DE FERRARS, R. M. et al. The pharmacokinetics of anthocyanins and their metabolites in humans. **British Journal of Pharmacology**, v. 171, n. 13, p. 3268–3282, 2014.

DE MORAIS, J. S. et al. Antioxidant activity and bioaccessibility of phenolic compounds in white, red, blue, purple, yellow and orange edible flowers through a simulated intestinal barrier. **Food Research International**, v. 131, p. 109046, 2020.

EKER, M. E. et al. A Review of Factors Affecting Anthocyanin Bioavailability: Possible Implications for the. **Foods**, v. 9, n. 2, p. 1–18, 2020.

ESCALANTE-ABURTO, A. et al. Consumption of dietary anthocyanins and their association with a reduction in obesity biomarkers and the prevention of obesity. **Trends in Food Science and Technology**, v. 140, p. 104140, 2023.

ETCHEVERRY, P.; GRUSAK, M. A.; FLEIGE, L. E. Application of *in vitro* bioaccessibility and bioavailability methods for calcium, carotenoids, folate, iron, magnesium, polyphenols, zinc, and vitamins B6, B12, D, and E. **Frontiers in Physiology**, v. 3, p. 1–22, 2012.

FALLAH, A. A. et al. Impact of dietary anthocyanins on systemic and vascular inflammation: Systematic review and meta-analysis on randomised clinical trials. **Food and Chemical Toxicology**, v. 135, p. 110922, 2020.

FALLAH, A. A.; SARMAST, E.; JAFARI, T. Effect of dietary anthocyanins on biomarkers of oxidative stress and antioxidative capacity: A systematic review and meta-analysis of randomized controlled trials. **Journal of Functional Foods**, v. 68, p. 103912, 2020.

FERNANDES, A. et al. Blackberry anthocyanins: β-Cyclodextrin fortification for thermal and gastrointestinal stabilization. **Food Chemistry**, v. 245, p. 426–431, 2018.

FLORES, G. et al. *In vitro* fermentation of anthocyanins encapsulated with cyclodextrins: Release, metabolism and influence on gut microbiota growth. **Journal of Functional Foods**, v. 16, p. 50–57, 2015.

FREDES, C. et al. The microencapsulation of maqui (*Aristotelia chilensis* (Mol.) Stuntz) juice by spray-drying and freeze-drying produces powders with similar anthocyanin stability and bioaccessibility. **Molecules**, v. 23, n. 5, 2018.

GIULIANI, A.; CERRETANI, L.; CICHELLI, A. Colors: Properties and Determination of Natural Pigments. In: CABALLERO, B.; FINGLAS, P.; TOLDRÁ, F. (Eds.). **Encyclopedia of Food and Health**. 1. ed. [s.l.] Elsevier Ltd., 2016. p. 273–283.

GONÇALVES, A. C.; NUNES, A. R.; ALVES, G. Dietary Effects of Anthocyanins in Human Health: A Comprehensive Review. **Pharmaceuticals**, v. 14, n. 690, p. 1–34, 2021.

GUERGOLETTO, K. B. et al. *In vitro* fermentation of juçara pulp (*Euterpe edulis*) by human colonic microbiota. **Food Chemistry**, v. 196, p. 251–258, 2016.

GUERRA, A. et al. Relevance and challenges in modeling human gastric and small intestinal digestion. **Trends in Biotechnology**, v. 30, n. 11, p. 591–600, 2012.

GUO, H.; XIA, M. Anthocyanins and Diabetes Regulation. Em: WATSON, R. R.; PREEDY, V. R.; ZIBADI, S. (Eds**.). Polyphenols: Mechanisms of Action in Human Health and Disease**. 2. ed. [s.l.] Academic Press, 2018. p. 135–145.

GUTIÉRREZ-GRIJALVA, E. P. et al. Effect of *In vitro* Digestion on the Total Antioxidant Capacity and Phenolic Content of 3 Species of Oregano (*Hedeoma patens*, *Lippia graveolens*, *Lippia palmeri*). **Journal of Food Science**, v. 82, n. 12, p. 2832–2839, 2017.

HAN, F. et al. Digestion and absorption of red grape and wine anthocyanins through the gastrointestinal tract. **Trends in Food Science & Technology**, v. 83, p. 211–224, 2019.

HAN, F. et al. *In vitro* gastrointestinal absorption of red wine anthocyanins – Impact of structural complexity and phase II metabolization. **Food Chemistry**, v. 317, p. 126398, 2020.

HANSKE, L. et al. Contribution of gut bacteria to the metabolism of cyanidin 3-glucoside in human microbiota-associated rats. **British Journal of Nutrition**, v. 109, n. 8, p. 1433–1441, 2013.

HE, J.; MONICA GIUSTI, M. Anthocyanins: Natural colorants with health-promoting properties. **Annual Review of Food Science and Technology**, v. 1, n. 1, p. 163–187, 2010.

HERRERA-BALANDRANO, D. D. et al. Blueberry anthocyanins: An updated review on approaches to enhancing their bioavailability. **Trends in Food Science & Technology**, v. 118, n. 2021, p. 808–821, 2021.

HERRERA-BALANDRANO, D. D. et al. Impact of *in vitro* gastrointestinal digestion on rabbiteye blueberry anthocyanins and their absorption efficiency in Caco-2 cells. **Food Bioscience**, v. 52, p. 102424, 2023.

HIDALGO, M. et al. Metabolism of anthocyanins by human gut microbiota and their influence on gut bacterial growth. **Journal of Agricultural and Food Chemistry**, v. 60, n. 15, p. 3882–3890, 2012.

HORNEDO-ORTEGA, R. et al. Bioavailability, Human Metabolic Pathways, and Potential Anti-Neuroinflammatory Activity. In: BADRIA, F. A.; BLUMENBERG, M. (Eds.). **Phenolic Compounds - Chemistry, Synthesis, Diversity, Non-Conventional Industrial, Pharmaceutical and Therapeutic Applications**. IntechOpen, 2021. p. 1–24.

HU, Y. et al. Bioaccessibility and bioavailability of phytochemicals: Influencing factors, improvements, and evaluations. **Food Hydrocolloids**, v. 135, p. 108165, 2023.

JAKOBEK, L.; BLESSO, C. Beneficial effects of phenolic compounds: native phenolic compounds vs metabolites and catabolites. **Critical Reviews in Food Science and Nutrition**, p. 9113–9129, 2023.

KALT, W. et al. Recent Research on the Health Benefits of Blueberries and Their Anthocyanins. **Advances in Nutrition**, v. 11, n. 2, p. 224–236, 2020.

KAMILOGLU, S. et al. Anthocyanin Absorption and Metabolism by Human Intestinal Caco-2 Cells — A Review. **International Journal of Molecular Sciences**, v. 16, p. 21555–21574, 2015.

KAMONPATANA, K. et al. Anthocyanin structure determines susceptibility to microbial degradation and bioavailability to the buccal mucosa. **Journal of Agricultural and Food Chemistry**, v. 62, n. 29, p. 6903–6910, 2014.

KAN, J. et al. Phytonutrients: Sources, bioavailability, interaction with gut microbiota, and their impacts on human health. **Frontiers in Nutrition**, v. 9, p. 960309, 2022.

KAWABATA, K.; YOSHIOKA, Y.; TERAO, J. Role of intestinal microbiota in the bioavailability and physiological functions of dietary polyphenols. **Molecules**, v. 24, n. 2, p. 1–25, 2019.

KENT, K.; HÖLZEL, N.; SWARTS, N. Polyphenolic compounds in sweet cherries: A focus on anthocyanins. In: **Polyphenols: Mechanisms of Action in Human Health and Disease**. Elsevier, 2018. p. 103–118.

KUNTZ, S. et al. Uptake and bioavailability of anthocyanins and phenolic acids from grape/blueberry juice and smoothie *in vitro* and *in vivo*. **British Journal of Nutrition**, v. 113, n. 7, p. 1044–1055, 2015.

LANG, Y. et al. Effects of α-casein on the excretion of blueberry anthocyanins via urine and feces: Analysis of their bioavailability. **Food Chemistry**, v. 413, p. 135565, 2024.

LIANG, A. et al. Anthocyanins-gut microbiota-health axis: A review. **Critical Reviews in Food Science and Nutrition**, p. 1–26, 2023.

LIANG, L. et al. *In vitro* bioaccessibility and antioxidant activity of anthocyanins from mulberry (*Morus atropurpurea* Roxb.) following simulated gastro-intestinal digestion. **Food Research International**, v. 46, n. 1, p. 76–82, 2012.

LILA, M. A. et al. Unraveling Anthocyanin Bioavailability for Human Health. **Annual Review of Food Science and Technology**, v. 7, p. 375–393, 2016.

MAKAREWICZ, M. et al. The interactions between polyphenols and microorganisms, especially gut microbiota. **Antioxidants**, v. 10, n. 2, p. 1–70, 2021.

MALLERY, S. R. et al. Effects of human oral mucosal tissue, saliva, and oral microbiota on intraoral metabolism and bioactivation of black raspberry anthocyanins. **Cancer Prevention Research**, v. 4, n. 8, p. 1209–1221, 2011.

MOLAN, A. L.; LIU, Z.; PLIMMER, G. Evaluation of the effect of blackcurrant products on gut microbiota and on markers of risk for colon cancer in humans. **Phytotherapy Research**, v. 28, n. 3, p. 416–422, 2014.

MUELLER, D. et al. Human intervention study to investigate the intestinal accessibility and bioavailability of anthocyanins from bilberries. **Food Chemistry**, v. 231, p. 275–286, 2017.

MUELLER, D. et al. Encapsulation of anthocyanins from bilberries – Effects on bioavailability and intestinal accessibility in humans. **Food Chemistry**, v. 248, p. 217–224, 2018.

MUKHERJEE, P. K. Phyto-Pharmaceuticals, Nutraceuticals and Their Evaluation. In: MUKHERJEE, P. K. (Ed.). **Quality Control and Evaluation of Herbal Drugs**. 1. ed. p. 707–722.

MUÑOZ-FARIÑA, O. et al. Bioaccessibility of phenolic compounds in fresh and dehydrated blueberries (*Vaccinium corymbosum* L.). **Food Chemistry Advances**, v. 2, p. 100171, 2023.

NASCIMENTO, A. L. A. A. et al. Exploring strategies to enhance anthocyanin bioavailability and bioaccessibility in food: A literature review. **Food Bioscience**, v. 56, p. 103388, 2023.

OLIVEIRA, H. et al. GLUT1 and GLUT3 involvement in anthocyanin gastric transport-Nanobased targeted approach. **Scientific Reports**, v. 9, n. 1, p. 1–14, 2019.

PASSAMONTI, S. et al. The stomach as a site for anthocyanins absorption from food. **FEBS Letters**, v. 544, n. 1–3, p. 210–213, 2003.

PEIXOTO, F. M. et al. Simulation of *in vitro* digestion coupled to gastric and intestinal transport models to estimate absorption of anthocyanins from peel powder of jabuticaba, jamelão and jambo fruits. **Journal of Functional Foods**, v. 24, p. 373–381, 2016.

PENG, Y. et al. Prebiotic effects *in vitro* of anthocyanins from the fruits of *Lycium ruthenicum* Murray on gut microbiota compositions of feces from healthy human and patients with inflammatory bowel disease. **LWT**, v. 149, p. 111829, 2021.

QUATRIN, A. et al. Bioaccessibility and catabolism of phenolic compounds from jaboticaba (*Myrciaria trunciflora*) fruit peel during *in vitro* gastrointestinal digestion and colonic fermentation. **Journal of Functional Foods**, v. 65, 2020.

RESEARCH AND MARKETS. **Anthocyanin Market by Product Type, Source, End User - Global Forecast 2025-2030**. 2024.

REYES, B. A. S. et al. **Selected Phyto and Marine Bioactive Compounds: Alternatives for the Treatment of Type 2 Diabetes**. 1. ed. Elsevier B.V., 2017. v. 55.

ROSALES, T. K. O. et al. A study of the oral bioavailability and biodistribution increase of Nanoencapsulation-driven Delivering radiolabeled anthocyanins. **Food Research International**, v. 197, p. 115125, 2024.

ROSALES-CHIMAL, S. et al. Optimal conditions for anthocyanin extract microencapsulation in taro starch: Physicochemical characterization and bioaccessibility in gastrointestinal conditions. **International Journal of Biological Macromolecules**, v. 227, p. 83–92, 2023.

SHARMA, S.; PANDITA, G.; BHOSALE, Y. K. Anthocyanin: Potential tool for diabetes management and different delivery aspects. **Trends in Food Science and Technology**, v. 140, p. 104170, 2023.

SHEHATA, E. et al. Spontaneous and Microbiota-Driven Degradation of Anthocyanins in an *In vitro* Human Colon Model. **Molecular Nutrition and Food Research**, v. 67, n. 19, 2023.

SHEN, Y. et al. Advanced approaches for improving bioavailability and controlled release of anthocyanins. **Journal of Controlled Release**, v. 341, p. 285–299, 2022.

STALMACH, A. et al. Gastrointestinal stability and bioavailability of (poly) phenolic compounds following ingestion of Concord grape juice by humans. **Molecular Medicine Reports**, v. 56, p. 497–509, 2012.

TALAVERA, S. et al. Anthocyanins Are Efficiently Absorbed from the Stomach in Anesthetized Rats Se. **American Society for Nutritional Sciences**, p. 4178–4182, 2003.

VAN DE VELDE, F.; PIROVANI, M. E.; DRAGO, S. R. Bioaccessibility analysis of anthocyanins and ellagitannins from blackberry at simulated gastrointestinal and colonic levels. **Journal of Food Composition and Analysis**, v. 72, p. 22–31, 2018.

VENDRAME, S. et al. Six-week consumption of a wild blueberry powder drink increases Bifidobacteria in the human gut. **Journal of Agricultural and Food Chemistry**, v. 59, n. 24, p. 12815–12820, 2011.

VERGARA, C. et al. Microencapsulation of Anthocyanin Extracted from Purple Flesh Cultivated Potatoes by Spray Drying and Its Effects on *In vitro* Gastrointestinal Digestion. **Molecules**, v. 25, n. 722, p. 1–14, 2020.

VICTORIA-CAMPOS, C. I. et al. Gastrointestinal metabolism and bioaccessibility of selected anthocyanins isolated from commonly consumed fruits. **Food Chemistry**, v. 383, p. 132451, 2022.

WANG, B. et al. Effects of *in vitro* fecal fermentation on the metabolism and antioxidant properties of cyanidin-3-O-glucoside. **Food Chemistry**, v. 431, p. 137132, 2024.

WANG, H.; LI, P.; ZHOU, W. Dyeing of Silk with Anthocyanins Dyes Extract from Liriope platyphylla Fruits. **Journal of textiles**, v. 2014, p. 1–9, 2014.

WANG, X.; QI, Y.; ZHENG, H. Dietary Polyphenol, Gut Microbiota, and Health Benefits. **Antioxidants**, v. 11, n. 6, p. 1212, 2022.

WOJTUNIK-KULESZA, K.; ONISZCZUK, A.; ONISZCZUK, T. Influence of *In vitro* Digestion on Composition, Bioaccessibility and Antioxidant Activity of Food Polyphenols — A Non-Systematic Review. **Nutrients**, v. 12, p. 1–29, 2020.

WU, Y. et al. *In vitro* gastrointestinal digestion and fecal fermentation reveal the effect of different encapsulation materials on the release, degradation and modulation of gut microbiota of blueberry anthocyanin extract. **Food Research International**, v. 132, p. 109098, 2020.

XIN, M. et al. Anthocyanins as natural bioactives with anti-hypertensive and atherosclerotic potential: Health benefits and recent advances. **Phytomedicine**, v. 132, p. 155889, 2024.

XUE, H. et al. Research Progress on Absorption, Metabolism, and Biological Activities of Anthocyanins in Berries: A Review. **Antioxidants**, v. 12, n. 1, p. 1–22, 1 jan. 2023.

XUE, H. et al. Factors affecting the stability of anthocyanins and strategies for improving their stability: A review. **Food Chemistry: X**, v. 24, p. 101883, 2024.

ZHONG, S. et al. Characterization of Wild Blueberry Polyphenols Bioavailability and Kinetic Profile in Plasma over 24-h Period in Human Subjects. **Molecular Nutrition and Food Research**, v. 61, n. 12, 2017.

ZOU, T. BIN et al. The role of sodium-dependent glucose transporter 1 and glucose transporter 2 in the absorption of cyanidin-3-O-β-glucoside in caco-2 cells. **Nutrients**, v. 6, n. 10, p. 4165–4177, 2014.

3. CHAPTER 2: Enhancement of phenolic compounds bioaccessibility in jabuticaba wine through fermentation by *Saccharomyces cerevisiae*

This paper was published in the journal Food and Bioproducts Processing: BORGES, L. L. R. et al. Enhancement of phenolic compounds bioaccessibility in jabuticaba wine through fermentation by *Saccharomyces cerevisiae*. **Food and Bioproducts Processing**, v. 148, p. 198–207, 2024. https://doi.org/10.1016/j.fbp.2024.09.009

Larissa Lorrane Rodrigues Borges[a*],Valdeir Viana Freitas[a], Amanda Lais Alves Almeida Nascimento[a], Janaina Gonçalves Fernandes[a], Hélia de Barros Kobi[a], Monique Renon Eller[a], Frederico Augusto Ribeiro de Barros[a], Luciana Ângelo de Souza[b], Gabriel Abranches Dias Castro[c], Arthur Figueira de Carvalho[b], Jaqueline de Araújo Bezerra[d], Sergio Antonio Fernandes[c], Gustavo Costa Bressan[b], Evandro Martins[a], Pedro Henrique Campelo[a], Paulo César Stringheta[a]

[a]Universidade Federal de Viçosa, Department of Food Technology, Avenida Peter Henry Rolfs, s/n, Viçosa, MG 36570-900, Brazil
[b]Universidade Federal de Viçosa, Department of Biochemistry and Molecular Biology, Avenida Peter Henry Rolfs, s/n, Viçosa, MG 36570-900, Brazil
[c]Universidade Federal de Viçosa, Department of Chemistry, Avenida Peter Henry Rolfs, s/n, Viçosa, MG 36570-900, Brazil
[d]Instituto Federal de Educação, Ciência e Tecnologia do Amazonas, Department of Chemistry, Avenida Sete de Setembro, 1975, Manaus, MA 69020-120, Brazil

*Corresponding author:
Larissa Lorrane Rodrigues Borges
Department of Food Technology, Universidade Federal de Viçosa
Avenida Peter Henry Rolfs, s/n, Viçosa, MG 36570-900, Brazil.
Email address: larissa.borges@ufv.br
Phone: +55 38 991790125

Abstract

Jabuticaba (*Plinia cauliflora*), a fruit native to Brazil, is known for the high phenolic content in its peel, which is usually discarded. The development of jabuticaba wine is an alternative for better nutritional and technological utilization of the fruit. In this context, this study is the first to investigate the biotransformation of phenolic compounds in jabuticaba during alcoholic fermentation by *Saccharomyces cerevisiae* and maturation. The research also explored the antioxidant and antiproliferative effects of the beverages, as well as their ability to inhibit α-glucosidase and lipase. Fermentation of jabuticaba significantly increased total phenolic compounds (4.91 ± 0.07-fold), total anthocyanins (5.62 ± 1.17-fold), cyanidin-3-glucoside (2.05 ± 0.74-fold), gallic acid (57.02 ± 3.70-fold), and protocatechuic acid (3.70 ± 0.51-fold), as well as the bioaccessibility of these compounds. The beverages also showed antiproliferative effects against cancer cells, antioxidant activities, and enzyme inhibition properties. Maturation at 4 ± 2 °C for 30 days reduced the cytotoxicity of the samples. Despite a reduction in phenolic concentration after digestion, the samples retained bioactive potential. These results establish reference data on the chemical composition and bioactive potential of jabuticaba wine.

Keywords: Bioactive compounds; Saccharomyces cerevisiae; Anthocyanins; *In vitro* digestion; Cytotoxicity; Antioxidant activity

1. Introduction

Jabuticaba (*Plinia cauliflora*) is a fruit native to Brazil, belonging to the Myrtaceae family, and a source of carbohydrates, fiber, minerals, and vitamins (Wu et al., 2013). The fruit is known for its high content of phenolic compounds, particularly anthocyanins, which are responsible for the fruit's pigmentation. The main anthocyanin found in jabuticaba is cyanidin-3-glucoside, and other phenolic compounds already identified in the fruit are quercetin, ellagitannins, gallotannins, and phenolic acids, such as gallic and ellagic acids (Inada et al., 2020; Neves et al., 2021, 2018).

In vitro and *in vivo* studies with jabuticaba have demonstrated that the phenolic compounds present exhibit promising effects on human health. The main biological effects reported in the literature include hypoglycemic action, prevention of insulin resistance, reduction of total cholesterol and triglycerides, antioxidant activities, anti-inflammatory properties, and antiproliferative effects against different cancer cell lines, such as NCI-H460

(lung carcinoma); MCF-7 (breast carcinoma); HepG2 (hepatocellular carcinoma), and HeLa (cervical carcinoma) (Albuquerque et al., 2020; Alezandro et al., 2013; Batista et al., 2014; Dragano et al., 2013; Moura et al., 2018; Plaza et al., 2016; Rodrigues et al., 2021).

Although jabuticaba has potential health benefits, this fruit is usually consumed fresh, and its peel, where the highest levels of phenolic compounds are concentrated, is usually discarded (Lima et al., 2008, 2011; Marquetti et al., 2018). In this context, developing products derived from jabuticaba is a promising alternative for better nutritional and technological use of the entire fruit. Some products derived from jabuticaba, such as jellies, juices, liqueurs, and alcoholic beverages, are already produced artisanally in some regions of Brazil (Inada et al., 2021; Jagtap and Bapat, 2015).

The production of an alcoholic beverage from jabuticaba, popularly known as jabuticaba wine, is an alternative for reducing post-harvest losses since large quantities of the fruit are wasted during peak harvest periods due to its high perishability (Garcia et al., 2019). Therefore, using the ripe fruit or its juice for wine production is considered an attractive means of utilizing surplus and over-ripen fruits. Moreover, fermentation improves fruit's sensory properties, through the production of alcohols, acids, and volatile compounds. The production of jabuticaba wine is also an alternative to increase the commercialization and consumption of jabuticaba products, addressing the growing consumer market for several fruit by-products, including wines, and creating a new source of income for producers (Jagtap and Bapat, 2015).

During production, the beverage can be prepared by crushing and macerating the whole fruit, allowing the extraction of phenolic compounds from the peel and generating a beverage rich in compounds with promising effects on human health. The peels are not normally consumed due to their stiffness and astringency; however, during winemaking, compounds like tannins and anthocyanins, that are important to the wine's color and flavor, can be extracted from the peels.

Furthermore, in addition to forming primary and secondary metabolites, fermentation can simultaneously biotransform phenolic compounds, significantly enhancing the health-promoting properties of the food (Cagno et al., 2016; Leonard et al., 2021). There is evidence that the fermentation process causes changes in the profile of phenolic compounds and can provide an increase in the antioxidant activity of fermented beverages (Braga et al., 2018; Chen et al., 2023; Dong et al., 2023).

Although the production of jabuticaba wine already happens artisanally in Brazil, there are few studies on the profile of phenolic compounds and the potential bioactive properties of this product. In this context, the objective of this study was to carry out, for the first time, a

detailed investigation of the biotransformation of phenolic compounds in jabuticaba after alcoholic fermentation and maturation, as well as the determination of the bioactive properties (antiproliferative, antioxidant and enzyme inhibition) of the beverages. Furthermore, the impact of *in vitro* digestion on these properties and the bioaccessibility of phenolic compounds was also evaluated.

2. Materials and methods

2.1. Production of the alcoholic fermented jabuticaba beverage

The jabuticaba fruits used in this study were of the Sabará variety (*Plinia cauliflora*), collected from the Fruit Culture sector of the Universidade Federal de Viçosa, Minas Gerais, Brazil, in November 2022. The fruits were carefully selected, washed with water, vacuum-packed, and stored in a freezer at -18 °C.

2.1.1. Yeast activation

A stock solution of frozen *Saccharomyces cerevisiae* (UFMG-CM-Y7130) was activated in YEPG (Yeast Extract Peptone Glucose) culture medium without gas restriction at 28 °C for 24 h at 200 rpm. Following activation, the yeast cells were counted using methylene blue staining in a Neubauer Chamber at a dilution of 1:20 (v/v), recovered by centrifugation, and resuspended in the must to achieve a concentration of 10^6 cells/mL after inoculation.

2.1.2. Must preparation

The must preparation was adapted from (Duarte et al., 2010). The must was prepared manually by crushing the whole fruit and removing the seeds. Then sucrose was added to obtain an initial must with 15 °Bx. The pH was corrected to 4.5 with calcium carbonate ($CaCO_3$), and potassium metabisulphite at a concentration of 100 mg/L was added to prevent unwanted microbial growth. Samples of the unfermented must were collected to serve as a baseline for the phenolic compounds already present in the must before fermentation (control (C)). The sample was frozen at -65 °C until analyses were carried out.

2.1.3. Alcoholic fermentation

For the alcoholic fermentation, the must was inoculated with *S. cerevisiae* at a concentration of 10^6 cells/mL. The inoculated must was placed in 4-liter amber vessels (without baffles) to protect the samples from photooxidation, equipped with airlocks for fermentation. The musts were fermented at 20 °C for 12 days under static conditions. The progress of the fermentation was monitored daily by analyzing the total soluble solids (ºBx) using a digital refractometer (AR200, Leica, São Paulo, Brazil) until the must concentration stabilized. At the end of fermentation, a strainer was used to filter out the peels from the beverage, which was transferred to other vessels, leaving the sedimented yeast behind. This sample was designated as alcoholic fermented beverage (AF). The beverage was submitted to physicochemical analysis and frozen at -65 °C until further analyses were carried out (total anthocyanin content, total phenolic content, antioxidant activity, HPLC-DAD, and simulated gastrointestinal digestion). Part of the fermented beverage without the peels was subjected to maturation at a temperature of 4 ± 2 °C for 30 days to assess the effect of these conditions on the phenolic profile and bioactive activities of the beverage. This sample was identified as the matured alcoholic fermented beverage (MAF). After 30 days, the beverage was submitted to the physicochemical analysis and frozen at -65 °C until the other analysis were carried out. Prior to analysis, all the samples were centrifuged at 2250 x g for 15 min (RA 280 rotor, Model NF 1200 R, Nüve, Akyurt/Ankara, Turkey).

For the enzymatic inhibition, cytotoxicity assays, and high-resolution mass spectrometry analysis (HRMS), the samples were previously powdered through rotary evaporation at 40 °C to remove ethanol, followed by freezing and lyophilization.

2.2. Physicochemical analysis

The pH of the samples was measured using a pHmeter (DM-20, Digimed, São Paulo, Brazil), and the total soluble solids content (°Bx) was measured using a digital refractometer (AR200, Leica, São Paulo, Brazil). Furthermore, total acidity was determined by titration with 0.1 N sodium hydroxide, using bromothymol blue as an indicator of the end of the reaction (OIV, 2021). To determine the volatile acidity, the volatile acids were separated from the wine by steam distillation and titrated with 0.1 N sodium hydroxide, using phenolphthalein as an indicator (OIV, 2021). Fixed acidity was calculated from the difference between total and

volatile acidity. The alcoholic content of the beverages was determined by relative density through distillation and the use of a pycnometer, as determined by the (OIV, 2021).

2.3. Total anthocyanin content (TAC) and Total phenolic content (TPC)

The total anthocyanin content was measured according to the method described by (Fuleki and Francis, 1968). An aliquot of the samples was diluted in a solution of ethanol:HCl 1.5 N (85:15 v/v), and the absorbance was measured at 535 nm (UV-M51, Bel Photonics, Monza, Italy), aiming to obtain a value between 0.200 and 0.800. The final results were expressed in µg of cyanidin-3-glucoside equivalents per mL of sample. Total phenolic compounds were quantified according to the method described by (Singleton and Rossi, 1965). In test tubes, 0.6 mL of diluted sample was mixed with 3 mL of Folin-Ciocalteau reagent (diluted 1:10 with water) and 2.4 mL of 7.5% Na_2CO_3 solution (m/v). After 1 h in the dark (23 ± 2 °C), the absorbance was measured at 765 nm (UV-M51, Bel Photonics, Monza, Italy). The results were expressed in µg gallic acid equivalent (GAE) per mL of the sample.

2.4. Identification of compounds through High-resolution mass spectrometry (HRMS) analysis

The samples were analyzed using a High-Performance Liquid Chromatograph Coupled to a High-Resolution Mass Spectrometer – HRMS ESI MicroTOF-Q II (Bruker Daltonics®, Fremont, CA, USA), calibrated with sodium formate at a concentration of 10 mM. The following parameters were used: capillary voltage of 3.5 kV and 4 .5 kV for ions in negative and positive modes. A ZORBAX Eclipse plus C18 column (4.6 x 250 mm, 5 µm) was used, with a flow of 4 mL/min, with solvents A (H_2O + 0.1% HCOOH), B (MeOH), and C (MeOH: H2O 1:1). Samples (10 µL) were injected using the following method: 0-5 min (2%), 5 – 34 min (2 – 55%), 34 – 38 min (55 – 100%), 38 – 42 min (100%) and 42 – 46 min (100 - 2%). Data were acquired and processed using Bruker® Compass Data Analysis 4.1 software.

2.5. Quantification of phenolic compounds by HPLC-DAD

High-performance liquid chromatography (HPLC) analyses were performed on a Thermo Scientific Accela LC system (diode array detector (DAD), autoinjector, and Accela pump) (Thermo Fisher Scientific, Austin, TX). The column used for the separation was the

Shim-pack VP-ODS reverse phase column (250 x 4.6 mm, with a particle size of 4.6 µm and a pore size of 12 nm) (Shimadzu, Shimadzu, Kyoto, Japan). For the phenolic acids analysis, the mobile phase consisted of acidified water with 1% acetic acid (A, v/v) and methanol acidified with 1% acetic acid (B, v/v). For cyanidin-3-glucoside, the mobile phase consisted of water acidified with 5% formic acid (A) and acetonitrile (B). The gradient programs are described in tables S1 and S2. The flow was 1000 µL/min, and the injection volume was 20 µL, with a temperature of 25 °C for the injector and the column. Peaks were detected at wavelengths of 280 nm for of gallic and protocatechuic acids and at 535 nm for cyanidin-3-glucoside. The peaks were identified by comparing the retention time in the chromatogram with those of the separately injected standards. The concentration of the compounds was calculated based on the area of each peak using a calibration curve. The calibration curves obtained for gallic acid and protocatechuic acid exhibited linearity within the concentration range of 0.01 mg/mL to 0.25 mg/ mL. The linear equation for gallic acid was y = 230993x – 387827 with an R^2 value of 0.9993. Similarly, for protocatechuic acid, the linear equation obtained was y = 119475x – 349576, with an R^2 value of 0.9991. For cyanidin-3-glucoside, the linear equation was y = 231136 x – 1000000 with and R^2 of 0.9970.

2.6. *In vitro* antiproliferative activity

Human cells MV3 (Metastatic Melanoma cell line), MCF-7 (Breast Cancer cell line), and HEK293T (Human Embrionary Kidney) were kindly provided by Dra. Anésia Aparecida dos Santos (General Biology Department, Universidade Federal de Viçosa, Minas Gerais, Brazil). The cells were plated in 96-well plates at a concentration of 5.0×10^3 cells per well for MV3 cells and a concentration of 1.0×10^4 cells per well for HEK293T and MCF-7 cells. The cells were allowed to grow for 24 h and then treated with the samples at concentrations ranging from 10 - 1000 µg/mL for IC50 determination. DMSO (Dimethylsulfoxide, Neon Comercial Reagentes Analíticos Ltda, SP, Brazil) was used as a diluent for the samples and as a negative control for the experiments. The samples were filtered using 0.22 µm filters before the experiments. After 48h of treatment, the cell viability was determined by MTT (3-(4,5 dimethylthiazol-2-yl)- 2,5 diphenyl tetrazolium bromide) (Sigma-Aldrich, MO, USA). The MTT solution in 1x PBS was added to each well (final concentration at 5 mg/mL) and the plate was incubated for 3 h. Finally, the MTT solution was removed and 100 µL of DMSO were added to each well and the absorbance was measured in a plate reader (Spectramax M5) at 540 nm. The assay is based on the ability of viable cells to reduce the yellow tetrazolium salt MTT

to formazan crystals. Cell viability results were quantified as percentage of untreated controls and the IC50 values (concentration of the sample that inhibits growth by 50%) were also calculated.

2.7. Antioxidant activity

2.7.1. ABTS (2,2'-azinobis-3-etil-benzotiazolina-6-sulfonado) radical scavenging activity

The ABTS radical assay followed a previously reported method (Re et al., 1999): In test tubes: 0.5 mL of sample solution (4 different dilutions) were added to 3.5 mL of ABTS radical solution (diluted in 80% ethanol up to an absorbance of 0.700 ± 0.05 at 734 nm). After 6 min of reaction in the dark (23 ± 2 °C), the absorbance was measured at 734 nm (UV-M51, Bel Photonics, Monza, Italy), and the results were expressed as µmol of Trolox equivalent (TE)/mL.

2.7.2. DPPH (2,2-diphenyl-1-picrylhydrazyl) radical scavenging activity

The DPPH assay followed the method described by (Kim et al., 2002). In test tubes: 0.5 mL of sample solution (4 different dilutions) was added to 3.5 mL of DPPH radical solution (0.1 mmol/L in 80% ethanol). Absorbance was measured at 517 nm (UV-M51, Bel Photonics, Monza, Italy) after 60 min of reaction in the dark (23 ± 2 °C). The results were expressed as µmol of Trolox equivalent (TE)/mL.

2.8. *In vitro* digestive enzyme inhibition

2.8.1. α-glucosidase inhibition assay

The assay was performed as previously described (Adisakwattana et al., 2009), with modifications. Samples were dissolved in 0.1 M phosphate buffer (pH 6.9). A crude enzymatic solution obtained from the intestine of rats was used as a source of α-glucosidases for sucrose hydrolysis. In 96-well plates: 5 µL of the sample (0.30 to 600 mg/mL) or phosphate buffer (negative control), 5 µL of α-glucosidase (9.42 ± 0.52 U/mL) and 57 µL of phosphate buffer (pH=6.9) were mixed. A pre-incubation was performed for 10 min at 37 °C, and the reaction was started by adding 71 µL of sucrose solution 5.0% (w/v). After incubation (30 min; 37 °C),

the glucose concentrations released from the reaction mixtures were determined by the glucose oxidase method using the Glucose Monoreagent K082 kit (Bioclin, Belo Horizonte, MG, Brazil). Absorbance was read at 492 nm (DR-200BS-NM-BI, Kasuaki). Acarbose was used as a positive control (0.01-5 mg/mL). Results were expressed as IC50 values, calculated by fitting sigmoidal dose-response curves of the logarithm of inhibitor concentration versus percent inhibition to the 4-parameter logistic regression model (Equation 1) using the R software.

$$Y = \left(\frac{(\text{max-min})}{1 + 10^{-((\text{logIC50-X})*\text{Hill slope})}} \right) \quad (1)$$

Y represents the % inhibition and its minimum (min) and maximum (max) values. X represents the inhibitor concentration, the IC50 is the inhibitor concentration required to reduce enzyme activity by 50%, and HillSlope is the slope factor.

2.8.2. Lipase inhibition assay

The lipase activity inhibition assay was adapted from (Borges et al., 2022). In 96-well plates, 5 µL of the sample (0.30-800 mg/mL) were mixed with 5 µL of a lipase solution (11.20 ± 0.28 U/mL), 100 µL of buffer and 10 µL of Dithionitrobenzoic acid (DTNB) color reagent. After 2 min of pre-incubation at 37 °C, the reaction was started by adding 10 µL of substrate solution 2-3-Dimercapto-1-Propanol Tributyrate (4.0 mM). The reaction mixture was incubated at 37 °C for another 30 min, and the reaction was stopped by adding 200 µL of reaction terminator solution. Released 2,3 dimercaptopropanol (BAL) was measured at 405 nm (DR-200BS-NM-BI, Kasuaki). The results were expressed as IC50 value, calculated according to item 2.8.1. Orlistat (0.02 to 10 mg/mL) was used as a positive control.

2.9. Simulated gastrointestinal digestion

The simulated gastrointestinal digestion system, which included two steps (gastric and intestinal digestion), was adapted from (Minekus et al., 2014). For the gastric digestion step, 10 mL of sample was mixed with: 7.5 mL of simulated gastric fluid (SGF), 1.6 mL of porcine pepsin stock solution (25000 U/mL; porcine gastric mucosal pepsin ≥ 500 U /mg protein, Sigma-Aldrich) prepared in SGF, 15 µL of CaCl2 (0.1 M), 1.0 M HCl to reach pH 2.0 and 175 µL of distilled water. The mixture was incubated (37 °C, 200 rpm) in the dark for 2 h. After

this period, 11 mL of simulated intestinal fluid (SIF), 5.0 mL of a pancreatin solution (800 U/mL; porcine pancreatin, 4 x USP, Sigma-Aldrich, prepared in SIF based on trypsin activity), 3.0 mL of a bile salt solution (200 mg/mL), 40 µL of $CaCl_2$ (0.3 M) and 1 M NaOH to reach pH 7.0 were added for the intestinal digestion process. The solutions were reincubated at 37 °C for 2 h at 200 rpm. At the end of the incubation, the digestion was interrupted in an ice bath for 10 min. The samples were centrifuged at 2250 x g for 10 min (RA 280 rotor, Model NF 1200 R, Nüve, Akyurt/Ankara, Turkey) to separate the bioaccessible fractions (Bernardes et al., 2019). Samples were then stored at -65 °C for further analysis. The bioaccessibility of phenolic compounds was calculated according to Equation 2.

$$\text{Bioaccessibility (\%)} = \frac{\text{Concentration in the digested sample}}{\text{Initial concentration}} \quad (2)$$

2.10. Statistical analysis

The experiments were conducted in 3 replicates, and the results were presented as mean ± standard deviation. The treatments included the control (C), alcoholic fermented beverage (AF), and matured alcoholic fermented beverage (MAF). The content of phenolic compounds and bioaccessibility in the 3 different samples were analyzed using one-way ANOVA, followed by Tukey's test. The antiproliferative activities of the samples were analyzed using the Dunnett's test. The data for antioxidant activity and enzyme inhibition were analyzed using two-way ANOVA, followed by Tukey's test for multiple comparisons, considering a 3x2 factorial design. The first factor corresponded to the different samples (C, AF, MAF) and the second to the digestion status (digested or non-digested). All the analyses were performed using the R software (R Core Team, Vienna, Austria). A statistically significant value was considered when $p<0.05$.

3. Results and discussion

3.1. Physicochemical parameters

The fermentation of jabuticaba was performed for 12 days and ended with a constant total soluble solids content of 6.00 ± 0.10 °Bx. The initial content of 15 °Bx under the fermentative conditions employed generated a beverage with an alcoholic content of 8.77 ±

0.60% (v/v). The pH of the alcoholic fermented sample (AF) decreased from 4.50 (control) to 3.75 ± 0.09 at the end of fermentation. Correspondingly, the total titratable acidity increased from 31.33 ± 4.18 to 166.00 ± 6.00 mmol/L. At the same time, the values found for volatile acidity and fixed acidity of the fermented alcoholic beverage were 5.67 ± 0.58 and 160.33 ± 5.51 mmol/L, respectively.

Maturation for 30 days at 4 ± 2 °C did not significantly affect the physicochemical properties of the fermented beverage for any of the parameters analysed after 30 days ($p>0.05$). The values obtained were 3.61 ± 0.04 for pH, 8.69 ± 0.33% of alcoholic content, 158.67 ± 2.31 mmol/L of total acidity, 5.33 ± 0.58 and 154.33 ± 2.08 mmol/L of volatile and fixed acidity, respectively.

The values obtained for the studied parameters (pH, alcoholic content, volatile acidity, and fixed acidity) were within the levels established for jabuticaba alcoholic fermented beverages in Brazil (BRASIL, 2012, Table S3). Except for total acidity, which was found above the established maximum limit of 130 mmol/L.

The same profile was observed in another study, where a comprehensive bromatological analysis was carried out on seven artisanal jabuticaba fermented products. The samples showed high total acidity (103.0 ±1.37-195.7 ±1.37), pH ranging from 3.6 to 4.1, soluble solids (°Bx) from 6.90 ± 0.10 to 15 .93 ± 0.11 and ethanol concentration within the expected levels for jabuticaba fermented products in Brazil (4% to 14% (v/v)) (Macedo et al., 2021). For the analysis of alcoholic fermented beverages produced artisanally by small producers in Minas Gerais, the values for total acidity exceeded 130 meq/L. Thus, jabuticaba fermented beverages can be considered highly acidic. Additionally, the samples ultra-passed the maximum limit established for volatile acidity, and most of the samples had an alcohol content between 10 and 13% (Da Silva et al., 2008).

3.2. Extraction and biotransformation of phenolic compounds during fermentation

Significant increases in total anthocyanins (TAC) and phenolics (TPC) contents were observed on the second day of fermentation, as shown in Figure 1. After this period, the concentration remained relatively stable until the tenth day. During alcoholic fermentation, ethanol produced by yeast activity acts as a solvent and can help extract phenolic compounds from jabuticaba peel to the must, which explains the increased concentration of these compounds during the fermentation process (Kowalczyk et al., 2022; Setford et al., 2017).

On the last day of fermentation, there was a significant decrease in the total anthocyanin content and an increase in the total phenolic concentration (Figure 1A). TPC increased by 49.31 ± 0.16%, and TAC reduced by 25.09 ± 4.18% compared to day 2. In general, studies have shown that the total phenolic content is higher and anthocyanin content is reduced at the end of the fermentation process. Similar findings have been reported in the fermentation of other plant-derived materials.

For jussara pulp fermentation, the degradation percentage of anthocyanins ranged from 12.7% to 100% (Braga et al., 2018). Similarly, fermented strawberry juice with lactic acid bacteria exhibited an increased phenolic content of 139.26 ± 1.19 mg/L, compared to 117.46 ± 1.26 mg/L in the unfermented juice. Conversely, the total anthocyanin content decreased to 21.19 ± 0.23 mg/L, while the unfermented juice contained 39.66 ± 0.19 mg/L (Chen et al., 2023). In the production of mulberry wine, a similar pattern was observed. The maximal level of total phenolic content (TPC) was reached on the final day of fermentation (2482.61 mg/L). However, the total anthocyanin content (TAC) initially increased to 911.73 mg/L from day 0 to 1, but subsequently decreased to approximately 700 mg/L between days 2 and 4 (Xie et al., 2017).

During the fermentation, the produced ethanol helps to extract phenolic compounds from the vegetal matrix while new compounds are generated in the media from the metabolization of parent compounds by the yeasts, such as anthocyanins. The association of these simultaneous events explain the results observed, i.e., increasing in TPC and decreasing in the anthocyanins contents after fermentation (Leonard et al., 2021).

During the alcoholic fermentation of jabuticaba, the anthocyanins present in the medium can be transformed into secondary phenolic compounds, such as phenolic acids. The major anthocyanin found in jabuticaba is cyanidin-3-glucoside (Inada et al., 2015; Neves et al., 2021). The yeast *S. cerevisiae* produces the β-glucosidase enzyme during fermentation, which can break down the glycosidic form of some phenolic compounds, including anthocyanins (Singh et al., 2016; Zhang et al., 2021). It has already been demonstrated that strains of *S. cerevisiae* with high β-glucosidase activity produced wines with lower concentrations of anthocyanins compared to wines produced by yeast strains with low β-glucosidase activity (Vernocchi et al., 2011). The formed aglycones appear transiently and are mainly degraded into phenolic acids (Ávila et al., 2009; Monteiro et al., 2019).

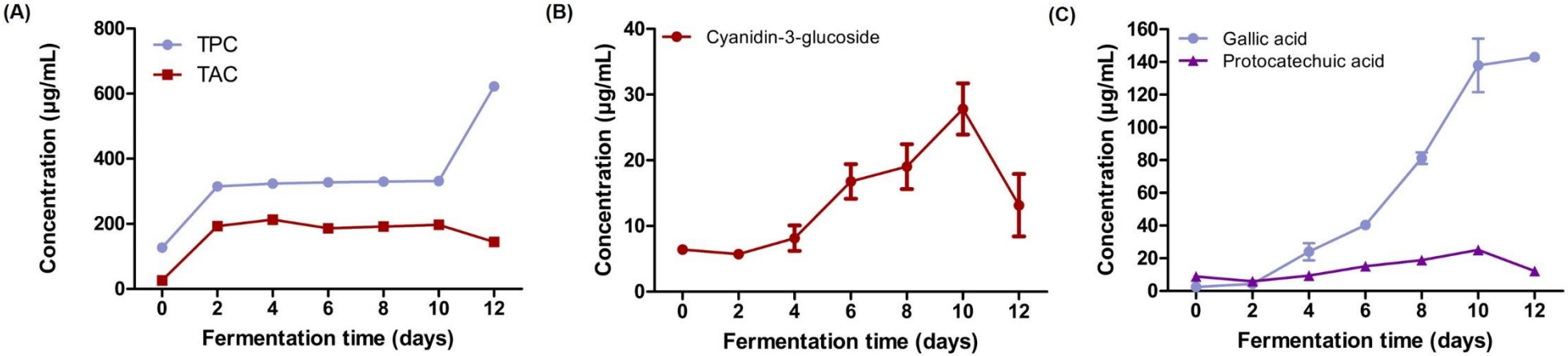

Figure 1

Behavior of phenolic compounds during the alcoholic fermentation of jabuticaba. (A) Total phenolic content (TPC) and total anthocyanin content (TAC) (B) Profile of cyanidin-3-glucoside (C) Profiles of gallic acid and protocatechuic acid. Error bars represent standard deviations (SD) with n = 3.

Throughout the fermentation process, the concentration of cyanidin-3-glucoside gradually increased until day 10, after which it declined on day 12 (Figure 1B). This behavior suggests that the anthocyanin underwent biotransformation towards the end of the fermentation process. Similarly, the concentration of protocatechuic acid also increased until day 10, and then decreased on day 12 (Figure 1C). Protocatechuic acid was identified as a primary degradation product of cyanidin-3-glucoside and was also detected in jabuticaba peel at a concentration of 33.9 ± 5.0 mg/100 g (Kay et al., 2009; Quatrin et al., 2019). Its formation may be associated with both the extraction of the peels and the degradation of anthocyanins. The decrease in the content of protocatechuic acid at the end of fermentation can be explained by other reactions occurring during alcoholic fermentation, such as the conversion of this phenolic acid to catechol formed through decarboxylation, and vanillic acid, produced via methylation (Leonard et al., 2021)

In this study, there was a significant increase in the concentration of gallic acid during fermentation (Figure 1C). This increase could be linked to the extraction of this compound from jabuticaba, as it is already found naturally in high concentrations in this fruit peel (16.979 ± 0.636 mg/100 g) (Neves et al., 2021).

As the process of extracting the compounds into the medium and the biotransformation can occur simultaneously, it can be challenging to identify the moment when the degradation of the compounds begins to occur. In addition, the biotransformation reactions are complex, which makes it difficult to identify in detail the degradation and derivatization pathways of specific phenolics (Chen et al., 2023). Gallic acid and protocatechuic acid, for example, can be formed by the metabolism of other compounds present in the medium, such as other flavonoids and tannins (Leonard et al., 2021).

3.3. Identification of compounds through HRMS

Eight compounds were identified in the alcoholic fermented beverage (AF) and matured alcoholic fermented beverage (MAF) through HRMS analysis (Table 1). It was observed that the obtained error values were low, indicating that the measured m/z values were close to the expected values for the [M-H]- ions of the compounds. Cyanidin-3-glucoside was identified in both samples, being the main anthocyanin present in jabuticaba and contributing significantly to its sensory and bioactive properties. Additionally, gallic, protocatechuic, and ellagic acids, categorized as hydroxybenzoic acids, were identified. Quinic acid, classified as a hydroxycinnamic acid, was also identified, enriching the diversity of detected phenolic

compounds. Furthermore, the organic acids, citric acid and dehydroascorbic acid, as well as ethyl gallate or syringic acid, which share the same m/z, were identified. The matured sample had the same profile of compounds as the AF sample, indicating that the maturation conditions applied did not result in significant changes in the sample composition for the compounds analyzed.

Table 1 – Compounds identified through High-resolution mass spectrometry (HRMS) analysis

Compounds	Ion formula [M-H]$^-$	m/z [M-H]$^-$	AF		MAF	
			meas. m/z	error (ppm)	meas. m/z	error (ppm)
Cyanidin-3-glucoside	$C_{21}H_{19}O_{11}$	447.0933	447.0950	-3.9	447.0950	-3.9
Protocatechuic acid	$C_7H_5O_4$	153.0193	153.0200	-4.5	153.0191	1.7
Gallic acid	$C_7H_5O_5$	169.0142	169.0144	1.1	169.0144	1.0
Dehydroascorbic acid	$C_6H_5O_6$	173.0092	173.0091	0.3	173.0091	0.3
Citric acid	$C_6H_7O_7$	191.0197	191.0201	1.8	191.0201	1.8
Quinic acid	$C_7H_{11}O_6$	191.0561	191.0556	-2.5	191.0556	-2.5
Ethyl gallate or syringic acid	$C_9H_9O_5$	197.0455	197.0469	-6.7	197.0469	-6.7
Ellagic acid	$C_{14}H_5O_8$	300.9990	301.0000	3.9	300.9986	-1.2

AF: alcoholic fermented beverage; MAF: matured a lcoholic fermented beverage.

3.4. Concentration of phenolic compounds and bioaccessibility after *in vitro* gastrointestinal digestion

The AF and MAF samples showed higher content of TPC, TAC, cyanidin-3-glucoside, gallic acid, and protocatechuic acid compared to the control ($p<0.05$) (Table 2). During maturation, phenolic compounds can undergo oxidative and polymerization reactions, resulting in new structures that contribute to changes in the color and flavor of wines and can also impact their bioactive properties (Jordão and Ricardo-da-Silva, 2019; Oliveira et al., 2015). However, for the maturation conditions employed, no significant differences were found in the concentrations of phenolic compounds analyzed for the MAF sample compared to the fermented sample (AF).

During fermentation, phenolic compounds are released from the food matrix and can possibly be bioconverted into more bioaccessible chemical forms, which can increase their absorption and utilization by the organism (Leonard et al., 2021). Bioaccessibility is defined as the amount of an ingested compound available for absorption after digestion and directly influences the absorption of compounds and their bioactive potential (Cianciosi et al., 2022). In the present study, despite the increase in the concentration of total phenolics at the end of alcoholic fermentation, there was no significant increase in the bioaccessibility of these compounds (Table 2). The bioaccessible fraction of total phenolics was lower for the AF and MAF samples compared to the control ($p<0.05$).

Regarding the bioaccessibility of total anthocyanins, there was no significant difference between samples ($p>0.05$). Anthocyanins are highly unstable in the intestinal environment due to pH and the presence of enzymes (Faria et al., 2013), which explains their low bioaccessibility.

Table 2 - Quantification of phenolics compounds and bioaccessibility after *in vitro* digestion

	Samples	Non-digested	Digested	Bioaccessibility (%)
Total phenolic content (TPC) (µg GAE/mL)	Control	126.67 ± 2.68^{B}	60.31 ± 0.13^{B}	47.63 ± 0.93^{A}
	AF	622.12 ± 5.40^{A}	125.15 ± 1.62^{A}	20.12 ± 0.09^{B}
	MAF	626.40 ± 1.71^{A}	126.92 ± 1.72^{A}	20.26 ± 0.22^{B}
Total anthocyanins content (TAC) (µg C3G/mL)	Control	26.30 ± 4.59^{B}	4.04 ± 0.92^{B}	15.35 ± 2.02^{A}
	AF	144.28 ± 6.01^{A}	23.96 ± 8.11^{A}	16.58 ± 5.52^{A}
	MAF	149.62 ± 7.46^{A}	31.73 ± 1.10^{A}	21.24 ± 1.38^{A}
Cyanidin-3-glucoside (µg/mL)	Control	6.40 ± 0.00^{B}	0.00 ± 0.00^{B}	0.00 ± 0.00^{B}
	AF	13.16 ± 4.75^{AB}	5.53 ± 0.14^{A}	36.30 ± 4.66^{A}
	MAF	14.62 ± 0.21^{A}	5.26 ± 0.80^{A}	35.98 ± 5.53^{A}
Gallic acid (µg/mL)	Control	2.53 ± 0.14^{B}	0.00 ± 0.00^{C}	0.00 ± 0.00^{C}
	AF	143.72 ± 1.83^{A}	3.18 ± 0.11^{B}	2.21 ± 0.09^{B}
	MAF	173.82 ± 31.08^{A}	5.65 ± 0.74^{A}	3.27 ± 0.14^{A}
Protocatechuic acid (µg/mL)	Control	8.89 ± 0.82^{B}	3.40 ± 0.14^{C}	38.40 ± 3.65^{B}
	AF	12.18 ± 0.66^{A}	9.11 ± 0.38^{B}	75.04 ± 6.44^{A}
	MAF	14.13 ± 1.17^{A}	11.51 ± 1.29^{A}	81.77 ± 10.60^{A}

Values are expressed as means ± standard deviation (n = 3). Means followed by different letters in the same column indicate significant difference ($p<0.05$). AF: alcoholic fermented beverage; MAF: matured alcoholic fermented beverage.

Fermentation can influence the bioaccessibility of phenolic compounds in foods differently, which may be associated with the type of microorganism used in fermentation and the food matrix, which can influence the release and solubility of phenolic compounds during the digestive process (Leonard et al., 2021). Some studies have reported an increase in the bioaccessibility of phenolic compounds after fermentation, as observed for Chinese goji pulp (Dong et al., 2023), orange juice (Barreto et al., 2023), pitaya pulp (Morais et al., 2019) and grapes (Lingua et al., 2018). In contrast, other studies have reported a reduction in the proportion of bioaccessible phenolics after *in vitro* digestion (Chen et al., 2019; Khan et al., 2020).

Despite the decrease in the bioaccessible fraction of total phenolic compounds, there was a significant increase in the bioaccessibility of cyanidin-3-glucoside, gallic acid and

protocatechuic acid. The AF and MAF samples showed greater bioaccessibility of these compounds than the control ($p<0.05$). Furthermore, maturation increased the bioaccessibility of gallic acid. During the digestion process, protocatechuic acid showed superior bioaccessibility compared to other compounds. This result can be attributed to its formation due to the degradation of cyanidin-3-glucoside. Thus, this may have contributed to a greater concentration of this compound at the end of digestion.

The effect of fermentation is also related to the type of phenolic compound present in the food, which may explain the results obtained. Opposite effects on bioaccessibility have already been observed for different compounds. For example, in a study with cajá and umbu pulp fermented with different yeasts, it was verified that fermentation reduced the bioaccessibility of procyanidin A2, caftaric acid, chlorogenic acid and syringic acid, regardless of the yeast used. On the other hand, there was an increase in the bioaccessibility of other phenolic compounds, such as procyanidin B2, gallic acid, p-coumaric acid, epicatechin and catechin (Macedo et al., 2023).

The alcoholic fermentation of jabuticaba proved to be efficient in extracting compounds from the food matrix into the medium and in the biotransformation of cyanidin-3-glucoside, generating a beverage with a higher content of phenolic compounds. This high concentration favored greater bioaccessibility of these compounds at the end of digestion. Besides that, the more complex matrix found in the jabuticaba wine may have contributed to the higher bioaccessibility of the compounds since the interaction with other components present in the sample can alter the digestion of phenolic compounds (Eseberri et al., 2022). Therefore, the alcoholic fermentation of jabuticaba offers a promising approach for obtaining a higher bioaccessible fraction of phenolic compounds, which may have bioactive effects on health.

3.5. Antiproliferative activity

Scientific studies have also investigated the antiproliferative activity of compounds present in foods, such as jabuticaba (Leite-legatti et al., 2012). However, to the best of our knowledge, this is the first study exploring the antiproliferative effect of jabuticaba alcoholic beverages against human cancer cell lines and non-cancerous cell line (Figure 2). All samples significantly reduced the viability of MCF-7 cancerous cells at concentrations of 1000 µg/mL and 100 µg/mL ($p<0.05$). For MV3 cells, only the AF and DMAF samples reduced viability at 100 µg/mL, while all samples significantly impacted this cell line at 1000 µg/mL ($p<0.05$).

Regarding non-cancerous HEK293T cells, only the control and digested samples showed a significant cytotoxic effect at a concentration of 1000 µg/mL ($p<0.05$) (Figure 2)

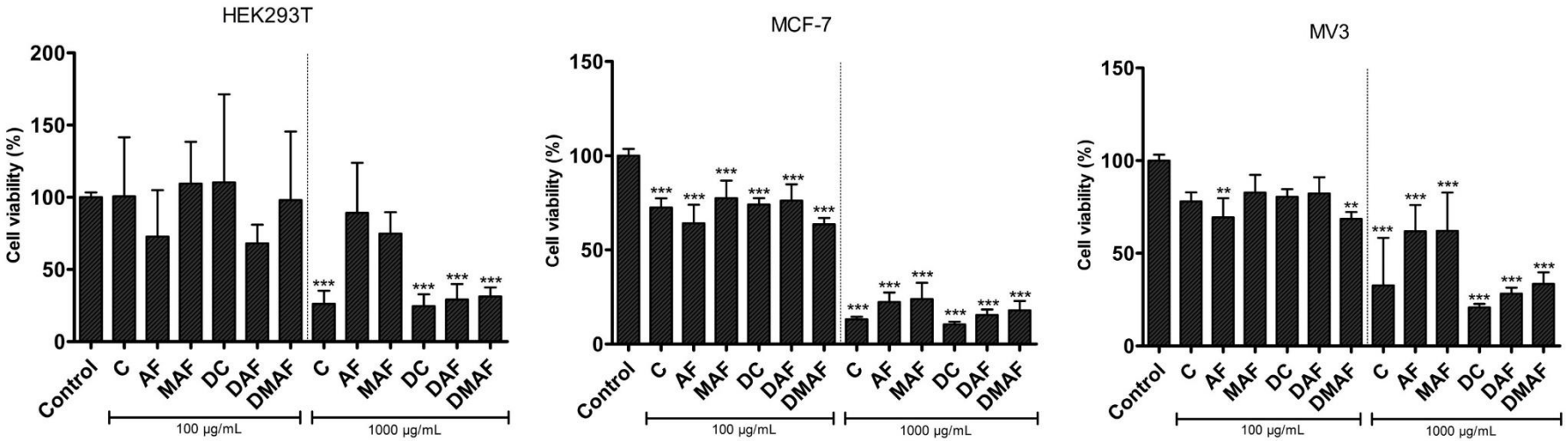

Figure 2

Inhibition of proliferation of metastatic melanoma cell line (MV3), breast cancer cell line (MCF-7), and Human Embrionary Kidney (HEK293T) after 48 h exposure to digested and non-digested jabuticaba beverages. Results were expressed as mean ± standard deviation of two independent assays with internal quadruplicates for each of them. Statistically significant differences between the control (untreated cells) and the samples were identified using Dunnett's test (∗p<0.05; ∗∗p<0.01; ∗∗∗ p<0.001). C: control; AF: alcoholic fermented beverage; MAF: matured alcoholic fermented beverage; DC: digested control; DAF: digested alcoholic fermented beverage; DMAF: digested matured alcoholic fermented beverage.

All tested samples exhibited a dose-dependent inhibitory effect on cell growth after 48 h of exposure. The concentrations of the samples that inhibited cell growth by 50% (IC50) are presented in Table 3. Jabuticaba beverages inhibited all the cell lines, but for the HEK293T cells, the IC50 values were higher than for the FA and FAM samples compared to the cancerous cells. These results suggest that the samples had a more significant cytotoxic impact on cancer cell lines than on normal cells.

Table 3 - Inhibition of proliferation (IC_{50}) of metastatic melanoma cell line (MV3), breast cancer cell line (MCF-7) and Human Embrionary Kidney cells (HEK293T) after 48 h exposure to digested and non-digested jabuticaba beverages

Samples	HEK293T		MCF-7		MV3	
	Non-digested	Digested	Non-digested	Digested	Non-digested	Digested
Control	391.60	281.50	463.2	472.6	458.4	571.2
AF	983.80	247.80	408.1	485.2	414.0	659.6
MAF	>1000	253.60	487.8	467.2	919.3	410.9

IC50: the concentration of the sample that inhibits growth by 50%.

The observed cytotoxic potential can be associated with the phenolic compounds present in the samples. Studies have shown that phenolic compounds can inhibit cell growth of several cancer cell lines. The antioxidant property of phenolic compounds is attributed as one of the primary mechanisms associated with the antiproliferative potential of these compounds (Chimento et al., 2023). In addition, polyphenols can interfere with different signaling pathways associated with cell proliferation, differentiation, migration, angiogenesis, metastasis, and cell death (Chimento et al., 2023).

Since this is a complex sample, it is important to consider that the cytotoxicity observed may result from the combined effects of the different compounds in the samples since other components can also exert this effect. This is the case, for example, of sodium metabisulphite added to the samples, which can inhibit cell proliferation (Alimohammadi et al., 2021; Ghasemi et al., 2022). The sucrose concentration may also have contributed to this result since high sucrose concentrations can also affect cytotoxicity (Yamamoto et al., 2015).

Despite having a significantly lower concentration of phenolic compounds than the fermented samples, the control (C) showed a considerable cytotoxic effect. This result can be explained by the presence of sodium metabisulphite in this sample and the higher concentration of sucrose, which may have affected cytotoxicity. During alcoholic fermentation, sulfite can be

available in two main forms, including free forms (SO2, SO32-, HSO3- e H2SO3) and bound forms (bound to ketones, aldehydes, and phenolics), reducing the amount of free sulfites to react. In addition, part of the metabisulfite can be released as sulfur dioxide during fermentation, which can also decrease the concentration of this compound (Varo et al., 2022).

The matured sample (MAF) exhibited higher IC50 values than C and AF for all three studied cell lines. These results indicate that maturation decreased the cytotoxic potential of the alcoholic fermented jabuticaba beverage against cancer cells. As previously mentioned, during maturation, the formation of new phenolic compounds with greater structural complexity can either impair or potentially confer new bioactive properties (Oliveira et al., 2015). Although no significant differences were observed in the concentration of the analyzed compounds between the AF and MAF samples, it is possible that biotransformation of other compounds, which were not covered by the analyses performed, may have occurred. Therefore, further analyses are necessary for a broader evaluation of the compounds present in the samples.

Regarding cytotoxic effects, it is also important to highlight that the transformation of phenolic compounds in the human gastrointestinal tract can influence their biological activity, including antiproliferative activity (Carmo et al., 2018). This is due to the metabolization and degradation reactions occurring during digestion. The digested samples exhibited lower IC50 values for HEK293T cells, indicating that digestion increased the cytotoxic potential of the samples against this cell type. For melanoma cells (MV3), digestion increased the cytotoxic potential of the matured sample and reduced the cytotoxicity of samples C and FA. For breast cancer cells, the IC50 values remained similar to those before digestion. It is noteworthy that the increased cytotoxicity observed could also have been impacted by the digestion residues present in the samples, as these residues per se can present toxicity to the cells depending on the concentration (Vital et al., 2024).

The different behaviors observed for the different cell lines can be attributed to the differences between cellular metabolic phenotypes, making the results cell-dependent (Carmo et al., 2018; Garcia-Guasch et al., 2023). However, in general, the results suggest that the compounds resulting from the digestion of the samples still possess the ability to interact with cells and exert inhibitory effects on their proliferation.

3.6. Antioxidant activity

Some studies have shown that fermentation can increase the antioxidant activity in certain foods, such as jussara and pitaya pulp and blueberry juice (Braga et al., 2018; Gao et

al., 2022; Morais et al., 2019). This effect may be associated with the biotransformation of phenolic compounds into compounds with greater antioxidant activity and the release of these compounds from the food matrix (Leonard et al., 2021). The antioxidant activity of the beverages before and after fermentation was estimated by the free radical scavenging methods ABTS and DPPH to determine how fermentation and maturation of jabuticaba beverages affect this property and the behavior after *in vitro* digestion.

Considering the ABTS and DPPH assays, jabuticaba fermentation resulted in remarkably significant increases in antioxidant activity. The antioxidant activity of the AF and MAF samples was approximately 5 times greater than that of the control sample. This result can be attributed both to the increase in phenolic content in these beverages due to the extraction of phenolic compounds, and to the biotransformation reactions that occurred during fermentation (Figure 3).

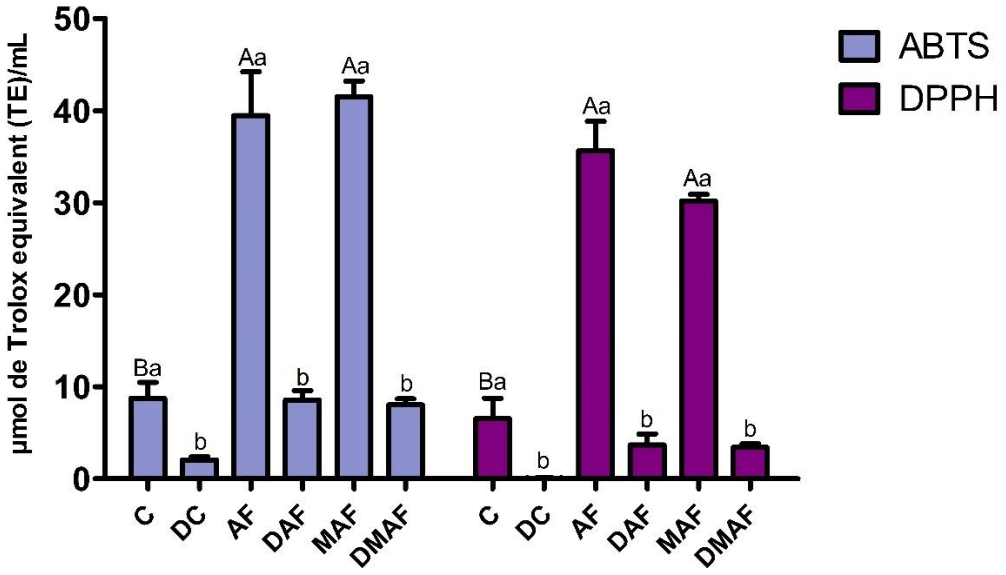

Figure 3

Effects of alcoholic fermentation, maturation and *in vitro* digestion on the antioxidant activity of jabuticaba. Values are expressed as means ± standard deviation (n = 3). Different uppercase letters indicate significant difference between undigested samples ($p<0.05$). Different lowercase letters indicate significant difference between the undigested sample and the correspondent digested sample ($p<0.05$). C: control; AF: alcoholic fermented beverage; MAF: matured alcoholic fermented beverage; DC: digested control; DAF: digested alcoholic fermented beverage; DMAF: digested matured alcoholic fermented beverage.

After undergoing *in vitro* digestion, the antioxidant activity of samples C, AF, and MAF decreased by 75.95 ± 4.49%, 78.29 ± 0.70%, and 80.64 ± 0.74%, respectively, for the ABTS method, and 98.77 ± 0.69%, 89.79 ± 2.36%, and 88.67 ± 0.97% for the DPPH method. Although the fermented samples had a lower bioaccessibility of total phenolics at the end of digestion when compared to the control, they still exhibited higher antioxidant activity. This can be attributed to the higher concentration of phenolic compounds in these samples. Therefore, despite the reduction in antioxidant activity, the samples still had significant antioxidant potential at the end of digestion and could potentially help protect against oxidative stress.

3.7. *In vitro* digestive enzyme inhibition

Another investigated bioactive property of phenolic compounds is their ability to inhibit enzymes associated with human diseases, such as diabetes mellitus and obesity, and reduce the risk of development and complications of these diseases. It has already been demonstrated that phenolic extracts from jabuticaba peel have *in vitro* potential to inhibit α-glucosidase and lipase (Borges et al., 2022). These enzymes are involved in the metabolism of carbohydrates and lipids, respectively, and their inhibition may help control glycemia and fat absorption. Thus, enzymatic inhibition assays were carried out to estimate how the alcoholic fermentation of jabuticaba affects these properties (Table 4).

Table 4 - *In vitro* inhibitory activities (IC50: mg/mL) of jabuticaba beverages towards digestive enzymes

Samples	α-glucosidase		Lipase	
	Non-digested	Digested	Non-digested	Digested
Control	18.65 ± 1.99^{Ab}	51.62 ± 1.05^{Aa}	> 800	> 800
AF	4.97 ± 0.79^{Bb}	33.12 ± 1.68^{Ba}	76.95 ± 2.90^{A}	> 600
MAF	4.05 ± 0.60^{Bb}	33.31 ± 0.49^{Ba}	66.48 ± 0.67^{B}	> 600
Positive controls				
Acarbose	0.017 ± 0.00^{C}	-	-	-
Orlistat	-	-	0.21 ± 0.02^{C}	-

Values are expressed as means ± standard deviation (n = 3). Different uppercase letters in the same column indicate significant difference between the samples and means followed by different lowercase letters in the same line indicate significant difference between the undigested sample and the correspondent digested sample ($p<0.05$).

All samples inhibited the α-glucosidase in a dose-dependent manner, with the highest inhibitory potential being verified for the AF and MAF samples ($p<0.05$) (Table 4). Compared to the acarbose positive control, all samples showed less inhibition ($p<0.05$). After *in vitro* digestion, the samples had their inhibitory potential reduced, which was verified by the increase in IC50 values. At the end of digestion, the IC50 increased 2.79 ± 0.28, 6.79 ± 1.16, and 8.34 ± 1.17-fold for samples C, AF, and MAF, respectively.

Concerning the lipase enzyme, only the fermented samples showed inhibitory capacity, and it was not possible to estimate the IC50 value for the control sample at the tested concentrations. This result can be attributed to higher levels of phenolic compounds in the AF and MAF samples compared to the unfermented control. The matured sample had a lower IC50 value than the AF sample ($p<0.05$), which may be related to the phenolic profile of this sample. The samples had a lower inhibitory potential than orlistat, an inhibitory drug used to treat obesity ($p<0.05$).

After *in vitro* digestion, it was not possible to detect the IC50 for the samples tested at the maximum concentration of 600 mg/mL. The lower inhibitory potential verified against the lipase enzyme in the samples can be explained by the lower susceptibility of this enzyme to the action of the compounds present in the samples. A similar trend was observed for extracts from jabuticaba peel, which exhibited higher IC50 values for the lipase (15.05 ± 0.98 mg/mL)

compared to α-glucosidase (0.47 ± 0.04 mg/mL) (Borges et al., 2022). Similarly, compounds from native Chilean red strawberries exhibited a more significant inhibitory effect on α-glucosidase compared to lipase. The IC50 value for α-glucosidase was 0.80 ± 0.06 μg/mL, whereas, at a concentration of 50 μg/mL, the same sample inhibited lipase by only 41.36 ± 0.30% (Thomas-valdés et al., 2019).

During digestion, the concentration of compounds decreased, leading to a reduction in the inhibition capacity. Additionally, the digestive process may result in the formation of other metabolites, which have less inhibitory potential compared to the initial compounds. However, even after digestion, the samples still exhibited some inhibitory effects on the digestive enzymes. This finding is in agreement with previous reports, showing a reduction of the enzyme inhibition activity due to the effects of digestion (Burgos-edwards et al., 2017; Thomas-valdés et al., 2019; Thomas-Valdés et al., 2018).

4. Conclusion

This study has demonstrated that the fermentation of jabuticaba fruit using *Saccharomyces cerevisiae* significantly enhanced the levels of total phenolic content (4.91 ± 0.07-fold), total anthocyanin content (5.62 ± 1.17-fold), and phenolic acids (57.02 ± 3.70-fold for gallic acid and 3.70 ± 0.51-fold for protocatechuic acid). The fermentation process also increased the bioaccessibility of cyanidin-3-glucoside (36.30 ± 4.66%), gallic acid (2.21 ± 0.09%), and protocatechuic acid (75.04 ± 6.44%). The samples also showed antiproliferative effects against cancer cells, antioxidant activities, and enzyme inhibition properties. After digestion, the concentration of phenolic compounds was reduced, but the samples still showed bioactive potential, although to a minor extent. The maturation conditions increased the bioaccessibility of gallic acid and reduced the cytotoxicity against cells. The comprehensive analysis conducted pre- and post-fermentation has provided valuable insights into the specific changes in the phytochemical profile of jabuticaba wine, revealing mechanisms by which fermentation can enhance the potential health benefits of this underutilized fruit. This study also highlights the potential of jabuticaba in the production of wine with functional properties, offering an alternative for product development in the food and beverage industry. Future research should focus on exploring *in vivo* health benefits and evaluating consumer acceptance of jabuticaba wine.

CRediT authorship contribution statement

L. L. R. Borges: Conceptualization, Methodology, Validation, Investigation, Data curation, Formal analysis, Writing - original draft, Writing - review & editing. **V. V. Freitas**: Investigation, Writing - review & editing. **A. L. A. A. Nascimento**: Investigation, Writing - review & editing. **J. G. Fernandes**: Investigation, Writing - review & editing. **H. B. Kobi**: Investigation, Writing - review & editing. **M. R. Eller**: Conceptualization, Methodology, Resources, Writing - review & editing. **F. A. R. de Barros**: Conceptualization, Methodology, Writing - review & editing. **L. A. de Souza**: Investigation, Writing - review & editing. **G. A. D. Castro**: Investigation, Writing - review & editing. **A. F. de Carvalho**: Investigation. **J. A. Bezerra**: Resources, Investigation. **S. A. Fernandes**: Resources, Writing - review & editing. **G. C. Bressan**: Resources, Writing - review & editing. **E. Martins**: Writing - review & editing. **P. H. Campelo**: Conceptualization, Methodology, Writing - review & editing. **P. C. Stringheta**: Conceptualization, Methodology, Resources, Supervision, Project administration, Funding acquisition, Writing - review & editing.

Declaration of Competing Interest

The authors declare no conflict of interest.

Acknowledgments

We gratefully acknowledge Coordenação de Aperfeiçoamento de Pessoal de Nível Superior (CAPES, Finance Code 001) - Brazil, Conselho Nacional de Desenvolvimento Científico e Tecnológico (CNPq) - Brazil and Fundação de Amparo à Pesquisa do Estado de Minas Gerais (FAPEMIG) - Brazil for financial support. We would also like to thank Bioclin for donating kits for analyses and the Analytical Center of INPA (CA-LTQPN).

References

Adisakwattana, S., Chantarasinlapin, P., Thammarat, H., Yibchok-anun, S., 2009. A seriesof cinnamic acid derivatives and their inhibitory activity on intestinal α -glucosidase. J Enzyme Inhib Med Chem 24, 1194–1200. https://doi.org/10.1080/14756360902779326

Albuquerque, B.R., Pereira, C., Calhelha, R.C., Alves, M.J., Abreu, R.M.V., Barros, L., Oliveira, M.B.P.P., Ferreira, I.C.F.R., 2020. Jabuticaba residues (*Myrciaria jaboticaba* (Vell.)

Berg) are rich sources of valuable compounds with bioactive properties. Food Chem 309, Article 125735. https://doi.org/10.1016/j.foodchem.2019.125735

Alezandro, M.R., Granato, D., Genovese, M.I., 2013. Jaboticaba (*Myrciaria jaboticaba* (Vell.) Berg), a Brazilian grape-like fruit, improves plasma lipid profile in streptozotocin-mediated oxidative stress in diabetic rats. Food Research International 4, 650–659. https://doi.org/10.1016/j.foodres.2013.07.041

Alimohammadi, A., Moosavy, M., Amin, M., 2021. Sodium metabisulfite as a cytotoxic food additive induces apoptosis in. Food Chem 358, 129910. https://doi.org/10.1016/j.foodchem.2021.129910

Ávila, M., Hidalgo, M., Sánchez-moreno, C., Pelaez, C., Requena, T., Pascual-teresa, S. De, 2009. Bioconversion of anthocyanin glycosides by *Bifidobacteria* and *Lactobacillus*. Food Research International 42, 1453–1461. https://doi.org/10.1016/j.foodres.2009.07.026

Barreto, S.M.A., Silva, A.B.M. da, Dutra, M. da C.P., Bastos, D.C., Carvalho, A.J. de B.A., Viana, A.C., Narain, N., Marcos dos Santos Lima, 2023. Effect of commercial yeasts (*Saccharomyces cerevisiae*) on fermentation metabolites, phenolic compounds, and bioaccessibility of Brazilian fermented oranges. Food Chem 408, 135121. https://doi.org/10.1016/j.foodchem.2022.135121

Batista, Â.G., Lenquiste, S.A., Cazarin, C.B.B., Silva, J.K. da, Luiz-Ferreira, A., Bogusz, S., Hantao, L.W., Souza, R.N. de, Augusto, F., Prado, M.A., Maróstica, M.R., 2014. Intake of jaboticaba peel attenuates oxidative stress in tissues and reduces circulating saturated lipids of rats with high-fat diet-induced obesity. J Funct Foods 6, 450–461. https://doi.org/10.1016/j.jff.2013.11.011

Bernardes, A.L., Moreira, J.A., Tostes, M. das G.V., Costa, N.M.B., Silva, P.I., Costa, A.G.V., 2019. *In vitro* bioaccessibility of microencapsulated phenolic compounds of jussara (*Euterpe edulis* Martius) fruit and application in gelatine model-system. Lwt 102, 173–180. https://doi.org/10.1016/j.lwt.2018.12.009

Borges, L.L.R., Oliveira, L.L. de, Freitas, V.V., Leite Júnior, B.R. de C., Nascimento, A.L.A.A., Castro, G.A.D., Fernandes, S.A., Stringheta, P.C., 2022. Digestive enzymes inhibition, antioxidant and antiglycation activities of phenolic compounds from jabuticaba (*Plinia cauliflora*) peel. Food Biosci 50, 102195. https://doi.org/10.1016/j.fbio.2022.102195

Braga, A.R.C., Mesquita, L.M. de S., Martins, P.L.G., Habu, S., Rosso, V.V. de, 2018. Lactobacillus fermentation of jussara pulp leads to the enzymatic conversion of anthocyanins increasing antioxidant activity. Journal of Food Composition and Analysis 69, 162–170. https://doi.org/10.1016/j.jfca.2017.12.030

BRASIL, 2012. Instrução normativa n° 34 de 29 de dezembro de 2012. Dispõe sobre os padrões de identidade e qualidade para bebidas fermentadas.

Burgos-edwards, A., Jiménez-aspee, F., Thomas-valdés, S., Schmeda-hirschmann, G., Theoduloz, C., 2017. Qualitative and quantitative changes in polyphenol composition and bioactivity of *Ribes magellanicum* and *R . punctatum* after *in vitro* gastrointestinal digestion. Food Chem 237, 1073–1082. https://doi.org/10.1016/j.foodchem.2017.06.060

Cagno, R. Di, Filannino, P., Gobbetti, M., Aldo, B., 2016. Fermented Foods: Fermented Vegetables and Other Products, in: Caballero, B., Finglas, P., Toldrá, F. (Eds.), Encyclopedia of Food and Health. Academic Press, Oxford, pp. 668–674. https://doi.org/10.1016/B978-0-12-384947-2.00284-1

Carmo, M.A.V. do, Pressete, C.G., Marques, M.J., Granato, D., Azevedo, L., 2018. Polyphenols as potential antiproliferative agents: scientific trends. Curr Opin Food Sci 24, 26–35. https://doi.org/10.1016/j.cofs.2018.10.013

Chen, W., Xie, C., He, Q., Sun, J., Bai, W., 2023. Improvement in color expression and antioxidant activity of strawberry juice fermented with lactic acid bacteria: A phenolic-based research. Food Chem X 17, 100535. https://doi.org/10.1016/j.fochx.2022.100535

Chen, Y., Ma, Y., Dong, L., Jia, X., Liu, L., Huang, F., Chi, J., Xiao, J., Zhang, M., Zhang, R., 2019. Extrusion and fungal fermentation change the profile and antioxidant activity of free and bound phenolics in rice bran together with the phenolic bioaccessibility. Lwt 115, 108461. https://doi.org/10.1016/j.lwt.2019.108461
Chimento, A., Luca, A. De, Amico, M.D., Amicis, F. De, 2023. The Involvement of Natural Polyphenols in Molecular Mechanisms Inducing Apoptosis in Tumor Cells: A Promising Adjuvant in Cancer Therapy. Int J Mol Sci 24, 1680.

Cianciosi, D., Forbes-hern, T.Y., Regolo, L., Alvarez-suarez, M., Navarro-hortal, M.D., Xiao, J., Battino, M., Giampieri, F., 2022. The reciprocal interaction between polyphenols and other dietary compounds: Impact on bioavailability , antioxidant capacity and other physico-chemical and nutritional parameters. Food Biosci 375, 1–13.

Da Silva, P.H.A., De Faria, F.C., Tonon, B., José, S., Mota, D., Pinto, V.T., 2008. Avaliação da composição química de fermentados alcoólicos de jabuticaba (*Myrciaria jabuticaba*). Quim. Nova 31, 595–600.

Dong, X., Qi, J., Xu, K., Li, B., Xu, H., Tian, X., Lei, H., 2023. Effect of lactic acid fermentation and *in vitro* digestion on the bioactive compounds in Chinese wolfberry (*Lycium barbarum)* pulp. Food Biosci 53, 102558. https://doi.org/10.1016/j.fbio.2023.102558

Dragano, N.R.V., Marques, A.Y.C., Cintra, D.E.C., Solon, C., Morari, J., Leite-Legatti, A. V., Velloso, L.A., Maróstica-Júnior, M.R., 2013. Freeze-dried jaboticaba peel powder improves insulin sensitivity in high-fat-fed mice. British Journal of Nutrition 110, 447–455. https://doi.org/10.1017/S0007114512005090

Duarte, W.F., Dias, D.R., Oliveira, J.M., Vilanova, M., Teixeira, J.A., Almeida, J.B., Schwan, R.F., 2010. Raspberry (*Rubus idaeus* L.) wine: Yeast selection, sensory evaluation and instrumental analysis of volatile and other compounds. Food Research International 43, 2303–2314. https://doi.org/10.1016/j.foodres.2010.08.003

Eseberri, I., Trepiana, J., Léniz, A., Gómez-García, I., Carr-Ugarte, H., González, M., Portillo, M.P., 2022. Variability in the Beneficial Effects of Phenolic Compounds: A Review. Nutrients 14. https://doi.org/10.3390/nu14091925

Faria, A., Fernandes, I., Mateus, N., Calhau, C., 2013. Bioavailability of Anthocyanins, in: Ramawat, K.G., Merillon, J.M. (Eds.), Natural Products. Springer, Berlin, pp. 2465–2487. https://doi.org/10.1007/978-3-642-22144-6

Fuleki, T., Francis, F.J., 1968. Quantitative Methods for Anthocyanins. 1. Extraction and Determination of Total Anthocyanin in Cranberries. J Food Sci 33, 72–77. https://doi.org/10.1111/j.1365-2621.1968.tb00887

Gao, B., Wang, J., Wang, Y., Xu, Z., Li, B., Meng, X., Sun, X., Zhu, J., 2022. Influence of fermentation by lactic acid bacteria and *in vitro* digestion on the biotransformations of blueberry juice phenolics. Food Control 133, 1–9. https://doi.org/10.1016/j.foodcont.2021.108603

Garcia, L.G.C., da SILVA, E.P., E Silva Neto, C. de M., Vilas Boas, E.V. de B., Asquieri, E.R., Damiani, C., da SILVA, F.A., 2019. Effect of the addition of calcium chloride and different storage temperatures on the post-harvest of jabuticaba variety Pingo de mel. Food Science and Technology (Brazil) 39, 261–269. https://doi.org/10.1590/fst.02318

Garcia-Guasch, M., Escrich, E., Moral, R., Duarte, I.F., 2023. Metabolomics Insights into the Differential Response of Breast Cancer Cells to the Phenolic Compounds Hydroxytyrosol and Luteolin. Molecules 28. https://doi.org/10.3390/molecules28093886

Ghasemi, A., Salari, A., Amiryousefi, M.R., 2022. Sodium metabisulfite in dried plum and its cytotoxic effects on K-562 and L-929 normal cell lines. J Food Sci 856–866. https://doi.org/10.1111/1750-3841.16034

Inada, K.O.P., Leite, I.B., Martins, A.B.N., Fialho, E., Tomas-Barberan, F.A., Perrone, D., Monteiro, M., 2021. Jaboticaba berry: A comprehensive review on its polyphenol composition, health effects, metabolism, and the development of food products. Food Research International 147, 110518.

Inada, K.O.P., Oliveira, A.A., Revorêdo, T.B., Martins, A.B.N., Lacerda, E.C.Q., Freire, A.S., Braz, B.F., Santelli, R.E., Torres, A.G., Perrone, D., Monteiro, M.C., 2015. Screening of the chemical composition and occurring antioxidants in jabuticaba (*Myrciaria jaboticaba*) and jussara (*Euterpe edulis*) fruits and their fractions. J Funct Foods 17, 422–433. https://doi.org/10.1016/j.jff.2015.06.002

Inada, K.O.P., Silva, T.B.R., Lobo, L.A., Domingues, R.M.C.P., Perrone, D., Monteiro, M., 2020. Bioaccessibility of phenolic compounds of jaboticaba (*Plinia jaboticaba*) peel and seed after simulated gastrointestinal digestion and gut microbiota fermentation. J Funct Foods 67, Article 103851. https://doi.org/10.1016/j.jff.2020.103851

Jagtap, U.B., Bapat, V.A., 2015. Wines from fruits other than grapes: Current status and future prospectus. Food Biosci 9, 80–96. https://doi.org/10.1016/j.fbio.2014.12.002

Jordão, A.M., Ricardo-da-Silva, J.M., 2019. Evolution of Proanthocyanidins During Grape Maturation, Winemaking, and Aging Process of Red Wines, in: Red Wine Technology. pp. 177–193. https://doi.org/https://doi.org/10.1016/B978-0-12-814399-5.00012-8 177

Kay, C.D., Kroon, P.A., Cassidy, A., 2009. The bioactivity of dietary anthocyanins is likely to be mediated by their degradation products. Mol Nutr Food Res 53, 92–101. https://doi.org/10.1002/mnfr.200800461

Khan, S.A., Zhang, M., Liu, L., Dong, L., Ma, Y., Wei, Z., Chi, J., Zhang, R., 2020. Co-culture submerged fermentation by lactobacillus and yeast more effectively improved the profiles and bioaccessibility of phenolics in extruded brown rice than single-culture fermentation. Food Chem 326, 126985. https://doi.org/10.1016/j.foodchem.2020.126985

Kim, D.O., Lee, K.W., Lee, H.J., Lee, C.Y., 2002. Vitamin C equivalent antioxidant capacity (VCEAC) of phenolic phytochemicals. J Agric Food Chem 50, 3713–3717. https://doi.org/10.1021/jf020071

Kowalczyk, B., Bieniasz, M., Kostecka-Gugała, A., 2022. The Content of Selected Bioactive Compounds in Wines Produced from Dehydrated Grapes of the Hybrid Variety 'Hibernal' as a Factor Determining the Method of Producing Straw Wines. Foods 11, 1027. https://doi.org/10.3390/foods11071027

Leite-legatti, A.V., Batista, Â.G., Dragano, N.R.V., Marques, A.C., Malta, L.G., Riccio, M.F., Eberlin, M.N., Machado, A.R.T., Carvalho-silva, L.B., Ruiz, A.L.T.G., Carvalho, J.E., Pastore, G.M., Júnior, M.R.M., 2012. Jaboticaba peel: Antioxidant compounds, antiproliferative and antimutagenic activities 49, 596–603. https://doi.org/10.1016/j.foodres.2012.07.044

Leonard, W., Zhang, P., Ying, D., Adhikari, B., Fang, Z., 2021. Fermentation transforms the phenolic profiles and bioactivities of plant-based foods. Biotechnological Progress and Beverage Consumption 49, 107763.

Lima, A. de J.B., Corrêa, A.D., Alves, A.P.C., Abreu, C.M.P., Dantas-Barros, A.M., 2008. Caracterização química do fruto jabuticaba (*Myrciaria cauliflora* Berg) e de suas frações. ALAN 58, 1–8.

Lima, A.D.J.B., Corrêa, A.D., Saczk, A.A., Martins, M.P., Castilho, R.O., 2011. Anthocyanins, pigment stability and antioxidant activity in jabuticaba [Myrciaria cauliflora (Mart.) O. Berg]. Rev. Bras. Frutic., Jaboticabal-SP 33, 877–887.

Lingua, M.S., Wunderlin, D.A., Baroni, M. V., 2018. Effect of simulated digestion on the phenolic components of red grapes and their corresponding wines. J Funct Foods 44, 86–94. https://doi.org/10.1016/j.jff.2018.02.034

Macedo, E. de L.C., Pimentel, T.C., Melo, D. de S., Souza, A.C. de, Morais, J.S. de, Lima, M. dos S., Dias, D.R., Schwan, R.F., Magnani, M., 2023. Yeasts from fermented Brazilian fruits as biotechnological tools for increasing phenolics bioaccessibility and improving the volatile profile in derived pulps. Food Chem 401, 134200. https://doi.org/10.1016/j.foodchem.2022.134200

Macedo, E.H.B.C., Jr., G.C.S., Santana, M.N., Jesus, E.F.O., Araújo, U.B. de, Anjos, M.J., Pinheiro, A.S., Carneiro, C.S., Rodrigues, I.A., 2021. Unveiling the physicochemical properties and chemical profile of artisanal jabuticaba wines by bromatological and NMR-based metabolomics approaches. LWT - Food Science and Technology 146, 111371. https://doi.org/10.1016/j.lwt.2021.111371

Marquetti, C., Batista, T., Fabiana, K., Kaipers, C., Böger, B.R., Tonial, I.B., Junior, A.W., Lucchetta, L., Vieira, N., 2018. Jaboticaba skin flour: analysis and sustainable alternative source to incorporate bioactive compounds and increase the nutritional value of cookies. Food Science and Technology 2061, 629–638.

Minekus, M., Alminger, M., Alvito, P., Ballance, S., Bohn, T., Bourlieu, C., Carrière, F., Boutrou, R., Corredig, M., Dupont, D., Dufour, C., Egger, L., Golding, M., Karakaya, S., Kirkhus, B., Le Feunteun, S., Lesmes, U., MacIerzanka, A., MacKie, A., Marze, S., McClements, D.J., Ménard, O., Recio, I., Santos, C.N., Singh, R.P., Vegarud, G.E., Wickham, M.S.J., Weitschies, W., Brodkorb, A., 2014. A standardised static *in vitro* digestion method suitable for food-an international consensus. Food Funct 5, 1113–1124. https://doi.org/10.1039/c3fo60702

Monteiro, L.M.O., Pereira, M.G., Vici, A.C., Heinen, P.R., Buckeridge, M.S., Polizeli, M. de L.T. de M., 2019. Efficient hydrolysis of wine and grape juice anthocyanins by Malbranchea pulchella β-glucosidase immobilized on MANAE-agarose and ConA-Sepharose supports. Int J Biol Macromol 136, 1133–1141. https://doi.org/10.1016/j.ijbiomac.2019.06.106

Morais, S.G.G., da Silva Campelo Borges, G., dos Santos Lima, M., Martín-Belloso, O., Magnani, M., 2019. Effects of probiotics on the content and bioaccessibility of phenolic compounds in red pitaya pulp. Food Research International 126, 108681. https://doi.org/10.1016/j.foodres.2019.108681

Moura, M.H.C., Cunha, M.G., Alezandro, M.R., Genovese, M.I., 2018. Phenolic-rich jaboticaba (*Plinia jaboticaba* (Vell.) Berg) extracts prevent high-fat-sucrose diet-induced obesity in C57BL/6 mice. Food Research International 107, 48–60. https://doi.org/10.1016/j.foodres.2018.01.071

Neves, N. de A., Stringheta, P.C., Gómez-Alonso, S., Hermosín-Gutiérrez, I., 2018. Flavonols and ellagic acid derivatives in peels of different species of jabuticaba (*Plinia* spp.) identified by HPLC-DAD-ESI/MSn. Food Chem 252, 61–71. https://doi.org/10.1016/j.foodchem.2018.01.078

Neves, N. de A., Stringheta, P.C., Silva, I.F. da, García-Romero, E., Gómez-Alonso, S., Hermosín-Gutiérrez, I., 2021. Identification and quantification of phenolic composition from different species of Jabuticaba (*Plinia* spp.) by HPLC-DAD-ESI/MSn. Food Chem 355, Article 129605. https://doi.org/10.1016/j.foodchem.2021.129605

OIV, 2021. Compendium of international methods of wine and must analysis.

Oliveira, H., Fernandes, I., Freitas, V. De, Mateus, N., 2015. Ageing impact on the antioxidant and antiproliferative properties of. Food Research International 67, 199–205.

Plaza, M., Batista, Â.G., Cazarin, C.B.B., Sandahl, M., Turner, C., Östman, E., Maróstica Júnior, M.R., 2016. Characterization of antioxidant polyphenols from *Myrciaria jaboticaba* peel and their effects on glucose metabolism and antioxidant status: A pilot clinical study. Food Chem 211, 185–197. https://doi.org/10.1016/j.foodchem.2016.04.142

Quatrin, A., Pauletto, R., Maurer, L.H., Minuzzi, N., Nichelle, S.M., Carvalho, J.F.C., Maróstica, M.R., Rodrigues, E., Bochi, V.C., Emanuelli, T., 2019. Characterization and

quantification of tannins, flavonols, anthocyanins and matrix-bound polyphenols from jaboticaba fruit peel: A comparison between *Myrciaria trunciflora* and *M. jaboticaba*. Journal of Food Composition and Analysis 78, 59–74. https://doi.org/10.1016/j.jfca.2019.01.018

Re, R., Pellegrini, N., Proteggente, A., Pannala, A., Yang, M., Rice-Evans, C., 1999. Antioxidant activity applying an improved ABTS radical cation decolorization assay. Free Radic Biol Med 26, 1231–1237. https://doi.org/10.1016/S0891-5849(98)00315-3

Rodrigues, L., Donado-pestana, C.M., Moura, H.C., Rossi, R., Pessoa, E.V.M., In, M., 2021. Phenolic compounds from jaboticaba (*Plinia jaboticaba* (Vell.) Berg) ameliorate intestinal inflammation and associated endotoxemia in obesity. Food Research International 141, 110139. https://doi.org/10.1016/j.foodres.2021.110139

Setford, P.C., Jeffery, D.W., Grbin, P.R., Muhlack, R.A., 2017. Factors affecting extraction and evolution of phenolic compounds during red wine maceration and the role of process modelling. Trends Food Sci Technol 69, 106–117. https://doi.org/10.1016/j.tifs.2017.09.005

Singh, G., Verma, A.K., Kumar, V., 2016. Catalytic properties, functional attributes and industrial applications of β-glucosidases. 3 Biotech 6, 1–14. https://doi.org/10.1007/s13205-015-0328

Singleton, V.L., Rossi, J.A.J., 1965. Colorimetry of Total Phenolics with Phosmolybdicphosphotungstic Acid Reagents. Am J Enol Vitic 16, 144–158.

Thomas-Valdés, S., Theoduloz, C., Jiménez-Aspee, F., Burgos-Edwards, A., Schmeda-Hirschmann, G., 2018. Changes in polyphenol composition and bioactivity of the native Chilean white strawberry (*Fragaria chiloensis* spp. chiloensis f. chiloensis) after *in vitro* gastrointestinal digestion. Food Research International 105, 10–18. https://doi.org/10.1016/j.foodres.2017.10.074

Thomas-valdés, S., Theoduloz, C., Jiménez-aspee, F., Schmeda-hirschmann, G., 2019. Effect of simulated gastrointestinal digestion on polyphenols and bioactivity of the native Chilean red strawberry (*Fragaria chiloensis* ssp. chiloensis f. patagonica). Food Research International 123, 106–114. https://doi.org/10.1016/j.foodres.2019.04.039

Varo, M.A., Martin-Gomez, J., Serratosa, M.P., Merida, J., 2022. Effect of potassium metabisulphite and potassium bicarbonate on color, phenolic compounds, vitamin C and antioxidant activity of blueberry wine. LWT - Food Science and Technology 163, 113585. https://doi.org/10.1016/j.lwt.2022.113585

Vernocchi, P., Ndagijimana, M., Serrazanetti, D.I., López, C.C., Fabiani, A., Gardini, F., Guerzoni, M.E., Lanciotti, R., 2011. Use of *Saccharomyces cerevisiae* strains endowed with β-glucosidase activity for the production of Sangiovese wine. World J Microbiol Biotechnol 27, 1423–1433. https://doi.org/10.1007/s11274-010-0594-1

Vital, N., Gramacho, A.C., Silva, M., Cardoso, M., Alvito, P., Kranendonk, M., Silva, M.J., Louro, H., 2024. Challenges of the Application of *In vitro* Digestion for Nanomaterials Safety Assessment. Foods 13. https://doi.org/10.3390/foods13111690

Wu, S., Long, C., Kennelly, E.J., 2013. Phytochemistry and health-benefits of jaboticaba, an emerging fruit crop from Brazil. Food Research International 54, 148–159. https://doi.org/10.1016/j.foodres.2013.06.021

Xie, X., Zhang, L., Gao, X., 2017. Phenolic Compounds Content and Antioxidant Activity of Mulberry Wine During Fermentation and Aging. Am J Food Technol 12, 367–373. https://doi.org/10.3923/ajft.2017.367.373

Yamamoto, T., Uemura, K., Moriyama, K., Mitamura, K., Taga, A., 2015. Inhibitory effect of maple syrup on the cell growth and invasion of human colorectal cancer cells. Oncol Rep 33, 1579–1584. https://doi.org/10.3892/or.2015.3777

Zhang, P., Zhang, R., Sirisena, S., Gan, R., Fang, Z., 2021. Beta-glucosidase activity of wine yeasts and its impacts on wine volatiles and phenolics: A mini-review. Food Microbiol 100, 13. https://doi.org/10.1016/j.fm.2021.103859

Supplementary material

Table S1. HPLC gradient program for phenolic acids analysis

Time (min)	Mobile phase – A (%)	Mobile phase – B (%)
0 – 15	100	0
15 – 34	100 – 80	0 – 20
34 – 35	80	20
35 – 45	80 – 60	20 – 40
45 – 51	60 – 35	40 – 65
51 – 52	35 – 5	65 – 95
52 – 54	5	95
54 – 60	100	0

Table S2. HPLC gradient program for anthocyanins analysis

Time (min)	Mobile phase – A (%)	Mobile phase – B (%)
0 – 5	100 – 95	0 – 5
5 – 10	95 – 87	5 – 13
10 – 14	87	13
14 – 15	87 – 95	13 – 5
15 – 16	95	5

Table S3. Limits established in the legislation for jabuticaba fermented beverage

	Minimum limit	Maximum limit	Classification
Fixed acidity (meq/L)	30	-	-
Total acidity (meq/L)	50	130	-
Volatile acidity (meq/L)	-	20	-
Total sulfur dioxide (g/L)	-	0,35	-
Chaptalization (% of fruit sugars)	-	50	-
Total chlorides (g/L)	-	0,5	-
Reduced dry extract (g/L)	7	-	-
Alcohol by volume (% v/v at 20 °C))	4	14	-
Pressure, in atm	2	3	Aerated
Sugar content in g/L	-	≤ 3	Dry
	>3		Sweet or soft

BRAZIL. Normative Instruction No. 34 of December 29, 2012. Establishes the identity and quality standards for fermented beverages. Brasília-DF, 2012.

Figure S1. HPLC chromatogram of anthocyanins analysis

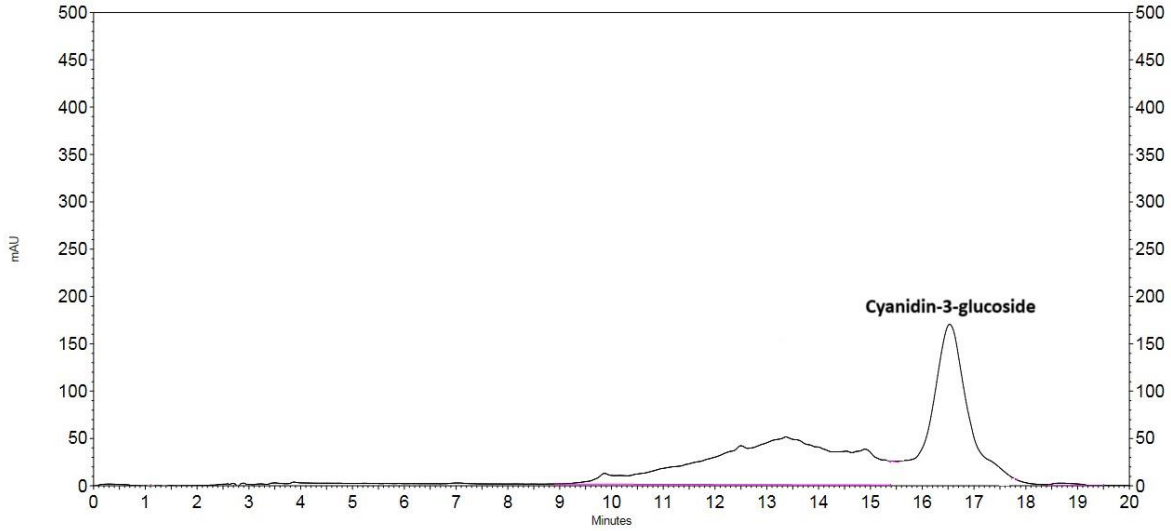

Figure S2. HPLC chromatogram of phenolic acid analysis

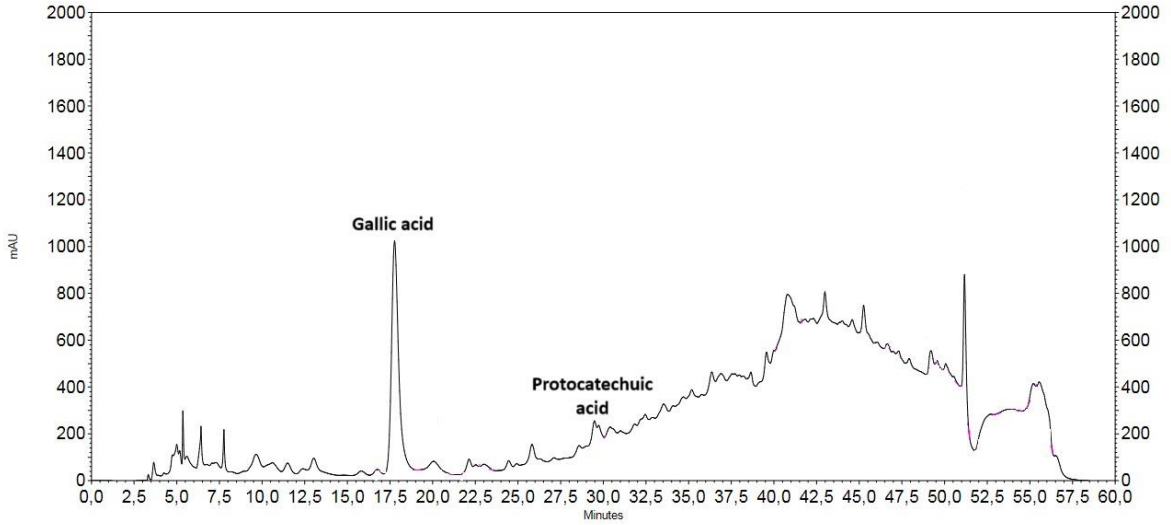

4. CHAPTER 3: Combination of whey or pea protein with gum arabic for anthocyanin encapsulation enhances bioaccessibility, alters anthocyanin metabolism, and promotes short chain fatty acid production

Abstract

This study investigated the impact of encapsulating jabuticaba extract with whey protein (WP) or pea protein (PP), combined with gum arabic (GA), on the release and bioaccessibility of anthocyanins, and on the production of phenolic metabolites and short-chain fatty acids (SCFAs), using an *in vitro* model of gastrointestinal digestion and fecal fermentation. The cross-linking interactions between the food biopolymers and the extract were confirmed by FTIR spectroscopy and the entrapment of anthocyanins and the formation of particles were verified through confocal laser scanning microscopy and scanning electron microscopy. Encapsulation improved anthocyanins bioaccessibility, with the highest increases in samples encapsulated with a higher proportion of GA (PP:GA 1:2 e WP:GA 1:2), showing an increase of 33% and 25%, respectively, compared to the free extract. Encapsulation also delayed compounds degradation during the first phases of digestion, retaining more anthocyanins and tannins in the particles and enhancing metabolites production in the colonic phase. The concentration of cyanidin-3-glucoside delivered to the colonic phase was ~18-fold higher in encapsulated samples with a higher protein ratio compared to the free extract. The wall materials influenced SCFA profiles, with WP-encapsulated samples presenting higher concentrations of straight-chain SCFAs and similar concentrations of branched-chain SCFAs to samples encapsulated with PP. Cyanidin-3-glucoside exhibited superior antioxidant and anti-inflammatory effects compared to its primary metabolites, reducing reactive oxygen species (ROS) and pro-inflammatory markers (TNF-α, IL-6, IL-8) in colon cancer cells (HT29-MTX). In conclusion, the combination of WP or PP with GA can be considered promising as a food-grade carrier for encapsulating anthocyanins, with potential applications in functional foods and dietary supplements.

Keywords: Cyanidinin-3-glucoside; Microbiota; Bioavailability; *In vitro* digestion; Colonic fermentation; Wall materials.

1. Introduction

Jabuticaba (*Plinia cauliflora*) is a fruit native to Brazil, recognized for its content of phenolic compounds, especially anthocyanins, which are responsible for the characteristic pigmentation of the peels. Other phenolic compounds already identified in the fruit are ellagitannins, gallotannins, and phenolic acids, such as gallic and ellagic acids (Inada et al.,

2020; Neves et al., 2018, 2021). The peels, representing around 30% of the mass of the fruit, are normally discarded during the fresh consumption and in the production of jabuticaba by-products (Quatrin et al., 2020). However, it is in the peels that the highest concentration of anthocyanins is found, which are recognized for their beneficial effects on human health. Thus, the peels are a potential source of anthocyanin extraction for different applications.

Several researches indicated that the continuous consumption of anthocyanins can contribute positively to human health through antioxidant, antidiabetic, anticancer, anti-inflammatory, antimicrobial, and anti-obesity effects (Albuquerque et al., 2020; Batista et al., 2014; Burton-freeman et al., 2016; Calloni et al., 2020; Lenquiste et al., 2012). Besides that, anthocyanins can also improve human health by modulating the intestinal microbiota, increasing the diversity and presence of beneficial groups such as *Bifidobacterium* and *Lactobacillus*, and stimulating the production of short-chain fatty acids (SCFAs) (Liang et al., 2023). In this context, there is a growing interest in the global market for these compounds for application as natural colorants, in the development of functional foods and beverages, and in dietary supplements (Cory et al., 2018).

However, the potential health effects of anthocyanins depend on their bioaccessibility and bioavailability. After consumption, anthocyanins can undergo several changes throughout the digestive tract due to factors such as pH, food matrix, enzymes, bile acids and intestinal microbiota (Ayvaz et al., 2023). Current evidence suggests that the bioavailability of anthocyanins *in vivo* is very low, with values below 2% (De Ferrars et al., 2014; Hornedo-Ortega et al., 2021; Zhong et al., 2017). This indicates that the observed health effects are associated not only with intact anthocyanins but also with their bioactive metabolites formed during digestion. If only the parent compounds and primary degradation products of anthocyanins are considered, the bioavailability value may be underestimated (Lila et al., 2016). Considering unmetabolized parent compounds, degradation products, phase I and phase II compounds (formed through oxidation, reduction, hydrolysis, or conjugation reactions), and metabolites generated by the microbiota, the total bioavailability may be higher (Lila et al., 2016). In particular, the role of the intestinal microbiota in metabolizing anthocyanins is considered essential in the production of diverse functional metabolites that can mediate the bioactivities of anthocyanins (Liang et al., 2023; Wang et al., 2024).

The low bioaccessibility and bioavailability of anthocyanins have raised the question of whether it is more important to enhance the bioaccessibility and bioavailability of intact anthocyanins or focus on their degradation products, which may be responsible for their physiological effects (Mueller et al., 2018). This question is important to determine the best

approach for maximizing the health benefits of anthocyanins. However, these questions do not yet have answers. Aiming to increase the stability and achieve the targeted delivery of compounds to the intestinal region, designing and developing novel encapsulation delivery systems has attracted increasing interest. Encapsulation can increase the stability of anthocyanins under different conditions during processing and storage and also provide increased bioaccessibility and possibly bioavailability through protection against conditions in the gastrointestinal tract and providing controlled release at a specific absorption site (Dias et al., 2015; Hu et al., 2023; Ribeiro & Veloso, 2021).

Complex coacervation is one of the most used techniques to enhance the stability of sensitive compounds, including anthocyanins. Polyelectrolyte complexes are formed through electrostatic interactions between oppositely charged polymers, entrapping the target compound (Timilsena et al., 2019). This technique is appropriate for application in the food industry, due to its simplicity, low cost, scalability, and the flexibility to employ various combinations of food biopolymers such as proteins and polysaccharides. In particular, whey protein and pea protein have attracted interest in the field of encapsulation due to their desirable intrinsic properties such as biocompatibility, biodegradability and their functional properties, including gelation, emulsification, and binding capacity (Hadidi et al., 2022; Song et al., 2022). Pea protein, is also a sustainable alternative for the growing demand for plant-derived proteins for the encapsulation of compounds in the food industry. Both whey protein and pea protein have shown potential to interact electrostatically with gum arabic under specific pH conditions to form coacervates (Comunian et al., 2022; Wan et al., 2023). However, these combinations have yet to be extensively explored for encapsulating anthocyanins to enhance their functional properties.

Although there are several techniques, the encapsulation of anthocyanins is still challenging. Delivery systems such as nanoencapsulation, microencapsulation, and protein complexes are some methods used to increase the stability of anthocyanins (Chang et al., 2022; Jafari et al., 2023; Semenova et al., 2021). The results indicated an increase in the stability of anthocyanins to conditions such as temperature and light (Cai et al., 2019; Cui et al., 2022; Ge et al., 2018; Liu et al., 2023; Rosa et al., 2019; Zhao et al., 2020). Studies also showed that encapsulation resulted in a controlled release of anthocyanins during digestion and delayed their degradation, which led to a moderate increase in their bioaccessibility around 10 to 20% (Fernandes et al., 2018; Fredes et al., 2018; Rosales-Chimal et al., 2023; C. Vergara et al., 2020).

Despite some promising results, the majority of the studies have focused on increasing the bioaccessibility of intact anthocyanins and mainly on the controlled released during gastric and small intestine phases. It is also important to analyze the impact of encapsulation on the formation of metabolites during different phases of digestion, including the colonic phase, which has shown to be a potential site for the absorption of metabolites that can contribute to the physiological effects of anthocyanins (Mueller et al., 2017). In this context, the objective of this study was to investigate the effect of encapsulation of jabuticaba peel extract with food polymers on the bioaccessibility of anthocyanins and formation of functional metabolites, applying an *in vitro* model of gastrointestinal digestion and fecal fermentation.

2. Material and methods

2.1. Materials

The fruit used in this study was jabuticaba (*Plinia cauliflora*), which was obtained in November 2022 from the Fruit Culture sector of the Universidade Federal de Viçosa, Minas Gerais, Brazil. The fruits were carefully selected, washed with water, vacuum-packed, and stored in a freezer at -18 °C. Commercially available pea protein (PP, 80% protein content) in powder form was purchased from a local market in Viçosa-MG (Vivenda Naturales, Viçosa, Brazil). The product composition per 20 g was described as: 16 g of proteins, 1.5 g of carbohydrates, 1.4 g of total fat, 1.2 g of fiber and 0.3 mg of sodium. Commercially available whey protein (WP, 82-86 % protein content) in powder form was purchased from Arla Food Ingredients (Nutrilac BE-8405, Viby, Denmark). Pure gum arabic was purchased from LabSynth (Synth, Diadema-SP, Brazil).

2.2. Preparation of the jabuticaba extract

The extraction of phenolic compounds was performed according to (Rocha et al., 2018). Briefly, 100 g of jabuticaba peel was mixed and macerated with 1000 mL of an ethanol solution 75 % (v/v) acidified with citric acid to pH 2.0. The sample was then ultrasonicated at 45 kHz at 40 °C for 50 min (Elmasonic TI-H10, Elma, Singen, BW, Germany), filtered (Whatman No.1 filter paper), and concentrated in a rotary evaporator (RV 10 digital V, IKA, Staufen, BW, Germany) at 40 °C. Residual water was removed by lyophilization, and the powder was packed in metalized bags and kept in a freezer at −20 °C until the time of analysis.

2.3. Total phenolic content (TPC)

Total phenolic compounds were quantified using a method adapted from Singleton & Rossi, (1965), and the results were expressed in mg of gallic acid equivalent (GAE) per g. In a 96-well microplate, 20 µL of diluted sample was mixed with 100 µL of Folin-Ciocalteau reagent (diluted 1:10 with water) and 75 µL of 7.5% Na_2CO_3 solution (m/v). After 1 h in the dark (23 ± 2 °C), the absorbance was measured at 760 nm (CLARIOstar Plus plate reader, BMG Labtech Inc., Durham, NC, USA).

2.4. Encapsulation of jabuticaba extract

Stock solutions (5% w/v) of whey protein (WP), pea protein (PP) and gum arabic (GA) were prepared by dissolving the powders in deionized water. The solutions were allowed to stand overnight under refrigeration at 4 °C to allow complete hydration. The WP or PP solution was mixed with the extract (100 mL) and the resulting solution was stirred for 10 min at room temperature (23 ± 2°C). After that, gum arabic solution was added to the mixture and the pH was adjusted to 3.5 using 1 M $NaCO_3$. It has been shown that at pH 3.5 to 4.0, the electrostatic repulsion between the WP or PP-GA reached its lowest, leading to the highest electrostatic attraction between the proteins and GA, and the maximum formation of coacervates (Comunian et al., 2022; Wan et al., 2023). The resulting solution (500 mL) was stirred for 10 more minutes. The mixtures were prepared in two different ratios: 2:1 e 1:2 v/v of protein (WP or PP) to GA, to assess the effect of higher concentration of protein or gum arabic in the encapsulation of the compounds. The samples were further frozen and stored at −60 °C. After that, the samples were freeze-dried for 72 h. Finally, the powder was packed in metalized bags and kept in a freezer at −20 °C for later analyses.

2.5. Identification of compounds in the powders through LC-ESI-MS/MS analysis

Identification and quantification of compounds in the jabuticaba extract and encapsulated powders was performed using an Thermo Scientific Vanquish™ HPLC equipped with a Thermo Scientific TSQ Altis triple quadrupole mass spectrometer with an ESI source. Separations were carried out on a SunFireTM C18 column (150 × 3 mm, 5 µm) with acidified water 0.1% (v/v) formic acid as mobile phase A and acidified methanol 0.1% (v/v) formic acid as mobile phase B. The flow rate was 0.4 mL/min, and gradient elution began with 5 % B,

which increased to 40% B after 5 min and then to 95% B after 15 min. After 15.50 min, the column was re-equilibrated with 5% B until 17 min. MS data was acquired in both negative and positive polarity. The parameters consisted of a 3912.7 V spray voltage, a sheath gas of 24, auxiliary gas of 2, ion transfer tube temperature at 325 °C and vaporizer temperature at 400 °C. Compound identification was carried out by comparing retention times, fragmentation patterns, and relative ion abundances with known analytical standards or through database searches. Quantification was conducted using calibration curves generated from analytical standards.

2.6. Powder characterization

2.6.1. Encapsulation efficiency (%)

The total anthocyanin content (TAC) and the surface anthocyanin content (SAC) were quantified in order to evaluate the encapsulation efficiency. To determine the TAC, 300 mg of microcapsules were mixed with 1.5 mL of methanol: acetic acid: water (50: 8: 42 v/v/v), vortexed for 3 min and ultrasonicated for 10 min. For the SAC, 200 mg of microcapsules were washed with ethanol in a vortex for 5 min (Adapted from Oancea et al., 2018). Both, TAC and SAC mixtures were centrifuged at 10000 x g for 5 min. The clear supernatant was collected and the quantification of anthocyanins was carried out according to the pH-differential method described by Lee et al., (2005). Encapsulation efficiency (EE %) was calculated according to Eq. (1):

$$\text{EE (\%)} = \frac{\text{TAC - SAC}}{\text{TAC}} * 100 \quad (1)$$

2.6.2. Confocal laser scanning microscopy (CLSM)

The confocal microscopy analysis of the encapsulated samples was performed based on the fluorescence properties of the anthocyanins, present in the jabuticaba extract. The samples were analyzed using a Zeiss Laser Scanning Confocal Microscope (LSM510 META, Carl Zeiss AG, Germany) with the 20× objective lens. The images were observed using a 488 nm excitation laser, with a detection range between 499 and 563 nm.

2.6.3. Scanning electron microscopy (SEM)

For SEM observation, all the samples were freeze-dried, mounted on aluminum stubs, and coated with gold. The morphology of the particles was examined using SEM (Leo 1430VP, Zeiss, Germany) at 300x, 500x and 1000x magnification.

2.6.4. Fourier transform infrared spectroscopy (FTIR)

The samples were analyzed by FTIR using a Cary 630 FTIR spectrophotometer (Agilent Technologies). The scans were performed from 4000 to 400 cm^{-1} with a resolution of 4.00 cm^{-1}. Mean spectra were calculated from triplicate of independent measurements. The resulting spectra were visualized and analyzed with the software Spectragryph v. 1.2.16.1.

2.6.5. Zeta potential (ζ)

The ζ-potential of the wall materials and encapsulated samples were determined using a Zeta Sizer NanoSeries (Malvern, UK).

2.7. *In vitro* gastrointestinal digestion

The simulated gastrointestinal digestion system, which included two steps (gastric and small intestinal digestion), was adapted from Minekus et al., (2014). For the anthocyanin release profile study, the mass of the encapsulated samples added for digestion was normalized to the same anthocyanin content as 1 g of free extract. For the gastric digestion step, 7.5 mL of gastric fluid, containing 0.5% pepsin (S25695A, Fisher Scientific, Nazareth, USA) and supplemented with the salts described by Minekus et al. (2014), was added to the samples. The pH was adjusted to 2.0 using 1.0 M HCl, and the mixture was incubated at 37°C with continuous shaking at 100 rpm for 2 h (C76 Shaking Water Bath, New Brunswick Scientific, Edison, NJ, USA). After this period, 11 mL of simulated intestinal fluid (SIF), 5.0 mL of a pancreatin solution (800 U/mL; porcine pancreatin, 4 x USP, Sigma-Aldrich) prepared in SIF based on trypsin activity, 3.0 mL of a bile salt solution (200 mg/mL), $CaCl_2$ (0.3 M), and 1 M NaOH to reach pH 7.0 were added for the intestinal digestion process. The solutions were reincubated at 37 °C for 2 h at 100 rpm. Every 30 minutes, aliquots were collected for analysis and immediately placed on ice. The samples were subjected to centrifugation at 10000 x g for 5

minutes (Megafuge 16, Thermo Scientific, Waltham, MA, USA). The content of anthocyanins released from the particles in the supernatant was quantified according to the pH-differential method (Lee et al., 2005). The bioaccessibility of anthocyanins in the gastric and intestinal phases was calculated according to Equation 2.

$$\text{Bioaccessibility (\%)} = \frac{\text{Concentration in the digested sample}}{\text{Initial concentration}} * 100 \quad (2)$$

2.8. *In vitro* colonic phase

In vitro colonic metabolism of residues obtained after *in vitro* digestion was performed following the procedures of Sirven et al., (2021). Stool samples were collected from ten lean adults (BMI: 18-25 kg/m2, ages between 18 and 65, and no intake of antibiotics in the last 6 months) and processed inside an anaerobic chamber (Coy Laboratory Products, Grass Lake, MI, USA) at 37 °C and regulated with nitrogen, hydrogen (5%), and carbon dioxide (5%). Anaerobic conditions were confirmed using Resazurin strips (Sigma Aldrich, St Louis, MO, USA). To prepare the fecal slurry, 5 g of feces were mixed with 50 mL of phosphate-buffered saline (PBS). The fecal fermentation medium (FFM) used was produced by Anaerobe Systems (Morgan Hill, CA, USA) and was formulated with 2.0 g peptone water, 0.5 g bile salts, 2.0 g yeast extract, 0.5 g L-cysteine, 0.05 g haemin, 0.01 mL vitamin K, 0.001 g resazurin, 0.01 g $CaCl_2 \cdot 6H_2O$, 0.01 g $MgSO_4 \cdot 7H_2O$, 0.04 g KH_2PO_4, 0.04 g K_2HPO_4, 0.10 g NaCl, 2.0 g $NaHCO_3$, 2.0 mL tween 80 per 1 L. To simulate the metabolism of samples in the colon, the digestion residues were mixed with 18 mL of FFM and 2 mL of fecal slurry. Two controls were prepared: one with 18 mL of media and 2 mL of fecal slurry to eliminate the interference of phenolic compounds already present in the feces, and another with the digestion residues, 18 mL of FFM, and 2 mL of PBS to identify the metabolization derived from the spontaneous degradation of the compounds in the medium. Fermentation was carried out for 48 h, with aliquots collected at 0, 3, 6, 12, 24, and 48 h time points. For chemical analysis of metabolites, 500 µL aliquots were mixed with 500 µL of acidified methanol (0.1% formic acid), followed by centrifugation at 10000 x g for 5 minutes (Megafuge 16, Thermo Scientific, Waltham, MA, USA). The resulting supernatants were stored at −80 °C until further analysis.

2.9. Identification of metabolites through LC-ESI-MS/MS analysis

Identification and quantification of parent compounds and metabolites produced during fecal fermentations was performed as described before (Section 2.5). The following compounds were analyzed in the samples: cyanidin-3-glucoside, cyanidin, phloroglucinol aldehyde, phloroglucinol acid, protocatechuic acid, catechol, vanillic acid, 4-hidroxybenzoic acid, 4-hidroxybenzoaldehyde, gentisic acid, 3,4-dihidroxyphenylpropionic acid, 4-hydroxyphenylpropionic acid, 3- hydroxyphenylpropionic acid, phenylpropionic acid, 3,4-dihydroxyphenylacetic acid, 4-hydroxyphenylacetic acid, 3-hydroxyphenylacetic acid, phenylacetic acid, 3-hydroxybenzoic acid, benzoic acid, hippuric acid, 4-hydroxyphenylethanol, gallic acid, syringic acid, pyrogallol, methyl gallate, 1-GG (monogalloyl glucose), 2-GG (Digalloyl glucose), 3-GG (Trigalloyl glucose), and 4-GG (Tetragalloyl glucose).

2.10. Short-chain fatty acids (SCFAs)

Short-chain fatty acids were extracted by combining 50 μL of fermentation aliquot with 800 μL of 30 mM HCl. The solution was then vortexed for 1 min and centrifuged at 12000 x g for 10 min at 4 °C (LD-2910, GMI, Ramsey, MN, USA). The supernatant (400 μL) was extracted with 400 μL of ethyl acetate, vortexed for 20 min, and centrifuged again at 12000 x g for 10 min at 4 °C. The supernatant was stored at −80 °C until analysis by GC-MS (Sirven et al., 2021). The whole extraction was performed on ice. SCFAs were analyzed on a gas chromatography (TRACE 1310, Thermo Scientific, Waltham, MA, USA) coupled with a triple quadrupole mass spectrometer (TSQ 9000, Thermo Scientific, Waltham, MA, USA). Chromatographic separation was achieved on a DB WAX column (60 m × 0.25 mm × 0.25 μm; Agilent, Santa Clara, CA, USA), and 1 μL of the samples was injected with a split ratio of 17: 1. The ionization was carried out in the electron impact (EI) mode at 70 eV. The MS transfer line, and ion source were maintained at 200 °C and 250 °C, respectively. The flow rate of helium carrier gas was 1 mL/min. The target compounds were analyzed in the Selected Reaction Monitoring (SRM) mode using the following product ions (m/z) for each compound: acetic acid 60, propionic acid 74.1,73.1, 57.1, isobutyric acid 73.1, 88.1, 89.1, butyric acid 60, 73.1, 89.1, 2-methylbutyric/isovaleric 74.1, 60.1, 87.1, valeric acid 60, 87.1, 103.1. A short-chain fatty acid mixture containing acetic, propionic, isobutyric, n-butyric, 2-methylbutyric, isovaleric, and valeric acids was used as the standard (Cayman Chemicals, Ann Arbor, MI,

USA). The results for the encapsulated samples and free extract were adjusted by subtracting the control (no digestion residue) to eliminate interference from SCFAs already present in the fecal slurry or produced in the absence of digestion residues.

2.11. *In vitro* study of the effects of cyanidin-3-glucoside and metabolites on HT29-MTX cells

2.11.1. Cell line and culture maintenance

Cell culture and treatment were performed according to the recommendations of the American Type Culture Collection (ATCC®, Manassas, VA, USA). HT29-MTX cells (Human colorectal adenocarcinoma cell line) were cultured in high glucose Dulbecco's modified Eagle's medium (DMEM; Invitrogen, Carlsbad, CA, USA) supplemented with 10% (v/v) fetal bovine serum (FBS), 1% (v/v) non-essential amino acids, and 1% (v/v) penicillin–streptomycin (Arbizu et al., 2020). Cells were maintained at 37 °C with a humidified 5% CO_2 atmosphere.

2.11.2. Cell viability

HT29-MTX cells (1.0×10^5) were seeded in a 96-well plate and incubated for 48 h to allow cell attachment before treatment with various concentrations of the compounds for 48 h. The cells were treated with cyanidin-3-glucoside (Cya-3-glu), protocatechuic acid (PA), phloroglucinol aldehyde (PGA), gallic acid (GA), methyl gallate (MG), vanillic acid (VA), and two different mixtures at concentrations ranging from 250 to 1.95 µM. The mixtures were prepared with different proportions of the compounds (1000 µM), based on the concentrations observed after *in vitro* digestion. Mix 1 simulated the free extract with a higher concentration of metabolites (31.37% cya-3-glu, 63.00% PA, 1.77% GA, 0.02% PGA, 3.47% VA, and 0.46% MG), while Mix 2 simulated the encapsulated samples (68.10% cya-3-glu, 30.57% PA, 1.26% PGA, 0.01% PGA, 0.00% VA, and 0.06% MG). Cell viability was assessed using the Resazurin *in vitro* assay kit (Sigma-Aldrich, St. Louis, MO, USA) following the manufacturer's protocol. Fluorescence intensity was measured using a CLARIOstar Plus plate reader (BMG Labtech Inc., Durham, NC, USA) set at 560 nm excitation and 590 nm emission. Cell viability results were quantified as a percentage of the untreated controls (Arbizu et al., 2020).

2.11.3. Reactive oxygen species (ROS) assay

Intracellular reactive oxygen species (ROS) generation was assessed using the DCFH-DA assay as described by Arbizu et al., (2020). HT29-MTX cells (1.0 x 10^5) were seeded in a 96-well plate and incubated for 48 h to allow cell attachment until reaching 90% confluency. After that, the cells were pretreated for 2 h with different concentrations (0-125 µM) of the phenolic compounds followed by LPS (4 µg/mL, Lipopolysaccharides from Escherichia coli O111:B4, Sigma Aldrich, Saint Louis, MO, USA) challenge for 3 h at 37 °C. ROS production was detected using DCFH-DA at 10 µM for 45 min at 37 °C and 200 rpm (H5000-HC MultiTherm™, Benchmark Scientific, Sayreville, NJ, USA). Fluorescence intensity was monitored at 520 nm emission and 480 nm excitation using a CLARIOstar Plus plate reader (BMG Labtech Inc., Durham, NC, USA). Cells were then washed with PBS (2×) and fixed with methanol for 3 min at room temperature. Methanol was then completely removed and 100 µL of Janus green (1 mg/mL) was added to the wells for 3 min. Following removal of Janus green, cultures were washed with PBS (2×) and 100 µL of 50% MeOH was added to each well. Cell density was determined at 654 nm. Results were expressed as RFU (relative fluorescence units)-fold of untreated control. RFU values were normalized to absorbance values corresponding to cell densities. The experiments were conducted with two independent assays with internal quadruplicates for each of them.

2.11.4 Gene expression

HT29-MTX cells were seeded in 12-well plates at 90% confluence and were pretreated for 2 h with the phenolic compounds followed by LPS (4 µg/mL) challenge for 3 h at 37 °C. For all experiments, total RNA was isolated using the RNA Mini Kit (Zymo Research, Irvine, CA, USA) according to the manufacturer's protocol. The quality and quantity of RNA samples were assessed using the NanoDrop Lite Plus Spectrophotometer (Thermo Scientific, Waltham, MA, USA). Extracted RNA was used to synthetize cDNA using the iScript Reverse Transcription Supermix (BioRad, Hercules, CA, USA). The sequences of the primers used were as follows: GAPDH (forward: 5'-ACAGTTGCCATGTAGACC; reverse: 5'-TTTTTGGTT G AGCACAGG); TNF-α (forward: 5'-TCCTCCAGACACCCTCAACC-3'; reverse: 5'-AGGCCCCAGTTTGAATTCTT-3'); IL-8 (forward: 5'- CACCGGAAGGAACCATCTCA-3'; reverse: 5'- AGAGCCACGGCCAGCTT-3'); IL-6 (forward: 5'-GCAGAAAAAGGCAAA GAA-TC; reverse: 5'- CTACATTTGCCGAAGAGC); COX-2 (forward: 5'-AGGGTTGCT

GGTGGTAGGAA-3'; reverse: 5'-GGTCAATGGAAGCCTGTGATACT-3'). Real time polymerase chain reaction (RT-PCR) was performed using a CFX384 Touch Real Time PCR Detection System (BioRad; Hercules, CA, USA). Each reaction was performed in duplicates and relative mRNA levels were calculated by the comparative CT method (Schmittgen & Livak, 2008) using GAPDH as a housekeeping gene.

2.12. Statistical analyses

The analyses were conducted in 3 replicates, and the results were presented as mean ± standard deviation (SD). Data were analyzed using one-way ANOVA followed by Tukey's test or using Dunnett's test. All the analyses were performed using the R software (R Core Team, Vienna, Austria). A statistically significant value was considered when $p<0.05$.

3. Results and discussion

3.1. Identification and quantification of phenolic compounds in the powders

Seventeen phenolic compounds were identified in the jabuticaba extract through LC-ESI-MS/MS analysis (Table 1), including flavonoids, phenolic acids, gallotannins, and ellagitannins. The relative abundance of each compound was calculated using the ratio of the peak area of each compound to the total peak area of all compounds, and the main compound identified in the extract was cyanidin-3-glucoside, with a relative abundance of 96.77 ± 0.04%. Therefore, this anthocyanin can be considered the primary functional compound of the jabuticaba extract.

Table 1 - Identification of individual polyphenols in the jabuticaba extract by LC-ESI-MS/MS analysis

Compounds	$[M-H]^-$	MS^2	Relative abundance (%)
Cyanidin-3-glucoside*	449.18	287.125, 213.125, 241.042	96.77 ± 0.04
Quercetin	301.09	151.04, 179.04, 107.04	0.12 ± 0.02
Quercetin-3-glucoside	462.86	255.125, 271.077, 299.768	0.09 ± 0.00
Rutin	609.00	254.97, 271.04, 300.04	0.03 ± 0.00
Phloroglucinol aldehyde	152.90	83.042, 107.042, 151.083	0.01 ± 0.00
Gallic acid	168.90	124.97, 81.054, 79.071	0.72 ± 0.05
Protocatechuic acid	153.05	81.054, 91.042, 109.042	0.24 ± 0.00
Caffeic acid glycoside	341.00	131.018, 179.042, 220.929	0.03 ± 0.00
Ellagic acid	301.09	145.04, 229.04, 284.04	0.34 ± 0.04
Ellagic acid hexoside	463.00	257, 284, 301	0.03 ± 0.00
1-GG (monogalloyl glucose)	331.04	169.040, 210.960, 271.070	0.04 ± 0.01
2-GG (Digalloyl glucose)	482.91	169.130, 271.040, 331.050	0.06 ± 0.01
3-GG (Trigalloyl glucose)	635.14	330.910, 465.160, 482.990	0.10 ± 0.01
4-GG (Tetragalloyl glucose)	787.15	617.125, 635.155, 465.095	0.21 ± 0.01
Casuarinin (Galloyl-bis-HHDP-glucose)	935.15	451.083, 633.125, 301.071	0.20 ± 0.00
Tellimagrandin I (HHDP-digalloylglucose)	785.15	301.042, 275.071, 623.071	0.26 ± 0.00
Castalagin/Vescalagin	933.20	451.042, 301.042, 275.083	0.75 ± 0.01

*All compounds were analyzed with negative polarity, with the exception of cyanidin-3-glucoside which were analyzed with positive polarity ($[M + H]^+$).

The concentrations of cyanidin-3-glucoside and the total phenolic content (TPC) in the samples are presented in Table 2. Variations in cyanidin-3-glucoside and TPC among the powders can be attributed to the different polymers used and their proportions.

Table 2 - Cyanidin-3-glucoside concentration and total phenolic content (TPC) in jabuticaba extract and encapsulated powders

Samples	Cyanidin-3-glucoside (mg/g)	Total phenolic content (TPC, mg of GAE/g)
Jabuticaba extract	13.85 ± 0.68	180.26 ± 1.92
WP:GA 1:2	3.82 ± 0.05	26.08 ± 0.46
WP:GA 2:1	3.12 ± 0.01	38.63 ± 0.74
PP:GA 1:2	4.04 ± 0.00	23.69 ± 0.04
PP:GA 2:1	4.39 ± 0.00	21.94 ± 0.12

3.2. Encapsulation efficiency (EE) (%)

The EE (%) of the encapsulated samples WP:GA 1:2, WP:GA 2:1, PP:GA 1:2 and PP:GA 2:1 were 96.50 ± 0.17, 94.95 ± 0.23, 93.99 ± 0.31 and 91.37 ± 0.30%, respectively. All values were higher than 90%, indicating successful anthocyanins encapsulation in all formulations. Samples encapsulated with WP presented encapsulation efficiency significantly ($p<0.05$) higher than the samples encapsulated with PP.

The EE of hydrophilic substances tends to be much lower than that of lipophilic substances, since the former tend to migrate to the aqueous phase during the coacervation process (de Souza et al., 2018). However, the combination of complex coacervation with freeze-drying in the present study showed a high EE for the jabuticaba extract, mainly composed of anthocyanins. This result may be related to the ability of anthocyanins to bind proteins and polysaccharides (Dangles & Fenger, 2018). During the coacervation process, proteins and polysaccharides form electrostatic complexes under specific pH conditions. Initially, anthocyanins can interact with proteins through hydrophobic and hydrogen bonds. Subsequently, the loaded proteins can be cross-linked through electrostatic interactions with oppositely charged polysaccharides, entrapping the anthocyanins within the structure, which may have contributed to the high EE observed (Song et al., 2022).

High values of EE were also found for the encapsulation of red raspberry anthocyanins using soy protein isolate, gum arabic, and their combination as wall material. The EE of the

freeze-dried produced capsules ranged between 93.05% and 98.87% (Mansour et al., 2020). The combination of pea protein/carrageenan and pea protein/tragacanth for the encapsulation of blackberry juice also resulted in high EE, with values ranging from 89.88 to 94.20% (L. P. Vergara et al., 2023). For the encapsulation of anthocyanins from sour cherries skins extract with whey protein and gum arabic the EE was 70.30 ± 2.20% (Oancea et al., 2018).

3.3. Morphology by Confocal laser scanning microscopy (CLSM) and Scanning Electron Microscopy (SEM)

The fluorescence of anthocyanins was explored using confocal laser scanning microscopy to evaluate their distribution in the particles after the complex coacervation reaction. The ability of anthocyanins to emit fluorescence has been demonstrated in previous studies (Cai et al., 2019; Carvalho et al., 2016; Li et al., 2023, 2024; Lu et al., 2015; Tarone et al., 2021). To ensure accurate interpretation of microscopy results, the wall materials were individually analyzed for their fluorescence emission and potential interference prior to the confocal analysis of the encapsulated samples. Among the wall materials, only PP exhibited fluorescence. These findings indicate that the red regions observed in the samples encapsulated with WP and GA resulted exclusively from anthocyanin fluorescence. In contrast, for the samples encapsulated with PP, the fluorescence originated from both anthocyanins and PP.

These results align with the known fluorescence characteristics of these hydrocolloids. The maximum excitation and emission wavelengths for fluorescent groups in proteins, primarily associated with the aromatic amino acids tryptophan, tyrosine, and phenylalanine, typically occur around 280 nm for excitation and between 280-350 nm for emission (Du et al., 2020; Ghisaidoobe & Chung, 2014). However, some secondary emission or background fluorescence may be observed in other ranges. The fluorescence observed in GA is mainly attributed to the intrinsic fluorescent properties of the amino acids tyrosine and phenylalanine, located in the protein components of its structure (Dhenadhayalan et al., 2014; Sethuraman & Rajendran, 2018). At 278 nm excitation, GA exhibited a maximum emission at 315 nm and a broad shoulder from 390 to 450 nm (Dhenadhayalan et al., 2014; Sethuraman & Rajendran, 2018), while no fluorescence was observed at 420 nm excitation (Mohammadian et al., 2019).

The results indicated that the anthocyanins were trapped in the particles in both protein-to-polysaccharide ratios studied (Figure 1). However, two different behaviors were observed. In the samples encapsulated with WP, the particles presented a larger size, an irregular shape, and the anthocyanins were concentrated around the center of the particle

(Figure 1). This distinct distribution suggests a different encapsulation behavior, where the anthocyanins might be preferentially localized or aggregated in the walls of the particles. On the other hand, the samples encapsulated with PP showed a spherical shape and a more uniform distribution of anthocyanins in the particles (Figure 1). This behavior may also be influenced by the fluorescence of pea protein (PP), which could have affected the imaging results.

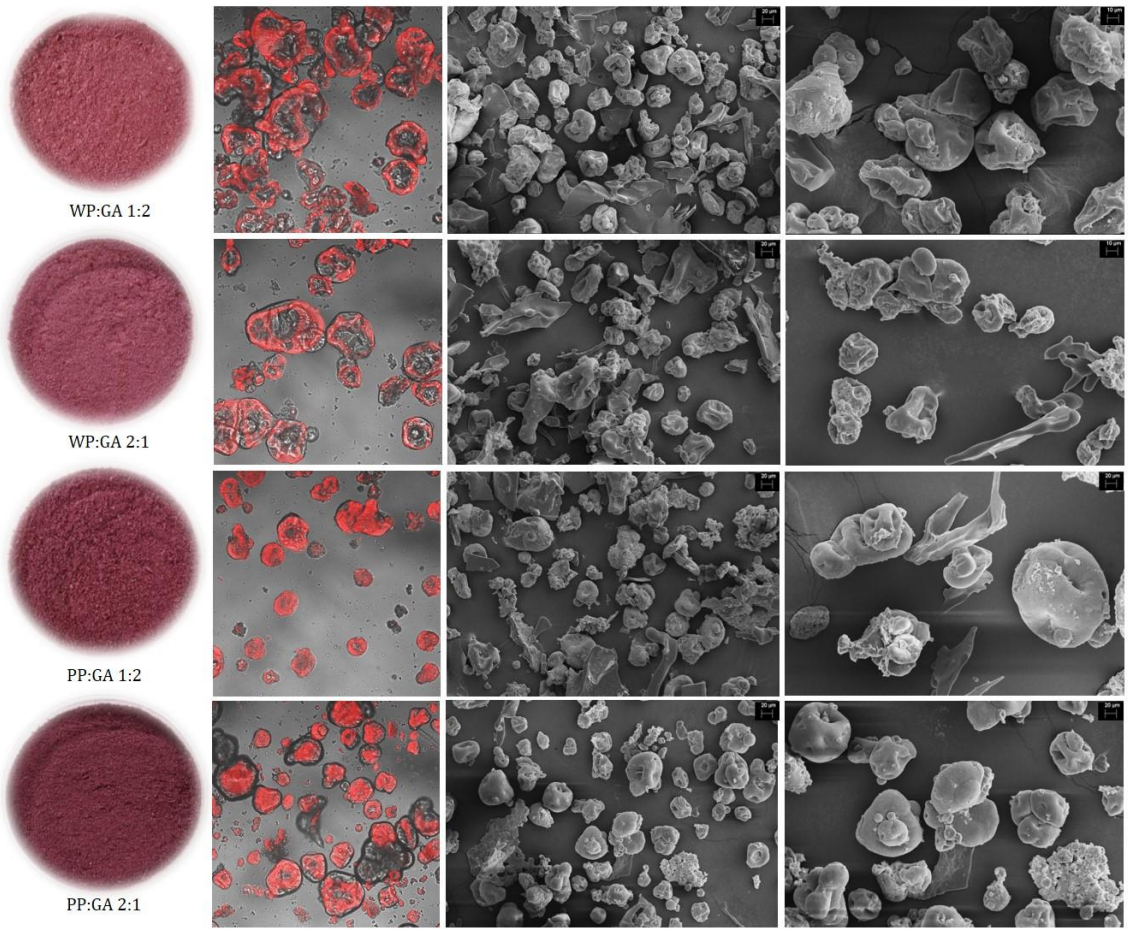

Figure 1 – Physical appearance of the freeze-dried powders, confocal laser scanning microscopy (CLSM)* and scanning electron microscopy (SEM) images of the encapsulated samples at 500 and 1000x magnification. *The anthocyanins are represented in red in the CLSM images for better visualization, but the fluorescence was emitted in the green spectrum (499–563 nm) following excitation at 488 nm.

The coacervation process is influenced by various factors such as temperature, ionic strength, pH of the reaction medium, the mixing ratio of polymers, their molecular weight, and charge densities. In addition, the interactions between the participating biopolymers affect the

structure, morphology, size, and stability of coacervates and the core material (Timilsena et al., 2019). Since the processing conditions were the same for all the samples, the different behaviors in the particles can be associated with the chemical characteristics of the proteins and how they interacted with the gum arabic and the extract. Pea proteins are one of the most popular plant proteins, mainly consisting of globulins (70-80%), with minor fractions of albumins and glutelins. Pea globular proteins are mainly constituted of legumin (300 to 400 kDa, isoelectric point (pI) ≈ 5-6) and vicilin (150 to 170 kDa, pI ≈ 4-6) (Lam et al., 2018; Shanthakumar et al., 2022). Whey proteins, on the other hand, are a mixture of globular protein molecules primarily composed of β-lactoglobulin (∼18.3 kDa, pI of 5.2) and α-lactalbumin (∼14.2 kDa; pI of 4-5) (Y.-R. Lee & Hong, 2003; Permyakov, 2020).

After the coacervation reaction, drying is considered essential to obtain the particles in a powder form for further application (Timilsena et al., 2019). The surface morphology of the dried samples encapsulated with WP revealed particles with irregular, quasi-spherical shapes, a wrinkled surface, and concavities. The particles also exhibited heterogeneous sizes and tendencies for agglomeration (Figure 1). On the other hand, particles from samples encapsulated with PP showed a more uniform spherical shape with fewer concavities and a less pronounced wrinkled surface. Similarly to the whey protein samples, the particles also exhibited heterogeneous sizes and agglomeration (Figure 1).

Particles with irregular shape are typically observed when freeze drying is used as a drying method (L. P. Vergara et al., 2023). A similar morphology has been observed in lyophilized particles of blackberry juice encapsulated by complex coacervation, using carrageenan, tragacanth, and xanthan in combination with pea protein as wall material (L. P. Vergara et al., 2023). These characteristics have also been observed for the encapsulation of *Lactobacillus plantarum* using whey protein isolate and gum arabic by complex coacervation, but in this case, spray drying was used as the drying method (Sharifi et al., 2021).

3.4. FTIR spectrum

The spectra of the jabuticaba extract, wall materials and encapsulated samples were evaluated to identify the possible chemical interactions occurring within the encapsulation matrix. The FTIR spectrum of the jabuticaba extract and the walls materials provides a baseline reference for the molecular vibrations present in each of them. In the encapsulated samples, the interactions of functional groups can lead to the appearance of new bands and changes in

absorption band or location in the FTIR spectra (Carpentier et al., 2021). The FTIR spectrum of the wall materials, jabuticaba extract, and the mixtures are shown in Figure 2.

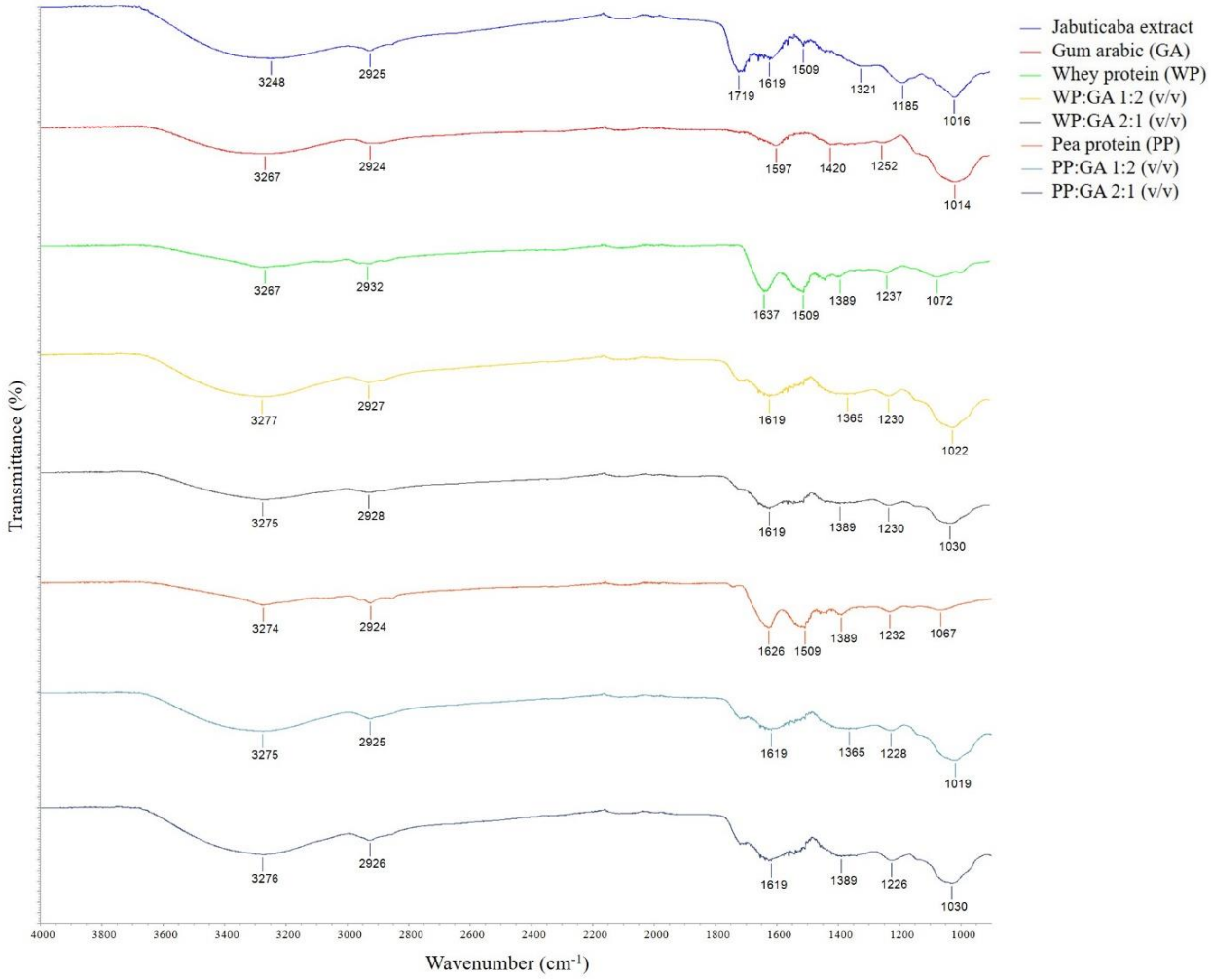

Figure 2 - FTIR spectra of the jabuticaba extract, gum arabic (GA), whey protein (WP), pea protein (PP) and the encapsulated samples with varying protein-to-GA ratios.

In the jabuticaba extract (Figure 2), the peak at 3248 cm^{-1} represents the O–H stretching vibration, and the peak at 2925 cm^{-1} represents the aliphatic C-H stretching vibrations. The peaks observed at 1719 cm^{-1} and 1619 cm^{-1} are related to the C=O and C=C stretching vibrations in the aromatic ring skeleton, respectively (Sampaio et al., 2019). Similarly, a peak at 1509 cm^{-1} corresponds to the deformation of the C=C bond in aromatic rings (Silva et al., 2019). The jabuticaba extract also showed a band at 1321 cm^{-1}, which is characteristic of C-OH deformations of phenols, and at 1185 cm^{-1} related to the stretching vibration of C–O (Shurvell, 2006). Besides, the peak at 1016 cm^{-1} is related to the C–H deformation of the aromatic ring (Cai et al., 2019; Heneczkowski et al., 2001).

For the gum arabic (GA) (Figure 2), the peak at 3267 cm^{-1} corresponded to the O–H stretching vibration, while the peak observed at 2924 cm^{-1} was assigned to the vibrational modes of C–H. Two bands at 1597 cm^{-1} and 1420 cm^{-1} were related to the presence of COOH (carboxylic group) due to asymmetric and symmetric stretching vibration of the carboxylic acid salt −COO−. The 1252 cm^{-1} and 1014 cm^{-1} peaks corresponded to the stretching of the C–O bond (Bashir & Haripriya, 2016; Espinosa-Andrews et al., 2010; Shurvell, 2006).

In the case of WP (Figure 2), the peak observed at 3267 cm^{-1} corresponded to the O–H stretching vibration, while the band at 2932 cm^{-1} corresponded to C(sp2)-H stretching vibration in aliphatic groups. Other notable peaks were observed at 1637 cm^{-1} and 1509 cm^{-1}, which correspond to the amide I band (1600−1690 cm^{-1}, C=O stretching) and amide II bands (1480−1575 cm^{-1}, CN stretching, NH bending). These specific peaks are known to well characterize the whey proteins (Gbassi et al., 2012; Shen et al., 2023). In addition, a peak at 1237 cm^{-1} related to the amide III band (1229−1301 cm^{-1}, CN stretching, NH bending) was also observed. The bands observed at 1389 cm^{-1} and 1072 cm^{-1} corresponded to the CH-OH angular deformation and C–O stretching, respectively (Gbassi et al., 2012; Shen et al., 2023).

Regarding the pea protein (PP) (Figure 2), the peak at 3274 cm^{-1} represented the O–H stretching vibration, while the band at 2932 cm^{-1} was related to a C-H stretching band. The peaks at 1626 cm^{-1}, 1509 cm^{-1}, and 1232 cm^{-1} corresponded to the amide I, amide II, and amide III bands. While, the peaks at 1389 cm^{-1} and 1067 cm^{-1} were associated with the C–O stretching (Aguilar-Vázquez et al., 2018; Carpentier et al., 2021).

Regarding the spectra of the samples encapsulated with WP, some characteristic peaks of the jabuticaba extract disappeared (1719, 1509, 1321, and 1185 cm^{-1}) when mixed with the wall materials, indicating that jabuticaba extract was successfully encapsulated in both treatments (Cui et al., 2022). A decrease in the intensity of amide I (1637 to 1619 cm^{-1}) and the disappearance of the amide II band (1509 cm^{-1}) was also observed in the complexes compared to the pure whey protein. This could indicate interactions between the biopolymers and the extract, resulting in a decrease in free functional groups (Carpentier et al., 2021). Comparing the mixtures to the pure GA spectra, the encapsulated samples did not show the symmetric and asymmetric -COO- stretching vibrations (1597 and 1420 cm^{-1}) found for GA. There was also an increase in the C–O bond stretching due to a shift in the peak values from 1014 to 1022 and 1030 cm^{-1}. Overall, the carbonyl-amide region was affected during the encapsulation process, indicating the establishment of electrostatic interactions between the amino groups of whey protein and the carboxylic groups of GA and also interactions with the extract (Carpentier et al., 2021).

The results were similar for the samples encapsulated with PP in combination with GA. Some of the characteristic peaks in the jabuticaba extract disappeared, and the carbonyl-amide region was also affected. There was a decrease in the intensity of amide I (1626 to 1619 cm^{-1}) and the disappearance of the amide II band (1509 cm^{-1}). The peaks for the symmetric and asymmetric -COO- stretching vibrations in GA were not detected either. Thus, the results indicated interactions between the PP, GA, and the extract.

3.5. Zeta potential (ζ)

Pea protein and WP showed a cationic nature at pH 3.5 because of the protonation of the amino groups. The zeta potential of WP was 11.70 ± 0.17 mV and of PP was 9.45 ± 1.69 mV. Gum arabic, on the other hand, showed a negative zeta potential of -17.00 ± 2.12 mV, because of the deprotonation of carboxylic groups. Regarding WP:GA mixtures, the values of zeta potential were -9.66 ± 0.56 and -15.00 ± 0.56 mV for the proportions 2:1 and 1:2, respectively. For PP:GA mixtures, the zeta potential was -11.33 ± 0.47 for the sample PP:GA 2:1 and -16.8 ± 0.40 mV for the sample PP:GA 1:2. The net charge of all the mixtures was negative, suggesting the dominance of negative charges in the mixtures.

The surface charge density (zeta potential) is considered an important parameter for optimizing the complex coacervation process and verifying the complexation and stability of the formed coacervates (Eghbal & Choudhary, 2018). When the zeta potential value is equal to zero, the complex coacervation reaction is considered optimal, which means that all the groups from the anionic polymer interacted with all the positive groups of the cationic polymer at the mixing ratio (Kayitmazer et al., 2015). The 2:1 protein-to-gum arabic mixtures showed a less negative zeta potential because there was more protein available to partially neutralize the negative charge of gum arabic. In contrast, the 1:2 mixtures had a more negative zeta potential because there was more gum arabic present, increasing the overall negative charge.

The interactions between the polymers and the extract may have also influenced the results. Anthocyanins, for example, can interact with the proteins through hydrophobic or hydrogen bonding (Song et al., 2022). These interactions could have reduced the number of groups available on the protein to interact with the gum arabic, thereby affecting the overall zeta potential. Although the complete neutralization between the polymers was not achieved, the coacervation reaction was still observed (evidenced by phase separation during the reaction), and the interaction between the polymers, as well as the encapsulation of anthocyanins, was confirmed through FTIR and microscopy analysis, as previously discussed.

3.6. *In vitro* release of anthocyanins during simulated digestion

The impact of encapsulation on the release of anthocyanins during *in vitro* simulated gastrointestinal digestion was investigated, and the content of total anthocyanins over time, as well as the bioaccessibility at the end of the gastric and intestinal phases are presented in Figure 3. It was found that encapsulation significantly reduced the release ratio of anthocyanins during the gastric digestion. In simulated gastric fluid (pH = 2.0), the percentage of anthocyanins released from the particles after 30 min was 64.85 ± 1.21%, 43.94 ± 3.08%, 61.20 ± 1.63% and 34.07 ± 4.11 % for the samples WP:GA 1:2, WP:GA 2:1, PP:GA 1:2, PP:GA 2:1, respectively. The rate of anthocyanins released from the particles was significantly lower than that of the free extract in solution (89.72 ± 2.37 %).

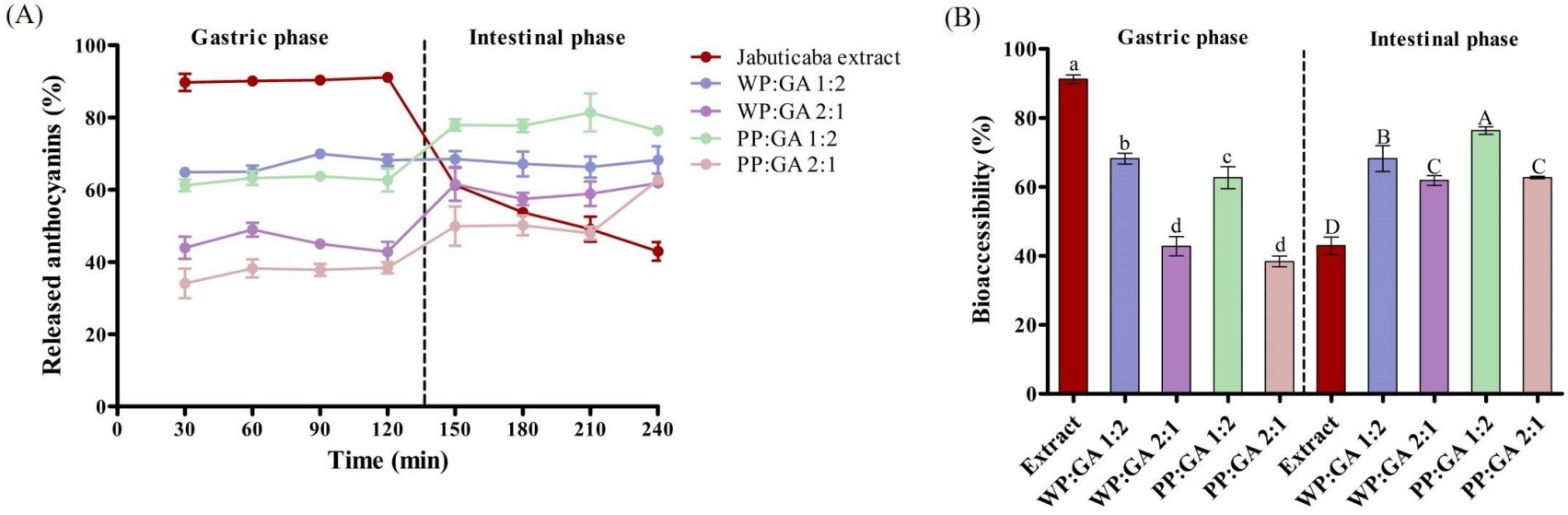

Figure 3 - Release (A) and bioaccessibility (B) of anthocyanins from jabuticaba extract and encapsulated samples with whey protein (WP) or pea protein (PP) combined with gum arabic (GA) during simulated digestion (gastric phase at pH 2.0 and small intestinal phase at pH 7.0). Values are presented as mean ± standard deviation (n=3). Mean values with different lowercase letters (gastric phase) or uppercase letters (intestinal phase) are significantly different (Tukey's multiple comparisons test, $p<0.05$).

In an acidic environment, anthocyanins are in the flavylium cation form with red color and are stable (Ayvaz et al., 2023), which explains the stable behavior of anthocyanins in the free extract and the encapsulated samples when subjected to the simulated gastric conditions. At the end of gastric digestion, the bioaccessibility of anthocyanins in the encapsulated samples were also significant lower compared to the control (free extract) ($p<0.05$). The lowest release ratios of anthocyanins were obtained in the extract encapsulated with the higher proportion of proteins WP:GA 2:1 (42.78 ± 2.80%) and PP:GA 2:1 (38.40 ± 1.56%). Comparing the samples with higher content of gum arabic, the one encapsulated with PP (62.20 ± 1.57%) showed a lower bioaccessibility ($p<0.05$) compared to the one with WP (68.20 ± 1.57%).

After intestinal digestion (pH = 7.0) for 30 min, anthocyanins release rates increased significantly for the samples WP:GA 2:1, PP:GA 1:2 e PP:GA 2:1, and was constant for the sample WP:GA 1:2 over time. For the jabuticaba extract, on the other hand, there was a significant decrease in the concentration of anthocyanins over time, due to the degradation of this compound. Anthocyanins are unstable at high pH, and the change from acidic pH in the stomach to pH 7-8 in the intestine is responsible for the hydrolysis and degradation of anthocyanins. Besides that, the presence of digestive enzymes and bile salts can also contribute to the degradation of anthocyanins (Ayvaz et al., 2023).

The bioaccessibility of anthocyanins at the end of intestinal digestion was significantly higher for all the encapsulated samples compared to the free extract ($p<0.05$). The results indicated that encapsulation treatment improved anthocyanins stability under a higher pH environment during intestinal digestion, minimizing the loss of anthocyanins and increasing the concentration of intact anthocyanins after 4 h of digestion. The highest bioaccessibility of total anthocyanins were obtained in samples encapsulated with a higher proportion of GA, PP:GA 1:2 (76.32 ± 1.11 %) followed by the WP:GA 1:2 (68.22 ± 3.76 %) ($p<0.05$). These samples showed an absolute increase in bioaccessibility of approximately 33% and 25%, respectively, compared to the free extract (42.93 ± 2.56%). The samples with a higher proportion of proteins, PP:GA 2:1 (62.71 ± 0.36 %) and WP:GA 2:1 (61.86 ± 1.40 %), retained more anthocyanins in the particles, showing a lower bioaccessibility than the other treatments.

The observed increase in the bioaccessibility of anthocyanins was higher compared to previous studies. For the microencapsulation of maqui Juice (MJ) with maltodextrin (MD) and soy protein isolate by spray-drying (SD) and freeze-drying (FD), the bioaccessibility of anthocyanins in MJ powders (44.1% for SD and 43.8% for FD powders) was significantly higher than in the MJ (35.2%) (Fredes et al., 2018). In another study with coacervates prepared with pectin and chitosan, the bioaccessibility of the coacervate formulation (~24%) was higher

than the crude extract (~12%), as well as that of purified anthocyanins (~19%) (Sarkar et al., 2021). For the encapsulation of anthocyanin extract using taro starch by spray drying, the bioaccessibility of the anthocyanins was 10 % higher than that observed in the extract without encapsulation during gastrointestinal digestion (Rosales-Chimal et al., 2023). Similarly, in the encapsulation of purple flesh cultivated potato extract with maltodextrin (MD) and spray-drying, the bioaccessibility of anthocyanins was approximately 20% higher than the free extract, though still lower than in the present study (C. Vergara et al., 2020).

A change in the external pH environment in which the particles are dispersed can change the charge state of the wall materials and affect the electrostatic attraction between wall materials and the extract (Kim et al., 2019). GA is negatively charged at pH above 2.2 due to the deprotonation of the residual carboxyl groups (Sabet et al., 2021; Weinbrreck et al., 2004). The proteins, on the other hand, presents a positive charge below its isoelectric point (pI) and negative charge above its pI (Timilsena et al., 2019). At pH 2.0, there was some disintegration of the particles, however, in less extent compared to the pH 7.0 of intestinal digestion (Figure 4). The release of anthocyanins in the gastric phase can be attributed to some weakened of the electrostatic attraction between the proteins and GA, due to the lower number of deprotonated carboxyl groups in GA, and also due to the effects of the enzyme pepsin on the proteins. The results revealed that samples encapsulated with a higher proportion of proteins displayed a better retention of anthocyanins during gastric digestion, indicating that a higher concentration of proteins helped to maintain the structure of the particles and retain the anthocyanins in a more acidic environment. At pH 7.0, the electrostatic attraction between the proteins and GA was further weakened. Since pH 7.0 is above the pI of WP and PP, the deprotonation of the amino groups in the proteins led to a decrease in binding between the two polymers, causing greater disintegration of the particles and releasing more anthocyanins, as observed in Figure 4.

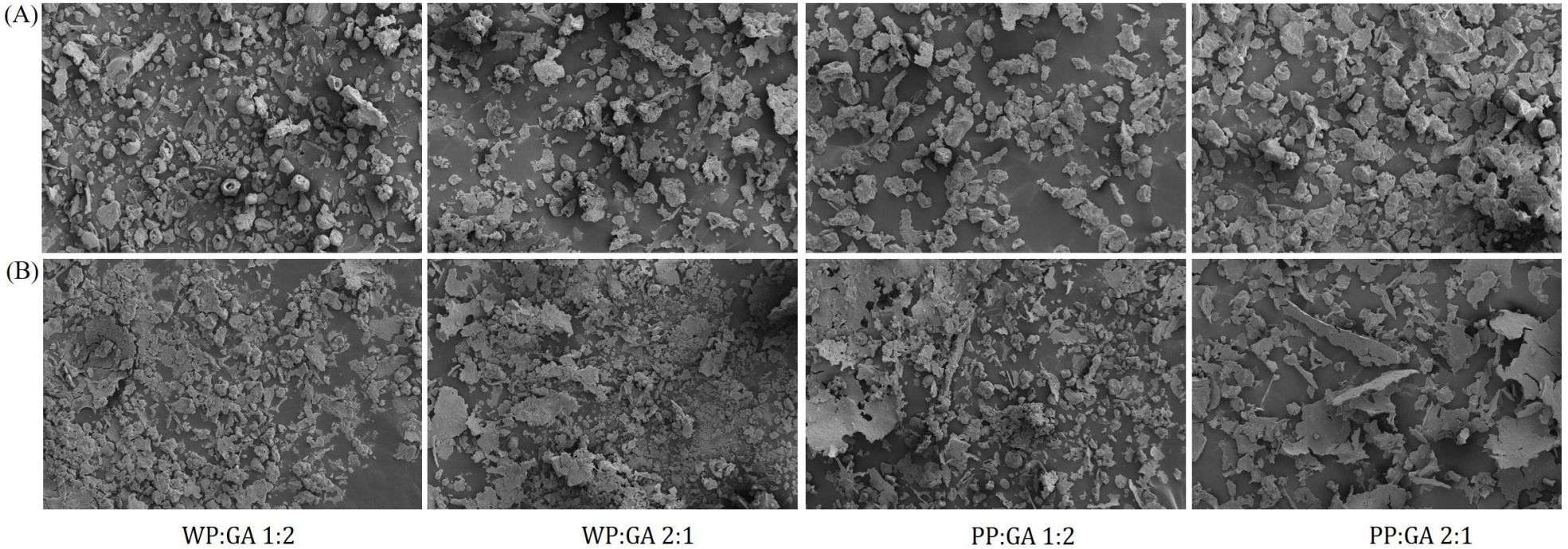

Figure 4 – Scanning electron microscopy (SEM) images of the digested samples (encapsulated samples with whey protein (WP) or pea protein (PP) combined with gum arabic (GA) in two different proportions, 1:2 or 2:1 (v/v)) at 300x magnification. (A) Gastric digestion (B) Small intestine digestion.

The higher degradation of anthocyanins in the free extract resulted in more detected metabolites in the media at the end of the 4 h digestion process (Table 3). As discussed before, during digestion, the pH and digestive enzymes can degrade anthocyanins into the corresponding aldehyde and phenolic acids, that can be further metabolized. Higher concentrations of protocatechuic acid, gallic acid, vanillic acid, methyl gallate and 1-GG were detected for the free extract compared to the encapsulated samples ($p<0.05$). Higher areas for the compounds gentisic acid, 2-GG, 3-GG and 4-GG were also found for the extract.

The results showed that encapsulation with different proportions of proteins and GA effectively reduced the release of anthocyanins under gastric conditions, while maintaining a controlled release in the intestinal phase, where the anthocyanins are mainly absorbed. This led to a higher bioaccessibility of anthocyanins and consequently to a lower concentration of metabolites, since less anthocyanins were degraded in the first phases of digestion.

Table 3 – Concentration (mg/L) or area of phenolic compounds detected by LC-ESI-MS/MS after 4-h *in vitro* digestion

Compounds	JE	WP:GA 1:2	WP:GA 2:1	PP:GA 1:2	PP:GA 2:1
Cyanidin-3-glucoside (mg/L)	93.21 ± 7.16^{d}	183.14 ± 1.49^{a}	168.52 ± 8.38^{b}	185.31 ± 7.44^{a}	113.04 ± 4.82^{c}
Protocatechuic acid (mg/L)	187.79 ± 9.91^{a}	52.54 ± 5.61^{d}	69.25 ± 8.04^{c}	83.18 ± 6.00^{c}	120.62 ± 7.30^{b}
Gallic acid (mg/L)	5.29 ± 0.33^{a}	2.89 ± 0.13^{d}	3.07 ± 0.14^{cd}	3.43 ± 0.07^{c}	4.62 ± 0.38^{b}
Phloroglucinol aldehyde (mg/L)	0.05 ± 0.01^{ab}	0.02 ±0.00^{b}	0.03 ± 0.01^{b}	0.04 ± 0.00^{b}	0.11 ± 0.07^{a}
Vanillic acid (mg/L)	10.34 ± 0.66^{a}	n.d.	n.d.	n.d.	n.d.
Gentisic acid (area)	28060.75 ± 1749.97^{a}	8158.75 ± 860.65^{d}	10625 ± 1640.39^{d}	14131.75 ± 1573.43^{c}	20004.75 ± 827.95^{b}
Methyl gallate (mg/L)	1.38 ± 0.08^{a}	0.05 ± 0.01^{c}	0.31 ± 0.07^{b}	0.17 ± 0.02^{c}	0.34 ± 0.09^{b}
Monogalloyl glucose (mg/L)	1.92 ± 0.04^{a}	n.d.	n.d.	n.d.	n.d.
Digalloyl glucose (área)	17009.88 ± 384.32^{a}	3045.00 ± 277.52^{c}	5223.75 ± 432.65^{b}	5249.25 ± 888.03^{b}	3287.50 ± 414.18^{c}
Trigalloyl glucose (área)	15245.25 ± 2673.50^{a}	879.25 ± 379.64^{b}	3021.75 ± 633.19^{b}	2148.00 ± 658.87^{b}	1785.00 ± 473.80^{b}
Tetragalloyl glucose (área)	19113.25 ± 2039.04^{a}	n.d.	1167.00 ± 353.87^{b}	1376.25 ± 299.25^{b}	1087.75 ± 482.24^{b}

Values are presented as mean ± standard deviation (n=3). Mean values with different lowercase letters within the same row are significantly different (Tukey's multiple comparisons test, $p<0.05$). n.d. = not detected

3.7. *In vitro* colonic metabolism

Following the gastric and small intestine phases, to evaluate the release and biotransformation of the compounds in conditions mimicking the colon, the residues from the *in vitro* digestion were incubated with fecal samples. Figure 5 shows the concentration of the compounds over time. The concentration of cyanidin-3-glucoside in the fecal fermentation media first increased indicating its release from the residue right after being added and mixed with the medium, followed by a decreasing trend (Figure 5A). The higher concentrations of cyanidin-3-glucoside were detected at 0 h in the samples PP:GA 2:1 (57.89 ± 4.45 mg/L) and WP:GA 2:1 (56.19 ± 1.20 mg/L) ($p<0.05$), indicating that these samples retained more anthocyanins in the residue after the digestion, which is in accordance with the results observed previously. The concentration of anthocyanins delivered to the fecal fermentation media was ~18-fold higher compared to the free extract (3.17 ± 1.03 mg/L).

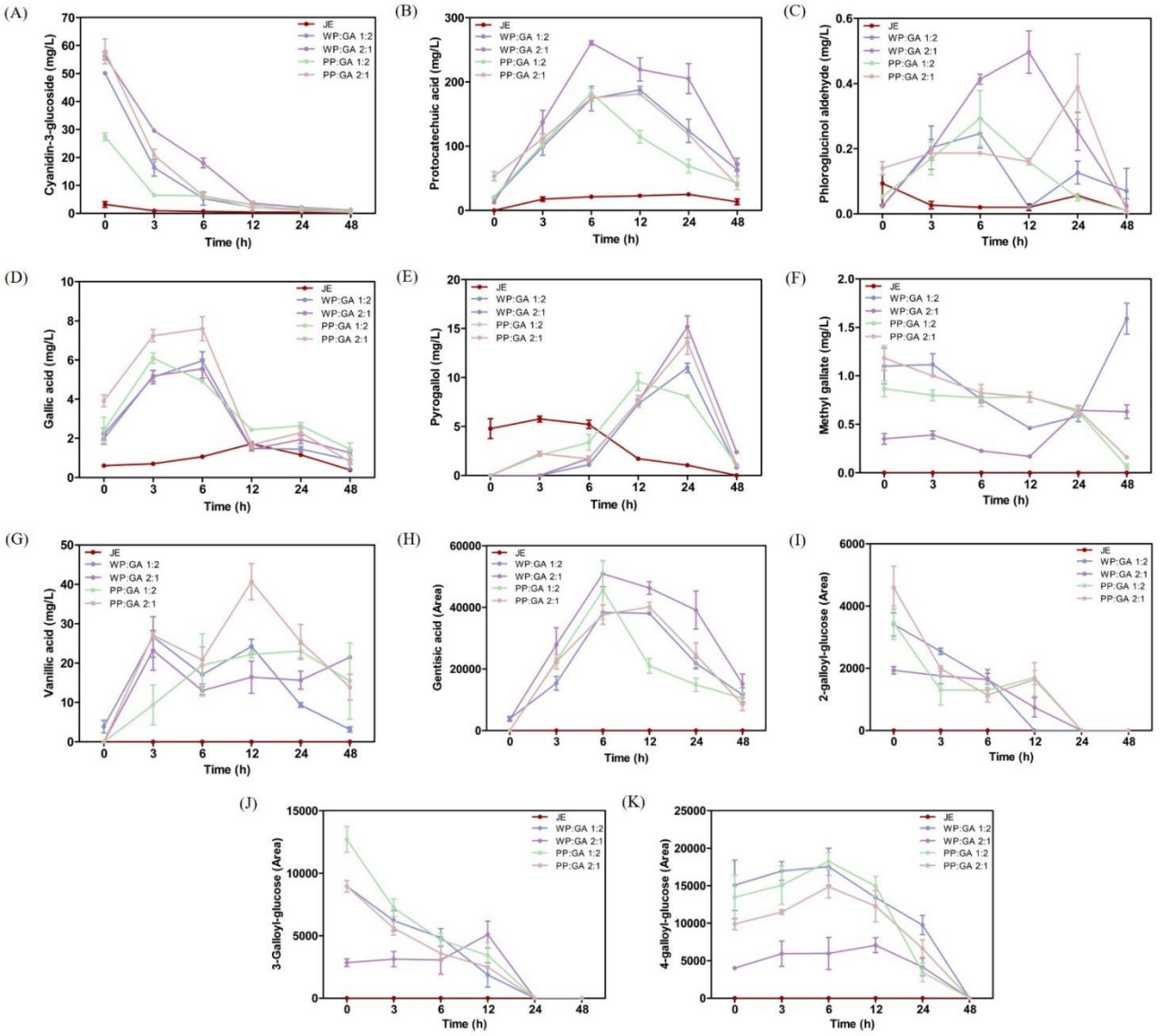

Figure 5 – Changes in the content of phenolic compounds during 48 h of *in vitro* colonic metabolism. Values are expressed as mean ± SD. Cyanidin-3-glucoside (A), protocatechuic acid (B), phloroglucinol aldehyde (C), gallic acid (D), pyrogallol (E), methyl gallate (F), vanillic acid (G), gentisic acid (H), 2-galloyl-glucose (I), 3-galloyl-glucose (J), 4-galloyl-glucose (K).

After 48 h, the degradation rate of cyanidin-3-glucoside reached more than 90%, indicating that cyanidin-3-glucoside was almost completely metabolized by the gut microbiota. A control without the fecal microbiota was performed to differentiate the metabolization derived from spontaneous degradation of the compounds in the media at pH 7.0 and the metabolization derived from microbial metabolism. The concentration of cyanidin-3-glucoside also decreased in the

control over time; however, to a lesser extent compared to samples metabolized by the microbiota ($p<0.05$) (Table S1). The initial concentration in the control was reduced in average by ~ 42% after 24 h and 70% after 48 h, indicating that were spontaneous degradation of cyanidin-3-glucoside in the FFM.

The evolutions of metabolites at different stages of the colonic phase were also monitored and the results are presented in Figure 5. In summary, besides cyanidin-3-glucoside, ten phenolic compounds were identified. The other compounds listed in the methodology (section 2.9) were not detected under any of the collection times assayed, including the aglycone cyanidin.

The effects of the medium conditions and bacterial metabolism led to the breakdown of glycosidic bonds and cleavage of the anthocyanin heterocycle ring. Protocatechuic acid, phenolic acid originated from B ring of cyanidin-3-glucoside, was detected in the samples. The concentration of this phenolic acid increased up to 6 h or 12 h, then decreased gradually until 48 h (Figure 5B). After 24 h, the concentration of this acid was higher for all the samples compared to the control (Table S1), which is in accordance with the higher degradation of cyanidin-3-glucoside in those samples due to the microbial metabolism. The decrease in the concentrations after 6 h indicated that protocatechuic acid was produced and then utilized by the microbiota. The other product formed from the cleavage of the anthocyanin ring is phloroglucinol aldehyde and it was also detected during fermentation. The concentration of this compound oscillated during 24 h for all the samples and declined at the end of the fermentation (Figure 5C).

Gallic acid was also detected in the samples (Figure 5D). This phenolic acid was originally present in the samples and the increase in its concentration over time may have originated from the degradation of the gallotannins (2-GG, 3-GG and 4-GG). It reached the maximum concentration at 6 h for the encapsulated samples and at 12 h for the free extract. The decrease in the area detected for the gallotannins indicated that were microbiota-mediated hydrolysis of the tannins leading to the production of gallic acid. Gallic acid is considered a highly bioaccessible metabolite of gallotannins, which have been extensively studied and are primarily responsible for the health benefits associated with tannins (Sallam et al., 2021).

The metabolism of gallotannins varied over time. After 3 h of fermentation, significant metabolism of 2-GG (Figure 5I) and 3-GG (Figure 5J) was observed, whereas 4-GG (Figure 5K) showed substantial metabolism after 12 h of fermentation. Encapsulated samples exhibited higher content of 2-GG, 3-GG, and 4-GG in the fermentation media compared to the free extract.

Gallotannins from the free extract were released earlier during the digestive process, being metabolized during the gastric and small intestinal phases, resulting in undetected concentrations in the residue and consequently in the fecal fermentation media. Conversely, encapsulated samples retained a higher concentration of these compounds in the residue, retarding their release and metabolism during gastric and small intestinal digestion, and delivering these compounds for microbiota metabolism. Degradation of gallotannins was also observed in the control; however, it occurred to a lesser extent than in the samples metabolized by the microbiota (Table S1).

The decrease in gallic acid concentration after 6 h can be attributed to the metabolization of this compound by the microbiota. The bacterial enzyme gallate decarboxylase catalyzes the decarboxylation of gallic acid, leading to the formation of pyrogallol (Pulido-Mateos et al., 2022). The concentration of pyrogallol increased after 6 h of fermentation, reaching its maximum concentration at 24 h for the samples WP:GA 2:1, PP:GA 2:1 and WP:GA 1:2 (Figure 5E). For the free extract, a higher concentration of pyrogallol were observed at 0 h and the concentration started to decrease after 6 h. The decline in the concentration of this compound towards the end of fermentation, indicated that pyrogallol, once formed, underwent additional metabolic transformations within the gut microbiota.

Another compound that can be derived from gallic acid and was detected is methyl gallate, the methyl ester of gallic acid (Abdullah et al., 2023). The evolution of methyl gallate was different between the samples. For the samples encapsulated with PP, there was a decrease in the concentration from 0 h. For the samples encapsulated with WP, the concentration declined after 3 h and increased after 12 h, being the higher concentration of methyl gallate detected for the sample WP:GA 1:2 after 48 h of fermentation (Figure 5F).

Other metabolites identified in the samples were vanillic acid and gentisic acid. Vanillic acid was not detected in the control, so your formation can be attributed only to the microbial metabolism. The concentration of this phenolic acid showed oscillations within the time of fermentation and was not detectable for the free extract (Figure 5G). For gentisic acid, an increase in area were observed until 6 h, followed by a decline. This metabolite was not detected either for the free extract (Figure 5H).

In summary, the results from the colonic phase showed that encapsulated samples retained more phenolic compounds in the residue following gastric and small intestine digestion, delivering more intact anthocyanins and tannins to the colon phase. This led to the formation of higher

concentrations of metabolites compared to the free extract. It has already been demonstrated the beneficial effects of bioactive phytochemicals, such as anthocyanins, on colon health, including reducing inflammation, inhibiting colon cancer cells, promoting the growth of beneficial bacteria, suppressing the harmful bacteria growth, and increasing the production of SCFAs (Feng et al., 2020; Liang et al., 2023). The large intestine also plays an important role in the bioavailability of anthocyanins. This was demonstrated by the results of anthocyanin absorption for subjects with an intact healthy gut compared to ileostomies with an interrupted intestinal passage lacking a colon (Mueller et al., 2017). The amounts of anthocyanins in the plasma and urine of healthy subjects were 79% and 44% higher, respectively, than in the plasma and urine of ileostomists (Mueller et al., 2017).

However, the challenge lies in the susceptibility of these compounds to degradation in the gastrointestinal tract. This degradation can compromise their effectiveness before reaching the colon and exert their benefits. Therefore, alternatives to protect the bioactive compounds until they reach the colon are necessary (Feng et al., 2020). In this study, the encapsulation treatments showed potential as an alternative approach for targeted delivery of compounds to the colon to be metabolized by the intestinal microbiota, particularly the samples encapsulated with a higher proportion of proteins, which delivered increased concentrations of intact anthocyanins.

3.8. Short-chain fatty acids

Colonic metabolism of polyphenols can also promote health increasing the biosynthesis of microbial short-chain fatty-acids (SCFAs), that have been associated with different health benefits, such as anti-inflammatory, immunoregulatory, anti-obesity, anti-diabetes, anticancer, cardiovascular protective, hepatoprotective, and neuroprotective activities (Xiong et al., 2022).

All the encapsulated samples presented higher contents of SCFAs compared to the free extract ($p<0.05$). The increased concentration of SCFAs in the encapsulated samples can be associated with the higher content of phenolic compounds delivered for microbial metabolism, since previous studies have shown that polyphenols can increase SCFAs production by promoting the abundance of specific bacteria (Zhang et al., 2022). Furthermore, the wall materials, GA, and proteins could potentially act as substrates for the synthesis of SCFAs. Branched-Chain SCFAs (isobutyric acid, isovaleric acid, and 2-methylbutyric acid) are primarily formed from the

degradation of proteins, while straight-chain SCFAs are primarily formed from the fermentation of carbohydrates (acetic, propionic, and butyric acids) (Comino et al., 2018).

Different SCFA profiles were observed for the encapsulated samples, indicating that the type and ratio of polymers used influenced the SCFA production during fermentation (Figure 6). Across all samples, butyric acid was consistently the most abundant, followed by propionic acid in WP-encapsulated samples and 2-methylbutyric acid/isovaleric acid in PP-encapsulated samples. Butyric and propionic acids, along with acetic acid, are the major SCFAs produced in the gut and they have been extensively studied (Rios-Covian et al., 2020).

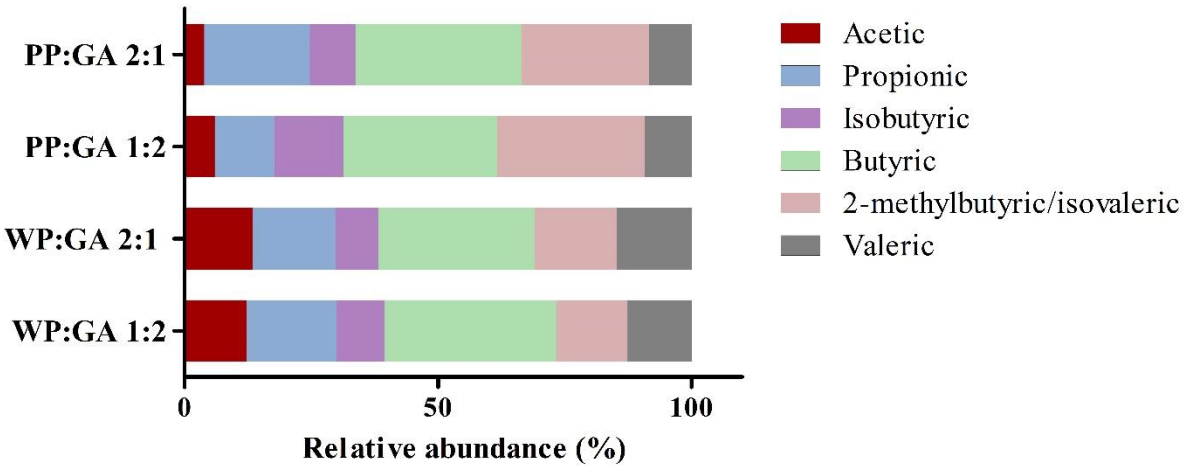

Figure 6 - Relative abundance of short chain fatty acids (SCFAs) produced during 48 h of *in vitro* fecal fermentation.

Concerning the concentration of SCFAs (Figure 7), the WP:GA 2:1 sample resulted in higher concentrations of acetic, propionic, butyric, and valeric acids. The sample WP:GA 1:2 followed these sample presenting the second highest concentration for those SCFAs. Regarding isobutyric acid, the content did not significantly differ between the encapsulated samples. For 2-methylbutyric acid/isovaleric acid, the samples WP:GA 2:1, PP:GA 1:2 and PP:GA 2:1 presented the highest concentrations.

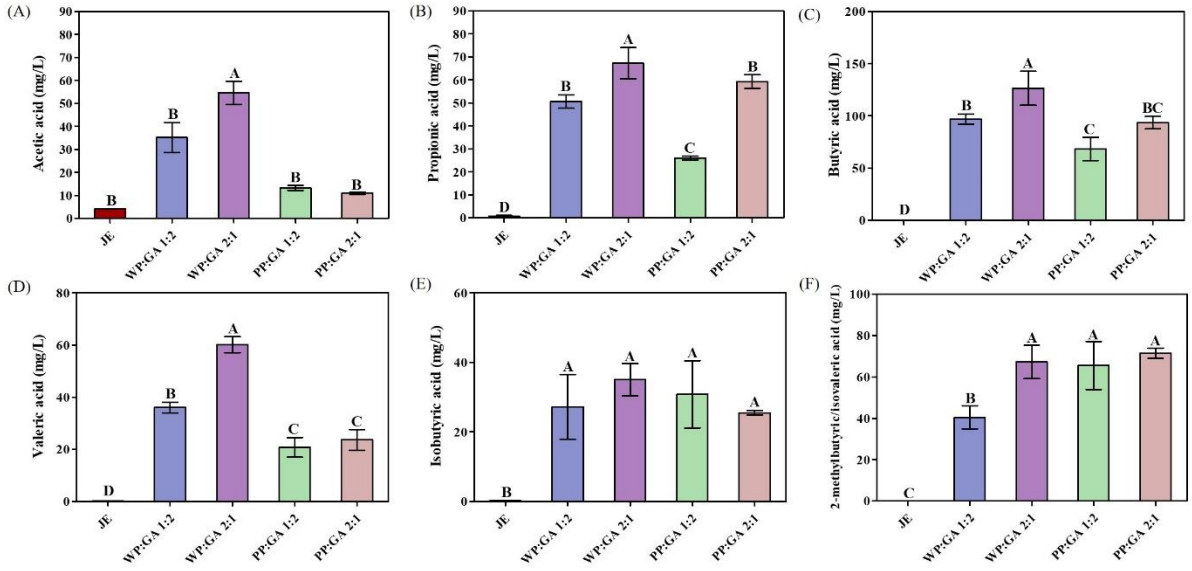

Figure 7 - Concentration (mg/L) of short-chain fatty acids (SCFAs) produced during 48 h of *in vitro* fecal fermentation. Acetic acid (A), propionic acid (B), butyric acid (C), valeric acid (D), Isobutyric acid (E), and 2-methylbutyric acid/isovaleric acid (F). Concentration is expressed as mean ± SD. Mean values with different letters are significantly different (Tukey's multiple comparisons test, $p<0.05$).

Branched short-chain fatty acids (BCFAs) are usually produced in less amounts and have been suggested as indicators of protein fermentation (Rios-Covian et al., 2020). The similar concentrations observed among the treatments suggest that both PP and WP residues were efficiently fermented by the bacteria, stimulating the production of isobutyric acid and 2-methylbutyric acid/isovaleric acid in both ratios studied. However, for 2-methylbutyric acid/isovaleric acid, the sample with a lower proportion of WP showed a reduced concentration.

In summary, the encapsulated samples showed potential as an alternative approach for targeted delivery of compounds to the colon to increase the production of SCFAs, particularly the samples encapsulated with WP, which generated higher concentrations of straight-chain SCFAs and similar concentrations of branched-Chain SCFAs compared to the samples encapsulated with PP.

3.9. *In vitro* study of the effects of cyanidin-3-glucoside and metabolites on HT29-MTX cells

In the present study, the *in vitro* gastrointestinal digestion simulation revealed that encapsulation can delay the release of compounds during the gastric and small intestinal phases and increase the bioaccessibility of anthocyanins. However, this also resulted in the formation of lower concentrations of metabolites in the medium at the end of digestion compared to the free extract. To investigate this further, the bioactivity of cyanidin-3-glucoside (cya-3-glu) and the main metabolites was compared in the colon cancer cell line HT29-MTX. The isolated compounds and two different mixtures were tested: one with a higher cya-3-glu content and another with a higher concentration of metabolites, as detailed in section 2.11.2.

The generation of ROS was assessed in HT29-MTX human colon adenocarcinoma cell line with different concentration of the compounds. The concentrations were selected based on cell viability results showing no significant suppression of growth by the compounds (Figure S1). Results indicated that ROS levels increased up to 1.84-fold compared to the control following LPS challenge. This effect was significantly prevented by cya-3-glu and other metabolites, exhibiting a dose-dependent response (Figure 8).

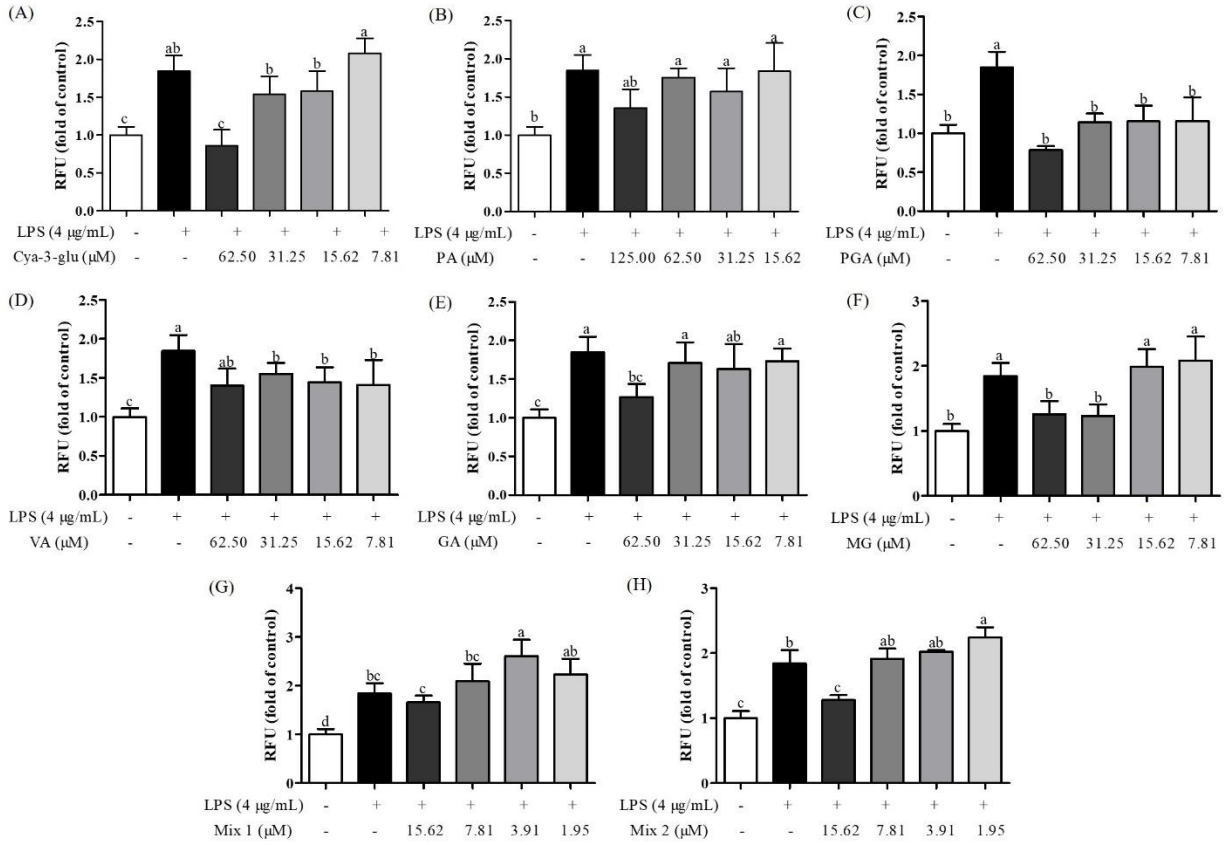

Figure 8 - Reactive Oxygen Species (ROS) in HT29-MTX cells treated with different concentrations of the phenolic compounds followed by LPS (4 µg/mL) challenge for 3 h. Cyanidin-3-glucoside (A), protocatechuic acid (B), phloroglucinol aldehyde (C), vanillic acid (D), gallic acid (E), methyl gallate (F), mixture 1 (G), mixture 2 (H). Results were expressed as RFU (relative fluorescence units)-fold of untreated control. Values are presented as the mean ± standard deviation of two independent assays with internal quadruplicates for each of them. Mean values with different lowercase letters are significantly different (Tukey's multiple comparisons test, $p<0.05$).

Cya-3-glu showed a higher antioxidant activity compared to its primary metabolite PA at a concentration of 62.50 µM (Figure 9). On the other hand, cya-3-glu showed similar activity to other compounds like GA, VA, PGA, and MG, which suggests that these phenolic compounds, despite having different structures, share a similar ability to mitigate ROS production in HT29-MTX cells challenged with LPS. Regarding the mixtures, the one with a higher content of cya-3-glu (Mix 2) was more effective in reducing ROS production compared to the mixture with a higher

content of metabolites (Mix 1). This result aligns with the individual activity of cya-3-glu, suggesting that its higher concentration enhanced the overall antioxidant activity of the mixture.

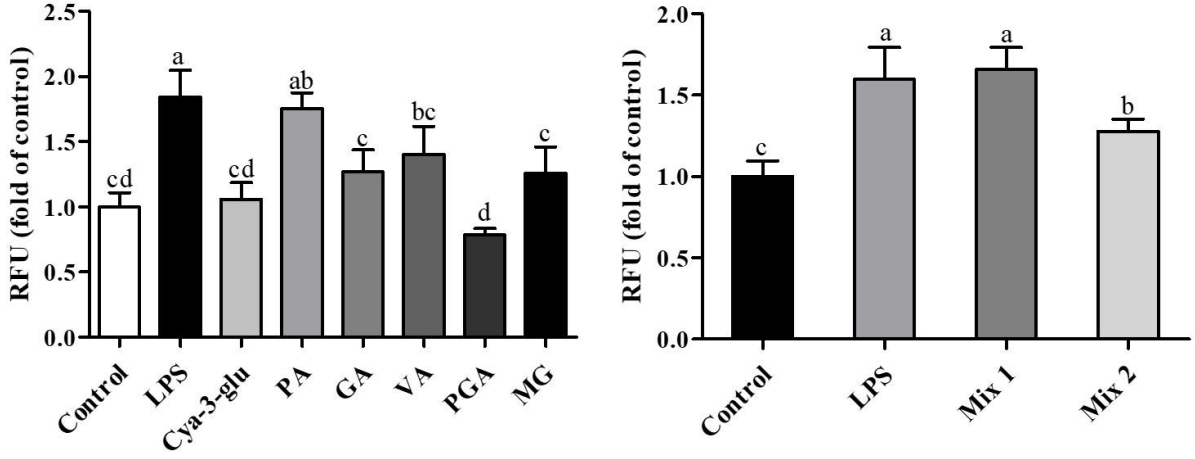

Figure 9 - Reactive Oxygen Species (ROS) in HT29-MTX cells treated with phenolic compounds at a concentration of 62.50 µM, followed by an LPS (4 µg/mL) challenge for 3 h. Results were expressed as RFU (relative fluorescence units)-fold of untreated control. Values are presented as the mean ± standard deviation of two independent assays with internal quadruplicates for each of them. Mean values with different lowercase letters are significantly different (Tukey's multiple comparisons test, $p<0.05$).

Phenolic compounds are also widely recognized for their anti-inflammatory properties. However, limited evidence is available comparing the biological activity of parent compounds and its metabolites. Phenolic compounds can inhibit the activity of enzymes like cyclooxygenase (COX), particularly COX-2, which are responsible for the synthesis of pro-inflammatory mediators like prostaglandins (Yahfoufi et al., 2018). The mRNA expression of COX-2 was upregulated by LPS challenge by 1.6-fold (Figure 10). All the compounds were able to prevent the up-regulation by LPS, except for MG. Additionally, gallic acid (GA) was the only compound that caused a downregulation of this enzyme.

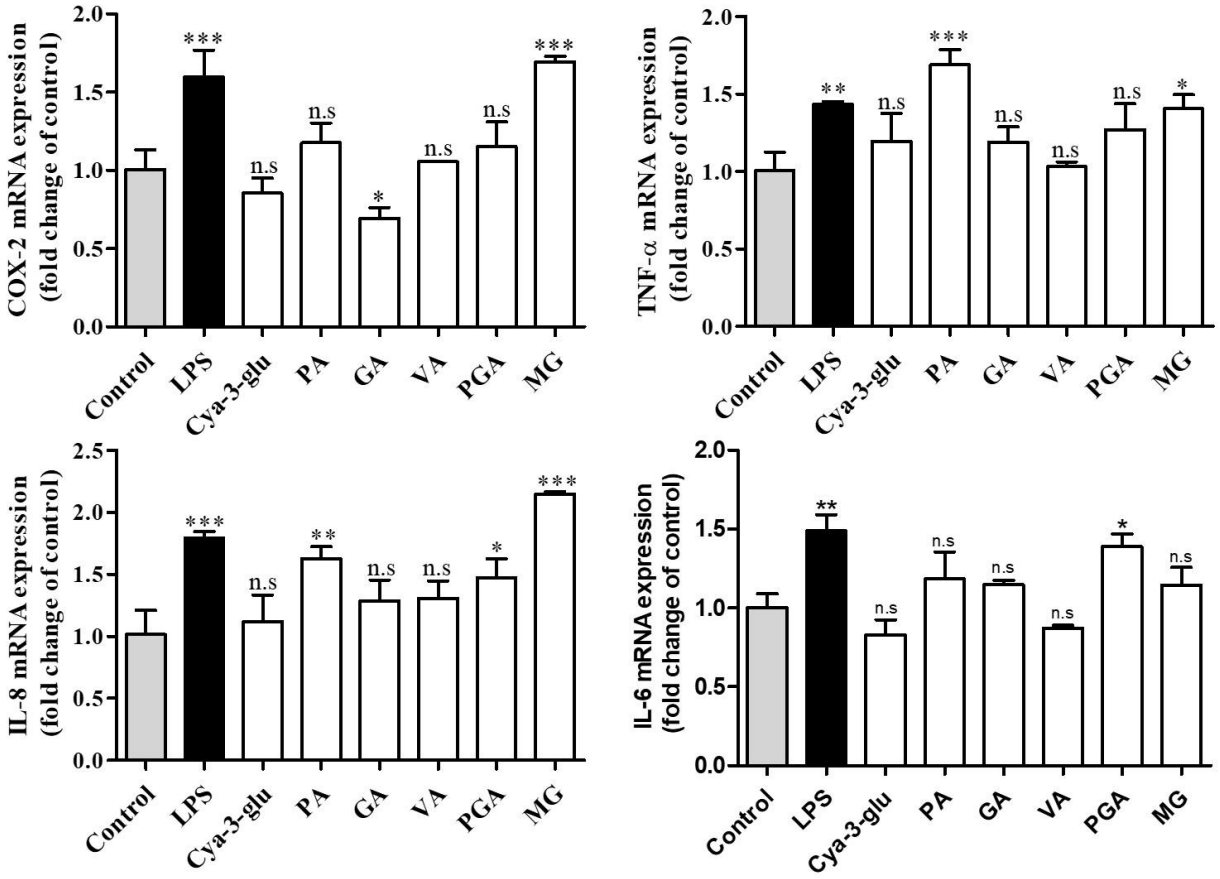

Figure 10 – Gene expression of COX-2 and inflammatory cytokines (TNF-α, IL-6, and IL-8) in HT29-MTX cells treated with phenolic compounds at a concentration of 15.62 µM. Values are presented as mean ± standard deviation (n=3). Statistically significant differences between the control (untreated cells) and the cells treated with different phenolic compounds were identified using Dunnett's test (∗p<0.05; ∗∗p<0.01; ∗∗∗ p<0.001).

Phenolic compounds can also modulate key signaling pathways involved in inflammation, such as nuclear factor-kappa B (NF-κB), and regulate the expression of various pro-inflammatory cytokines, including TNF-α, IL-6, and IL-8 (Yahfoufi et al., 2018). After an LPS challenge, mRNA expression of TNF-α increased by 1.4-fold (Figure 10). This effect was reduced by cya-3-glu and the metabolites to levels comparable to the unchallenged control, except for PA and MG. Similarly, the mRNA expression of pro-inflammatory cytokines/chemokines IL-6 and IL-8 was significantly upregulated by LPS stimulation, with IL-6 increasing by 1.5-fold and IL-8 by 1.8-fold. Only cya-3-glu, GA, and VA were effective in preventing the increase in IL-8 expression. On the other hand,

all the compounds, except for PGA, prevented the LPS-induced upregulation of IL-6 in HT29-MTX cells.

Regarding the mixtures, Mix 2 downregulated TNF-α expression and prevented the LPS-induced upregulation of IL-8, while both Mix 1 and Mix 2 were able to regulate the expression of COX-2 and IL-6 to levels similar to the untreated control (Figure 11).

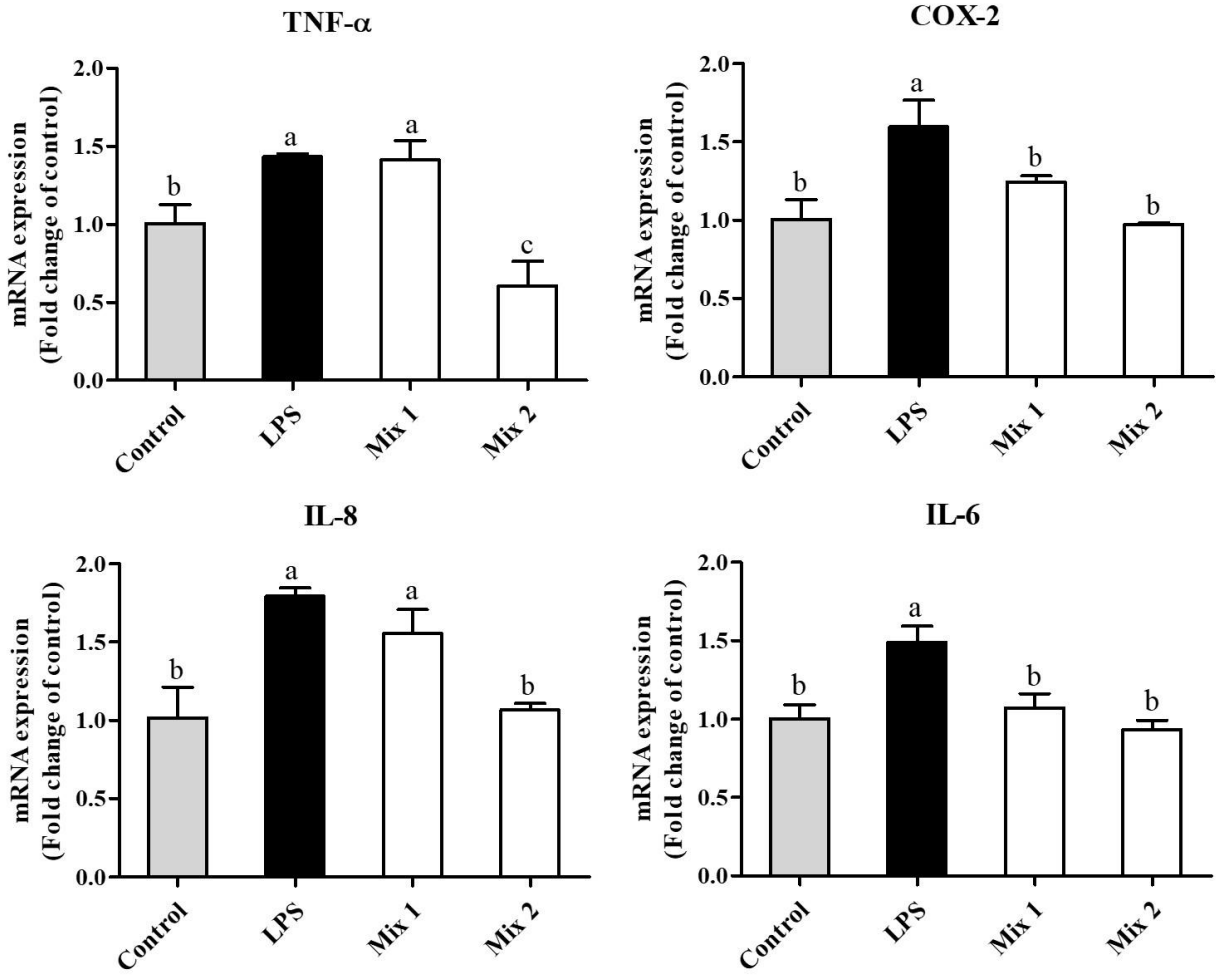

Figure 11 – Gene expression of COX-2 and inflammatory cytokines (TNF-α, IL-6, and IL-8) in HT29-MTX cells treated with the mixtures at a concentration of 15.62 µM. Values are presented as mean ± standard deviation (n=3). Mean values with different lowercase letters are significantly different (Tukey's multiple comparisons test, $p<0.05$).

The results showed the superior antioxidant and anti-inflammatory properties of cya-3-glu compared to its primary metabolites, particularly PA. Cya-3-glu was more effective in preventing ROS formation and the upregulation of key pro-inflammatory markers such as TNF-α

and IL-8, compared to PA. Cya-3-glu was also more effective in preventing the LPS-induced upregulation of IL-6 compared to its other primary metabolite PGA. The mixture with a higher content of cya-3-glu (Mix 2) also showed higher antioxidant activity and was more effective in downregulating TNF-α and preventing the upregulation of IL-8 compared to Mix 1, which contained more of the metabolites.

4. Conclusion

The encapsulation of jabuticaba extract achieved high encapsulation efficiency with both proteins and ratios studied. The results also showed that encapsulation increased the bioaccessibility of anthocyanins, providing a reduced and controlled release during *in vitro* gastric and small intestine phases. Encapsulation delayed the degradation of the compounds during the initial phases of digestion, effectively retaining more anthocyanins and tannins in the residue and delivering a higher concentration of parent compounds to the colonic phase, which resulted in the formation of a higher concentration of beneficial metabolites, including phenolic acids. The encapsulated samples also increased the production of short-chain fatty acids (SCFAs) compared to the free extract, particularly the samples encapsulated with whey protein, which generated higher concentrations of straight-chain SCFAs. Cyanidin-3-glucoside showed higher antioxidant and anti-inflammatory properties compared to its primary metabolites against HT29-MTX colon cancer cell line, suggesting that increased concentrations of this anthocyanin could offer enhanced health benefits. Based on the results, the combination of whey protein or pea protein with gum arabic can be considered promising as a food-grade carrier for the encapsulation of bioactive compounds like anthocyanins. Pea protein is also a sustainable alternative for the growing demand for plant-derived proteins for the encapsulation of compounds in the food industry. Future studies should include human trials to elucidate how encapsulation affects the pharmacokinetics of anthocyanins and their metabolites *in vivo*, as well as the impact of the different formulations on the gut microbiota.

5. References

Abdullah, H., Ismail, I., Suppian, R., & Zakaria, N. M. (2023). Natural Gallic Acid and Methyl Gallate Induces Apoptosis in Hela Cells through Regulation of Intrinsic and Extrinsic Protein

Expression. International Journal of Molecular Sciences, 24(10), 1–23. https://doi.org/10.3390/ijms24108495

Aguilar-Vázquez, G., Loarca-Piña, G., Figueroa-Cárdenas, J. D., & Mendoza, S. (2018). Electrospun fibers from blends of pea (*Pisum sativum*) protein and pullulan. Food Hydrocolloids, 83, 173–181. https://doi.org/10.1016/j.foodhyd.2018.04.051

Albuquerque, B. R., Pereira, C., Calhelha, R. C., Alves, M. J., Abreu, R. M. V., Barros, L., Oliveira, M. B. P. P., & Ferreira, I. C. F. R. (2020). Jabuticaba residues (*Myrciaria jaboticaba* (Vell.) Berg) are rich sources of valuable compounds with bioactive properties. Food Chemistry, 309, 1–8. https://doi.org/10.1016/j.foodchem.2019.125735

Arbizu, S., Chew, B., Mertens-Talcott, S. U., & Noratto, G. (2020). Commercial whey products promote intestinal barrier function with glycomacropeptide enhanced activity in downregulating bacterial endotoxin lipopolysaccharides (LPS)-induced inflammation: *In vitro*. Food and Function, 11(7), 5842–5852. https://doi.org/10.1039/d0fo00487a

Ayvaz, H., Cabaroglu, T., Akyildiz, A., Pala, C. U., Temizkan, R., Ağçam, E., Ayvaz, Z., Durazzo, A., Lucarini, M., Direito, R., & Diaconeasa, Z. (2023). Anthocyanins: Metabolic Digestion, Bioavailability, Therapeutic Effects, Current Pharmaceutical/Industrial Use, and Innovation Potential. Antioxidants, 12(1), 1–39. https://doi.org/10.3390/antiox12010048

Bashir, M., & Haripriya, S. (2016). Assessment of physical and structural characteristics of almond gum. International Journal of Biological Macromolecules, 93, 476–482. https://doi.org/10.1016/j.ijbiomac.2016.09.009

Batista, Â. G., Lenquiste, S. A., Cazarin, C. B. B., da Silva, J. K., Luiz-Ferreira, A., Bogusz, S., Wang Hantao, L., de Souza, R. N., Augusto, F., Prado, M. A., & Maróstica, M. R. (2014). Intake of jaboticaba peel attenuates oxidative stress in tissues and reduces circulating saturated lipids of rats with high-fat diet-induced obesity. Journal of Functional Foods, 6(1), 450–461. https://doi.org/10.1016/j.jff.2013.11.011

Burton-freeman, B., Sandhu, A., & Edirisinghe, I. (2016). Anthocyanins. In R. C. Gupta (Ed.), Nutraceuticals (1st ed., pp. 489–500). Academic Press. https://doi.org/10.1016/B978-0-12-802147-7.00035-8

Cai, X., Du, X., Cui, D., Wang, X., Yang, Z., & Zhu, G. (2019). Improvement of stability of blueberry anthocyanins by carboxymethyl starch/xanthan gum combinations microencapsulation. Food Hydrocolloids, 91, 238–245. https://doi.org/10.1016/j.foodhyd.2019.01.034

Calloni, C., Martínez, L. S., Gil, D. F., da Silva, D. M., Rosales, P. F., Agostini, F., Moura e Silva, S., Parmegiani Jahn, M., & Salvador, M. (2020). Jabuticaba (*Plinia trunciflora* (O. Berg) Kausel) improved the lipid profile and immune system and reduced oxidative stress in streptozotocin-induced diabetic rats. Journal of Food Biochemistry, 44(9), 1–12. https://doi.org/10.1111/jfbc.13383

Carpentier, J., Conforto, E., Chaigneau, C., Vendeville, J. E., & Maugard, T. (2021). Complex coacervation of pea protein isolate and tragacanth gum: Comparative study with commercial polysaccharides. Innovative Food Science and Emerging Technologies, 69. https://doi.org/10.1016/j.ifset.2021.102641

Carvalho, A. G. da S., Machado, M. T. da C., da Silva, V. M., Sartoratto, A., Rodrigues, R. A. F., & Hubinger, M. D. (2016). Physical properties and morphology of spray dried microparticles containing anthocyanins of jussara (*Euterpe edulis* Martius) extract. Powder Technology, 294, 421–428. https://doi.org/10.1016/j.powtec.2016.03.007

Chang, C., Li, J., Su, Y., Gu, L., Yang, Y., & Zhai, J. (2022). Protein particle-based vehicles for encapsulation and delivery of nutrients: Fabrication, digestion, and release properties. Food Hydrocolloids, 123, 106963. https://doi.org/10.1016/j.foodhyd.2021.106963

Comino, P., Williams, B. A., & Gidley, M. J. (2018). *In vitro* fermentation gas kinetics and end-products of soluble and insoluble cereal flour dietary fibres are similar. Food and Function, 9(2), 898–905. https://doi.org/10.1039/c7fo01724

Comunian, T. A., Archut, A., Gomez-Mascaraque, L. G., Brodkorb, A., & Drusch, S. (2022). The type of gum arabic affects interactions with soluble pea protein in complex coacervation. Carbohydrate Polymers, 295, 119851. https://doi.org/10.1016/j.carbpol.2022.119851

Cory, H., Passarelli, S., Szeto, J., Tamez, M., & Mattei, J. (2018). The Role of Polyphenols in Human Health and Food Systems: A Mini-Review. Frontiers in Nutrition, 5, 1–9. https://doi.org/10.3389/fnut.2018.00087

Cui, H., Si, X., Tian, J., Lang, Y., Gao, N., Tan, H., Bian, Y., Zang, Z., Jiang, Q., Bao, Y., & Li, B. (2022). Anthocyanins-loaded nanocomplexes comprising casein and carboxymethyl cellulose: stability, antioxidant capacity, and bioaccessibility. Food Hydrocolloids, 122. https://doi.org/10.1016/j.foodhyd.2021.107073

Dangles, O., & Fenger, J. A. (2018). The chemical reactivity of anthocyanins and its consequences in food science and nutrition. Molecules, 23(8). https://doi.org/10.3390/molecules23081970

De Ferrars, R. M., Czank, C., Zhang, Q., Botting, N. P., Kroon, P. A., Cassidy, A., & Kay, C. D. (2014). The pharmacokinetics of anthocyanins and their metabolites in humans. British Journal of Pharmacology, 171(13), 3268–3282. https://doi.org/10.1111/bph.12676

de Souza, V. B., Thomazini, M., Echalar Barrientos, M. A., Nalin, C. M., Ferro-Furtado, R., Genovese, M. I., & Favaro-Trindade, C. S. (2018). Functional properties and encapsulation of a proanthocyanidin-rich cinnamon extract (*Cinnamomum zeylanicum*) by complex coacervation using gelatin and different polysaccharides. Food Hydrocolloids, 77, 297–306. https://doi.org/10.1016/j.foodhyd.2017.09.040

Weinbreck Dhenadhayalan, N., Mythily, R., & Kumaran, R. (2014). Fluorescence spectral studies of Gum Arabic: Multi-emission of Gum Arabic in aqueous solution. Journal of Luminescence, 155, 322–329. https://doi.org/10.1016/j.jlumin.2014.06.022

Dias, M. I., Ferreira, I. C. F. R., & Barreiro, M. F. (2015). Microencapsulation of bioactives for food applications. Food & Function, 6, 1035–1052. https://doi.org/10.1039/c4fo01175a

Du, R., Yang, D., Jiang, G., Song, Y., & Yin, X. (2020). An approach for in situ rapid detection of deep-sea aromatic amino acids using laser-induced fluorescence. Sensors (Switzerland), 20(5), 1330. https://doi.org/10.3390/s20051330

Eghbal, N., & Choudhary, R. (2018). Complex coacervation: Encapsulation and controlled release of active agents in food systems. LWT, 90, 254–264. https://doi.org/10.1016/j.lwt.2017.12.036

Espinosa-Andrews, H., Sandoval-Castilla, O., Vázquez-Torres, H., Vernon-Carter, E. J., & Lobato-Calleros, C. (2010). Determination of the gum Arabic-chitosan interactions by Fourier Transform Infrared Spectroscopy and characterization of the microstructure and rheological features of their coacervates. Carbohydrate Polymers, 79(3), 541–546. https://doi.org/10.1016/j.carbpol.2009.08.040

Feng, K., Wei, Y. shan, Hu, T. gen, Linhardt, R. J., Zong, M. hua, & Wu, H. (2020). Colon-targeted delivery systems for nutraceuticals: A review of current vehicles, evaluation methods and future prospects. Trends in Food Science and Technology, 102, 203–222). https://doi.org/10.1016/j.tifs.2020.05.019

Fernandes, A., Rocha, M. A. A., Santos, L. M. N. B. F., Brás, J., Oliveira, J., Mateus, N., & de Freitas, V. (2018). Blackberry anthocyanins: β-Cyclodextrin fortification for thermal and gastrointestinal stabilization. Food Chemistry, 245, 426–431. https://doi.org/10.1016/j.foodchem.2017.10.109

Fredes, C., Becerra, C., Parada, J., & Robert, P. (2018). The microencapsulation of maqui (*Aristotelia chilensis* (Mol.) Stuntz) juice by spray-drying and freeze-drying produces powders with similar anthocyanin stability and bioaccessibility. Molecules, 23(5). https://doi.org/10.3390/molecules23051227

Gbassi, G., Yolou, F., Sarr, S., Atheba, P., Amin, C., & Ake, M. (2012). Whey proteins analysis in aqueous medium and in artificial gastric and intestinal fluids. International Journal of Biological and Chemical Sciences, 6(4). https://doi.org/10.4314/ijbcs.v6i4.38

Ge, J., Yue, P., Chi, J., Liang, J., & Gao, X. (2018). Formation and stability of anthocyanins-loaded nanocomplexes prepared with chitosan hydrochloride and carboxymethyl chitosan. Food Hydrocolloids, 74, 23–31.

Ghisaidoobe, A. B. T., & Chung, S. J. (2014). Intrinsic tryptophan fluorescence in the detection and analysis of proteins: A focus on förster resonance energy transfer techniques. International Journal of Molecular Sciences, 15(12), 22518–22538. https://doi.org/10.3390/ijms151222518

Hadidi, M., Boostani, S., & Jafari, S. M. (2022). Pea proteins as emerging biopolymers for the emulsification and encapsulation of food bioactives. Food Hydrocolloids, 126, 107474. https://doi.org/10.1016/j.foodhyd.2021.107474

Heneczkowski, M., Kopacz, M., Nowak, D., & Kuzniar, A. (2001). Infrared spectrum analysis of some flavonoids. Acta Poloniae Pharmaceutica, 58(6), 415–420.

Hornedo-Ortega, R., Rasines-Perea, Z., Cerezo, A. B., Teissedre, P.-L., & Jourdes, M. (2021). Anthocyanins: Dietary Sources, Bioavailability, Human Metabolic Pathways, and Potential Anti-Neuroinflammatory Activity. In F. A. Badria & M. Blumenberg (Eds.), Phenolic Compounds - Chemistry, Synthesis, Diversity, Non-Conventional Industrial, Pharmaceutical and Therapeutic Applications (pp. 1–24). IntechOpen.

Hu, Y., Lin, Q., Zhao, H., Li, X., Sang, S., McClements, D. J., Long, J., Jin, Z., Wang, J., & Qiu, C. (2023). Bioaccessibility and bioavailability of phytochemicals: Influencing factors, improvements, and evaluations. Food Hydrocolloids, 135, 108165. https://doi.org/10.1016/j.foodhyd.2022.108165

Inada, K. O. P., Silva, T. B. R., Lobo, L. A., Domingues, R. M. C. P., Perrone, D., & Monteiro, M. (2020). Bioaccessibility of phenolic compounds of jaboticaba (*Plinia jaboticaba*) peel and seed after simulated gastrointestinal digestion and gut microbiota fermentation. Journal of Functional Foods, 67, Article 103851. https://doi.org/10.1016/j.jff.2020.103851

Jafari, S., Jafari, S. M., Ebrahimi, M., Kijpatanasilp, I., & Assatarakul, K. (2023). A decade overview and prospect of spray drying encapsulation of bioactives from fruit products: Characterization, food application and *in vitro* gastrointestinal digestion. Food Hydrocolloids, 134, 108068. https://doi.org/10.1016/j.foodhyd.2022.108068

Kayitmazer, A. B., Koksal, A. F., & Kilic Iyilik, E. (2015). Complex coacervation of hyaluronic acid and chitosan: Effects of pH, ionic strength, charge density, chain length and the charge ratio. Soft Matter, 11(44), 8605–8612. https://doi.org/10.1039/c5sm01829c

Kim, E. S., Kim, D. Y., Lee, J., & Lee, H. G. (2019). Mucoadhesive Chitosan–Gum Arabic Nanoparticles Enhance the Absorption and Antioxidant Activity of Quercetin in the Intestinal Cellular Environment. Journal of Agricultural and Food Chemistry, 67, 8609–8616. https://doi.org/10.1021/acs.jafc.9b00008

Lam, A. C. Y., Can Karaca, A., Tyler, R. T., & Nickerson, M. T. (2018). Pea protein isolates: Structure, extraction, and functionality. Food Reviews International, 34(2), 126–147. https://doi.org/10.1080/87559129.2016.1242135

Lee, J., Durst, R. W., Wrolstad, R. E., Barnes, K. W., Eisele, ; T, Giusti, ; M M, Haché, ; J, Hofsommer, ; H, Koswig, ; S, Krueger, D. A., Kupina, ; S, Martin, ; S K, Martinsen, ; B K, Miller, T. C., Paquette, ; F, Ryabkova, ; A, Skrede, ; G, Trenn, ; U, & Wightman, J. D. (2005). Determination of Total Monomeric Anthocyanin Pigment Content of Fruit Juices, Beverages, Natural Colorants, and Wines by the pH Differential Method: Collaborative Study. Journal of AOAC International, 88(5), 1269–1278.

Lee, Y.-R., & Hong, Y.-H. (2003). Electrophoretic Behaviors of α Lactalbumin and β-Lactoglobulin Mixtures Caused by Heat Treatment. Asian-Australasian Journal of Animal Sciences, 16, 1041–1045.

Lenquiste, S. A., Batista, A. G., Marineli, R. da S., Dragano, N. R. V., & Maróstica, M. R. (2012). Freeze-dried jaboticaba peel added to high-fat diet increases HDL-cholesterol and improves insulin resistance in obese rats. Food Research International, 49(1), 153–160. https://doi.org/10.1016/j.foodres.2012.07.052

Li, W., Bie, Q., Zhang, K., Linli, F., Yang, W., Chen, X., Chen, P., & Qi, Q. (2024). Regulated anthocyanin release through novel pH-responsive peptide hydrogels in simulated digestive environment. Food Chemistry: X, 23, 101645. https://doi.org/10.1016/j.fochx.2024.101645

Li, W., Linli, F., Yang, W., & Chen, X. (2023). Enhancing the stability of natural anthocyanins against environmental stressors through encapsulation with synthetic peptide-based gels. International Journal of Biological Macromolecules, 253, 127133. https://doi.org/10.1016/j.ijbiomac.2023.127133

Liang, A., Leonard, W., Beasley, J. T., Fang, Z., Zhang, P., & Ranadheera, C. S. (2023). Anthocyanins-gut microbiota-health axis: A review. Critical Reviews in Food Science and Nutrition, 1–26. https://doi.org/10.1080/10408398.2023.2187212

Lila, M. A., Burton-Freeman, B., Grace, M., & Kalt, W. (2016). Unraveling Anthocyanin Bioavailability for Human Health. Annual Review of Food Science and Technology, 7, 375–393. https://doi.org/10.1146/annurev-food-041715-033346

Liu, R., Wang, X., Yang, L., Wang, Y., & Gao, X. (2023). Coordinated encapsulation by β-cyclodextrin and chitosan derivatives improves the stability of anthocyanins. International Journal of Biological Macromolecules, 242. https://doi.org/10.1016/j.ijbiomac.2023.125060

Lu, M., Li, Z., Liang, H., Shi, M., Zhao, L., Li, W., Chen, Y., Wu, J., Wang, S., Chen, X., Yuan, Q., & Li, Y. (2015). Controlled release of anthocyanins from oxidized konjac glucomannan microspheres stabilized by chitosan oligosaccharides. Food Hydrocolloids, 51, 476–485. https://doi.org/10.1016/j.foodhyd.2015.05.036

Mansour, M., Salah, M., & Xu, X. (2020). Effect of microencapsulation using soy protein isolate and gum arabic as wall material on red raspberry anthocyanin stability, characterization, and simulated gastrointestinal conditions. Ultrasonics Sonochemistry, 63, 104927. https://doi.org/10.1016/j.ultsonch.2019.104927

Minekus, M., Alminger, M., Alvito, P., Ballance, S., Bohn, T., Bourlieu, C., Carrière, F., Boutrou, R., Corredig, M., Dupont, D., Dufour, C., Egger, L., Golding, M., Karakaya, S., Kirkhus, B., Le Feunteun, S., Lesmes, U., MacIerzanka, A., MacKie, A., … Brodkorb, A. (2014). A standardised static *in vitro* digestion method suitable for food-an international consensus. Food and Function, 5(6), 1113–1124. https://doi.org/10.1039/c3fo60702j

Mohammadian, M., Salami, M., Alavi, F., Momen, S., Emam-Djomeh, Z., & Moosavi-Movahedi, A. A. (2019). Fabrication and Characterization of Curcumin-Loaded Complex Coacervates Made of Gum Arabic and Whey Protein Nanofibrils. Food Biophysics, 14(4), 425–436. https://doi.org/10.1007/s11483-019-09591-1

Mueller, D., Jung, K., Winter, M., Rogoll, D., Melcher, R., Kulozik, U., Schwarz, K., & Richling, E. (2018). Encapsulation of anthocyanins from bilberries – Effects on bioavailability and intestinal accessibility in humans. Food Chemistry, 248, 217–224. https://doi.org/10.1016/j.foodchem.2017.12.058

Mueller, D., Jung, K., Winter, M., Rogoll, D., Melcher, R., & Richling, E. (2017). Human intervention study to investigate the intestinal accessibility and bioavailability of anthocyanins from bilberries. Food Chemistry, 231, 275–286. https://doi.org/10.1016/j.foodchem.2017.03.130

Neves, N. de A., Stringheta, P. C., Gómez-Alonso, S., & Hermosín-Gutiérrez, I. (2018). Flavonols and ellagic acid derivatives in peels of different species of jabuticaba (*Plinia* spp.) identified by HPLC-DAD-ESI/MSn. Food Chemistry, 252, 61–71. https://doi.org/10.1016/j.foodchem.2018.01.078

Neves, N. de A., Stringheta, P. C., Silva, I. F. da, García-Romero, E., Gómez-Alonso, S., & Hermosín-Gutiérrez, I. (2021). Identification and quantification of phenolic composition from different species of Jabuticaba (*Plinia* spp.) by HPLC-DAD-ESI/MSn. Food Chemistry, 355, Article 129605. https://doi.org/10.1016/j.foodchem.2021.129605

Noratto, G. D., Angel-Morales, G., Talcott, S. T., & Mertens-Talcott, S. U. (2011). Polyphenolics from Açaí (*Euterpe oleracea* Mart.) and red muscadine grape (*Vitis rotundifolia*) protect human umbilical vascular endothelial cells (HUVEC) from glucose- and lipopolysaccharide (LPS)-induced inflammation and target microRNA-126. Journal of Agricultural and Food Chemistry, 59(14), 7999–8012. https://doi.org/10.1021/jf201056x

Oancea, A., Hasan, M., Mihaela, A., Barbu, V., Enachi, E., Bahrim, G., Râpeanu, G., Silvi, S., & St, N. (2018). Functional evaluation of microencapsulated anthocyanins from sour cherries skins extract in whey proteins isolate. LWT - Food Science and Technology, 95, 129–134.

Permyakov, E. A. (2020). α-Lactalbumin, amazing calcium-binding protein. Biomolecules, 10(9), 1–50. https://doi.org/10.3390/biom10091210

Pulido-Mateos, E. C., Lessard-Lord, J., Guyonnet, D., Desjardins, Y., & Roy, D. (2022). Comprehensive analysis of the metabolic and genomic features of tannin transforming *Lactiplantibacillus plantarum* strains. Scientific Reports, 12(1). https://doi.org/10.1038/s41598-022-26005-4

Quatrin, A., Rampelotto, C., Pauletto, R., Maurer, L. H., Nichelle, S. M., Klein, B., Rodrigues, R. F., Maróstica Junior, M. R., Fonseca, B. de S., de Menezes, C. R., Mello, R. de O., Rodrigues, E., Bochi, V. C., & Emanuelli, T. (2020). Bioaccessibility and catabolism of phenolic compounds from jaboticaba (*Myrciaria trunciflora*) fruit peel during *in vitro* gastrointestinal digestion and colonic fermentation. Journal of Functional Foods, 65. https://doi.org/10.1016/j.jff.2019.103714

Ribeiro, J. S., & Veloso, C. M. (2021). Microencapsulation of natural dyes with biopolymers for application in food: A review. Food Hydrocolloids, 112, 106374. https://doi.org/10.1016/j.foodhyd.2020.106374

Rios-Covian, D., González, S., Nogacka, A. M., Arboleya, S., Salazar, N., Gueimonde, M., & de los Reyes-Gavilán, C. G. (2020). An Overview on Fecal Branched Short-Chain Fatty Acids Along Human Life and as Related With Body Mass Index: Associated Dietary and Anthropometric Factors. Frontiers in Microbiology, 11. https://doi.org/10.3389/fmicb.2020.00973

Rocha, J. de C. G., Procópio, F. R., Mendonça, A. C., Vieira, L. M., Perrone, Í. T., de Barros, F. A. R., & Stringheta, P. C. (2018). Optimization of ultrasound-assisted extraction of phenolic compounds from jussara (*Euterpe edulis* M.) and blueberry (*Vaccinium myrtillus*) fruits. Food Science and Technology, 38(1), 45–53. https://doi.org/10.1590/1678-457x.36316

Rosa, J. R. da, Nunes, G. L., Motta, M. H., Fortes, J. P., Weis, G. C. C., Hecktheuer, L. H. R., Muller, E. I., Menezes, C. R. de, & Rosa, C. S. da. (2019). Microencapsulation of anthocyanin compounds extracted from blueberry (*Vaccinium* spp.) by spray drying: Characterization, stability and simulated gastrointestinal conditions. Food Hydrocolloids, 89, 742–748.

Rosales-Chimal, S., Navarro-Cortez, R. O., Bello-Perez, L. A., Vargas-Torres, A., & Palma-Rodríguez, H. M. (2023). Optimal conditions for anthocyanin extract microencapsulation in taro starch: Physicochemical characterization and bioaccessibility in gastrointestinal conditions. International Journal of Biological Macromolecules, 227, 83–92. https://doi.org/10.1016/j.ijbiomac.2022.12.136

Sabet, S., Rashidinejad, A., Melton, L. D., Zujovic, Z., Akbarinejad, A., Nieuwoudt, M., Seal, C. K., & Mcgillivray, D. J. (2021). The interactions between the two negatively charged polysaccharides: Gum Arabic and alginate. Food Hydrocolloids, 112, 106343. https://doi.org/10.1016/j.foodhyd.2020.106343

Sallam, I. E., Abdelwareth, A., Attia, H., Aziz, R. K., Homsi, M. N., von Bergen, M., & Farag, M. A. (2021). Effect of gut microbiota biotransformation on dietary tannins and human health implications. Microorganisms, 9(5), 1–34. https://doi.org/10.3390/microorganisms9050965

Sampaio, D. M., Babu, R. S., Costa, H. R. M., & de Barros, A. L. F. (2019). Investigation of nanostructured TiO2 thin film coatings for DSSCs application using natural dye extracted from jabuticaba fruit as photosensitizers. Ionics, 25(6), 2893–2902. https://doi.org/10.1007/s11581-018-2753-6

Sarkar, R., Dutta, A., Patra, A., & Saha, S. (2021). Bio-inspired biopolymeric coacervation for entrapment and targeted release of anthocyanin. Cellulose, 28(1), 377–388. https://doi.org/10.1007/s10570-020-03523-w

Schmittgen, T. D., & Livak, K. J. (2008). Analyzing real-time PCR data by the comparative CT method. Nature Protocols, 3(6), 1101–1108. https://doi.org/10.1038/nprot.2008.73

Semenova, M., Antipova, A., Martirosova, E., Zelikina, D., Palmina, N., & Chebotarev, S. (2021). Essential contributions of food hydrocolloids and phospholipid liposomes to the formation of carriers for controlled delivery of biologically active substances via the gastrointestinal tract. Food Hydrocolloids, 120, 106890. https://doi.org/10.1016/j.foodhyd.2021.106890

Sethuraman, S., & Rajendran, K. (2018). Multicharacteristic Behavior of Tyrosine Present in the Microdomains of the Macromolecule Gum Arabic at Various pH Conditions. ACS Omega, 3(12), 17602–17609. https://doi.org/10.1021/acsomega.8b02928

Shanthakumar, P., Klepacka, J., Bains, A., Chawla, P., Dhull, S. B., & Najda, A. (2022). The Current Situation of Pea Protein and Its Application in the Food Industry. Molecules, 27(16), 1–28. https://doi.org/10.3390/molecules27165354

Sharifi, S., Rezazad-Bari, M., Alizadeh, M., Almasi, H., & Amiri, S. (2021). Use of whey protein isolate and gum Arabic for the co-encapsulation of probiotic *Lactobacillus plantarum* and phytosterols by complex coacervation: Enhanced viability of probiotic in Iranian white cheese. Food Hydrocolloids, 113. https://doi.org/10.1016/j.foodhyd.2020.106496

Shen, H., Fu, C., Zhang, J., Feng, B., & Yu, S. (2023). Protocol for determining protein dynamics using FT-IR spectroscopy. STAR Protocols, 4(4). https://doi.org/10.1016/j.xpro.2023.102587

Shurvell, H. F. (2006). Spectra-Structure Correlations Spectra-Structure Correlations in the Mid- and Far-infrared. Handbook of Vibrational Spectroscopy, 1783–1816. https://doi.org/10.1002/9780470027325.s4101

Silva, H. R. da, Assis, D. da C. de, Prada, A. L., Silva, J. O. C., Sousa, M. B. de, Ferreira, A. M., Amado, J. R. R., Carvalho, H. de O., Santos, A. V. T. de L. T. dos, & Carvalho, J. C. T. (2019). Obtaining and characterization of anthocyanins from *Euterpe oleracea* (açaí) dry extract for nutraceutical and food preparations. Revista Brasileira de Farmacognosia, 29(5), 677–685. https://doi.org/10.1016/j.bjp.2019.03.004

Singleton, V. L., & Rossi, J. A. J. (1965). Colorimetry of Total Phenolics with Phosmolybdicphosphotungstic Acid Reagents. American Journal of Enology and Viticulture, 16, 144–158.

Sirven, M. A., Venancio, V. P., Shankar, S., Klemashevich, C., Castellón-Chicas, M. J., Fang, C., Mertens-Talcott, S. U., & Talcott, S. T. (2021). Ulcerative colitis results in differential metabolism of cranberry polyphenols by the colon microbiome: *In vitro*. Food and Function, 12(24), 12751–12764. https://doi.org/10.1039/d1fo03047g

Song, J., Yu, Y., Chen, M., Ren, Z., Chen, L., Fu, C., Ma, Z. feei, & Li, Z. (2022). Advancement of Protein- and Polysaccharide-Based Biopolymers for Anthocyanin Encapsulation. Frontiers in Nutrition, 9, 938829. https://doi.org/10.3389/fnut.2022.938829

Tarone, A. G., Silva, E. K., Barros, H. D. de F. Q., Cazarin, C. B. B., & Roberto Marostica Junior, M. (2021). High-intensity ultrasound-assisted recovery of anthocyanins from jabuticaba by-products using green solvents: Effects of ultrasound intensity and solvent composition on the extraction of phenolic compounds. Food Research International, 140, 110048. https://doi.org/10.1016/j.foodres.2020.110048

Timilsena, Y. P., Akanbi, T. O., Khalid, N., Adhikari, B., & Barrow, C. J. (2019). Complex coacervation: Principles, mechanisms and applications in microencapsulation. International

Journal of Biological Macromolecules, 121, 1276–1286. https://doi.org/10.1016/j.ijbiomac.2018.10.144

Vergara, C., Zamora, O., Parada, J., Ricardo, P., Uribe, M., & Kalazich, J. (2020). Microencapsulation of Anthocyanin Extracted from Purple Flesh Cultivated Potatoes by Spray Drying and Its Effects on *In vitro* Gastrointestinal Digestion. Molecules, 25(722), 1–14.

Vergara, L. P., dos Santos Hackbart, H. C., Jansen Alves, C., Reissig, G. N., Wachholz, B. S., Borges, C. D., Chim, J. F., & Zambiazi, R. C. (2023). Encapsulation of phenolic compounds through the complex coacervation technique for the enrichment of diet chewable candies. Food Bioscience, 51. https://doi.org/10.1016/j.fbio.2022.102256

Wan, X., Zhao, M., Guo, M., Li, P., Shi, H., Zhang, X., Liu, Z., & Xia, G. (2023). Characterization of coacervation behavior between whey protein isolate and gum Arabic: Effects of heat treatment. Food Chemistry: X, 18. https://doi.org/10.1016/j.fochx.2023.100703

Wang, B., Tang, X., Mao, B., Zhang, Q., Tian, F., Zhao, J., Chen, W., & Cui, S. (2024). Effects of *in vitro* fecal fermentation on the metabolism and antioxidant properties of cyanidin-3-O-glucoside. Food Chemistry, 431. https://doi.org/10.1016/j.foodchem.2023.137132

Weinbrreck, F., Tromp, R. H., & de Kruif, C. G. (2004). Composition and structure of whey protein/gum arabic coacervates. Biomacromolecules, 5(4), 1437–1445. https://doi.org/10.1021/bm049970v

Xiong, R. G., Zhou, D. D., Wu, S. X., Huang, S. Y., Saimaiti, A., Yang, Z. J., Shang, A., Zhao, C. N., Gan, R. Y., & Li, H. Bin. (2022). Health Benefits and Side Effects of Short-Chain Fatty Acids. Foods, 11(18), 1–24. https://doi.org/10.3390/foods11182863

Yahfoufi, N., Alsadi, N., Jambi, M., & Matar, C. (2018). The immunomodulatory and anti-inflammatory role of polyphenols. Nutrients, 10(11), 1618. https://doi.org/10.3390/nu10111618

Zhang, Y., Yu, W., Zhang, L., Wang, M., & Chang, W. (2022). The Interaction of Polyphenols and the Gut Microbiota in Neurodegenerative Diseases. Nutrients, 14, 14245373. https://doi.org/10.3390/nu

Zhao, X., Zhang, X., Tie, S., Hou, S., Wang, H., Song, Y., Rai, R., & Tan, M. (2020). Facile synthesis of nano-nanocarriers from chitosan and pectin with improved stability and biocompatibility for anthocyanins delivery: An *in vitro* and *in vivo* study. Food Hydrocolloids, 109. https://doi.org/10.1016/j.foodhyd.2020.106114

Zhong, S., Sandhu, A., Edirisinghe, I., & Burton-Freeman, B. (2017). Characterization of Wild Blueberry Polyphenols Bioavailability and Kinetic Profile in Plasma over 24-h Period in Human Subjects. Molecular Nutrition and Food Research, 61(12). https://doi.org/10.1002/mnfr.201700405

Supplementary material

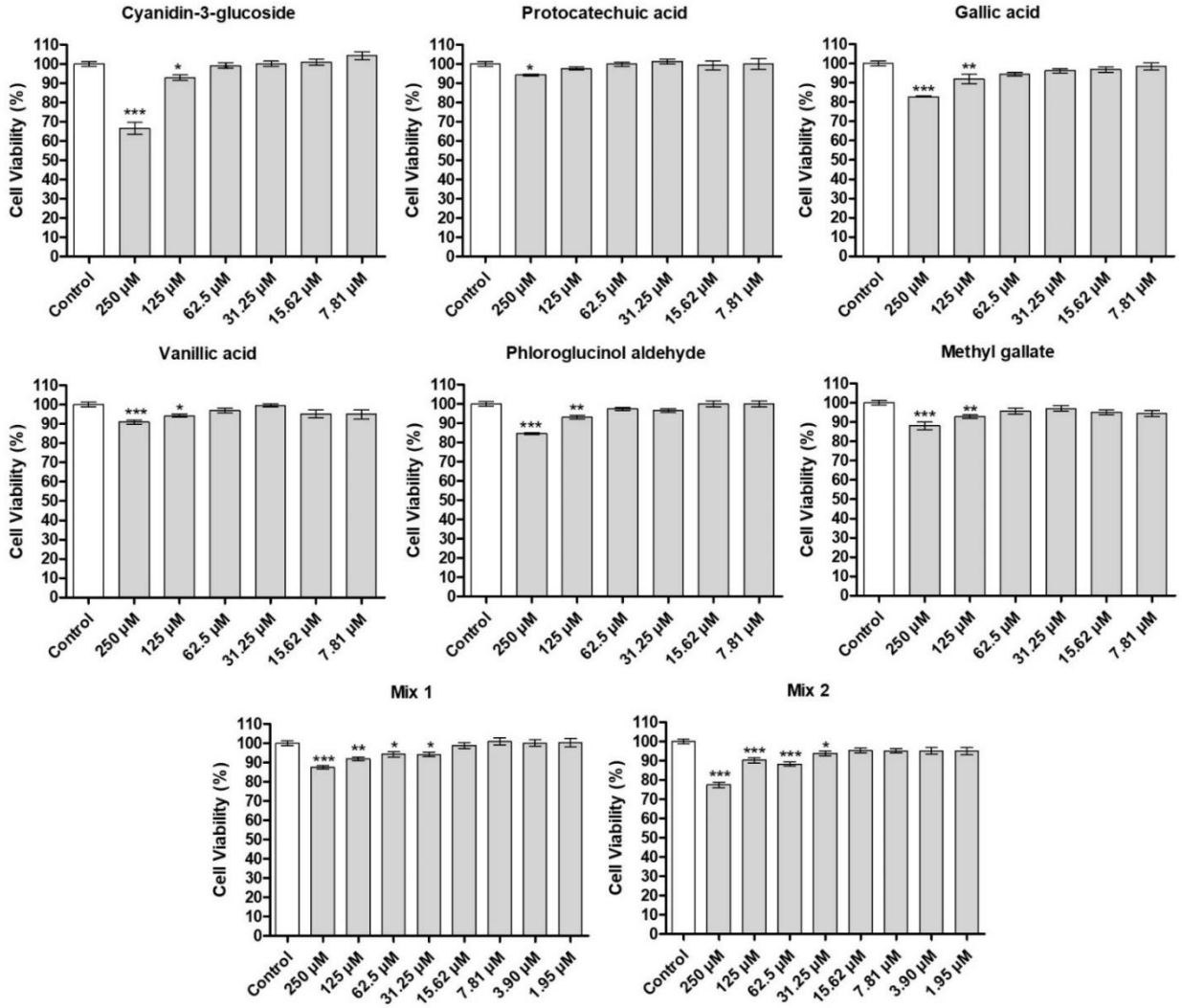

Figure S1 - Dose-dependent effects of the phenolic compounds on cell viability in HT29-MTX Cells. Values are presented as mean ± standard deviation of two independent assays with internal quadruplicates for each of them. Statistically significant differences between the control (untreated cells) and the cells treated with different compounds were identified using Dunnett's test (∗p<0.05; ∗∗p<0.01; ∗∗∗ p<0.001).

Table S1 – Concentration (mg/L) or area of phenolic compounds detected by LC-ESI-MS/MS after 24 h of *in vitro* colonic metabolism

Compounds		CE	WP:GA 1:2	WP:GA 2:1	PP:GA 1:2	PP:GA 2:1
Cyanidin-3-glucoside (mg/L)	F	0.36 ± 0.09^{B}	1.11 ± 0.16^{B}	2.09 ± 0.06^{B}	1.69 ± 0.31^{B}	0.84 ± 0.00^{B}
	C	1.40 ± 0.07^{A}	13.88 ± 0.72^{A}	57.22 ± 5.15^{A}	39.45 ± 0.94^{A}	27.73 ± 1.30^{A}
Protocatechuic acid (mg/L)	F	25.13 ± 2.78^{A}	123.88 ± 18.18^{A}	205.20 ± 23.30^{A}	69.04 ± 10.33^{A}	118.61 ± 3.15^{A}
	C	10.99 ± 1.78^{B}	29.58 ± 6.33^{B}	29.57 ± 3.98^{B}	35.84 ± 3.43^{B}	33.63 ± 5.57^{B}
Phloroglucinol aldehyde (mg/L)	F	0.06 ± 0.00^{A}	0.13 ± 0.04^{A}	0.25 ± 0.06^{A}	0.14 ± 0.02^{A}	0.39 ± 0.10^{A}
	C	0.01 ± 0.00^{B}	0.02 ± 0.00^{B}	0.03 ± 0.01^{B}	0.05 ± 0.01^{B}	0.06 ± 0.01^{B}
Gallic acid (mg/L)	F	1.15 ± 0.10^{A}	1.45 ± 0.12^{B}	1.94 ± 0.20^{B}	2.64 ± 0.17^{B}	2.28 ± 0.30^{B}
	C	0.85 ± 0.05^{B}	25.53 ± 1.18^{A}	19.67 ± 0.44^{A}	25.50 ± 0.14^{A}	20.58 ± 2.11^{A}
Pyrogallol (mg/L)	F	1.04 ± 0.06	11.00 ± 0.48^{A}	15.18 ± 1.12^{A}	8.07 ± 0.18^{A}	13.60 ± 1.22^{A}
	C	n.d.	1.70 ± 0.11^{B}	0.97 ± 0.00^{B}	1.24 ± 0.25^{B}	0.81 ± 0.22^{B}
Methyl gallate (mg/L)	F	n.d.	0.65 ± 0.05^{A}	0.64 ± 0.05^{A}	0.63 ± 0.06^{B}	0.58 ± 0.06^{A}
	C	n.d.	0.77 ± 0.06^{A}	0.20 ± 0.00^{B}	0.81 ± 0.05^{A}	0.69 ± 0.03^{A}
Vanillic acid (mg/L)	F	n.d.	9.36 ± 0.59	15.65 ± 2.32	23.03 ± 1.69	25.38 ± 4.44
	C	n.d.	n.d.	n.d.	n.d.	n.d.
Gentisic acid (area)	F	n.d.	21819 ± 1789.00^{A}	39066.67 ± 6161.92^{A}	14869.00 ± 2143.00^{A}	24502.00 ± 3980.10^{A}
	C	n.d.	6931.00 ± 493.56^{B}	7249 ± 1865.35^{B}	8218.00 ± 3063.19^{A}	12178.00 ± 0.00^{B}
2-GG (area)	F	n.d.	n.d.	n.d.	n.d.	n.d.
	C	n.d.	7428.00 ± 178.19	5698.00 ± 384.67	10513 ± 1658.87	6715.00 ± 878.23
3-GG (area)	F	n.d.	n.d.	n.d.	n.d.	n.d.
	C	n.d.	9373.00 ± 7.07	3881.00 ± 866.91	11134.00 ± 73.54	6773.00 ± 176.78
4-GG (area)	F	n.d.	9746.00 ± 1282.00^{B}	4156.67 ± 1180.10^{B}	3456.00 ± 1238.00^{B}	6614.00 ± 1160.05^{B}
	C	n.d.	16875.00 ± 1028.13^{A}	9617.00 ± 615.18^{A}	26775.00 ± 3491.69^{A}	16449.00 ± 1257.24^{A}

Values are presented as mean ± standard deviation (n = 3). Different uppercase letters in the same column indicate a significant difference between the fecal fermentation sample (F) and the control (C) by F-test ($p<0.05$). n.d. = not detected

5. CHAPTER 4: Encapsulation with chitosan and gum arabic enhances the bioaccessibility and targeted delivery of anthocyanins to the colon during simulated digestion and fecal fermentation

Abstract

The encapsulation of anthocyanins extract using chitosan (CH) and gum arabic (GA) as wall materials was investigated as a technique to improve the stability, bioaccessibility, and targeted delivery of anthocyanins to the colon. Two formulations (CH:GA ratios of 1:2 and 2:1 v/v) were evaluated. FTIR results revealed interactions between the encapsulating agents and the extract, and encapsulation efficiency exceeded 90% for both formulations. Results from *in vitro* digestion showed that both formulations retained anthocyanins during gastric digestion and improved stability in the small intestine phase compared to the unencapsulated extract. The CH:GA 1:2 formulation exhibited higher bioaccessibility of anthocyanins (73.73 ± 1.91%), while the CH:GA 2:1 (43.98 ± 2.60%) demonstrated greater retention. The encapsulated samples also enhanced the release and microbiota metabolism of phenolic compounds during the colonic phase. The sample CH:GA 1:2 delivered the highest levels of cyanidin-3-glucoside (C3G) (30.57 ± 0.01-fold higher than the unencapsulated extract) and promoted significant increases in short-chain fatty acids (SCFAs), including propionic, valeric, and isobutyric acids. C3G and phenolic metabolites showed potential to improve vascular health by reducing ROS levels and modulating key inflammatory mediators in HUVEC cells. These findings showed the potential of CH and GA as encapsulation materials to protect and control anthocyanins release, improving their target delivery to the colon.

Keywords: Bioavailability; Gut microbiota; Short-chain fatty acids; Functional foods; Controlled release.

1. Introduction

Chitosan represents a linear cationic polysaccharide that is constituted of D-glucosamine (deacetylated units) and N-acetyl-D-glucosamine (acetylated units) linked by β-(1–4) bonds (Júlia et al., 2021). It is obtained by the deacetylation of chitin from crustacean (Júlia et al., 2021). Chitosan presents mucoadhesive properties and is considered an excellent alternative to prolong the residence time and possibly the absorption of bioactive compounds in the gastrointestinal tract (Fathi & Julian, 2014; J. Liang et al., 2017). Additionally, the polymer is recognized as biocompatible and non-toxic (J. Liang et al., 2017). Due to these characteristics, chitosan has been extensively used in pharmaceutical industry for the development of drug delivery systems and has also been studied for the controlled release of

bioactive compounds, like anthocyanins, looking for their optimal functionality, bioaccessibility and bioavailability when consumed.

Anthocyanins have been extensively studied for their health benefits; however, they are unstable under many environmental conditions, including light, pH, temperature, and present low bioacessibilidade and bioavailability when consumed, which limit their applications (Ayvaz et al., 2023; Mueller et al., 2017; Zhong et al., 2017). Consequently, the application of encapsulation techniques has been investigated to enhance the stability of anthocyanins. The electrostatic interaction between food polymers for encapsulation has been explored due to its ability to improve the stability and controlled release of bioactive compounds. Under acidic conditions, the amino groups of chitosan (pKa = 6.3) become protonated, making the chitosan macromolecules positively charged (Gatto et al., 2019; Ways et al., 2018). Because of this cationic nature, chitosan can electrostatically interact with negatively charged components, enabling the formation of particles by interaction with other molecules, such as gum arabic (Gatto et al., 2019; Ways et al., 2018).

Gum arabic is a polysaccharide obtained from the exudate of *Senegalia senegal* (or *Acacia senegal*). Its structure presents a main chain of β-D-galactopyranose with (1➔3) linkages and (1➔6) branches and the side chains include glucuronic acid, galactose, arabinose, and rhamnose (Padil et al., 2021). At pH higher than 2.2 (approximate pKa), gum arabic presents negative charges due to the deprotonation of carboxyl groups in the glucuronic acid residues (Sabet et al., 2021; Tan et al., 2016). This property allows gum arabic to interact with chitosan, making it a good candidate for the encapsulation of compounds.

Different combinations with chitosan have been studied for the encapsulation of anthocyanins, such as in association with β-cyclodextrin (R. Liu et al., 2023), pectin (Xie et al., 2023; X. Zhao et al., 2020), and whey protein (S. Wang et al., 2021). However, to the best of our knowledge, this is the first study analyzing the combination of chitosan and gum arabic for the encapsulation of anthocyanins. The combination of chitosan with gum arabic have potential to protect the anthocyanins in the upper gastrointestinal tract and for the targeted delivery of anthocyanins to the colon, as both polymers are polysaccharides that are resistant to digestion and can be fermented by the gut microbiota in the colon (Al-Baadani et al., 2021; Yan et al., 2021).

This characteristic makes the chitosan-gum arabic combination promising for maximizing the benefits of anthocyanins, as targeted delivery to the colon can enhance the metabolism of these compounds into more bioavailable forms and potentially enhance their

bioactivity and therapeutic potential (S. Zhao et al., 2023). This approach is especially beneficial for compounds, such as anthocyanins, that have shown the potential to modulate the gut microbiota and improve the intestinal health and related conditions, such as inflammation, oxidative stress, and metabolic disorders (A. Liang et al., 2023; Verediano et al., 2021). In this context, this study aimed to assess the potential of combinations of chitosan and gum arabic for the encapsulation of anthocyanins and controlled release during different phases of digestion (gastric, small intestine, and colon) using an *in vitro* model.

2. Material and methods

2.1. Materials

The fruit used in this study was jabuticaba (*Plinia cauliflora*), harvested in November 2022 from the Fruit Culture sector of the Universidade Federal de Viçosa, Minas Gerais, Brazil. Chitosan (medium molecular weight, deacetylation ≥ 75%) was purchased from Sigma-Aldrich (Cotia, SP, Brazil), and pure gum arabic was obtained from LabSynth (Synth, Diadema-SP, Brazil).

2.2. Preparation of the extract

The extraction of phenolic compounds was carried out following the method described by Rocha et al., (2018). Briefly, 100 g of jabuticaba peel was combined with 1000 mL of a 75% (v/v) ethanol solution and acidified with citric acid to a pH of 2.0. The mixture was then subjected to ultrasonication at 45 kHz and 40 °C for 50 minutes (Elmasonic TI-H10, Elma, Singen, BW, Germany), filtered through Whatman No. 1 filter paper, and concentrated using a rotary evaporator (RV 10 digital V, IKA, Staufen, BW, Germany) at 40 °C. Any residual water was removed by lyophilization, and the resulting powder was stored in metalized bags in a freezer at −20 °C until analysis.

2.3. Encapsulation

Stock solutions of chitosan (CH) at 1.0% (w/v) and gum arabic (GA) at 2.5% (w/v) were prepared by dissolving the powders in acidified water (1% acetic acid) and deionized water, respectively. The solutions were allowed to stand overnight at 4 °C to allow complete

hydration. The concentrations were determined based on screening tests. The CH solution was mixed with 100 mL of the extract and stirred for 10 minutes at room temperature (23 ± 2°C). Subsequently, the gum arabic solution was added, and the pH was adjusted to 3.5 using 1M NaOH. The mixture (500 mL) was stirred for an additional 10 minutes. Two ratios were tested: CH:GA 2:1 and CH:GA 1:2 (v/v). The samples were frozen at −60 °C and freeze-dried for 72 h. Finally, the powder was stored in metalized bags in a freezer at −20 °C for later analysis.

2.4. Total phenolic content (TPC)

Total phenolic compounds were quantified using a method adapted from Singleton & Rossi, (1965), and the results were expressed in mg of gallic acid equivalent (GAE) per g. In a 96-well microplate, 20 µL of diluted sample was mixed with 100 µL of Folin-Ciocalteau reagent (diluted 1:10 with water) and 75 µL of 7.5% Na_2CO_3 solution (m/v). After 1 h in the dark (23 ± 2 °C), the absorbance was measured at 760 nm (CLARIOstar Plus plate reader (BMG Labtech Inc., Durham, NC, USA).

2.5. Identification and quantification of compounds in the powders through LC-ESI-MS/MS analysis

Identification and quantification of compounds in the jabuticaba extract and encapsulated powders were performed using a Thermo Scientific Vanquish™ HPLC system coupled with a Thermo Scientific TSQ Altis triple quadrupole mass spectrometer with an ESI source. The separations were carried out on a SunFire™ C18 column (150 × 3 mm, 5 µm), using acidified water (0.1% v/v formic acid) as mobile phase A and acidified methanol (0.1% v/v formic acid) as mobile phase B. The flow rate was set to 0.4 mL/min, and gradient elution began with 5% B, increasing to 40% B after 5 minutes, and then to 95% B after 15 minutes. After 15.50 minutes, the column was re-equilibrated with 5% B until 17 minutes. MS data were acquired in both negative and positive polarity. The instrument parameters included a spray voltage of 3912.7 V, a sheath gas flow of 24, an auxiliary gas flow of 2, an ion transfer tube temperature of 325 °C, and a vaporizer temperature of 400 °C. Compound identification was performed by comparing retention times, fragmentation patterns, and relative ion abundances with known analytical standards or by using database searches. Quantification was carried out using calibration curves generated from analytical standards.

2.6. Encapsulated samples characterization

2.6.1. Encapsulation efficiency (%)

The total anthocyanin content (TAC) and surface anthocyanin content (SAC) were quantified to evaluate the encapsulation efficiency. For TAC determination, 300 mg of microcapsules were mixed with 1.5 mL of acidified water (5% acetic acid), vortexed for 3 min, and then ultrasonicated for 10 minutes. For SAC, 200 mg of microcapsules were washed with ethanol in a vortex for 5 minutes (Adapted from Oancea et al., 2018). Both the TAC and SAC mixtures were centrifuged at 10000 x g for 5 minutes. The clear supernatant was collected, and the quantification of anthocyanins was carried out using the pH-differential method described by Lee et al., (2005). Encapsulation efficiency (% EE) was calculated using Eq. (1):

$$\text{EE (\%)} = \frac{\text{TAC - SAC}}{\text{TAC}} * 100 \quad (1)$$

2.6.2. Scanning electron microscopy (SEM)

For SEM analysis, all samples were freeze-dried, placed on aluminum stubs, and gold-coated. The particle morphology was observed using a scanning electron microscope (SEM) (Leo 1430VP, Zeiss, Germany) at magnifications of 200x and 500x.

2.6.3. Fourier transform infrared spectroscopy (FTIR)

The samples were analyzed by FTIR using a Cary 630 FTIR spectrophotometer (Agilent Technologies). Scans were conducted over the range of 4000 to 400 cm^{-1} with a resolution of 4.00 cm^{-1}. Mean spectra were calculated from three independent measurements. The resulting spectra were visualized and analyzed using Spectragryph software (v. 1.2.16.1).

2.6.4. Zeta potential (ζ)

The ζ-potential of the wall materials and encapsulated samples were determined using a Zeta Sizer NanoSeries (Malvern, UK).

2.7. *In vitro* gastric and small intestinal digestion

The simulated gastrointestinal digestion system, consisting of two stages (gastric and small intestinal digestion), was adapted from Minekus et al., (2014). For the anthocyanin release profile study, the mass of encapsulated samples added for digestion was adjusted to match the anthocyanin content of 1 g of unencapsulated extract. In the gastric digestion step, 7.5 mL of gastric fluid, containing 0.5% pepsin (S25695A, Fisher Scientific, Nazareth, USA) and supplemented with salts as described by Minekus et al. (2014), was added to the samples. The pH was adjusted to 2.0 using 1.0 M HCl, and the mixture was incubated at 37°C with continuous shaking at 100 rpm for 2 h (C76 Shaking Water Bath, New Brunswick Scientific, Edison, NJ, USA). Afterward, 11 mL of simulated intestinal fluid (SIF), 5.0 mL of a pancreatin solution (800 U/mL; porcine pancreatin, 4 x USP, Sigma-Aldrich), 3.0 mL of a bile salt solution (200 mg/mL), CaCl2 (0.3 M), and 1 M NaOH were added to adjust the pH to 7.0 for the intestinal digestion step. The mixture was reincubated at 37°C for 2 h at 100 rpm. Every 30 minutes, aliquots were collected for analysis and placed on ice immediately. The samples were then centrifuged at 10000 x g for 5 minutes (Megafuge 16, Thermo Scientific, Waltham, MA, USA). The anthocyanin content released into the supernatant was quantified using the pH-differential method (Lee et al., 2005). The residues remaining after centrifugation were frozen for subsequent analysis in the colonic phase. The bioaccessibility of anthocyanins at the end of the gastric and intestinal phases was calculated using Equation 2:

$$\text{Bioaccessibility (\%)} = \frac{\text{Concentration in the digested sample}}{\text{Initial concentration}} * 100 \quad (2)$$

2.8. *In vitro* colonic metabolism

In vitro colonic metabolism of the residues obtained after *in vitro* digestion was conducted following the method described by Sirven et al., (2021). Stool samples were collected from ten lean adults (BMI: 18-25 kg/m², ages between 18 and 65, with no antibiotic use in the past 6 months) and processed inside an anaerobic chamber (Coy Laboratory Products, Grass Lake, MI, USA), maintained at 37 °C and regulated with nitrogen, hydrogen (5%), and carbon dioxide (5%). Anaerobic conditions were confirmed using Resazurin strips (Sigma Aldrich, St Louis, MO, USA). To prepare the fecal slurry, 5 g of feces were mixed with 50 mL of phosphate-buffered saline (PBS). The fecal fermentation medium (FFM) used was

formulated by Anaerobe Systems (Morgan Hill, CA, USA) and contained: 2.0 g peptone water, 0.5 g bile salts, 2.0 g yeast extract, 0.5 g L-cysteine, 0.05 g haemin, 0.01 mL vitamin K, 0.001 g resazurin, 0.01 g $CaCl_2 \cdot 6H_2O$, 0.01 g $MgSO_4 \cdot 7H_2O$, 0.04 g KH_2PO_4, 0.04 g K_2HPO_4, 0.10 g NaCl, 2.0 g $NaHCO_3$, 2.0 mL tween 80 per 1 L, To simulate the metabolism of the samples, digestion residues were mixed with 18 mL of FFM and 2 mL of fecal slurry. A control with 18 mL of FFM and 2 mL of fecal slurry was prepared to eliminate the interference of phenolic compounds naturally present in the feces. Fermentation was carried out for 48 h, with aliquots collected at 0, 3, 6, 12, 24, and 48 h time points. For chemical analysis of metabolites, 500 µL aliquots were mixed with 500 µL of acidified methanol (0.1% formic acid), followed by centrifugation at 10000 x g for 5 minutes (Megafuge 16, Thermo Scientific, Waltham, MA, USA). The resulting supernatants were stored at −80 °C until further analysis by LC-ESI-MS/MS as described in section 2.5.

2.9. Short-chain fatty acids

Short-chain fatty acids (SCFAs) were extracted by mixing 50 µL of the fermentation aliquot with 800 µL of 30 mM HCl. The mixture was vortexed for 1 minute and then centrifuged at 12000 x g for 10 minutes at 4 °C (LD-2910, GMI, Ramsey, MN, USA). The supernatant (400 µL) was then extracted with 400 µL of ethyl acetate, vortexed for 20 minutes, and centrifuged again at 12000 x g for 10 minutes at 4 °C (Sirven et al., 2021). The final supernatant was stored at −80 °C for subsequent analysis by GC-MS. SCFAs were quantified using a gas chromatograph (TRACE 1310, Thermo Scientific, Waltham, MA, USA) coupled to a triple quadrupole mass spectrometer (TSQ 9000, Thermo Scientific, Waltham, MA, USA). Separation was achieved on a DB WAX column (60 m × 0.25 mm × 0.25 µm; Agilent, Santa Clara, CA, USA), and 1 µL of the sample was injected with a split ratio of 17:1. Ionization was performed in electron impact (EI) mode at 70 eV. The MS transfer line and ion source were maintained at 200 °C and 250 °C, respectively, with a helium carrier gas flow rate of 1 mL/min. The analysis was carried out in Selected Reaction Monitoring (SRM) mode, monitoring the following product ions (m/z) for each compound: acetic acid 60, propionic acid 74.1, 73.1, 57.1, isobutyric acid 73.1, 88.1, 89.1, butyric acid 60, 73.1, 89.1, 2-methylbutyric/isovaleric 74.1, 60.1, 87.1, and valeric acid 60, 87.1, 103.1. A standard mixture of SCFAs, including acetic, propionic, isobutyric, n-butyric, 2-methylbutyric, isovaleric, and valeric acids, was obtained from Cayman Chemicals (Ann Arbor, MI, USA).

2.10. Analyses of cell viability, ROS production and gene expression in HUVEC cells

2.10.1. Cell line and culture maintenance

The human umbilical vascular endothelial cells (HUVEC) were cultured using ECM medium supplemented with 5% of fetal bovine serum, 1% of endothelial growth supplement (ECGS), and 1% of penicillin/streptomycin solution (ScienCell). Cells were maintained at 37 °C with a humidified 5% CO_2 atmosphere.

2.10.2. Cell viability

HUVEC cells (6.0 x 10^4) were seeded in a 96-well plate and incubated for 24 h to allow cell attachment before treatment with various concentrations of the compounds for 48 h. Cell viability was assessed using the Resazurin *in vitro* assay kit (Sigma-Aldrich, St. Louis, MO, USA) following the manufacturer's protocol. Fluorescence intensity was measured using a CLARIOstar Plus plate reader (BMG Labtech Inc., Durham, NC, USA) set at 560 nm excitation and 590 nm emission. Cell viability results were quantified as a percentage of the untreated controls. The cells were treated with isolated standards of cyanidin-3-glucoside (C3G), protocatechuic acid (PA), phloroglucinol aldehyde (PGA), gallic acid (GA), and methyl gallate (MG). Mixtures of these compounds were also tested. Mix 1 contained higher concentrations of metabolites (31 % C3G, 63 % PA, 2 % GA, 0.02% PGA, 3.5% vanillic acid (VA), and 0.5% MG). Mix 2 contained a higher concentration of C3G, with 68% C3G, 31% PA, 1% GA, 0.01% PGA, 0.00% VA, and 0.06% MG.

2.10.3. Intracellular reactive oxygen species (ROS) generation

Intracellular reactive oxygen species (ROS) generation was assessed using the DCFH-DA assay as described by Arbizu et al., (2020). HUVEC cells (6.0 × 10^4 per well) were seeded into a 96-well plate and incubated for 24 h to achieve 90% confluency. Cells were then pretreated for 2 h with phenolic compounds at varying concentrations (0–250 µM), followed by a 3 h challenge with LPS (4 µg/mL, Lipopolysaccharides from Escherichia coli O111:B4, Sigma Aldrich, Saint Louis, MO, USA) at 37 °C. ROS production was measured using 10 µM DCFH-DA for 45 minutes under incubation at 37 °C and 200 rpm (H5000-HC MultiTherm™, Benchmark Scientific, Sayreville, NJ, USA). Fluorescence intensity was measured at 520 nm

(emission) and 480 nm (excitation) using a CLARIOstar Plus plate reader (BMG Labtech Inc., Durham, NC, USA). After fluorescence measurement, cells were washed twice with PBS and fixed with methanol for 3 minutes at room temperature. Methanol was completely removed, and 100 µL of Janus Green solution (1 mg/mL) was added to each well for 3 minutes. Following the removal of Janus Green, cells were washed twice with PBS, and 100 µL of 50% methanol was added to each well to measure cell density at 654 nm. Results were expressed as RFU (relative fluorescence units)-fold of untreated control. RFU values were normalized to absorbance values corresponding to cell densities. The experiments were conducted with two independent assays with internal quadruplicates for each of them.

2.10.4. Gene expression

HUVEC cells were seeded in 12-well plates at 90% confluence and were pretreated for 2 h with the compounds followed by LPS (4 µg/mL) challenge for 3 h at 37 °C. For all experiments, total RNA was isolated using the RNA Mini Kit (Zymo Research, Irvine, CA, USA) according to the manufacturer's protocol. The quality and quantity of RNA samples were measured using the NanoDrop Lite Plus Spectrophotometer (Thermo Scientific, Waltham, MA, USA). Extracted RNA was used to synthetize cDNA using the iScript Reverse Transcription Supermix (BioRad, Hercules, CA, USA). The sequences of the primers used were as follows: GAPDH (forward: 5'-ACAGTTGCCATGTAGACC; reverse: 5'-TTTTTGGTTGAGCACAG G); TNF-α (forward: 5'-TCCTCCAGACACCCTCAACC-3'; reverse: 5'-AGGCCCCAGTTT GAATTCTT-3'); COX-2 (forward: 5'-AGGGTTGCTGGTGGTAGGAA-3'; reverse: 5'-GGT CAATGGAAGCCTGTGATACT-3'); NF-κβ1 (forward: 5'-CACAAGGAGACATGA AAC-AG; reverse: 5'-CCCAGAGACCTCATAGTTG). Real time polymerase chain reaction (RT-PCR) was performed using a CFX384 Touch Real Time PCR Detection System (BioRad; Hercules, CA, USA). Each reaction was performed in duplicates and relative mRNA levels were calculated by the comparative CT method (Schmittgen & Livak, 2008) using GAPDH as a housekeeping gene.

2.11. Statistical analyses

The analyses were conducted in 3 replicates, and the results were presented as mean ± standard deviation (SD). Data were analyzed using one-way ANOVA followed by Tukey's test

or using Dunnett's test. All the analyses were performed using the R software (R Core Team, Vienna, Austria). A statistically significant value was considered when $p<0.05$.

3. Results and discussion

3.1. Quantification of phenolic compounds in the powders

The compounds identified in the extract have been previously described (Chapter 3) and included flavonoids, phenolic acids, gallotannins, and ellagitannins, with cyanidin-3-glucoside identified as the predominant compound. The total phenolic content (TPC), and concentrations of cyanidin-3-glucoside, protocatechuic acid, and gallic acid in the unencapsulated extract and the encapsulated samples are presented in Table 1.

Table 1 – Concentration (mg/g) of phenolic compounds in the samples

Compounds	Extract	CH:GA 1:2	CH:GA 2:1
Total phenolic content	180.26 ± 1.92	67.70 ± 0.19	54.12 ± 3.32
Cyanidin-3-glucoside	13.85 ± 0.68	5.88 ± 0.24	6.67 ± 0.09
Protocatechuic acid	3.12 ± 0.22	2.04 ± 0.17	1.84 ± 0.40
Gallic acid	0.12 ± 0.00	0.05 ± 0.00	0.06 ± 0.01

3.2. Zeta potential (ζ) and Encapsulation efficiency (EE) (%)

Chitosan showed a cationic nature at pH 3.5, with a zeta potential of 31.75 ± 1.20 mV, due to the protonation of the amino groups under acidic conditions (theoretical pKa of 6.3). In contrast, gum arabic exhibited a negative surface charge of -17.00 ± 2.12 mV, reflecting the deprotonation of the carboxyl groups at this pH (theoretical pKa of 2.2). For the encapsulated samples, there was no complete neutralization of the charges between the polymers for any of the formulations. The CH:GA 1:2 formulation had a negative surface charge of -10.35 ± 0.21 mV, suggesting that gum arabic dominated the particle surface due to the higher concentration in this formulation and the strong contribution of negatively charged carboxyl groups. On the other hand, the CH:GA 2:1 formulation presented a positive surface charge of 30.50 ± 0.71 mV, indicating the predominant cationic nature of chitosan on the surface charge of the particles due to its higher proportion.

The anthocyanin encapsulation efficiency (EE) determined was 92.80 ± 0.28% for the formulation CH:GA 2:1 and 94.61 ± 0.34% for the formulation CH:GA 1:2, which represents an efficient percentage of incorporation of the anthocyanins in the matrix of the particles. Under acidic pH conditions, anthocyanins predominantly exist in their flavylium cation form. The hydroxyl groups of anthocyanins are capable of interacting with the amino ($-NH_2$) groups of chitosan and the hydroxyl groups in gum arabic (Chung et al., 2016; Fernandes et al., 2020; Song et al., 2022). These interactions at pH 3.5 may have contributed to the high EE observed, making the combination of positively charged chitosan and negatively charged gum arabic effective for encapsulation of anthocyanins.

3.3. Morphology by Scanning Electron Microscopy (SEM)

The morphology is considered a fundamental parameter for the characterization and stability of the particles (Rosales et al., 2023). As shown in Figure 1, the morphology of the freeze-dried powders for both formulations were similar to a broken glass structure with variable sizes. These characteristics have been previously observed in other studies and are associated with the freeze-drying process (Kuck & Noreña, 2016; Mansour et al., 2020; Saikia et al., 2015; Yamashita et al., 2017). Microencapsulated anthocyanins powders with maltodextrin by freeze-drying also showed an external morphology resembling a broken glass structure of variable sizes (Yamashita et al., 2017). This type of structure has also been observed for freeze-dried microparticles of grape skin aqueous extract microencapsulated with different formulations using gum arabic, guar gum and polydextrose (Kuck & Noreña, 2016), for polyphenols from star fruit (Averrhoa carambola) encapsulated with maltodextrin by freeze drying (Saikia et al., 2015) and for encapsulation of red raspberry anthocyanin using soy protein isolate and gum arabic (Mansour et al., 2020).

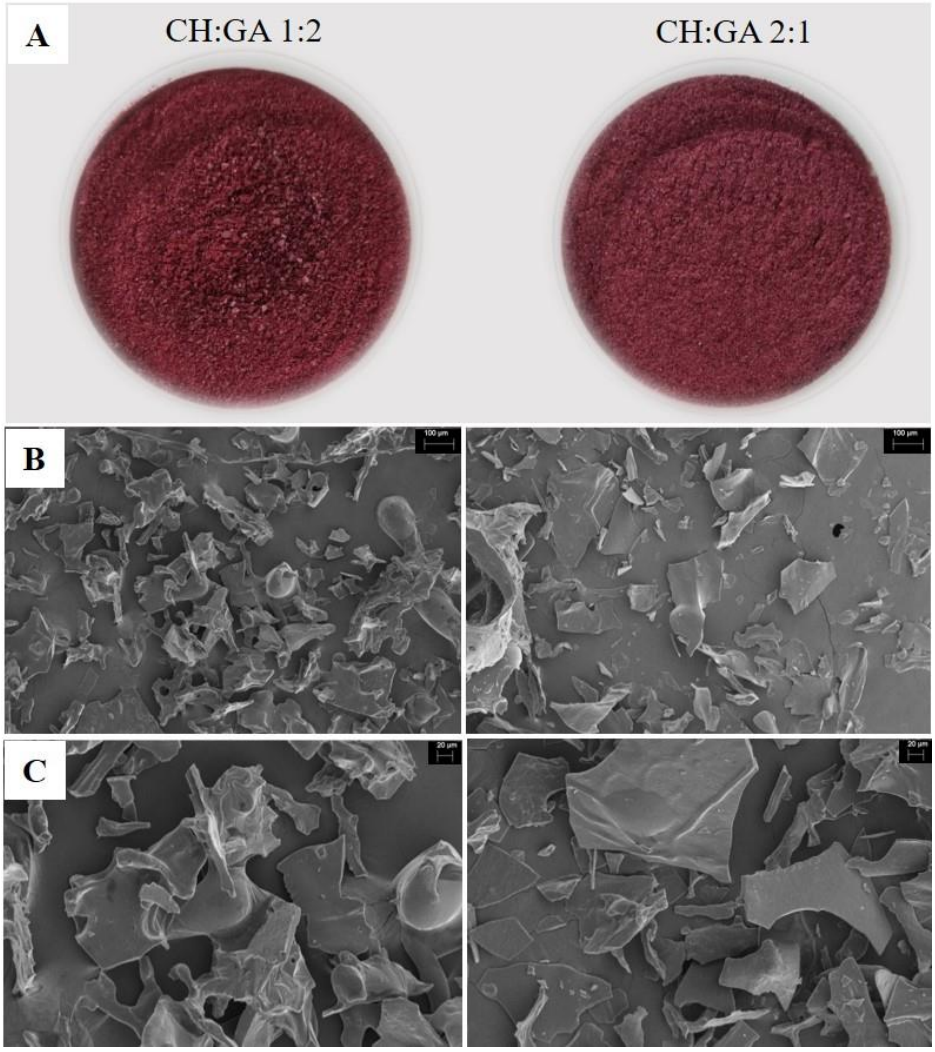

Figure 1 – (A) Image of the of freeze-dried powders and scanning electron micrographs of freeze-dried powders at (B) 200 and (C) 500x magnification.

3.4. FTIR spectrum

FTIR spectroscopy was used to confirm the presence of cross-linking and structural changes in the encapsulated samples. The FTIR spectra of the unencapsulated extract, chitosan, gum arabic and the encapsulated samples are presented in Figure 2. The FTIR spectrum of the unencapsulated extract showed different peaks: O–H stretching at 3248 cm^{-1}, C–H stretching at 2925 cm^{-1}, and C=O and C=C stretching at 1719 cm^{-1} and 1619 cm^{-1}, respectively, indicating aromatic structures (Sampaio et al., 2019). Peaks at 1509 cm^{-1}, 1321 cm^{-1}, and 1185 cm^{-1} corresponded to aromatic C=C deformation, phenol C–OH deformation, and C–O stretching. Finally, a peak at 1016 cm^{-1} was linked to aromatic C–H deformation (Cai et al., 2019; Heneczkowski et al., 2001; Shurvell, 2006; Silva et al., 2019).

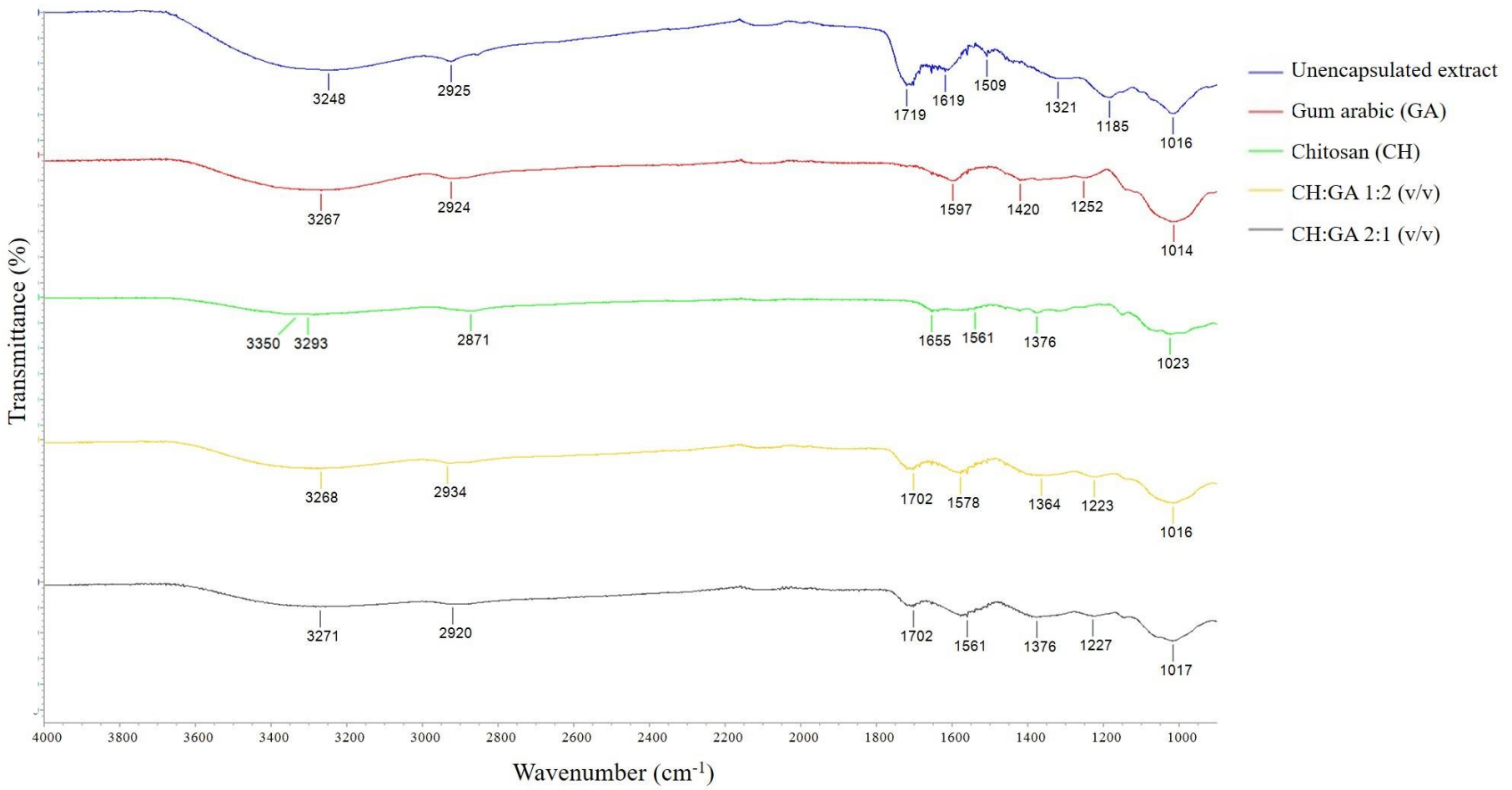

Figure 2 - FTIR spectra of the unencapsulated extract, gum arabic (GA), chitosan (CH), and the encapsulated samples with CH and GA at two different proportions (CH:GA 1:2 (v/v) and CH:GA 2:1 (v/v))

For gum arabic, the FTIR spectrum showed O–H stretching at 3267 cm^{-1}, C–H stretching at 2924 cm^{-1}, and bands at 1597 cm^{-1} and 1420 cm^{-1} attributed to carboxyl group vibrations. Peaks at 1252 cm^{-1} and 1014 cm^{-1} corresponded to C–O stretching (Bashir & Haripriya, 2016; Espinosa-Andrews et al., 2010; Shurvell, 2006). For chitosan, the region 3350-3293 cm−1 band corresponded to N-H and O-H stretching vibration (Espinosa-Andrews et al., 2010; Queiroz et al., 2015). The absorption band at 2871 cm^{-1} can be attributed to C-H stretching (Espinosa-Andrews et al., 2010; Queiroz et al., 2015). The peak observed at 1655 cm^{-1} is characteristic of the amide I band attributed to the C=O vibration of the acetylated units and the peak at 1376 cm^{-1} is associated with the amide III (-$NH3^{+}$ groups) (Espinosa-Andrews et al., 2010; Queiroz et al., 2015). A small band at 1561 cm^{-1} was also observed, which is related to the N-H bending of amide II and is the third band characteristic of N-acetyl groups. The peak at 1023 cm^{-1} was associated with the C-O stretching vibration (Espinosa-Andrews et al., 2010; Queiroz et al., 2015).

The spectra changed significantly in the carbonyl-amide region for the encapsulated samples. The peaks corresponded to the amide I band of CH shifted from 1655 to 1702 cm^{-1} in both treatments. The peaks related to the amide II band were shifted from 1561 to 1578 cm-1 in the 1:2 sample and were kept the same at 1561 cm^{-1} for the 2:1 sample. A decrease was observed in the amide III band for the 1:2 sample (1376 to 1364 cm^{-1}), and the same value was observed for 2:1 (1376 cm^{-1}). On the other hand, the symmetric and asymmetric -COO- stretching vibrations in AG disappeared in both samples, indicating the electrostatic interaction between the amine groups of CH and carboxyl groups of GA (Espinosa-Andrews et al., 2010). The results also suggested that the different proportions of CH in the samples can lead to different interactions and structural rearrangements in the amide region. Some characteristic peaks in the jabuticaba extract also disappeared (1719, 1619, 1509, 1321, and 1185 cm^{-1}) when mixed with the wall materials, indicating that jabuticaba extract was successfully encapsulated in both treatments (Cui et al., 2022).

3.5. *In vitro* gastric and intestinal release of anthocyanins during simulated digestion

The effect of encapsulation on the release and bioaccessibility of anthocyanins was evaluated during simulated *in vitro* digestion. The total anthocyanin content released from the unencapsulated extract and encapsulated samples was evaluated every 30 min. As shown in Figure 3, there was a rapid release of anthocyanins in the unencapsulated extract, with 89.72 ± 2.37% of the anthocyanins detected in the medium after 30 min of gastric digestion. In contrast,

only 50.79 ± 3.64% and 36.15 ± 4.62% were detected for the samples CH:GA 1:2 and CH:GA 2:1, respectively. For the CH:GA 1:2 sample, an increase in anthocyanin release was observed throughout gastric digestion, while the CH 2:1 sample showed slight variation in release. The unencapsulated extract showed the highest anthocyanins release and bioaccessibility at the end of the gastric phase, followed by the samples CH:GA 1:2 and CH:GA 2:1. The bioaccessibility of anthocyanins was significantly lower in the sample with a higher proportion of chitosan compared to the other samples ($p<0.05$), indicating that this formulation retained more anthocyanins in its structure.

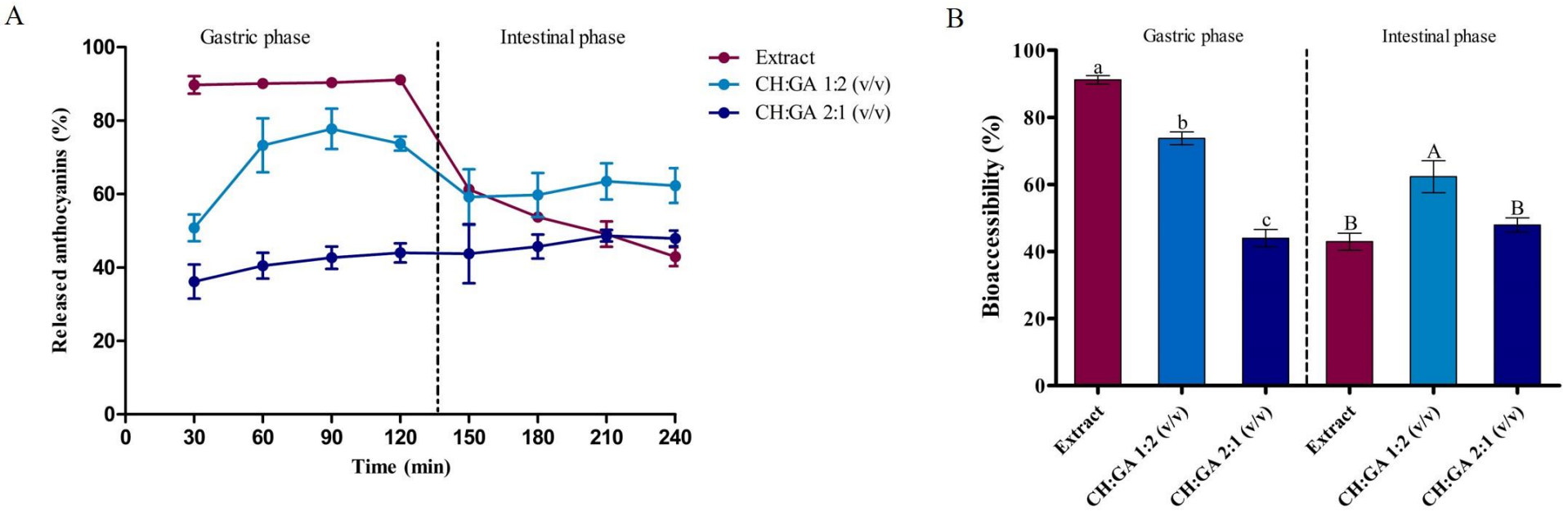

Figure 3 - (A) Percentage of anthocyanins released during the gastric and intestinal phases from the unencapsulated extract and encapsulated samples. (B) Bioaccessibility of anthocyanins from the unencapsulated extract and encapsulated samples after the gastric and intestinal phases. Values are presented as mean ± standard deviation (n=3). Mean values (bars) with different lowercase letters (gastric phase) or uppercase letters (intestinal phase) are significantly different (Tukey's multiple comparisons test, $p<0.05$).

After entering the gastrointestinal tract, the particles are subjected to variations in pH, the presence of ions, and different digestive enzymes, factors that can influence the ability of the particles to release bioactive compounds (Z. Li et al., 2015). Chitosan is soluble in aqueous media with low pH conditions, such as in the stomach (pH ≈ 2.0), due to the protonation of the amino groups in its structure (Du et al., 2015). This characteristic can lead to a greater release of anthocyanins in the stomach, limiting their delivery and absorption in the intestinal mucosa. On the other hand, the carboxyl groups in gum arabic becomes negatively charged at pH above 2.2 (Sabet et al., 2021; Weinbrreck et al., 2004). This characteristic may also have contributed to the partial degradation of the particles and the consequent release of anthocyanins during the digestive process, because of the lower percentage of deprotonated carboxyl groups. However, the results of this study indicated that the combination of CH with GA was effective in the partial retention of anthocyanins during the gastric phase, especially in the formulation with a higher proportion of CH. These results suggest that the addition of GA in combination with CH may contribute to improving the retention of anthocyanins under gastric conditions, favoring their controlled release in the intestine.

In the intestinal phase, a fast degradation of anthocyanins was observed in the unencapsulated extract in the first 30 minutes, with a continuous reduction throughout digestion, showing the susceptibility of anthocyanins to intestinal conditions (Figure 3). For the CH:GA 1:2 sample, the anthocyanin concentration showed an initial reduction, followed by an increase during the digestive process and a slight decrease at the end. In the formulation with a higher concentration of chitosan (CH:GA 2:1), the release of anthocyanins occurred gradually and in a more controlled manner, although with modest increases. Regarding bioaccessibility, the CH:GA 2:1 sample presented the highest value (62.31 ± 4.76%), while the unencapsulated extract and the CH:GA 1:2 sample did not differ statistically from each other ($p>0.05$) (Figure 3).

The solubility of chitosan in neutral pH environments is low due to the deprotonation of the amino groups, thus the structure can be maintained without chitosan dissolution (B. Li et al., 2020). The results demonstrated that, despite an initial degradation, the CH:GA 1:2 formulation increased the bioaccessibility of anthocyanins at the end of digestion, promoting a controlled release under intestinal conditions and protecting the compounds from degradation. This result is particularly relevant when compared to the unencapsulated extract, which showed fast degradation of anthocyanins after the transition to the intestinal environment. On the other hand, the CH:GA 2:1 formulation did not significantly impact the bioaccessibility of anthocyanins, probably due to the greater retention of the molecules within the encapsulating

matrix, delaying their release. These results showed the potential of encapsulation using CH and GA to optimize the bioaccessibility of anthocyanins, especially the formulation CH:GA 1:2, with promising applications in functional foods and dietary supplements.

Other studies have evaluated the effect of chitosan on the encapsulation of anthocyanins and have shown results of increased anthocyanin bioaccessibility, mainly by protecting anthocyanins from degradation during gastric digestion and in the small intestine. However, to the best of our knowledge, this is the first study analyzing the combination of chitosan and gum arabic for the entrapment of anthocyanins extract. Nanoparticles of carboxymethyl chitosan and chitosan hydrochloride loaded with blueberry anthocyanins showed slower degradation during *in vitro* digestion (He et al., 2017). The rate of anthocyanins released from chitosan nanoparticles (47.73%) was lower than that of free anthocyanins (68.53%) in solution, throughout gastric digestion (He et al., 2017). In intestinal digestion, the percentage of anthocyanins released from nanoparticles was 30.61%, compared with 50.49% of free anthocyanins (He et al., 2017). For *Aronia melanocarpa* anthocyanins nanoencapsulated with chitosan and sodium tripolyphosphate, the retention rate of anthocyanins (96.24%) in nanoparticles was clearly higher than that of free anthocyanins (88.21%) when the samples were subjected to gastric digestion for 1 h (M. Wang et al., 2021). Furthermore, the retention rate of free anthocyanins rapidly decreased to 38.52%, while that of nanoparticles was 79.13% after simulated intestinal digestion (M. Wang et al., 2021). When pectin was added as a wall material together with chitosan, the release rate of anthocyanins after 12 h of digestion was 26% in gastric juice and 56% in intestinal juice (X. Zhao et al., 2020).

3.6. *In vitro* colonic phase

The evolution of phenolic compounds at different stages of the colonic phase was monitored, and the results are presented in Figures 4 and 5. In summary, eleven phenolic compounds (cyanidin-3-glucoside, protocatechuic acid, phloroglucinol aldehyde, gallic acid, pyrogallol, methyl gallate, vanillic acid, gentisic acid, 2-galloyl-glucose, 3-galloyl-glucose, 4-galloyl-glucose) were identified in the colonic samples.

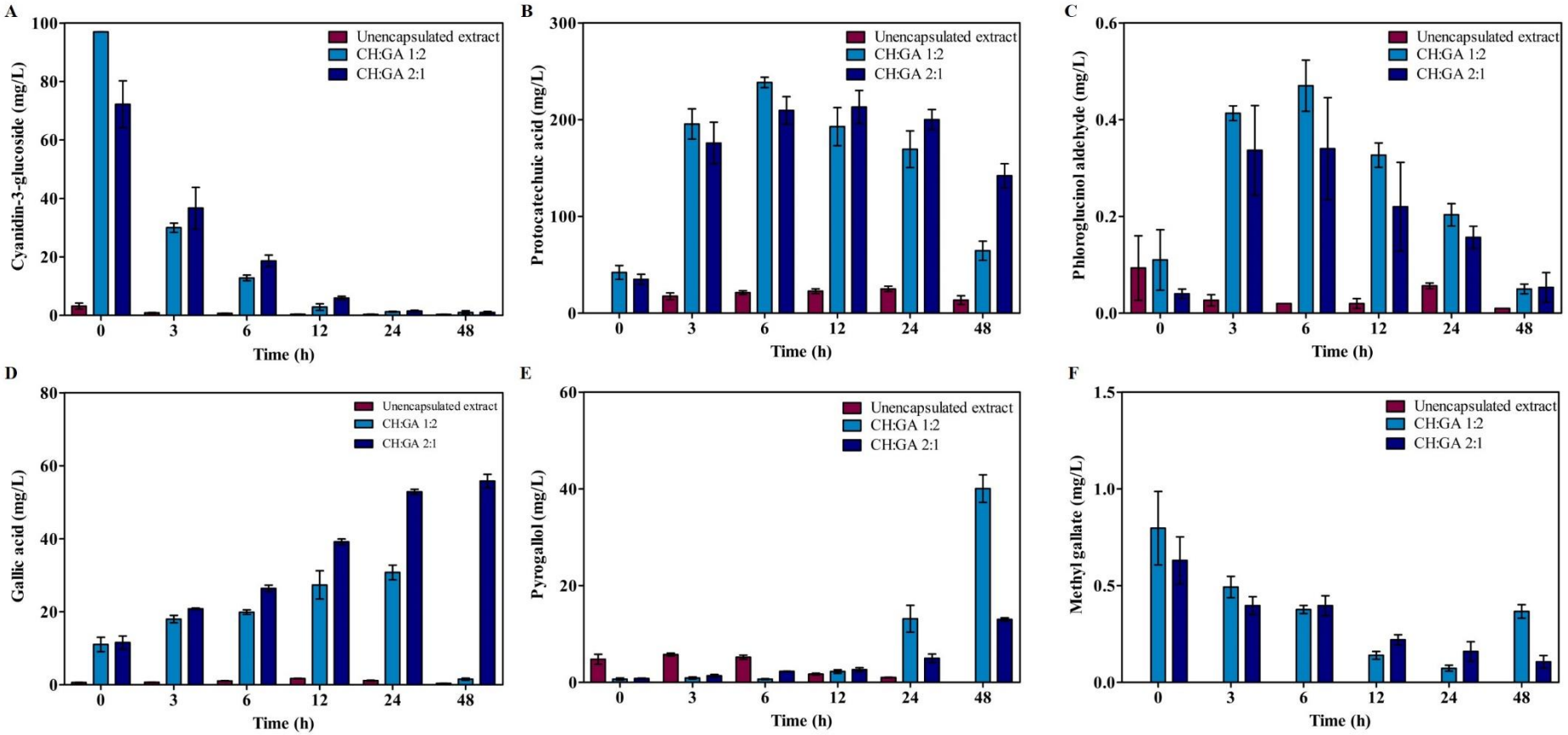

Figure 4 - Time-dependent changes in phenolic compounds during *in vitro* colonic metabolism of digestion residues from the unencapsulated extract and encapsulated samples using chitosan and gum arabic at different ratios (1:2 and 2:1 v/v). Values are expressed as mean ± SD (n=3). Cyanidin-3-glucoside (A), protocatechuic acid (B), phloroglucinol aldehyde (C), gallic acid (D), pyrogallol (E), methyl gallate

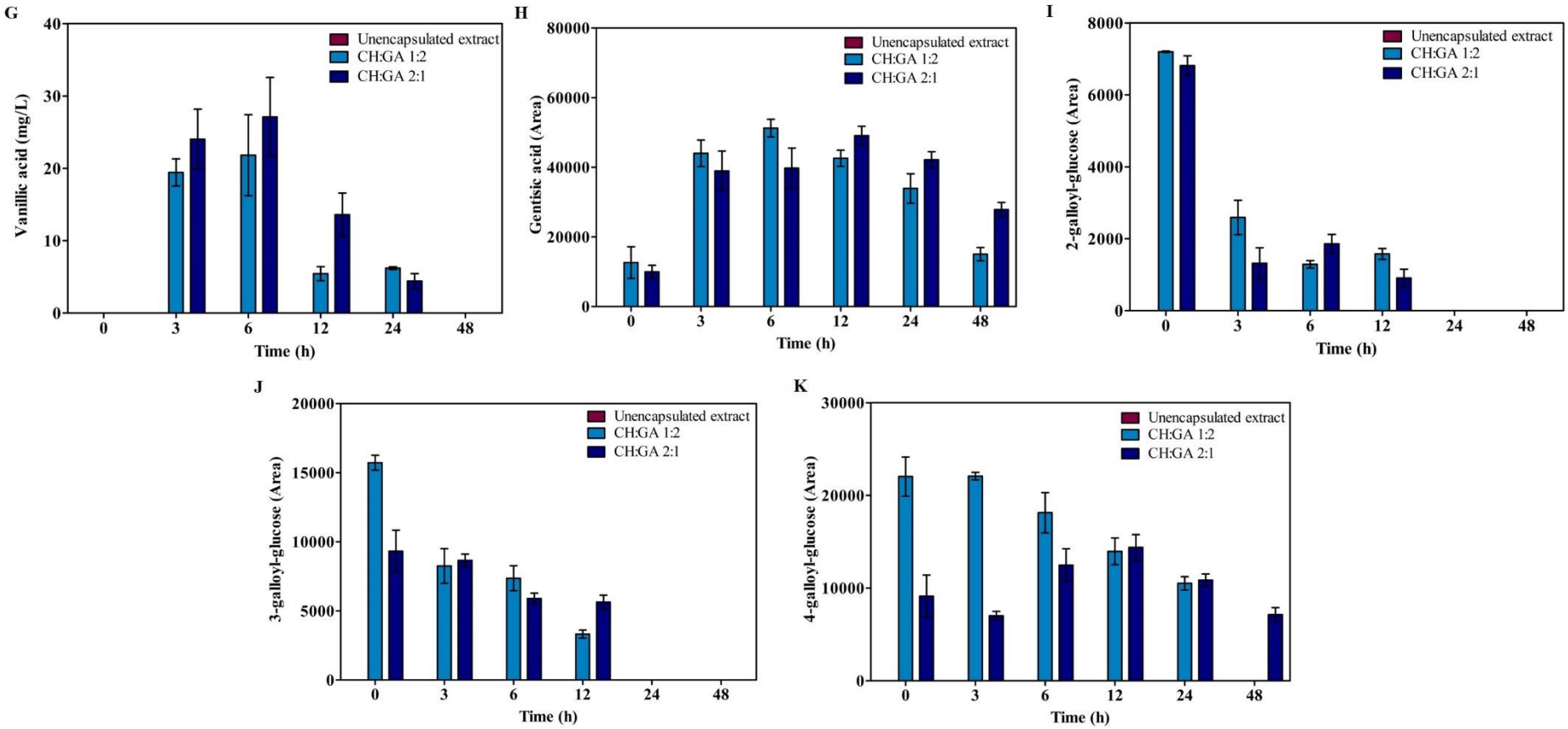

Figure 5 – Time-dependent changes in phenolic compounds during *in vitro* colonic metabolism of digestion residues from the unencapsulated extract and encapsulated samples using chitosan and gum arabic at different ratios (1:2 and 2:1 v/v). Values are expressed as mean ± SD. vanillic acid (G), gentisic acid (H), 2-galloyl-glucose (I), 3-galloyl-glucose (J), 4-galloyl-glucose (K).

The parent compound cyanidin-3-glucoside (C3G) exhibited a significant decrease overtime during fermentation, indicating rapid consumption by the microbiota (Figure 4). The sample CH:GA 1:2 delivered the highest concentration of C3G to be metabolized by the microbiota, followed by the sample CH:GA 2:1 and the unencapsulated extract ($p<0.05$). The concentrations of C3G delivered to the colonic phase were 30.57 ± 0.01-fold (CH:GA 1:2) and 22.77 ± 2.53-fold (CH:GA 2:1) higher compared to the unencapsulated extract. These results indicated that the encapsulated samples retained more C3G in the digestion residues, increasing the concentration of intact C3G delivered for microbiota metabolism.

Furthermore, the concentrations of protocatechuic acid (PCA) and phloroglucinol aldehyde (PGA) significantly increased during fermentation (Figure 4). These compounds can be considered as biomarkers for C3G metabolism, as they are formed from the breakdown of this anthocyanin (Makarewicz et al., 2021). The concentrations of PCA and PGA were higher for the encapsulated samples in comparison with the unencapsulated extract, which is in accordance with the higher concentration of C3G delivered for those samples. Towards the end of fermentation, there was a decrease in the content of PCA and PGA, indicating that these compounds were further metabolized by the microbiota.

Other compounds detected during the colonic phase were gallic acid (GA), pyrogallol (PG) and methyl gallate (MG) (Figure 4). Gallic acid was originally presented in the samples and its concentration increased during fermentation, with a more pronounced increase observed for the encapsulated samples (CH:GA 1:2 and CH:GA 2:1). The increase in concentration of GA over the fermentation can be associated with the release from the digestion residues and also from the metabolization of the gallotannins. For PG, a secondary metabolite resulting from the microbial degradation of gallic acid, there was an increase in concentration over time, with the highest concentration detected at 48 h for the sample CH:GA 1:2. On the other hand, MG was not detected in the medium for the unencapsulated extract and its concentration decreased gradually over time in the encapsulation treatments.

Vanillic acid (VA) and gentisic acid (GA) were detected only in the encapsulated samples (CH:GA 1:2 and CH:GA 2:1) (Figure 5). This suggests that encapsulation had a critical role in stabilizing these compounds or their precursors, making them available during fermentation. The concentrations of VA and GA increased during the initial hours of fermentation. However, towards the end of fermentation, their concentrations decreased, likely due to further microbial degradation into other metabolites.

The gallotannins, 2-galloyl-glucose (2-GG), 3-galloyl-glucose (3-GG) and 4-galloyl-glucose (4-GG) were also only detected for the encapsulated samples (Figure 5), indicating that

those samples were able to retain intact tannins in their structure and release these compounds during the colonic phase. The concentration 2-GG and 3-GG declined in all samples, particularly within the first 6 h, indicating its rapid metabolism by the microbiota. In contrast, the concentration of 4-GG remained relatively stable during the initial hours (0–6 h), followed by a gradual decrease over time.

The results showed that encapsulation of the extract increased the release and metabolic utilization of phenolic compounds during colonic metabolism. This indicates that the use of CH and GA in combination may be a promising alternative for the targeted delivery of phenolic compounds to the colon. The tested formulations protected anthocyanins and also tannins from degradation under stomach and small intestine conditions, ensuring that these compounds reached the colon in their intact forms to interact with the gut microbiota and be metabolized.

3.7. Short-chain fatty acids (SCFAs)

Gut microbiota can produce some metabolites like SCFAs that are essential for preserving the structure and functionality of the intestine (Al-Baadani et al., 2021). The concentrations of SCFAs produced after 48h of *in vitro* colonic metabolism in the control (no digestion residue) and in the samples (unencapsulated extract and encapsulated samples) are shown in Table 2.

Table 2 - Concentration (mg/L) of short-chain fatty acids (SCFAs) produced during the *in vitro* colonic metabolism of digestion residues from the unencapsulated extract and encapsulated samples (CH:GA 1:2 and CH:GA 2:1 v/v).

SCFA (mg/L)	Control*	Extract	CH:GA 1:2	CH:GA 2:1
Acetic acid	97.18 ± 2.08^{a}	98.58 ± 3.68^{a}	92.69 ± 8.56^{a}	92.73 ± 0.81^{a}
Propionic acid	20.45 ± 0.25^{b}	21.17 ± 0.12^{b}	49.40 ± 7.97^{a}	17.61 ± 0.56^{b}
Butyric acid	17.34 ± 0.86^{a}	13.18 ± 2.41^{a}	14.47 ± 3.57^{a}	3.09 ± 0.28^{b}
Valeric acid	25.46 ± 0.12^{b}	25.56 ± 0.05^{b}	28.70 ± 1.55^{a}	22.78 ± 0.14^{c}
Isobutyric acid	7.33 ± 0.09^{b}	7.39 ± 0.07^{b}	20.10 ± 4.12^{a}	5.86 ± 0.22^{b}
2-methylbutyric/ isovaleric acid	4.73 ± 0.33^{a}	4.31 ± 0.46^{a}	0.71 ± 0.17^{b}	n.d.

Concentration is expressed as mean ± SD. Mean values with different lowercase letters within the same row are significantly different (Tukey's multiple comparisons test, $p<0.05$). * The control refers to the sample without any digestion residue. n.d. = not detected

The CH:GA 1:2 formulation significantly increased propionic acid, valeric acid, and isobutyric acid concentrations, suggesting that the addition of anthocyanin extract encapsulated with a higher proportion of gum arabic promoted the synthesis of this SCFAs. On the other hand, the formulation with a higher proportion of chitosan did not positively affect the production of SCFAs, but showed reduced concentrations of butyric, valeric and 2-methylbutyric/isovaleric acid compared to the control. Regarding the unencapsulated extract, no increases in concentrations were observed, as all the values were similar to the control ($p>0.05$).

Gum arabic and chitosan are not digested in the upper gastrointestinal tract and reach the colon, where they can be fermented by the gut microbiota to produce SCFAs (Al-Baadani et al., 2021; Yan et al., 2021). However, the results suggested that a higher proportion of gum arabic in the formulation promoted the production of specific SCFAs, whereas chitosan did not exhibit similar effects. It has been observed in other study that the production of overall SCFAs was reduced after treatment with chitosan during *in vitro* fermentation, which was associated to the decrease of key SCFA-producing species (Ruiz-Rico et al., 2022).

3.8. Antioxidant and anti-inflammatory effects of cyanidin-3-glucoside and metabolites in HUVEC cells

The effects of cyanidin-3-glucoside (C3G) and some of the metabolites (PA, GA, PGA, MG) were analyzed in HUVEC cells to compare the bioactivity of these compounds in this cell line. A mixture of compounds was also tested. One mixture with a higher concentration of metabolites (Mix 1) and another one with a higher content of C3G (Mix 2). Human umbilical vein endothelial cells (HUVECs) are widely recognized as a valuable model for studying endothelial cell function, representing human vascular tissue (Duranova et al., 2024; Medina-Leyte et al., 2020). Since the endothelium plays a crucial role in vascular homeostasis and in the pathophysiology of several diseases, including diabetes, hypertension, and cardiovascular diseases, these cells have been used in different studies (Duranova et al., 2024; Medina-Leyte et al., 2020). The studies with these cells can provide insights into endothelial dysfunction,

disease mechanisms, and cellular responses to various drugs and treatments (Duranova et al., 2024; Medina-Leyte et al., 2020).

Resazurin assays were performed to assess the cytotoxicity of the compounds on HUVEC cells. All compounds showed a dose-dependent inhibitory effect on cell viability (Figure 6). C3G reduced cell viability only at the higher concentrations of 125 µM and 250 µM. Protocatechuic acid (PA), one of the primary metabolites of C3G, showed higher cytotoxicity compared to the parent compound, while PGA exhibited a similar cytotoxicity profile to C3G. Gallic acid (GA) reduced cell viability only at the higher concentration of 250 µM and Mix 2 was more cytotoxic than Mix 1.

The viability results were used to determine the concentrations for the ROS assay, ensuring that the selected concentrations did not significantly suppress cell growth. The results showed that ROS levels increased up to 1.60-fold compared to the control after LPS challenge. All the compounds reduced the concentration of ROS in the cells treated with LPS, showing a dose-dependent effect (Figure 7). Comparing the activity of the compounds at a concentration of 15.62 µM (Figure 7H), all treatments significantly reduced ROS production compared to LPS treated group ($p>0.05$), showing effective antioxidant activity. Regarding the mixtures, both mixtures reduced ROS levels at all concentrations tested, with no significant differences between the two formulations ($p>0.05$). Excessive ROS can lead to oxidative stress, causing endothelial dysfunction, which is an important factor in the development of cardiovascular diseases (CVD) (Scioli et al., 2020). Then, by neutralizing ROS, these antioxidant compounds help preserve endothelial function and prevent CVD (Scioli et al., 2020).

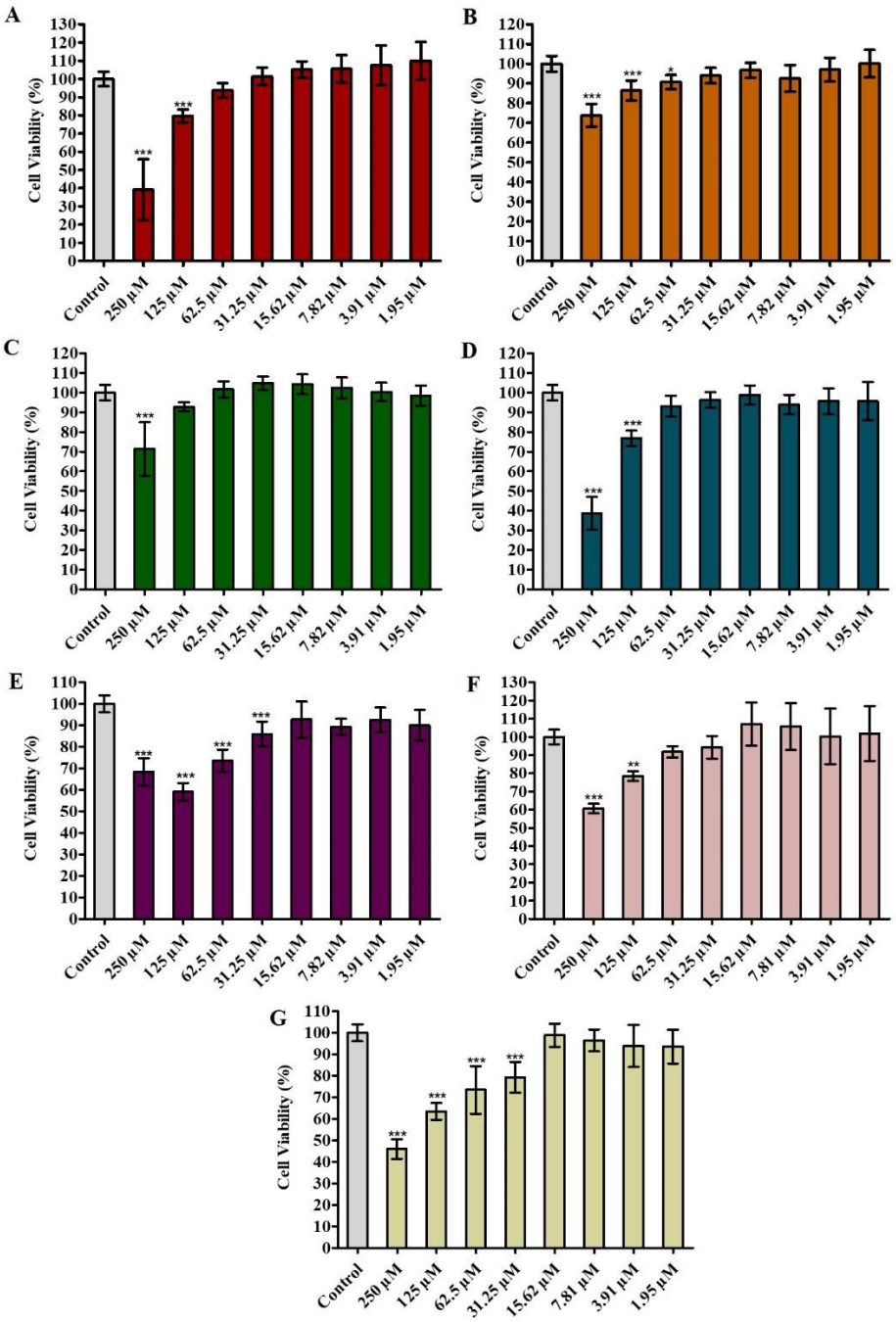

Figure 6 - Dose-dependent effects of bioactive compounds on cell viability in HUVEC Cells. Cyanidin-3-glucoside (A), protocatechuic acid (B), gallic acid (C), phloroglucinol aldehyde (D), methyl gallate (E), mix 1 (F), mix 2 (G). Values are presented as the mean ± standard deviation of two independent assays with internal quadruplicates for each of them. Statistically significant differences between the control (untreated cells) and the cells treated with different compounds were identified using Dunnett's test (∗p<0.05; ∗∗p<0.01; ∗∗∗ p<0.001).

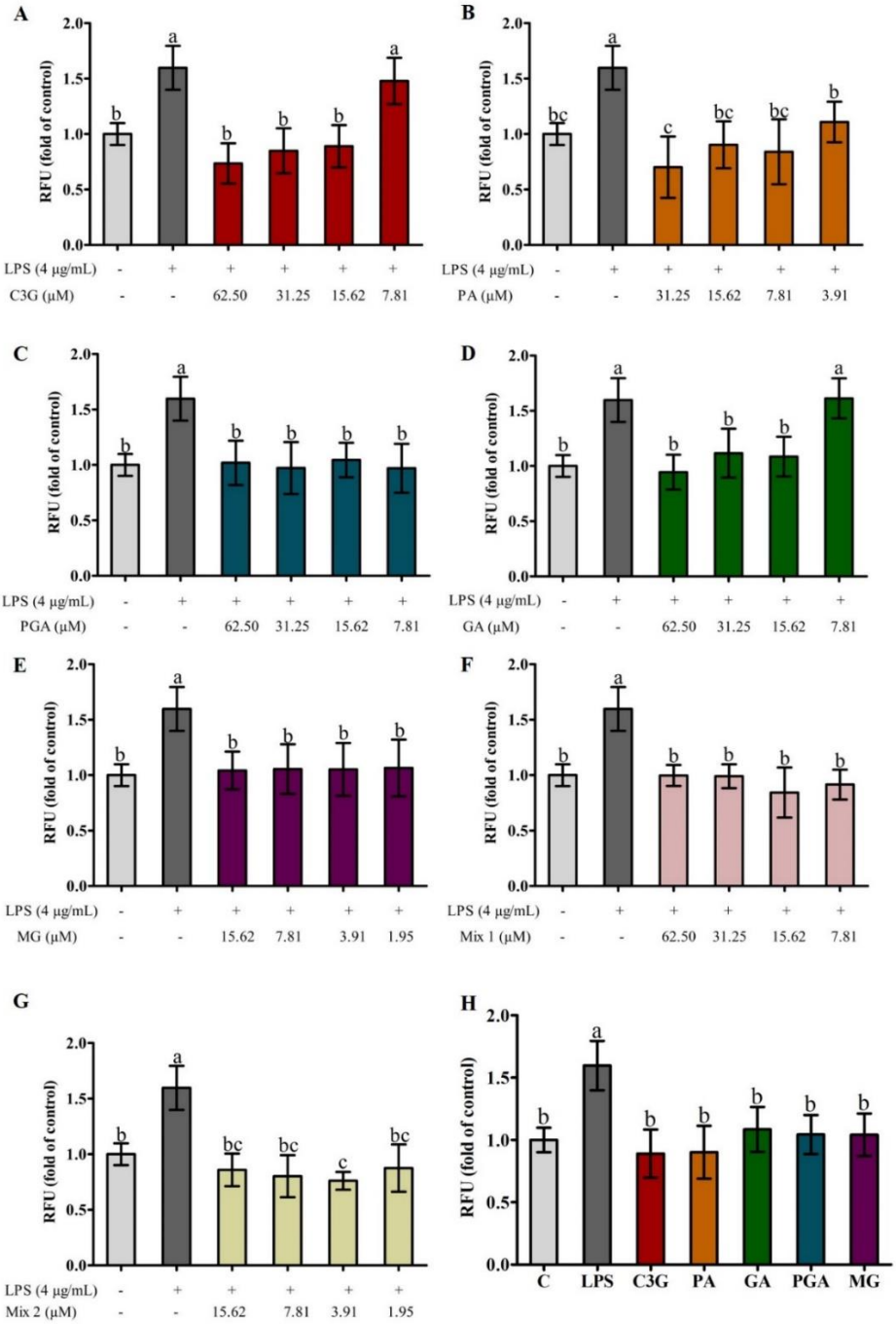

Figure 7 - Reactive Oxygen Species (ROS) in HUVEC cells treated with different concentrations of phenolic compounds followed by LPS (4 µg/mL) challenge for 3 h. Cyanidin-3-glucoside (A), protocatechuic acid (B), gallic acid (C), phloroglucinol aldehyde (D), methyl gallate (E), mix 1 (F), mix 2 (G), comparison of the compounds in the concentration of 15.62 µM (H). Values are presented as the mean ± standard deviation of two independent assays with internal quadruplicates for each of them. Mean values (bar) with different lowercase letters are significantly different (Tukey's multiple comparisons test, $p<0.05$).

Reducing inflammation is another key mechanism through which phenolic compounds can influence the endothelial function and the development and progression of cardiovascular diseases. The results showed that LPS induced the expression of TNF-α, NF-κB1, and COX-2 genes after 3 h of stimulation, with fold increases of 1.47, 4.66 and 4.29, respectively, compared to untreated control cells. TNF-α is a pro-inflammatory cytokine that plays a key role in regulating immune cells, inflammation, and endothelial function (Jang et al., 2021; Zhang et al., 2009). All the compounds were able to prevent the up-regulation of TNF-α by LPS to levels similar to the untreated control, with no significant differences between them ($p>0.05$) (Figure 8A).

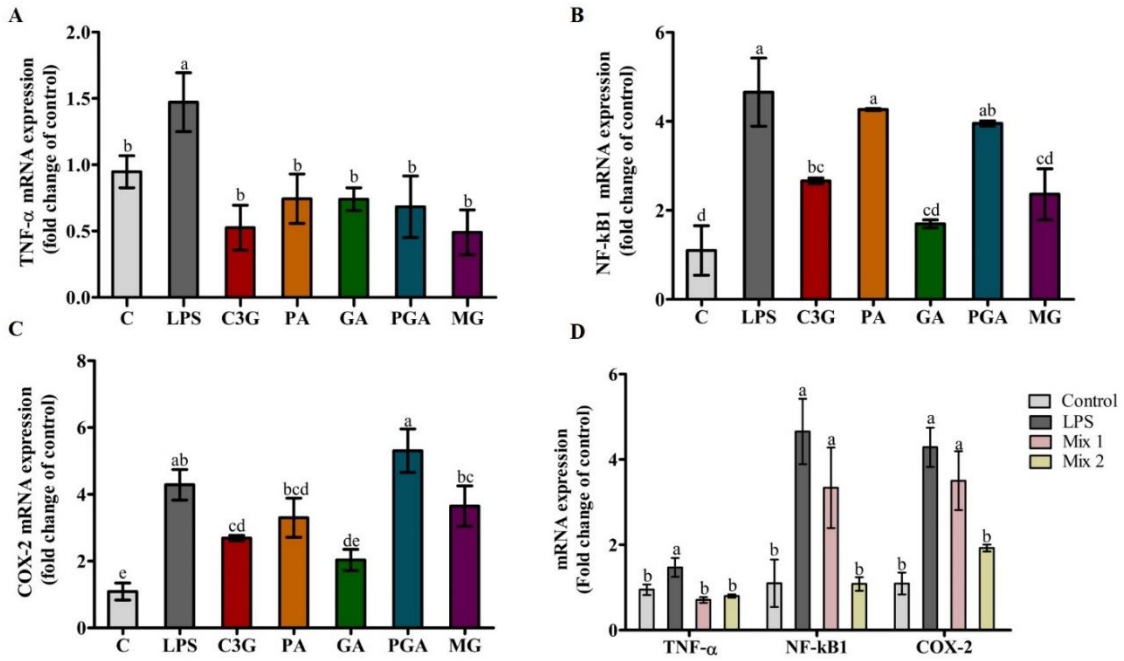

Figure 8 - Gene expression of TNF-α, NF-kB1 and COX-2 in HUVEC cells treated with phenolic compounds at a concentration of 15.62 µM. Values are presented as mean ± standard deviation (n=3). Mean values (bar) with different lowercase letters are significantly different (Tukey's multiple comparisons test, $p<0.05$).

NF-κB is a transcription factor involved in the expression of genes involved in inflammation, cell adhesion, and immune responses (T. Liu et al., 2017). Because of its central role in inflammation, NF-κB is often studied as a target for therapeutic interventions aiming to reduce inflammatory diseases (Roberti et al., 2022). C3G, GA and MG were the most effective compounds in preventing the upregulation of NF-kB1 by LPS, indicating their potential in modulating inflammation (Figure 8B). These compounds were able to inhibit the NF-κB1

activation triggered by LPS, suggesting they could reduce the inflammatory response in endothelial cells. In contrast, the metabolites of C3G, PA and PGA presented similar levels of NF-κB1 to LPS treated samples, which suggests that the parent compound (C3G) may be more potent in preventing NF-κB1 activation than its metabolites (Figure 8B).

Cyclooxygenase-2 (COX-2) is an enzyme involved in the synthesis of prostaglandins, which are key mediators of inflammation (Gandhi et al., 2017). The results indicated that C3G, PA, GA and MG significantly reduced COX-2 mRNA expression compared to the LPS-treated group (Figure 8C). While, PGA did not show an inhibitory effect on COX-2 mRNA expression (Figure 8C). By inhibiting COX-2 expression, these compounds may help reduce inflammation and vascular dysfunction, making them potential candidates for managing inflammatory diseases.

Regarding the mixtures, Mix 2 reduced the mRNA expression of NF-κB1 and COX-2 to levels similar to the control (Figure 8D). In contrast, Mix 1 showed no significant effect in reducing the expression of these inflammatory mediators, as its levels remained similar to those observed in the LPS-treated group (Figure 8D). On the other hand, both mixtures were effective in preventing the upregulation of TNF-α, showing comparable activity. These results are in accordance with the observations for the isolated compounds, as Mix 2 contains a higher proportion of C3G, which demonstrated superior activity in reducing inflammatory markers. In contrast, Mix 1 contains a higher concentration of C3G metabolites, such as PA and PGA, which showed lower anti-inflammatory potential compared to the parent compound.

The data presented in this study demonstrated that phenolic compounds have the potential to improve vascular health by reducing ROS levels and modulating key inflammatory mediators. The C3G metabolites, PA and PGA, showed reduced anti-inflammatory activity compared to the parent compound. These results suggest that increase the bioaccessibility and bioavailability of C3G, providing increased absorption, could be beneficial for improving vascular health.

4. Conclusion

This study evaluated the potential of combining chitosan and gum arabic as wall materials for the encapsulation of anthocyanins extracted from jabuticaba peel. The encapsulated samples showed high encapsulation efficiency, effectively retained anthocyanins during gastric digestion, and improved their stability in the small intestinal phase. The CH:GA 1:2 formulation showed the highest bioaccessibility of anthocyanins in the intestinal phase,

whereas CH:GA 2:1 promoted greater retention of anthocyanins. During the *in vitro* colonic phase, encapsulated samples enhanced the delivery of cyanidin-3-glucoside and other phenolic compounds, such as gallic acid and gallotannins, compared to the unencapsulated extract. Besides that, the CH:GA 1:2 formulation showed a higher potential to promote SCFAs production, enhancing the production of propionic, valeric, and isobutyric acids. In HUVEC cells, cyanidin-3-glucoside and other phenolic compounds showed the potential to improve vascular health by reducing ROS levels and the expression of inflammatory mediators, such as TNF-α, NF-κB1, and COX-2. The C3G metabolites, protocatechuic acid and phloroglucinol aldehyde, showed reduced anti-inflammatory activity compared to the parent compound. Based on the results, the combination of chitosan and gum arabic, particularly the CH:GA 1:2 formulation, proved to be effective for the encapsulation of anthocyanins and for the targeted delivery of phenolic compounds to the colon, presenting the potential for the development of functional food products and dietary supplements with controlled release profiles of anthocyanins and increased production of SCFAs.

5. References

Al-Baadani, H. H., Al-Mufarrej, S. I., Al-Garadi, M. A., Alhidary, I. A., Al-Sagan, A. A., & Azzam, M. M. (2021). The use of gum Arabic as a natural prebiotic in animals: A review. Animal Feed Science and Technology, 274, 114894. https://doi.org/10.1016/j.anifeedsci.2021.114894

Arbizu, S., Chew, B., Mertens-Talcott, S. U., & Noratto, G. (2020). Commercial whey products promote intestinal barrier function with glycomacropeptide enhanced activity in downregulating bacterial endotoxin lipopolysaccharides (LPS)-induced inflammation: *In vitro*. Food and Function, 11(7), 5842–5852. https://doi.org/10.1039/d0fo00487a

Ayvaz, H., Cabaroglu, T., Akyildiz, A., Pala, C. U., Temizkan, R., Ağçam, E., Ayvaz, Z., Durazzo, A., Lucarini, M., Direito, R., & Diaconeasa, Z. (2023). Anthocyanins: Metabolic Digestion, Bioavailability, Therapeutic Effects, Current Pharmaceutical/Industrial Use, and Innovation Potential. Antioxidants, 12(1). https://doi.org/10.3390/antiox12010048

Bashir, M., & Haripriya, S. (2016). Assessment of physical and structural characteristics of almond gum. International Journal of Biological Macromolecules, 93, 476–482. https://doi.org/10.1016/j.ijbiomac.2016.09.009

Cai, X., Du, X., Cui, D., Wang, X., Yang, Z., & Zhu, G. (2019). Improvement of stability of blueberry anthocyanins by carboxymethyl starch/xanthan gum combinations microencapsulation. Food Hydrocolloids, 91, 238–245. https://doi.org/10.1016/j.foodhyd.2019.01.034

Chung, C., Rojanasasithara, T., Mutilangi, W., & McClements, D. J. (2016). Enhancement of colour stability of anthocyanins in model beverages by gum arabic addition. Food Chemistry, 201, 14–22. https://doi.org/10.1016/j.foodchem.2016.01.051

Cui, H., Si, X., Tian, J., Lang, Y., Gao, N., Tan, H., Bian, Y., Zang, Z., Jiang, Q., Bao, Y., & Li, B. (2022). Anthocyanins-loaded nanocomplexes comprising casein and carboxymethyl cellulose: stability, antioxidant capacity, and bioaccessibility. Food Hydrocolloids, 122. https://doi.org/10.1016/j.foodhyd.2021.107073

Du, H., Liu, M., Yang, X., & Zhai, G. (2015). The design of pH-sensitive chitosan-based formulations for gastrointestinal delivery. Drug Discovery Today, 20(8), 1004–1011. https://doi.org/10.1016/j.drudis.2015.03.002

Duranova, H., Kuzelova, L., Borotova, P., Simora, V., & Fialkova, V. (2024). Human Umbilical Vein Endothelial Cells as a Versatile Cellular Model System in Diverse Experimental Paradigms: An Ultrastructural Perspective. Microscopy and Microanalysis, 30(3), 419–439. https://doi.org/10.1093/mam/ozae048

Espinosa-Andrews, H., Sandoval-Castilla, O., Vázquez-Torres, H., Vernon-Carter, E. J., & Lobato-Calleros, C. (2010). Determination of the gum Arabic-chitosan interactions by Fourier Transform Infrared Spectroscopy and characterization of the microstructure and rheological features of their coacervates. Carbohydrate Polymers, 79(3), 541–546. https://doi.org/10.1016/j.carbpol.2009.08.040

Fathi, M., & Julian, D. (2014). Nanoencapsulation of food ingredients using carbohydrate, based delivery systems. Trends in Food Science & Technology, 39, 18–39.

Fernandes, A., Oliveira, J., Fonseca, F., Ferreira-da-Silva, F., Mateus, N., Vincken, J. P., & de Freitas, V. (2020). Molecular binding between anthocyanins and pectic polysaccharides – Unveiling the role of pectic polysaccharides structure. Food Hydrocolloids, 102, 105625. https://doi.org/10.1016/j.foodhyd.2019.105625

Gandhi, J., Khera, L., Gaur, N., Paul, C., & Kaul, R. (2017). Role of modulator of inflammation cyclooxygenase-2 in gammaherpesvirus mediated tumorigenesis. Frontiers in Microbiology, 8, 538. https://doi.org/10.3389/fmicb.2017.00538

Gatto, M., Ochi, D., Yoshida, C. M. P., & da Silva, C. F. (2019). Study of chitosan with different degrees of acetylation as cardboard paper coating. Carbohydrate Polymers, 210, 56–63. https://doi.org/10.1016/j.carbpol.2019.01.053

He, B., Ge, J., Yue, P., Yue, X., Fu, R., Liang, J., & Gao, X. (2017). Loading of anthocyanins on chitosan nanoparticles influences anthocyanin degradation in gastrointestinal fluids and stability in a beverage. Food Chemistry, 221, 1671–1677.

Heneczkowski, M., Kopacz, M., Nowak, D., & Kuzniar, A. (2001). Infrared spectrum analysis of some flavonoids. Acta Poloniae Pharmaceutica, 58(6), 415–420.

Jang, D. I., Lee, A. H., Shin, H. Y., Song, H. R., Park, J. H., Kang, T. B., Lee, S. R., & Yang, S. H. (2021). The role of tumor necrosis factor alpha (Tnf-α) in autoimmune disease and current

tnf-α inhibitors in therapeutics. International Journal of Molecular Sciences, 22(5), 1–16. https://doi.org/10.3390/ijms22052719

Júlia, E., Souza, D. De, Hüttner, D., Renato, A., Dias, G., & Zavareze, R. (2021). Polysaccharides as wall material for the encapsulation of essential oils by electrospun technique. Carbohydrate Polymers, 265, 1180068.

Kuck, L. S., & Noreña, C. P. Z. (2016). Microencapsulation of grape (*Vitis labrusca* var. Bordo) skin phenolic extract using gum Arabic, polydextrose, and partially hydrolyzed guar gum as encapsulating agents. Food Chemistry, 194, 569–576. https://doi.org/10.1016/j.foodchem.2015.08.066

Lee, J., Durst, R. W., Wrolstad, R. E., Barnes, K. W., Eisele, ; T, Giusti, ; M M, Haché, ; J, Hofsommer, ; H, Koswig, ; S, Krueger, D. A., Kupina, ; S, Martin, ; S K, Martinsen, ; B K, Miller, T. C., Paquette, ; F, Ryabkova, ; A, Skrede, ; G, Trenn, ; U, & Wightman, J. D. (2005). Determination of Total Monomeric Anthocyanin Pigment Content of Fruit Juices, Beverages, Natural Colorants, and Wines by the pH Differential Method: Collaborative Study. Journal of AOAC International, 88(5), 1269–1278.

Li, B., Elango, J., & Wu, W. (2020). Recent advancement of molecular structure and biomaterial function of chitosan from marine organisms for pharmaceutical and nutraceutical application. Applied Sciences, 10(14), 4719. https://doi.org/10.3390/app10144719

Li, Z., Jiang, H., Xu, C., & Gu, L. (2015). A review: Using nanoparticles to enhance absorption and bioavailability of phenolic phytochemicals. Food Hydrocolloids, 43, 153–164. https://doi.org/10.1016/j.foodhyd.2014.05.010

Liang, A., Leonard, W., Beasley, J. T., Fang, Z., Zhang, P., & Ranadheera, C. S. (2023). Anthocyanins-gut microbiota-health axis: A review. Critical Reviews in Food Science and Nutrition, 1–26. https://doi.org/10.1080/10408398.2023.2187212

Liang, J., Yan, H., Puligundla, P., Gao, X., & Zhou, Y. (2017). Applications of chitosan nanoparticles to enhance absorption and bioavailability of tea polyphenols: A review. 69, 286–292.

Liu, R., Wang, X., Yang, L., Wang, Y., & Gao, X. (2023). Coordinated encapsulation by β-cyclodextrin and chitosan derivatives improves the stability of anthocyanins. International Journal of Biological Macromolecules, 242. https://doi.org/10.1016/j.ijbiomac.2023.125060

Liu, T., Zhang, L., Joo, D., & Sun, S. C. (2017). NF-κB signaling in inflammation. Signal Transduction and Targeted Therapy, 2, 17023. https://doi.org/10.1038/sigtrans.2017.23
Makarewicz, M., Drożdż, I., Tarko, T., & Duda-Chodak, A. (2021). The interactions between polyphenols and microorganisms, especially gut microbiota. Antioxidants, 10(2), 1–70. https://doi.org/10.3390/antiox10020188

Mansour, M., Salah, M., & Xu, X. (2020). Effect of microencapsulation using soy protein isolate and gum arabic as wall material on red raspberry anthocyanin stability, characterization, and simulated gastrointestinal conditions. Ultrasonics Sonochemistry, 63, 104927. https://doi.org/10.1016/j.ultsonch.2019.104927

Medina-Leyte, D. J., Domínguez-Pérez, M., Mercado, I., Villarreal-Molina, M. T., & Jacobo-Albavera, L. (2020). Use of human umbilical vein endothelial cells (HUVEC) as a model to study cardiovascular disease: A review. Applied Sciences (Switzerland), 10(3). https://doi.org/10.3390/app10030938

Minekus, M., Alminger, M., Alvito, P., Ballance, S., Bohn, T., Bourlieu, C., Carrière, F., Boutrou, R., Corredig, M., Dupont, D., Dufour, C., Egger, L., Golding, M., Karakaya, S., Kirkhus, B., Le Feunteun, S., Lesmes, U., MacIerzanka, A., MacKie, A., … Brodkorb, A. (2014). A standardised static *in vitro* digestion method suitable for food-an international consensus. Food and Function, 5(6), 1113–1124. https://doi.org/10.1039/c3fo60702j

Mueller, D., Jung, K., Winter, M., Rogoll, D., Melcher, R., & Richling, E. (2017). Human intervention study to investigate the intestinal accessibility and bioavailability of anthocyanins from bilberries. Food Chemistry, 231, 275–286. https://doi.org/10.1016/j.foodchem.2017.03.130

Noratto, G. D., Angel-Morales, G., Talcott, S. T., & Mertens-Talcott, S. U. (2011). Polyphenolics from Açaí (*Euterpe oleracea* Mart.) and red muscadine grape (*Vitis rotundifolia*) protect human umbilical vascular endothelial cells (HUVEC) from glucose- and lipopolysaccharide (LPS)-induced inflammation and target microRNA-126. Journal of Agricultural and Food Chemistry, 59(14), 7999–8012. https://doi.org/10.1021/jf201056x

Oancea, A., Hasan, M., Mihaela, A., Barbu, V., Enachi, E., Bahrim, G., Râpeanu, G., Silvi, S., & St, N. (2018). Functional evaluation of microencapsulated anthocyanins from sour cherries skins extract in whey proteins isolate. LWT - Food Science and Technology, 95, 129–134.

Padil, V. V. T., Zare, E. N., Makvandi, P., & Černík, M. (2021). Nanoparticles and nanofibres based on tree gums: Biosynthesis and applications. In Comprehensive Analytical Chemistry (Vol. 94, pp. 223–265). Elsevier. https://doi.org/10.1016/bs.coac.2020.12.002

Queiroz, M. F., Melo, K. R. T., Sabry, D. A., Sassaki, G. L., & Rocha, H. A. O. (2015). Does the use of chitosan contribute to oxalate kidney stone formation? Marine Drugs, 13(1), 141–158. https://doi.org/10.3390/md13010141

Roberti, A., Chaffey, L. E., & Greaves, D. R. (2022). NF-κB Signaling and Inflammation—Drug Repurposing to Treat Inflammatory Disorders? Biology, 11(3), 372. https://doi.org/10.3390/biology11030372

Rocha, J. de C. G., Procópio, F. R., Mendonça, A. C., Vieira, L. M., Perrone, Í. T., de Barros, F. A. R., & Stringheta, P. C. (2018). Optimization of ultrasound-assisted extraction of phenolic compounds from jussara (*Euterpe edulis* M.) and blueberry (*Vaccinium myrtillus*) fruits. Food Science and Technology, 38(1), 45–53. https://doi.org/10.1590/1678-457x.36316

Rosales, T. K. O., Pedrosa, L. de F., Nascimento, K. R., Fioroto, A. M., Toniazzo, T., Tadini, C. C., Purgatto, E., Hassimotto, N. M. A., & Fabi, J. P. (2023). Nanoencapsulated anthocyanins: A new technological approach to increase physical-chemical stability and bioaccessibility. Food Hydrocolloids, 139, 108516. https://doi.org/10.1016/j.foodhyd.2023.108516

Ruiz-Rico, M., Renwick, S., Vancuren, S. J., Robinson, A. V., Gianetto-Hill, C., Allen-Vercoe, E., & Barat, J. M. (2022). Influence of free and immobilized chitosan on a defined human gut

microbial ecosystem. Food Research International, 161, 111890. https://doi.org/10.1016/j.foodres.2022.111890

Sabet, S., Rashidinejad, A., Melton, L. D., Zujovic, Z., Akbarinejad, A., Nieuwoudt, M., Seal, C. K., & Mcgillivray, D. J. (2021). The interactions between the two negatively charged polysaccharides: Gum Arabic and alginate. Food Hydrocolloids, 112, 106343. https://doi.org/10.1016/j.foodhyd.2020.106343

Saikia, S., Mahnot, N. K., & Mahanta, C. L. (2015). Optimisation of phenolic extraction from Averrhoa carambola pomace by response surface methodology and its microencapsulation by spray and freeze drying. Food Chemistry, 171, 144–152. https://doi.org/10.1016/j.foodchem.2014.08.064

Sampaio, D. M., Babu, R. S., Costa, H. R. M., & de Barros, A. L. F. (2019). Investigation of nanostructured TiO2 thin film coatings for DSSCs application using natural dye extracted from jabuticaba fruit as photosensitizers. Ionics, 25(6), 2893–2902. https://doi.org/10.1007/s11581-018-2753-6

Schmittgen, T. D., & Livak, K. J. (2008). Analyzing real-time PCR data by the comparative CT method. Nature Protocols, 3(6), 1101–1108. https://doi.org/10.1038/nprot.2008.73

Scioli, M. G., Storti, G., D'amico, F., Guzmán, R. R., Centofanti, F., Doldo, E., Miranda, E. M. C., & Orlandi, A. (2020). Oxidative stress and new pathogenetic mechanisms in endothelial dysfunction: Potential diagnostic biomarkers and therapeutic targets. Journal of Clinical Medicine, 9(6), 1–39. https://doi.org/10.3390/jcm9061995

Shurvell, H. F. (2006). Spectra-Structure Correlations Spectra-Structure Correlations in the Mid-and Far-infrared. Handbook of Vibrational Spectroscopy, 1783–1816. https://doi.org/10.1002/9780470027325.s4101

Silva, H. R. da, Assis, D. da C. de, Prada, A. L., Silva, J. O. C., Sousa, M. B. de, Ferreira, A. M., Amado, J. R. R., Carvalho, H. de O., Santos, A. V. T. de L. T. dos, & Carvalho, J. C. T. (2019). Obtaining and characterization of anthocyanins from Euterpe oleracea (açaí) dry extract for nutraceutical and food preparations. Revista Brasileira de Farmacognosia, 29(5), 677–685. https://doi.org/10.1016/j.bjp.2019.03.004

Singleton, V. L., & Rossi, J. A. J. (1965). Colorimetry of Total Phenolics with Phosmolybdicphosphotungstic Acid Reagents. American Journal of Enology and Viticulture, 16, 144–158.

Sirven, M. A., Venancio, V. P., Shankar, S., Klemashevich, C., Castellón-Chicas, M. J., Fang, C., Mertens-Talcott, S. U., & Talcott, S. T. (2021). Ulcerative colitis results in differential metabolism of cranberry polyphenols by the colon microbiome: *In vitro*. Food and Function, 12(24), 12751–12764. https://doi.org/10.1039/d1fo03047g

Song, J., Yu, Y., Chen, M., Ren, Z., Chen, L., Fu, C., Ma, Z. feei, & Li, Z. (2022). Advancement of Protein- and Polysaccharide-Based Biopolymers for Anthocyanin Encapsulation. Frontiers in Nutrition, 9, 938829. https://doi.org/10.3389/fnut.2022.938829

Tan, C., Xie, J., Zhang, X., Cai, J., & Xia, S. (2016). Polysaccharide-based nanoparticles by chitosan and gum arabic polyelectrolyte complexation as carriers for curcumin. Food Hydrocolloids, 57, 236–245.

Verediano, T. A., Stampini Duarte Martino, H., Dias Paes, M. C., & Tako, E. (2021). Effects of anthocyanin on intestinal health: A systematic review. Nutrients, 13(4), 1331. https://doi.org/10.3390/nu13041331

Wang, M., Li, L., Wan, M., Lin, Y., Tong, Y., & Cui, Y. (2021). Preparing, optimising, and evaluating chitosan nanocapsules to improve the stability of anthocyanins from *Aronia melanocarpa*. RSC Advances, 11(1), 210–218. https://doi.org/10.1039/d0ra08162k

Wang, S., Ye, X., Sun, Y., Liang, J., Yue, P., & Gao, X. (2021). Nanocomplexes derived from chitosan and whey protein isolate enhance the thermal stability and slow the release of anthocyanins in simulated digestion and prepared instant coffee. Food Chemistry, 336, 127707.

Ways, T. M. M., Lau, W. M., & Khutoryanskiy, V. V. (2018). Chitosan and Its Derivatives for Application in Mucoadhesive Drug Delivery Systems. Polymers, 10(267), 1–37.

Weinbrreck, F., Tromp, R. H., & de Kruif, C. G. (2004). Composition and structure of whey protein/gum arabic coacervates. Biomacromolecules, 5(4), 1437–1445. https://doi.org/10.1021/bm049970v

Xie, C., Huang, M., Ying, R., Wu, X., Hayat, K., Shaughnessy, L. K., & Tan, C. (2023). Olive pectin-chitosan nanocomplexes for improving stability and bioavailability of blueberry anthocyanins. Food Chemistry, 417, 135798.

Yamashita, C., Chung, M. M. S., dos Santos, C., Mayer, C. R. M., Moraes, I. C. F., & Branco, I. G. (2017). Microencapsulation of an anthocyanin-rich blackberry (*Rubus* spp.) by-product extract by freeze-drying. LWT, 84, 256–262. https://doi.org/10.1016/j.lwt.2017.05.063

Yan, D., Li, Y., Liu, Y., Li, N., Zhang, X., & Yan, C. (2021). Antimicrobial properties of chitosan and chitosan derivatives in the treatment of enteric infections. Molecules, 26(23), 7136. https://doi.org/10.3390/molecules26237136

Zhang, H., Park, Y., Wu, J., Chen, X. P., Lee, S., Yang, J., Dellsperger, K. C., & Zhang, C. (2009). Role of TNF-α in vascular dysfunction. Clinical Science, 116(3), 219–230. https://doi.org/10.1042/CS20080196

Zhao, S., Zhao, Y., Yang, X., & Zhao, T. (2023). Recent research advances on oral colon-specific delivery system of nature bioactive components: A review. Food Research International, 173, 113403. https://doi.org/10.1016/j.foodres.2023.113403

Zhao, X., Zhang, X., Tie, S., Hou, S., Wang, H., Song, Y., Rai, R., & Tan, M. (2020). Facile synthesis of nano-nanocarriers from chitosan and pectin with improved stability and biocompatibility for anthocyanins delivery: An *in vitro* and *in vivo* study. Food Hydrocolloids, 109, 106114.

Zhong, S., Sandhu, A., Edirisinghe, I., & Burton-Freeman, B. (2017). Characterization of Wild Blueberry Polyphenols Bioavailability and Kinetic Profile in Plasma over 24-h Period in

Human Subjects. Molecular Nutrition and Food Research, 61(12). https://doi.org/10.1002/mnfr.201700405

6. CHAPTER 5: *In vitro* metabolism of anthocyanins by human gut microbiota from lean, overweight and obese subjects

Abstract

This study investigated the differences in anthocyanin metabolism and short-chain fatty acid (SCFA) production by the gut microbiota of subjects with different body mass index (BMI) (lean, overweight, and obese) using an *in vitro* fermentation model. After the incubation of fecal samples with an anthocyanin-rich jabuticaba extract, it was observed that 37.45–54.01% of cyanidin-3-glucoside was metabolized in the lean group, 40.84–61.74% in the overweight group, and 36.06–69.16% in the obese group by the end of fermentation (48 h). Principal component analysis (PCA) of anthocyanin metabolism did not show a clear separation between the three groups. In addition, SCFA production varied widely across individuals, with acetic acid as the dominant compound. The anthocyanin extract increased SCFAs levels compared to control fermentations at specific time points and groups, indicating altered microbiota function due to anthocyanin metabolism. These findings showed the complex interaction between anthocyanins and the gut microbiota, emphasizing interindividual variations in gut microbiota composition as a critical factor of anthocyanin biotransformation and SCFAs production.

Keywords: Cyanidin-3-glucoside; Microbiota; BMI; Short-chain fatty acids; Fecal fermentation.

1. Introduction

The gut microbiota has an important role in modulating the bioavailability, bioactivity, and health benefits of phenolic compounds, like anthocyanins (Cardona et al., 2013). After ingestion, only a small part of the dietary anthocyanins is absorbed due to their instability in the digestive tract, chemical structure, and limited intestinal absorption (Liang et al., 2024). The ingested anthocyanins that are not absorbed or degraded in the gastrointestinal tract enter the colon, where they undergo biotransformation by the gut microbiota into low-molecular-weight phenolic metabolites (X. Wang et al., 2022). There are also studies showing that phenolic compounds have the ability to modulate the gut microbiota, promoting the growth of beneficial bacteria and/or reducing the abundance of harmful species (X. Wang et al., 2022).

In the colon, anthocyanins are hydrolyzed by enzymes produced by the microbiota (e.g. β-glucosidase), capable of cleaving sugar linkages, releasing anthocyanidin aglycones (Verediano et al., 2021). These aglycones are unstable and are quickly metabolized into

phloroglucinol aldehyde derived from the A ring of the anthocyanin structure, and a phenolic acid derived from the B ring (Liang et al., 2024). These compounds can be further metabolized by the gut microbiota and different metabolites are generated (Makarewicz et al., 2021). The metabolites produced by the microbiota often have greater bioavailability and distinct biological activities compared to their parent compounds (Ozdal et al., 2016).

A few studies have investigated the metabolism of anthocyanins using *in vitro* models of the human colon and distinct metabolites were produced from the metabolism of different anthocyanins. In the case of cyanidin derivatives, the identified metabolites were cyanidin, protocatechuic acid, phloroglucinol aldehyde, 4-hydroxybenzoic acid, and 4-hydroxyphenylacetic acid (Aura et al., 2005; B. Wang et al., 2024). On the other hand, for malvidin-glucoside, syringic acid was the main metabolite generated, and hydroxyphenylpropionic acid and vanillic acid also increased during the *in vitro* fermentation (Hazas et al., 2017). For pelargonidin-glucoside the main microbial metabolite generated was tyrosol, and other phenolic metabolites detected as microbial catabolism were hydroxyphenylpropionic acid, hydroxyphenylacetic acid, and p-hydroxybenzoic acid (Hazas et al., 2017).

The composition of the colonic microbiota differs among and within individuals and can be affected by various intrinsic and extrinsic factors, including genetic factors, age, race/ethnicity, sex, dietary habits, medication use, physical activity levels, chronic stress, alcohol intake, and smoking (Boronat et al., 2021). Interindividual differences in gut microbiota composition can impact the extent of biotransformation of phenolic compounds, which helps to explain the variability in health outcomes associated with phenolic-rich diets (Boronat et al., 2021). These differences are linked to distinct metabotypes, which are defined by an individual's capacity to produce specific metabolites (Corrêa et al., 2019).

The definition of a healthy microbiota is still challenging, due to the complexity of the microbiota, and the variation between and within individuals. However, high bacterial diversity is considered a marker of good gut health (Hou et al., 2022; Hul et al., 2024). Besides that, a higher prevalence of genera such as *Bifidobacterium* and *Lactobacillus* is often associated with beneficial gut functions (Hul et al., 2024). These beneficial bacteria can contribute in different ways to human health, improving intestinal homeostasis and barrier function, modulating the immune system, and regulating the production/secretion of microbiota-associated metabolites and reactive small molecules, such as short-chain fatty acids (SCFAs) (Ma et al., 2023).

The gut microbiota of individuals with different body mass indexes (BMIs) exhibits distinct characteristics, with underweight, overweight, and obese individuals often associated

with a less healthy microbiota (Rinninella et al., 2023). The diversity of gut microbiota composition has been reported to decrease with higher body mass index (Gao et al., 2018; Yun et al., 2017). In healthy individuals, Bacteroidetes and Firmicutes are the dominant phyla (Magne et al., 2020). In contrast, fecal samples from obese individuals are typically enriched with Proteobacteria and Firmicutes (Xu et al., 2024). The Firmicutes/Bacteroidetes (F/B) ratio (Bacillota/Bacteroidota ratio) has attracted attention as a potential indicator of health (Hul et al., 2024). In obesity, a higher Firmicutes/Bacteroidetes (F/B) ratio is observed compared to normal-weight individuals, along with reduced overall gut microbiota diversity (Cheng et al., 2022). This microbiota dysbiosis has been linked to increased energy harvest, chronic inflammation, compromised gut barrier function, and a heightened risk of metabolic disorders such as diabetes and cardiovascular disease (Hou et al., 2022; K. Zhang et al., 2024).

It was already demonstrated that anthocyanins can modulate the growth of colonic bacteria both *in vitro* and *in vivo*, increasing the abundance of beneficial bacteria such as *Bifidobacterium* spp. and *Lactobacillus* spp. (Boto-Ordóñez et al., 2014; Guergoletto et al., 2016; Hidalgo et al., 2012; Molan et al., 2014; Peng et al., 2021; Vendrame et al., 2011). Anthocyanins can also help to reduce the abundance of potentially harmful bacteria, including *Escherichia-Shigella*, *Clostridium*, and *Klebsiella*, which are often associated with dysbiosis and inflammation (Peng et al., 2021; Xu et al., 2024). An *in vitro* investigation examining the effect of blueberry anthocyanin extract (BAE) on the gut microbiota of obese individuals found that the proportion of *Proteobacteria* decreased from 59.84% to 42.70% following fermentation with BAE (Xu et al., 2024). The treatment with the BAE also reduced the Firmicutes-to-Bacteroidetes (F/B) ratio, suggesting that blueberry anthocyanins might possess anti-obesity properties by altering microbiota composition (Xu et al., 2024). In humans, the consumption of red wine or dealcoholized red wine over a period of 20 days resulted in enhanced levels of *Bifidobacterium*, *Enterococcus*, and *Eggerthella lenta*, with changes in *Bifidobacterium* being positively correlated with anthocyanin-derived metabolites (Boto-Ordóñez et al., 2014). Similarly, the ingestion of blackcurrant extract powder increased the population of lactobacilli and bifidobacteria, while reducing the populations of *Clostridium* spp. and *Bacteroides* spp. (Molan et al., 2014).

Despite positive results regarding gut microbiota modulation, the possible variations in anthocyanin metabolism across different body mass indexes (BMI) categories remains unexplored. Therefore, more studies are needed to determine how anthocyanin metabolism may vary due to individual differences in gut microbiota composition, as these variations may directly impact anthocyanin absorption and their potential health benefits. In this context, the

present study explored differences in anthocyanin metabolism and short-chain fatty acids (SCFAs) production by the gut microbiota of individuals with different BMI using an *in vitro* fermentation model.

2. Material and methods

2.1. Preparation of the jabuticaba extract

A jabuticaba extract was used as the source of anthocyanins for the study. For the extraction, 100 g of jabuticaba peel was mixed and macerated with 1000 mL of an ethanol solution 75 % (v/v) acidified with citric acid to pH 2.0. The sample was then ultrasonicated at 45 kHz at 40 °C for 50 min (Elmasonic TI-H10, Elma, Singen, BW, Germany), filtered (Whatman No.1 filter paper), and concentrated in a rotary evaporator (RV 10 digital V, IKA, Staufen, BW, Germany) at 40 °C (Rocha et al., 2018). Residual water was removed by lyophilization, and the powder was packed in metalized bags and kept in a freezer at −20 °C until analysis.

2.2.Total phenolic content (TPC)

Total phenolic compounds were quantified using a method adapted from Singleton & Rossi, (1965), and the results were expressed in mg of gallic acid equivalent (GAE) per g. In a 96-well microplate, 20 µL of diluted sample was mixed with 100 µL of Folin-Ciocalteau reagent (diluted 1:10 with water) and 75 µL of 7.5% Na_2CO_3 solution (m/v). After 1 h in the dark (23 ± 2 °C), the absorbance was measured at 760 nm (CLARIOstar Plus plate reader (BMG Labtech Inc., Durham, NC, USA).

2.3. Identification of compounds in the extract through LC-ESI-MS/MS analysis

Identification and quantification of compounds in the jabuticaba extract was performed using an Thermo Scientific Vanquish™ HPLC equipped with a Thermo Scientific TSQ Altis triple quadrupole mass spectrometer with an ESI source. The separations were carried out on a SunFire™ C18 column (150 × 3 mm, 5 µm), using acidified water (0.1% v/v formic acid) as mobile phase A and acidified methanol (0.1% v/v formic acid) as mobile phase

B. The flow rate was set to 0.4 mL/min, and gradient elution began with 5% B, increasing to 40% B after 5 minutes, and then to 95% B after 15 minutes. After 15.50 minutes, the column was re-equilibrated with 5% B until 17 minutes. MS data was acquired in both negative and positive polarity. The parameters consisted of a 3912.7 V spray voltage, a sheath gas of 24, auxiliary gas of 2, ion transfer tube temperature at 325 °C and vaporizer temperature at 400 °C. The identification of compounds was carried out by comparing retention times, fragmentation patterns, and relative ion abundances with known analytical standards or through database search. Quantification was performed using calibration curves obtained from analytical standards.

2.4. *In vitro* colonic metabolism

The protocol was approved by the Texas A&M University Institutional Review Board (IRB2023-1334D). Participants were recruited with their informed consent and according to the following inclusion and exclusion criteria. Subjects qualified if they were 18–65 years of age, within the specified BMI range, had no history of chronic diseases, and had not taken supplemental probiotics within the last 6 months. Subjects were excluded from the study if they had a history of acute cardiac events, stroke, or cancer; recurrent hospitalizations within the last 6 months; alcohol or substance abuse; smoked more than 1 pack per week; had a history of liver, intestinal, or renal dysfunction; had hepatitis B, C, or HIV; used systemic antibiotics within 1 month of screening; took herbal dietary supplements; used probiotics within the last 6 weeks; or were females who were pregnant or lactating. Stool samples were collected from 12 adults divided into 3 groups: lean group (BMI: 18-24.9 kg/m², 2 males and 2 females), overweight group (BMI: 25-30 kg/m², 2 males and 2 females), and obese group (BMI: 30-35 kg/m², 1 male and 3 females).

In vitro colonic metabolism was performed following the procedures of (Sirven et al., 2021). The samples were processed inside an anaerobic chamber (Coy Laboratory Products, Grass Lake, MI, USA) held at 37 °C and regulated with nitrogen, hydrogen (5%), and carbon dioxide (5%). Anaerobic conditions were confirmed using Resazurin strips (Sigma Aldrich, St Louis, MO, USA). To prepare the fecal slurry, 5 g of feces were mixed with 50 mL of phosphate-buffered saline (PBS). The fecal fermentation medium (FFM) used for colonic metabolism was produced by Anaerobe Systems (Morgan Hill, CA, USA) and contained: 2.0 g peptone water, 0.5 g bile salts, 2.0 g yeast extract, 0.5 g L-cysteine, 0.05 g haemin, 0.01 mL vitamin K, 0.001 g resazurin, 0.01 g $CaCl_2 \cdot 6H_2O$, 0.01 g $MgSO_4 \cdot 7H_2O$, 0.04 g KH_2PO_4, 0.04

g K_2HPO_4, 0.10 g NaCl, 2.0 g $NaHCO_3$, 2.0 mL tween 80 per 1 L. To simulate the metabolism of samples, 0.5 mL of jabuticaba extract were mixed with 4 mL of FFM and 0.5 mL of fecal slurry. A control with 4 mL of media, 0.5 mL of water and 0.5 mL of fecal slurry was prepared to eliminate the interference of phenolic compounds already present in the feces. Fermentation was carried out for 48 h, and fermentation vessels for each time point were collected at 0, 6, 12, 24, and 48 h. For chemical analysis of metabolites, 500 µL aliquots were mixed with 500 µL of acidified methanol (0.1% formic acid), followed by centrifugation at 10000 x g for 5 minutes (Megafuge 16, Thermo Scientific, Waltham, MA, USA). The resulting supernatants were stored at −80°C until further analysis (LC-ESI-MS/MS and CG-MS/MS). Identification and quantification of parent compounds and metabolites produced during fecal fermentations was performed as described before (Section 2.3).

2.5. Short-chain fatty acids

SCFAs were analyzed on a gas chromatography (TRACE 1310, Thermo Scientific, Waltham, MA, USA) coupled with a triple quadrupole mass spectrometer (TSQ 9000, Thermo Scientific, Waltham, MA, USA). Chromatographic separation was achieved on a D WAX column (60 m × 0.25 mm × 0.25 µm; Agilent, Santa Clara, CA, USA). 1 µL of the samples was injected with a split ratio of 17: 1. The ionization was carried out in the electron impact (EI) mode at 70 eV. The MS transfer line, and ion source were maintained at 200 °C and 250 °C, respectively. The flow rate of helium carrier gas was 1 mL/min. The target compounds were analyzed in the Selected Reaction Monitoring (SRM) mode using the following product ions (m/z) for each compound: acetic acid 60, propionic acid 74.1,73.1, 57.1, isobutyric acid 73.1, 88.1, 89.1, butyric acid 60, 73.1, 89.1, 2-methylbutyric/isovaleric 74.1, 60.1, 87.1, valeric acid 60, 87.1, 103.1. A short-chain fatty acid mixture containing acetic, propionic, isobutyric, n-butyric, 2-methylbutyric, isovaleric, and valeric acids was used as the standard (Cayman Chemicals, Ann Arbor, MI, USA).

2.6. Statistical analyses

The analyses were conducted in 3 replicates, and the results were presented as mean ± standard deviation. Data were analyzed using one-way ANOVA, followed by Tukey's test. All the analyses were performed using the R software (R Core Team, Vienna, Austria). A statistically significant value was considered when $p<0.05$. Additionally, Principal Component

Analysis (PCA) was conducted to identify potential clusters among subjects based on the metabolic profile of cyanidin-3-glucoside and production of short-chain fatty acids (SCFAs) over time. The PCA was performed using MetaboAnalyst 6.0 software.

3. Results and discussion

3.1. Identification and quantification of phenolic compounds in the extract

The total phenolic content (TPC) and individual phenolic compounds quantified in the extract, as well as their mass spectral data, are presented in Table 1. Cyanidin-3-glucoside was the predominant compound, with other bioactive compounds also identified in minor concentrations, including gallic acid, protocatechuic acid, ellagic acid, and 1-GG. Cyanidin-3-glucoside has been previously recognized as the primary anthocyanin in jabuticaba peel and can be considered the main bioactive compound in the jabuticaba extract (Albuquerque et al., 2020; Inada et al., 2015, 2020).

Table 1 – Quantification of TPC (Folin-Ciocalteu method) and individual polyphenols in the extract by LC-ESI-MS/MS analysis

	$[M-H]^-$	MS^2	Concentration (mg/g)
Total phenolic content	-	-	180.26 ± 1.92
Cyanidin-3-glucoside*	449.18	287.125, 213.125, 241.042	13.85 ± 0.68
Protocatechuic acid	153.05	81.054, 91.042, 109.042	3.12 ± 0.22
Gallic acid	168.90	124.97, 81.054, 79.071	0.12 ± 0.00
Ellagic acid	301.09	145.04, 229.04, 284.04	1.18 ± 0.21
1-GG (Galloyl glucose)	331.04	169.040, 210.960, 271.070	0.02 ± 0.00

*All compounds were analyzed with negative polarity, with the exception of cyanidin-3-glucoside which were analyzed with positive polarity ($[M + H]^+$).

3.2. Metabolization of anthocyanins by the microbiota

Anaerobic fecal fermentations were performed with jabuticaba extract to assess the metabolism of anthocyanins by the gut microbiota of lean, overweight, and obese individuals. Fast metabolization of cyanidin-3-glucoside were observed during the first hours of fermentation (Figure 1). After 6 h of fermentation, 16.60–38.85% of cyanidin-3-glucoside was

metabolized in the lean group, 35.82–46.68% in the overweight group, and 25.07–41.34% in the obese group. From 12–24 h, there were some fluctuations in the concentrations and the rate of metabolism slowed down over time. By the end of fermentation (48 h), 37.45–54.01% of cyanidin-3-glucoside was metabolized in the lean group, 40.84–61.74% in the overweight group, and 36.06–69.16% in the obese group. These results showed that there were variations in anthocyanin metabolism within each group, indicating that even among subjects with similar BMI, differences in gut microbiota composition may impact the metabolization of cyanidin-3-glucoside.

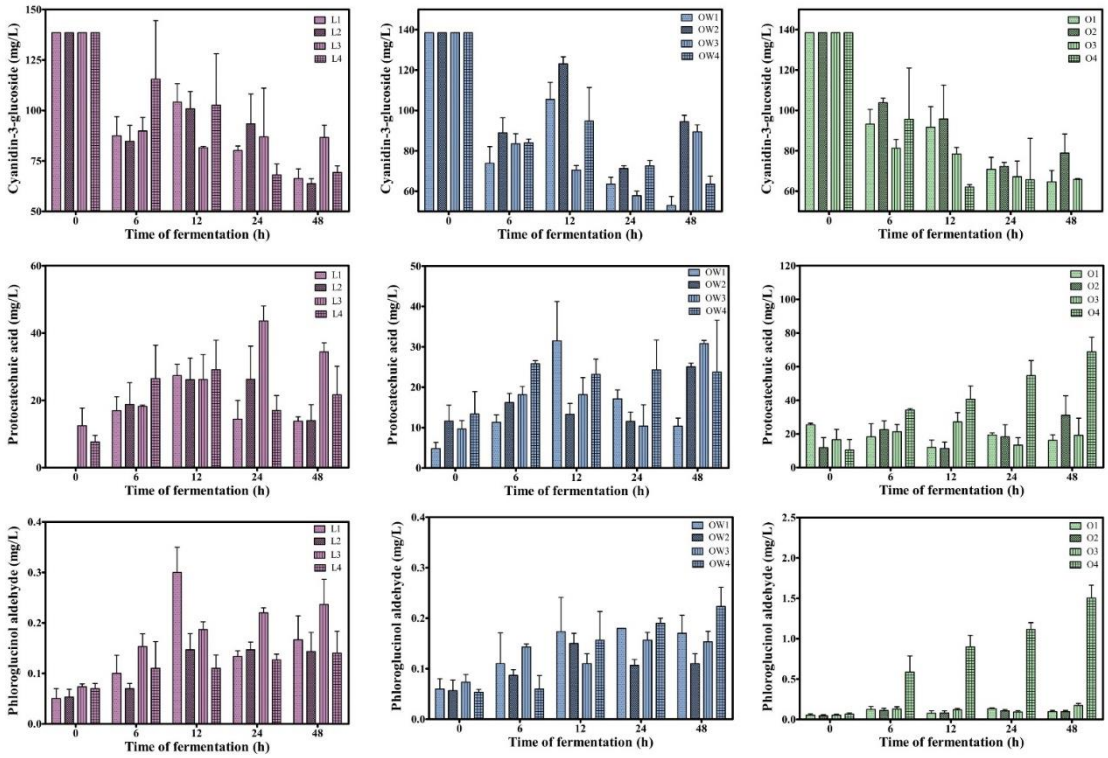

Figure 1 - Concentration of cyanidin-3-glucoside, protocatechuic acid, and phloroglucinol aldehyde during *in vitro* metabolism by the gut microbiota from lean (L), overweight (OW), and obese (O) individuals over 48 h. Each graph shows the mean concentrations (± standard deviation) for four individuals within each BMI group (L1–L4, OW1–OW4, and O1–O4).

The concentration of protocatechuic acid, a metabolite formed from the degradation of cyanidin-3-glucoside, increased over the fermentation period, with individuals reaching peak levels at different times (Figure 1). The observed decline in protocatechuic acid concentration at specific times suggests that bacteria may further metabolize protocatechuic acid, converting it into other compounds. It has been proposed that protocatechuic acid can be converted into

vanillic acid, catechol, and other derivatives (Makarewicz et al., 2021). However, these compounds were not detected in the current study. The variability in the observed results for protocatechuic acid concentrations may be attributed to differences in microbiota composition and activity specific to each individual.

Phloroglucinol aldehyde, another metabolite produced during the breakdown of cyanidin-3-glucoside, also showed an increase overtime of fermentation. However, at lower concentrations compared to protocatechuic acid (Figure 1). The rate and extent of phloroglucinol aldehyde production varied among individuals, with O4 showing a more pronounced increase. This variability might also reflect differences in microbiota composition between individuals. Unlike protocatechuic acid, which showed a decline in some individuals, the concentrations of phloroglucinol aldehyde continued to increase or remained stable over fermentation.

The PCA analysis revealed the distribution of lean, obese and overweight subjects as a function of the first two principal components (PC1 and PC2). The first two PCs explained 61.9% of the overall variance; 39.3% and 22.6% for PC1 and PC2, respectively. The resulting two-dimensional PCA score plot showed that that the three ellipses were overlapped, indicating that the metabolism of cyanidin-3-glucoside over time presents similar patterns among the groups of lean, obese and overweight subjects (Figure 2). This may indicate that other factors, besides BMI, more strongly influence the metabolic behavior of subjects for this compound.

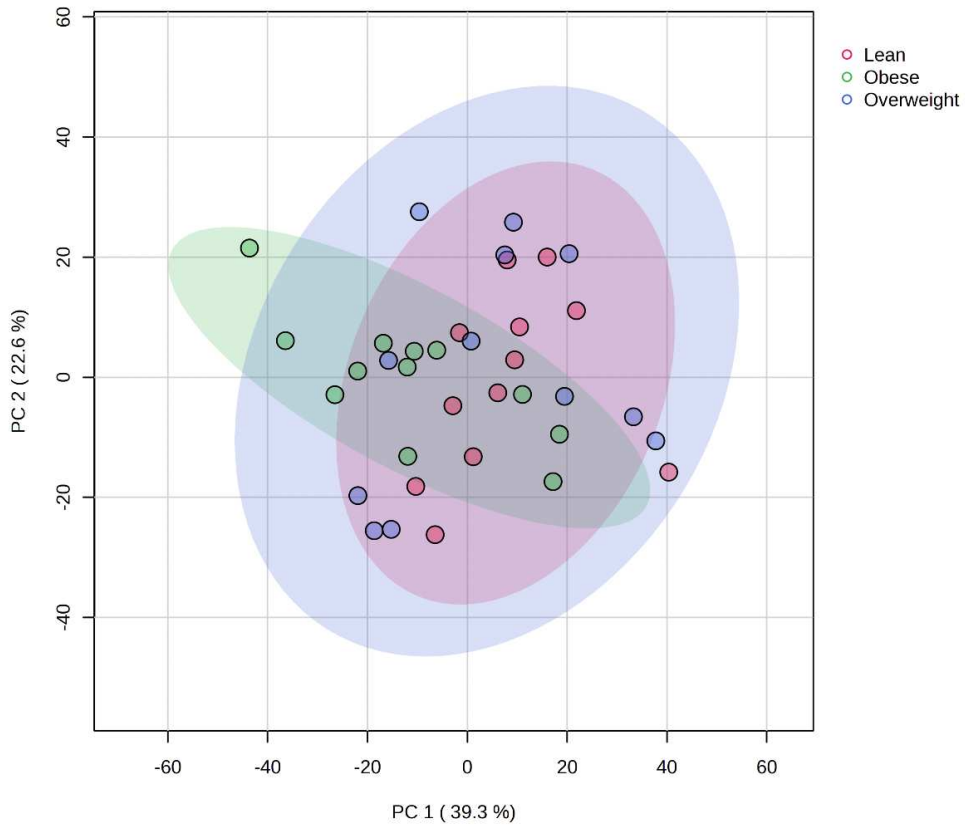

Figure 2 - 2D score plot of Principal Component Analysis (PCA) of cyanidin-3-glucoside metabolism over time, with samples from four lean (red), overweight (blue), and obese (green) subjects (n=3). Ellipses represent the confidence regions for each group.

Analyzing the grouped data over time, no significant differences were observed in the metabolism of cyanidin-3-glucoside between the groups (lean, overweight and obese), except for a significant difference at 24 h (Figure 3). At this time point the concentration of cyanidin-3-glucoside was lower in the overweight and obese groups, indicating faster metabolization of this anthocyanin in these groups. No significant differences were found for protocatechuic acid and phloroglucinol aldehyde analyzing the groups over time ($p<0.05$) (data not shown). These results suggest that differences in cyanidin-3-glucoside metabolism may not be directly related to BMI, but to interindividual variations in the gut microbiota. As previously discussed, the gut microbiota is influenced by different factors, including genetic background, age, race/ethnicity, sex, diet, medication, physical activity levels and chronic stress (Boronat et al., 2021). Some of these factors may have contributed to the observed metabolic outcomes and variability among subjects. These results emphasize the importance of considering not only BMI but also the diverse composition of the gut microbiota when evaluating anthocyanin metabolism.

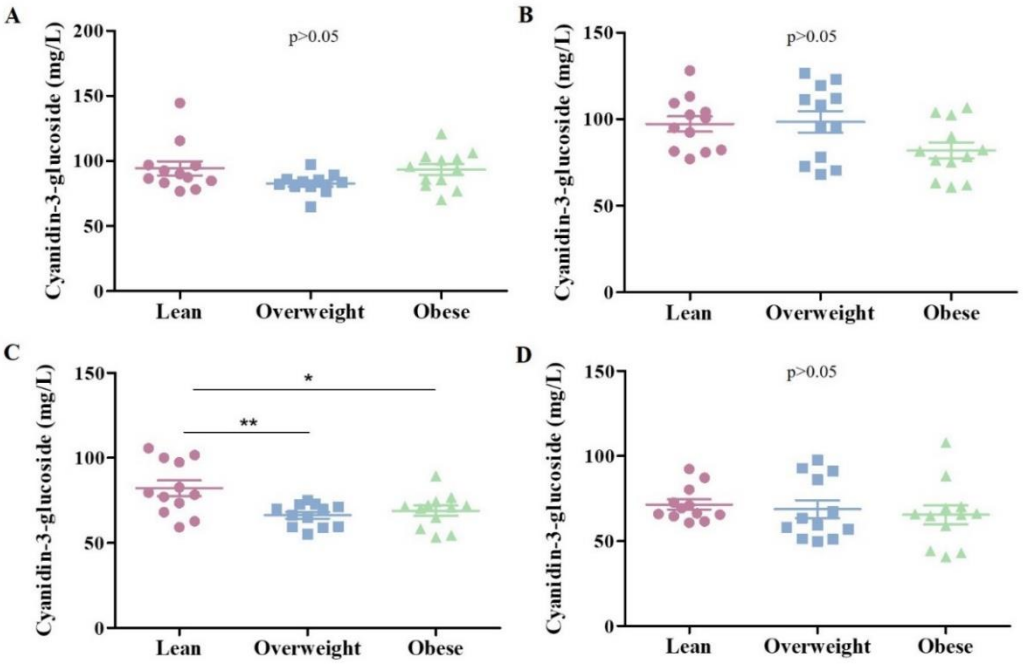

Figure 3 - Comparison of cyanidin-3-glucoside concentrations (mg/L) between lean, overweight and obese groups over time (A: 6h, B: 12h, C: 24h, D: 48h). Error bars represent mean ± standard deviation (n=12). Statistically significant differences between the groups were identified using Tukey's multiple comparisons test (∗p<0.05; ∗∗p<0.01).

Comparing the concentration of cyanidin-3-glucoside found for each subject at the end of fermentation, the results also showed considerable variability between individuals (Figure 4). Subjects within the same BMI category showed different levels of cyanidin-3-glucoside after 48 h of fermentation. The subjects O4, OW1, OW4, L2, O1, O3, L1 and L4 showed the highest reduction in cyanidin-3-glucoside concentration, which suggests they have a more active or efficient microbiota for metabolizing this anthocyanin. Besides, overweight and obese individuals, who are often linked to gut dysbiosis, also showed efficient capacity in metabolizing cyanidin-3-glucoside.

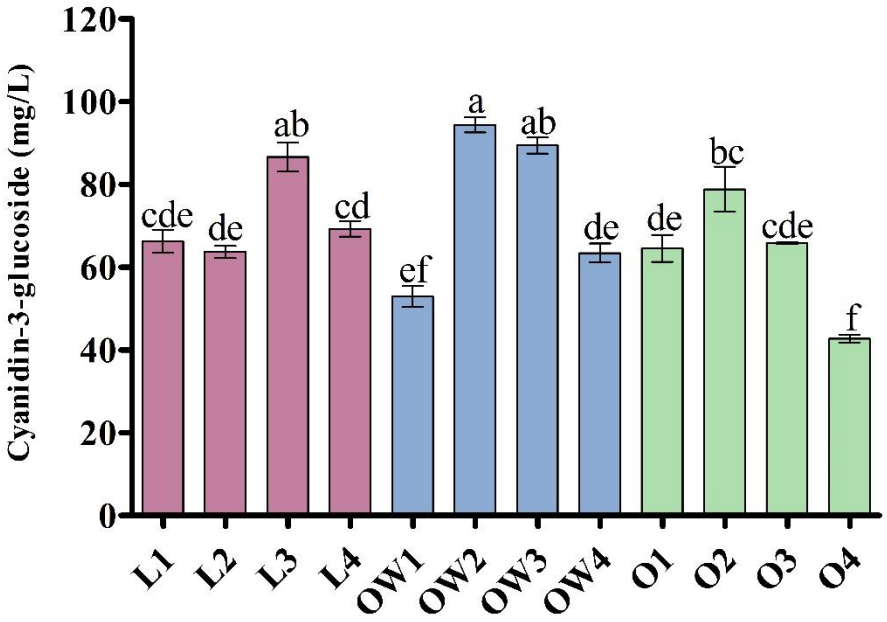

Figure 4 - Concentration of cyanidin-3-glucoside (mg/L) remaining at the end of the colonic metabolism (48 h) for each subject in the lean (L1–L4), overweight (OW1–OW4) and obese (O1–O4) groups. Error bars represent the mean ± standard deviation (n=3). Mean values with different lowercase letters are significantly different (Tukey's multiple comparisons test, $p<0.05$).

3.3. Production of short-chain fatty acids during *in vitro* colonic phase

Short-chain fatty acids (SCFAs) are metabolites produced by the gut microbiota from the fermentation of dietary fiber and proteins (Comino et al., 2018). The SCFAs have an essential role in promoting gut health by enhancing the integrity of the gut barrier and reducing inflammation. SCFAs can also contribute to immune system modulation and influence lipid and glucose homeostasis, promote satiety, and improve insulin sensitivity (Xiong et al., 2022). The time-trend production of acetic acid, propionic acid, butyric acid, valeric acid, and isobutyric acid during *in vitro* fermentation is presented in Figure 5. The compound 2-methylbutyric acid/isovaleric acid was not detected at quantifiable concentrations under any of the collection times assayed. Overall, the fermentation with the jabuticaba extract modified the production of SCFAs compared to the control (fermented sample without the extract), however, the results were time dependent and varied among the experimental groups.

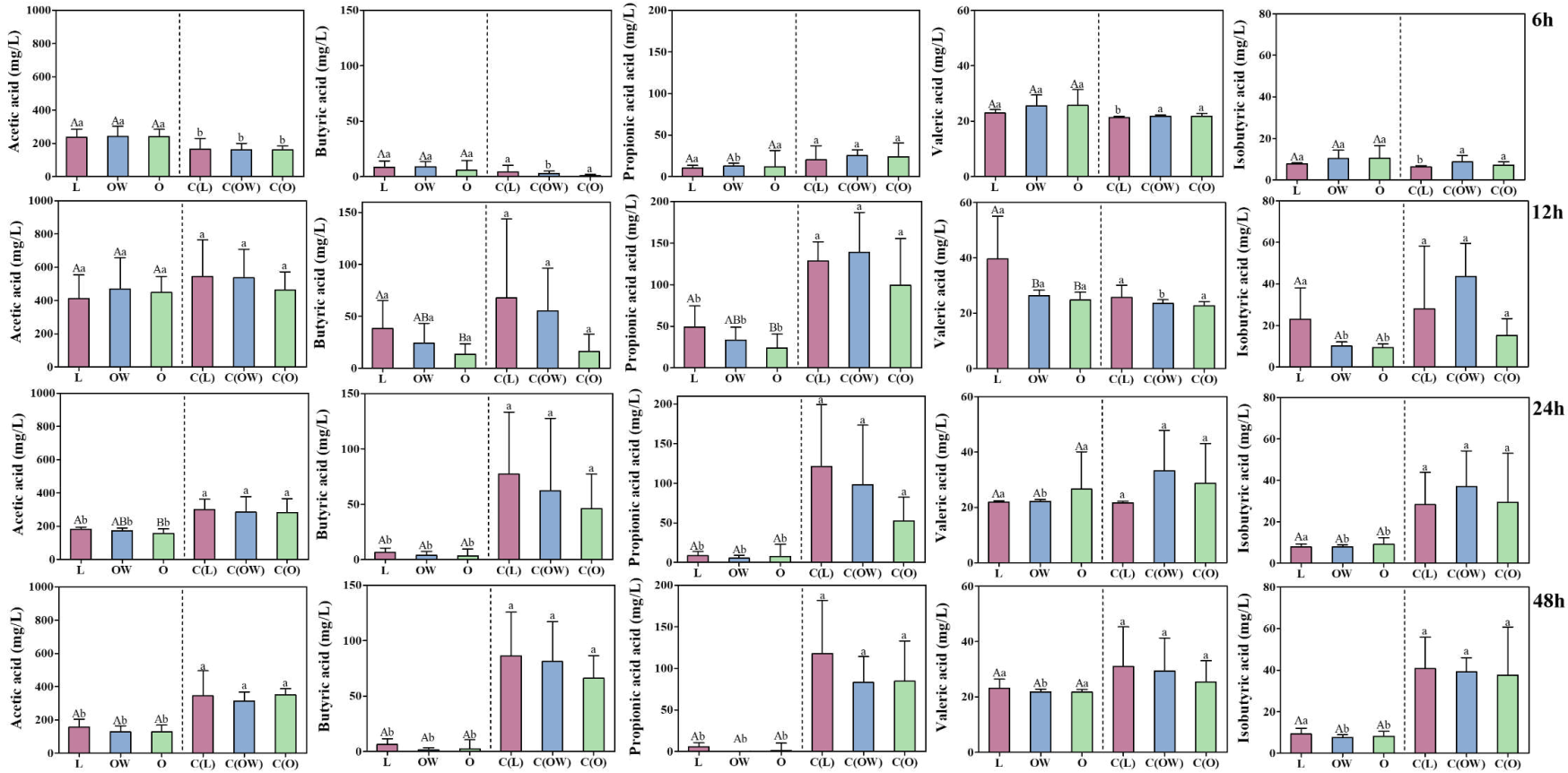

Figure 5 - Changes in short-chain fatty acid (SCFA) concentrations (acetic acid, butyric acid, propionic acid, valeric acid, and isobutyric acid) at different time points (6h, 12h, 24h, and 48h) across lean (L), overweight (OW), and obese (O) groups, along with their respective controls (C(L), C(OW), C(O)). Uppercase letters indicate significant differences between the lean, overweight, and obese groups (Tukey's test, $p < 0.05$), while lowercase letters denote significant differences between each experimental group and its respective control (t-test, $p < 0.05$). Bars represent the mean concentration (mg/L) ± standard deviation, illustrating SCFA production over time.

Acetic acid was the major SCFA produced, and the extract increased its formation at 6 h of fermentation, showing values higher than the control (no extract) (Figure 5). There were no significant differences between the L, OW, and O groups at this time point ($p>0.05$), suggesting a similar response to the extract among subjects with different BMIs. By 12 h, acetic acid concentrations continued to increase, but this rise was comparable between samples treated with the extract and their respective controls, indicating that the extract did not have a sustained effect on acetic acid production beyond the initial phase. After 24 h, acetic acid concentrations began to decline in both extract-treated samples and controls, however, the reduction was less pronounced in the control group. This suggests a time-dependent influence of the extract on acetic acid production, characterized by an early enhancement at 6 h followed by a gradual reduction.

The results for butyric acid production showed that at 6 h, fermentation with the extract led to a significant increase in butyric acid production only in the overweight (OW) group, while the lean (L) and obese (O) groups showed concentrations similar to their respective controls ($p>0.05$). As fermentation progressed, an increase in concentration was observed at 12 h followed by a decrease in the extract-treated samples across all groups. This decline suggests that butyric acid is being consumed or its production is being suppressed by the extract during fermentation, as concentrations in the control groups continued to rise throughout fermentation.

In contrast, the extract did not enhance propionic acid production in any of the groups across all time points. The concentrations observed in the extract-treated samples were either similar to or lower than those of the control, indicating that the extract had no stimulatory effect on propionic acid formation during fermentation.

The results for valeric acid also indicated that the extract stimulated the production of this SCFA, but the effect was limited to specific groups and time points. Increased concentrations were observed only in the lean group at 6 h and in the overweight group at 12 h. Overall, valeric acid concentrations were similar across the groups, with the only difference occurring at 12 h, where the lean group showed a higher concentration than the others. As fermentation progressed (24 h-48 h), valeric acid concentrations gradually declined in both the extract-treated and control samples.

The concentrations of isobutyric acid were only enhanced in the lean group at 6 h of fermentation, indicating a stimulatory effect of the extract specific to this group. Overweight and obese groups treated with the extract, showed levels similar to their respective controls ($p>0.05$). At 12 h, the concentration of isobutyric acid increased only in the lean group, while overweight and obese groups showed concentrations lower than the control. After 24 h,

isobutyric acid levels decreased across all groups, with extract-treated samples showing concentrations similar to or even lower than their controls.

There was substantial variability across all SCFAs data, suggesting individual differences in SCFAs production. In fact, SCFA concentrations varied significantly among all subjects, with individuals from different groups showing higher and lower levels. For acetic acid, the highest concentrations were observed in subjects O2 (116.18 ± 23.19), OW2 (108.54 ± 4.45), OW1 (99.05 ± 23.12), L3 (97.24 ± 7.66), O4 (86.47 ± 8.04), and L1 (81.80 ± 14.41) at 6 h. For propionic acid, only subjects L1 (1.54 ± 0.82) and L3 (7.76 ± 2.42) stimulated its production at 6 h of fermentation. The highest concentrations of butyric acid were observed after 12 h of fermentation in subjects L1 (22.72 ± 10.90), L3 (25.78 ± 5.84), and O4 (14.39 ± 7.36). For valeric acid, the highest levels were observed at 6 h in subject O2 (11.67 ± 2.26) and at 12 h in subjects L3 (38.82 ± 7.45) and L1 (18.80 ± 3.21). For isobutyric acid, subject L3 (29.54 ± 5.15) showed the highest concentration at 12 h.

The variability in the results indicates distinct microbiota responses to the anthocyanin extract, which might be associated with differences in microbiota composition and activity across subjects. The production of SCFAs by the gut microbiota is linked to the activity of different bacterial groups. Acetate, which is the most prevalent SCFA, is commonly produced by genera such as *Bacteroides*, *Bifidobacterium*, *Clostridium*, and *Prevotella*, and can be formed from pyruvate either via acetyl-CoA or via the Wood-Ljungdahl pathway (Koh et al., 2016). Propionate is primarily produced through the succinate pathway by bacteria such as *Bacteroides*, *Veillonella*, and *Dialister* (Koh et al., 2016; Louis & Flint, 2017). Butyrate, is predominantly produced by species like *Faecalibacterium prausnitzii*, *Roseburia, Eubacterium rectale*, and *Eubacterium hallii* (Koh et al., 2016; Louis & Flint, 2017). While, bacteria like *Clostridium* and *Bacteroides* generate isobutyrate and isovalerate from the fermentation of branched-chain amino acids (Rios-Covian et al., 2020).

During the course of fermentation, there was a reduction in concentrations of SCFAs in samples treated with the anthocyanin extract compared to the control, indicating two possible effects: an increase in the consumption of SCFAs, or a reduction in SCFA production. It has already been shown that anthocyanins can modulate the growth of colonic bacteria, promoting the growth of some groups and/or inhibiting the growth of others (Boto-Ordóñez et al., 2014; Guergoletto et al., 2016; Hidalgo et al., 2012; Molan et al., 2014; Peng et al., 2021; Vendrame et al., 2011). These possible changes in composition could have impacted the results observed in this study. Changes in microbiota composition caused by the anthocyanin extract may have influenced the production and consumption of SCFAs, contributing to the variability in the data.

In general, results from previous studies have shown that anthocyanins increase the formation of SCFAs over the time during *in vitro* fermentation, which has been associated with the ability of anthocyanins to increase the abundance of SCFAs producing bacteria (Guergoletto et al., 2016; Verediano et al., 2021; Xu et al., 2024; X. Zhang et al., 2016). For fermentation with blueberry anthocyanin extracts (BAE) and gut microbiota from obese subjects, the concentration of total SCFAs in the BAE group increased from 2.98 ± 0.14 mM to 78.06 ± 1.26 mM after 24h, which was significantly higher than the concentration in the control group. Acetate, propionate, and butyrate were the dominating metabolites (Xu et al., 2024). In another study of the effects of anthocyanins from the fruit of *Lycium ruthenicum* Murray during *in vitro* fermentation with feces from healthy volunteers, the contents of acetic, propionic and n-butyric acids were increased with the increase of fermentation time and i-butyric, n-valeric and i-valeric acids were all found in small amounts (Yan et al., 2018). The authors also observed that SCFAs accumulated with fast rate during 0–6 h fermentation and then increased slowly (Yan et al., 2018).

In contrast, other studies also observed lower concentrations of SCFAs at the end of fermentation. In another study with *Lycium ruthenicum* Murray the production of acetic, propionic, butyric and valeric acids was promoted by anthocyanins in healthy fecal fermentation and only acetic acid was promoted in IBD fecal fermentation (Peng et al., 2021). The concentration of isobutyric and isovaleric were not increased for both conditions (Peng et al., 2021). For the fermentation of cranberry, the concentration of isobutryic acid and isovaleric acid was also significantly lower ($p<0.05$) after 48 h in comparison to the non-polyphenol control (Sirven et al., 2021).

The results of PCA analysis did not reveal significant differences between the three groups, indicating that SCFA profiles may not be distinctly different based on BMI classifications alone (Figure 6). The principal components (PC1 and PC2) explained 78.6% of the variance in SCFA production. There was a substantial overlap between the lean, overweight and obese groups, which implies shared SCFA production characteristics. No statistically significant differences in SCFA production were observed between the groups ($p>0.05$). The lack of significant differences between the groups in this study suggests that factors beyond BMI, such as dietary intake, lifestyle, and differences in microbiota composition, may play a larger role in determining SCFA production.

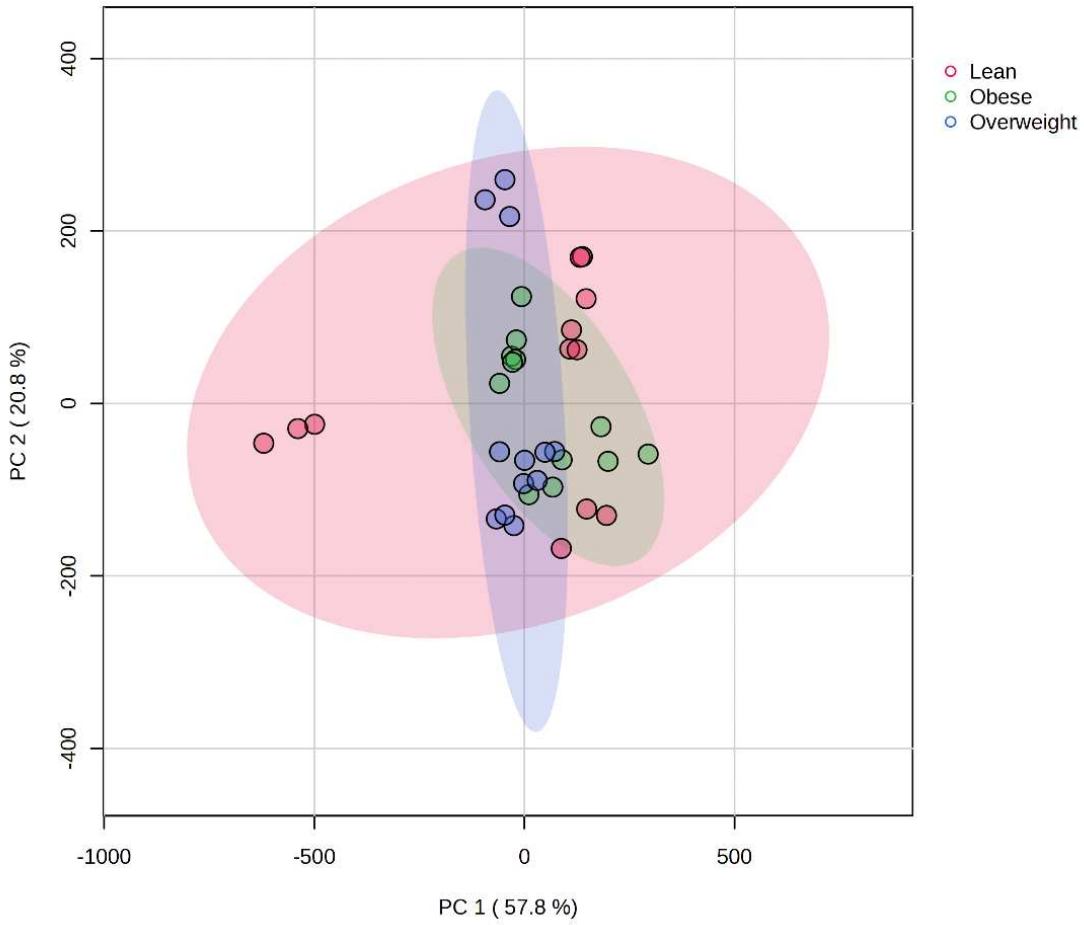

Figure 6 - 2D score plot of Principal Component Analysis (PCA) of SCFA production over time, with samples from four lean (red), overweight (blue), and obese (green) subjects (n=3). Ellipses represent the confidence regions for each group.

Although significant differences were not observed between normoweight, overweight and obese individuals in this study, previous studies have found a positive correlation between SCFAs levels and BMI. Total SCFAs were significantly higher in obese (214.01 ± 27.53 mM) compared to normoweight (119.70 ± 24.95 mM) individuals *in vitro* (Martínez-Cuesta et al., 2021). Significant differences were found between the two groups (normoweight and obese) for acetate and butyrate, with the highest concentrations found for obese individuals (Martínez-Cuesta et al., 2021). In a community-based study involving 441 Colombian adults between the ages of 18 and 62, higher fecal butyrate, acetate, propionate and total SCFAs were associated with BMI, body fat, and waist circumference (Cuesta-Zuluaga et al., 2019). An inverse correlation between fecal butyrate and gut microbiota diversity was also observed (Cuesta-Zuluaga et al., 2019). Similarly, in a population-based cohort of Chinese adults, positive associations were also found between butyrate/isobutyrate and BMI (Y. Wang et al., 2020).

Fecal SCFA concentrations were also significantly higher in overweight compared to lean individuals (81.3 ± 7.4 vs. 64.1 ± 10.4 mmol/kg), with these differences being linked with differences in colonic microbiota (Rahat-Rozenbloom et al., 2014).

4. Conclusion

In this study, differences in anthocyanin metabolism and SCFA production among subjects with different BMI (lean, overweight, and obese) were observed. Results showed that 36.06–69.16% of cyanidin-3-glucoside was metabolized after 48 h of fermentation. The anthocyanin extract influenced SCFA levels, improving the production of acetic, butyric, valeric, and isovaleric acids at specific time points and groups. Principal component analysis (PCA) did not show a clear separation between the three groups, indicating that the individual's microbiota composition may have a higher influence on anthocyanin metabolism and SCFAs production than BMI alone. Even though these results provided useful insights, this study is limited by the low number of subjects. More studies regarding anthocyanin–microbiota interactions will be essential to optimize anthocyanin metabolism for health benefits. Future studies should include microbiota analyses to characterize the gut microbiota of the subjects and identify bacterial groups associated with these metabolic activities.

5. References

Albuquerque, B. R., Pereira, C., Calhelha, R. C., José Alves, M., Abreu, R. M. V., Barros, L., Oliveira, M. B. P. P., & Ferreira, I. C. F. R. (2020). Jabuticaba residues (*Myrciaria jaboticaba* (Vell.) Berg) are rich sources of valuable compounds with bioactive properties. Food Chemistry, 309. https://doi.org/10.1016/j.foodchem.2019.125735

Aura, A. M., Martin-Lopez, P., O'Leary, K. A., Williamson, G., Oksman-Caldentey, K. M., Poutanen, K., & Santos-Buelga, C. (2005). *In vitro* metabolism of anthocyanins by human gut microbiota. European Journal of Nutrition, 44(3), 133–142. https://doi.org/10.1007/s00394-004-0502-2

Boronat, A., Rodriguez-Morató, J., Serreli, G., Fitó, M., Tyndale, R. F., Deiana, M., & De La Torre, R. (2021). Contribution of Biotransformations Carried out by the Microbiota, Drug-Metabolizing Enzymes, and Transport Proteins to the Biological Activities of Phytochemicals Found in the Diet. Advances in Nutrition, 12(6), 2172–2189. https://doi.org/10.1093/advances/nmab085

Boto-Ordóñez, M., Urpi-Sarda, M., Queipo-Ortuño, M. I., Tulipani, S., Tinahones, F. J., & Andres-Lacueva, C. (2014). High levels of *Bifidobacteria* are associated with increased levels

of anthocyanin microbial metabolites: A randomized clinical trial. Food and Function, 5(8), 1932–1938. https://doi.org/10.1039/c4fo00029c
Cardona, F., Andrés-Lacueva, C., Tulipani, S., Tinahones, F. J., & Queipo-Ortuño, M. I. (2013). Benefits of polyphenols on gut microbiota and implications in human health. Journal of Nutritional Biochemistry, 24(8), 1415–1422. https://doi.org/10.1016/j.jnutbio.2013.05.001

Cheng, Z., Zhang, L., Yang, L., & Chu, H. (2022). The critical role of gut microbiota in obesity. Frontiers in Endocrinology, 13, 1–14. https://doi.org/10.3389/fendo.2022.1025706

Comino, P., Williams, B. A., & Gidley, M. J. (2018). *In vitro* fermentation gas kinetics and end-products of soluble and insoluble cereal flour dietary fibres are similar. Food and Function, 9(2), 898–905. https://doi.org/10.1039/c7fo01724c

Corrêa, T. A. F., Rogero, M. M., Hassimotto, N. M. A., & Lajolo, F. M. (2019). The Two-Way Polyphenols-Microbiota Interactions and Their Effects on Obesity and Related Metabolic Diseases. Frontiers in Nutrition, 6, 188. https://doi.org/10.3389/fnut.2019.00188

Cuesta-Zuluaga, J. de la, Mueller, N. T., Álvarez-Quintero, R., Velásquez-Mejía, E. P., Sierra, J. A., Corrales-Agudelo, V., Carmona, J. A., Abad, J. M., & Escobar, J. S. (2019). Higher fecal short-chain fatty acid levels are associated with gut microbiome dysbiosis, obesity, hypertension and cardiometabolic disease risk factors. Nutrients, 11(1), 1–16. https://doi.org/10.3390/nu11010051

Gao, X., Zhang, M., Xue, J., Huang, J., Zhuang, R., Zhou, X., Zhang, H., Fu, Q., & Hao, Y. (2018). Body mass index differences in the gut microbiota are gender specific. Frontiers in Microbiology, 9, 1250. https://doi.org/10.3389/fmicb.2018.01250

Guergoletto, K. B., Costabile, A., Flores, G., Garcia, S., & Gibson, G. R. (2016). *In vitro* fermentation of juçara pulp (*Euterpe edulis*) by human colonic microbiota. Food Chemistry, 196, 251–258. https://doi.org/10.1016/j.foodchem.2015.09.048

Hazas, M. C. L. D. Las, Mosele, J. I., Macià, A., Ludwig, I. A., & Motilva, M. J. (2017). Exploring the Colonic Metabolism of Grape and Strawberry Anthocyanins and Their *in vitro* Apoptotic Effects in HT-29 Colon Cancer Cells. Journal of Agricultural and Food Chemistry, 65(31), 6477–6487. https://doi.org/10.1021/acs.jafc.6b04096

Hidalgo, M., Oruna-Concha, M. J., Kolida, S., Walton, G. E., Kallithraka, S., Spencer, J. P. E., Gibson, G. R., & De Pascual-Teresa, S. (2012). Metabolism of anthocyanins by human gut microbiota and their influence on gut bacterial growth. Journal of Agricultural and Food Chemistry, 60(15), 3882–3890. https://doi.org/10.1021/jf3002153

Hou, K., Wu, Z. X., Chen, X. Y., Wang, J. Q., Zhang, D., Xiao, C., Zhu, D., Koya, J. B., Wei, L., Li, J., & Chen, Z. S. (2022). Microbiota in health and diseases. Signal Transduction and Targeted Therapy, 7(1), 1. https://doi.org/10.1038/s41392-022-00974-4

Hul, M. Van, Cani, P. D., Petifils, C., De Vos, W. M., Tilg, H., & El Omar, E. M. (2024). What defines a healthy gut microbiome? Gut, 2024, 16. https://doi.org/10.1136/gutjnl-2024-333378

Inada, K. O. P., Oliveira, A. A., Revorêdo, T. B., Martins, A. B. N., Lacerda, E. C. Q., Freire, A. S., Braz, B. F., Santelli, R. E., Torres, A. G., Perrone, D., & Monteiro, M. C. (2015).

Screening of the chemical composition and occurring antioxidants in jabuticaba (*Myrciaria jaboticaba*) and jussara (*Euterpe edulis*) fruits and their fractions. Journal of Functional Foods, 17, 422–433. https://doi.org/10.1016/j.jff.2015.06.002

Inada, K. O. P., Silva, T. B. R., Lobo, L. A., Pilotto, R. M. C., Perrone, D., & Monteiro, M. (2020). Bioaccessibility of phenolic compounds of jaboticaba (*Plinia jaboticaba*) peel and seed after simulated gastrointestinal digestion and gut microbiota fermentation. Journal of Functional Foods, 67, 1–10. https://doi.org/10.1016/j.jff.2020.103851

Koh, A., De Vadder, F., Kovatcheva-Datchary, P., & Bäckhed, F. (2016). From dietary fiber to host physiology: Short-chain fatty acids as key bacterial metabolites. Cell, 165(6), 1332–1345. https://doi.org/10.1016/j.cell.2016.05.041

Liang, A., Leonard, W., Beasley, J. T., Fang, Z., Zhang, P., & Ranadheera, C. S. (2024). Anthocyanins-gut microbiota-health axis: A review. Critical Reviews in Food Science and Nutrition, 64(21), 7563–7588. https://doi.org/10.1080/10408398.2023.2187212

Louis, P., & Flint, H. J. (2017). Formation of propionate and butyrate by the human colonic microbiota. Environmental Microbiology, 19(1), 29–41. https://doi.org/10.1111/1462-2920.13589

Ma, T., Shen, X., Shi, X., Sakandar, H. A., Quan, K., Li, Y., Jin, H., Kwok, L. Y., Zhang, H., & Sun, Z. (2023). Targeting gut microbiota and metabolism as the major probiotic mechanism - An evidence-based review. Trends in Food Science and Technology, 138, 178–198. https://doi.org/10.1016/j.tifs.2023.06.013

Magne, F., Gotteland, M., Gauthier, L., Zazueta, A., Pesoa, S., Navarrete, P., & Balamurugan, R. (2020). The firmicutes/bacteroidetes ratio: A relevant marker of gut dysbiosis in obese patients? Nutrients, 12(5), 1474. https://doi.org/10.3390/nu12051474

Makarewicz, M., Drożdż, I., Tarko, T., & Duda-Chodak, A. (2021). The interactions between polyphenols and microorganisms, especially gut microbiota. Antioxidants, 10(2), 1–70. https://doi.org/10.3390/antiox10020188

Martínez-Cuesta, M. C., del Campo, R., Garriga-García, M., Peláez, C., & Requena, T. (2021). Taxonomic Characterization and Short-Chain Fatty Acids Production of the Obese Microbiota. Frontiers in Cellular and Infection Microbiology, 11, 598093. https://doi.org/10.3389/fcimb.2021.598093

Molan, A. L., Liu, Z., & Plimmer, G. (2014). Evaluation of the effect of blackcurrant products on gut microbiota and on markers of risk for colon cancer in humans. Phytotherapy Research, 28(3), 416–422. https://doi.org/10.1002/ptr.5009

Ozdal, T., Sela, D. A., Xiao, J., Boyacioglu, D., Chen, F., & Capanoglu, E. (2016). The reciprocal interactions between polyphenols and gut microbiota and effects on bioaccessibility. Nutrients, 8(2), 1–36. https://doi.org/10.3390/nu8020078

Peng, Y., Yan, Y., Wan, P., Chen, C., Chen, D., Zeng, X., & Cao, Y. (2021). Prebiotic effects *in vitro* of anthocyanins from the fruits of *Lycium ruthenicum* Murray on gut microbiota

compositions of feces from healthy human and patients with inflammatory bowel disease. LWT, 149, 111829. https://doi.org/10.1016/j.lwt.2021.111829

Rahat-Rozenbloom, S., Fernandes, J., Gloor, G. B., & Wolever, T. M. S. (2014). Evidence for greater production of colonic short-chain fatty acids in overweight than lean humans. International Journal of Obesity, 38(12), 1525–1531. https://doi.org/10.1038/ijo.2014.46

Rinninella, E., Tohumcu, E., Raoul, P., Fiorani, M., Cintoni, M., Mele, M. C., Cammarota, G., Gasbarrini, A., & Ianiro, G. (2023). The role of diet in shaping human gut microbiota. Best Practice and Research: Clinical Gastroenterology, 62–63, 101828. https://doi.org/10.1016/j.bpg.2023.101828

Rios-Covian, D., González, S., Nogacka, A. M., Arboleya, S., Salazar, N., Gueimonde, M., & de los Reyes-Gavilán, C. G. (2020). An Overview on Fecal Branched Short-Chain Fatty Acids Along Human Life and as Related With Body Mass Index: Associated Dietary and Anthropometric Factors. Frontiers in Microbiology, 11. https://doi.org/10.3389/fmicb.2020.00973

Rocha, J. de C. G., Procópio, F. R., Mendonça, A. C., Vieira, L. M., Perrone, Í. T., de Barros, F. A. R., & Stringheta, P. C. (2018). Optimization of ultrasound-assisted extraction of phenolic compounds from jussara (*Euterpe edulis* M.) and blueberry (*Vaccinium myrtillus*) fruits. Food Science and Technology, 38(1), 45–53. https://doi.org/10.1590/1678-457x.36316

Singleton, V. L., & Rossi, J. A. J. (1965). Colorimetry of Total Phenolics with Phosmolybdicphosphotungstic Acid Reagents. American Journal of Enology and Viticulture, 16, 144–158.

Sirven, M. A., Venancio, V. P., Shankar, S., Klemashevich, C., Castellón-Chicas, M. J., Fang, C., Mertens-Talcott, S. U., & Talcott, S. T. (2021). Ulcerative colitis results in differential metabolism of cranberry polyphenols by the colon microbiome: *In vitro*. Food and Function, 12(24), 12751–12764. https://doi.org/10.1039/d1fo03047g

Vendrame, S., Guglielmetti, S., Riso, P., Arioli, S., Klimis-Zacas, D., & Porrini, M. (2011). Six-week consumption of a wild blueberry powder drink increases Bifidobacteria in the human gut. Journal of Agricultural and Food Chemistry, 59(24), 12815–12820. https://doi.org/10.1021/jf2028686

Verediano, T. A., Stampini Duarte Martino, H., Dias Paes, M. C., & Tako, E. (2021). Effects of anthocyanin on intestinal health: A systematic review. Nutrients, 13(4), 1331. https://doi.org/10.3390/nu13041331

Wang, B., Tang, X., Mao, B., Zhang, Q., Tian, F., Zhao, J., Chen, W., & Cui, S. (2024). Effects of *in vitro* fecal fermentation on the metabolism and antioxidant properties of cyanidin-3-O-glucoside. Food Chemistry, 431, 137132. https://doi.org/10.1016/j.foodchem.2023.137132

Wang, X., Qi, Y., & Zheng, H. (2022). Dietary Polyphenol, Gut Microbiota, and Health Benefits. Antioxidants, 11(6), 1212. https://doi.org/10.3390/antiox11061212

Wang, Y., Wang, H., Howard, A. G., Meyer, K. A., Tsilimigras, M. C. B., Avery, C. L., Sha, W., Sun, S., Zhang, J., Su, C., Wang, Z., Zhang, B., Fodor, A. A., & Gordon-Larsen, P. (2020).

Circulating short-chain fatty acids are positively associated with adiposity measures in chinese adults. Nutrients, 12(7), 1–15. https://doi.org/10.3390/nu12072127
Xiong, R. G., Zhou, D. D., Wu, S. X., Huang, S. Y., Saimaiti, A., Yang, Z. J., Shang, A., Zhao, C. N., Gan, R. Y., & Li, H. Bin. (2022). Health Benefits and Side Effects of Short-Chain Fatty Acids. Foods, 11(18), 1–24. https://doi.org/10.3390/foods11182863

Xu, L., Tang, Z., Herrera-Balandrano, D. D., Qiu, Z., Li, B., Yang, Y., & Huang, W. (2024). *In vitro* fermentation characteristics of blueberry anthocyanins and their impacts on gut microbiota from obese human. Food Research International, 176, 113761. https://doi.org/10.1016/j.foodres.2023.113761

Yan, Y., Peng, Y., Tang, J., Mi, J., Lu, L., Li, X., Ran, L., Zeng, X., & Cao, Y. (2018). Effects of anthocyanins from the fruit of *Lycium ruthenicum* Murray on intestinal microbiota. Journal of Functional Foods, 48, 533–541. https://doi.org/10.1016/j.jff.2018.07.053

Yun, Y., Kim, H. N., Kim, S. E., Heo, S. G., Chang, Y., Ryu, S., Shin, H., & Kim, H. L. (2017). Comparative analysis of gut microbiota associated with body mass index in a large Korean cohort. BMC Microbiology, 17(1), 1. https://doi.org/10.1186/s12866-017-1052-0

Zhang, K., Zhang, Q., Qiu, H., Ma, Y., Hou, N., Zhang, J., Kan, C., Han, F., Sun, X., & Shi, J. (2024). The complex link between the gut microbiome and obesity-associated metabolic disorders: Mechanisms and therapeutic opportunities. Heliyon, 10(17), e37609. https://doi.org/10.1016/j.heliyon.2024.e37609

Zhang, X., Yang, Y., Wu, Z., & Weng, P. (2016). The Modulatory Effect of Anthocyanins from Purple Sweet Potato on Human Intestinal Microbiota *in vitro*. Journal of Agricultural and Food Chemistry, 64(12), 2582–2590. https://doi.org/10.1021/acs.jafc.6b00586

7. GENERAL CONCLUSION

This thesis provided a comprehensive evaluation of the metabolism, bioaccessibility and functional properties of anthocyanins, with particular focus on the use of fermentation and encapsulation techniques and the interaction with the intestinal microbiota. The fermentation of jabuticaba fruit significantly improved its phytochemical profile, increasing the levels of anthocyanins, phenolic compounds and the bioaccessibility of cyanidin-3-glucoside, gallic acid and protocatechuic acid. In addition, the produced beverage showed antiproliferative effects against cancer cells, antioxidant activities and inhibitory properties against enzymes linked to diabetes and obesity, highlighting jabuticaba wine as a promising functional beverage.

Encapsulation methods using the food-grade carriers whey protein, pea protein, chitosan and gum arabic were effective in protecting anthocyanins during digestion, retaining them in the gastric phase, increasing intestinal bioaccessibility, improving their targeted delivery to the colon phase and promoting the production of short-chain fatty acids. These findings highlight the formulations and encapsulation methods studied as innovative and efficient delivery systems to enhance the health benefits of anthocyanins and as alternatives to be used in the formulation of functional foods and dietary supplements. The increasing incidence of chronic diseases such as diabetes, obesity and cardiovascular diseases is a global challenge that demands effective solutions for health promotion and prevention of these conditions. In this context, encapsulation emerges as a promising strategy for the development of functional products and dietary supplements with high therapeutic potential, offering products with greater stability, controlled release, and improved bioaccessibility of bioactive compounds.

In the study of the metabolism of anthocyanins and the production of SCFAs by the gut microbiota of individuals with different BMI (lean, overweight and obese), no direct correlation between BMI and anthocyanins metabolism or SCFAs production were found. Although higher BMI is often associated with altered microbiota composition, these results suggested that the individual composition of the gut microbiota has a higher impact on these processes. These results could be explained by the complexity of colonic microbiota, which can be affected by various factors and differs among and within individuals. The variability in the results between individuals in the same BMI group, showed the importance for personalized approaches and additional investigation into microbiota-anthocyanin interactions.

In view of the five chapters presented, it is evident the importance of exploring the factors that influence the bioaccessibility and bioavailability of anthocyanins and the crucial

role of strategies such as encapsulation to increase the stability and potential health benefits of anthocyanins. Research focused on the interactions between anthocyanins and the gut microbiota can also be considered a promising area to optimize their health benefits. It is also important to highlight the role of jabuticaba, a Brazilian fruit that served as the basis for this study. The peels of jabuticaba, often discarded as waste, can be used as a source for anthocyanin extraction for applications in the development of functional products. Besides, jabuticaba fermentation proved to be a promising alternative in the production of wine with functional properties. As a future consideration, human studies should be conducted to validate and further investigate the observed effects *in vivo*.